Percolation theory using Python

Anders Malthe-Sørenssen

Department of Physics, University of Oslo

Apr 20, 2020

Preface

This textbook was developed for the course Fys4460 - Disordered media and percolation theory. The course was developed in 2004 and taught for twenty years at the University of Oslo. The original idea of the course was to provide an introduction to basic aspects of scaling theory to a cross-disciplinary student group. Both geoscience and physics students have successfully taken the course.

This book follows the underlying philosophy that learning a subject is a *hands-on* activity that requires student activities. The course that used the book was project driven. The students solved a set of extensive computational and theoretical exercises and were supported by lectures that provided the theoretical background and group sessions with a learning assistant. The exercises used in the course have been woven into the text, but are also given as a long project description in an appendix. This textbook provides much of the same information as provided in the lectures.

The underlying idea is that in order to learn a subject such as scaling, the student needs to gain hands on experience with real data. The student should learn to generate, analyze and understand data and models. The focus is not to generate perfect data. Instead, we aim to teach the student how to make sense of imperfect data. The data presented in the book and the data that students may generate using the supplied programs are therefore not for very long simulations, but instead from simulations that take a few minutes on an ordinary computer. Experience from this course has been that students learn most effectively by being guided through the process of building models and generating data. Some details of the computer programs have therefore been provided in the text, and we strive to use a similar notation in the computer code and in the mathematics in order to make the transfer from mathematics to computational modeling as simple as possible.

Another aspect of the book is that it tried to be complete in its exposition and worked examples. Not only are the theoretical arguments carried out in detail. The computer code needed to develop data are provided in such as form that they can be run and can generate the data in the examples. This provides students with a complete set of worked examples that contain theory, modeling (the transfer from theory to model), implementation, analysis and the resulting connection between theory and analysis.

In the full course, this textbook was only one half of the curriculum. For the first ten years the first part of the course focused on random walks and the last part focused on random growth processes. For the second ten years of the course, the course switched to be a course on cross-scale modeling of porous media. The first half of the course focused on molecular dynamics modeling of homogeneous systems in order to build an understanding of concepts from statistical physics from computational examples. The second part of the course used molecular dynamics simulations to model nanoscale porous media with focus on fluid transport (diffusion) and fluid flow in a nanoporous system and elastic properties of the porous matrix. Percolation theory was then introduced as a method to upscale the nanoscale systems, and we measured correlation functions, flow and diffusion problems across scales.

The course on percolation theory developed at the University of Oslo and that formed the basis for this textbook is inspired by a course given by Amnon Aharony on random systems several times in the 1990-ies. This course was a great inspiration for all students and faculty and the course served as an inspiration for this course and for this text. Thank you for your great inspiration Amnon.

This book is written as a practical textbook introduction to the field of percolation theory with particular emphasis on containing all the computational methods needed to study percolation theory because our experience is that students learn best by performing these studies themselves — students learn through their activities. Thus, we have focused on included computer code where it is needed. The textbook does not aim to provide a complete set of references to percolation theory. Instead, only a few key references are included for students how want to explore more. There are many other good text and reviews that provide a detailed set of references and a more historical description of the development of the field.

This textbook is the result of the contributions from many students in the course. Originally, the textbook was written with examples in matlab (and the whole book is available with all programs in matlab). However, as Python gradually have developed into the tool of choice for scientific computing, also the code in this course was updated. This was first done by Svenn-Arne Dragly, and some of the translations from matlab to Python was originally done by him. Later contributions from e.g. Øyvind Schøyen to the translation of matlab to Python code for diffusion are also acknowledged.

Thank you to all the students who have contributed in this course. It has been great fun to teach it because of your input and inspiration. I am greatly indebted to you!

Thank you also to my mentors Jens Feder, Torstein Jøssang and Bjørn Jamtveit who built up a cross-disciplinary research environment between physics, computer science and geoscience — the Center for the Physics of Geological Processes. You have always supported my work and inspired me to be a better researcher and a better teacher. Also thank you to my mentor in teaching, textbooks and computing, Hans Petter Langtangen. Without you, this book would never have been realized. Your vision, voice and spirit live on in us who worked with you. And thank you to my collegue Morten Hjorth-Jensen who has built up the group in computational physics at the University of Oslo, who generously included me in this group, and who has by example inspired me to be a better teacher.

This textbook was written using doconce — a document translation and formatting tool that allows simple integration of text, mathematics, and computer code developed by Hans Petter Langtangen.

April 2020 *Anders Malthe-Sørenssen*

Contents

Introduction to percolation 1

Percolation is the study of connectivity of random media and of other properties of connected subsets of random media [37, 30, 7]. Fig. 1.1 illustrates a porous material — a material with holes, pores, of various sizes. These are examples of random materials with built-in disorder. In this book, we will address the physical properties of such media, develop the underlying mathematical theory and the computational and statistical methods needed to discuss the physical properties of random media. In order to do that, we will develop a simplified model system, a model porous medium, for which we can develop a well-founded mathematical theory, and then afterwards we can apply this model to realistic random systems.

The porous media illustrated in the figure serves as a useful, fundamental model for random media in general. What characterizes the porous material in Fig. 1.1? The porous medium consists of regions with material and without material. It is therefore an extreme, binary version of a random medium. An actual physical porous material will be generated by some physical process, which will affect the properties of the porous medium in some way. For example, if the material is generated by sedimentary deposition, details of the deposition process may affect the shape and connectivity of the pores, or later fractures may generate straight fractures in addition to more round pores. These features are always present in the complex geometries found in nature, and they will generate correlations in the randomness of the material. While these correlations can be addressed in detailed, specific studies of random materials, we will here instead start with a simpler class of materials — uncorrelated random, porous materials.

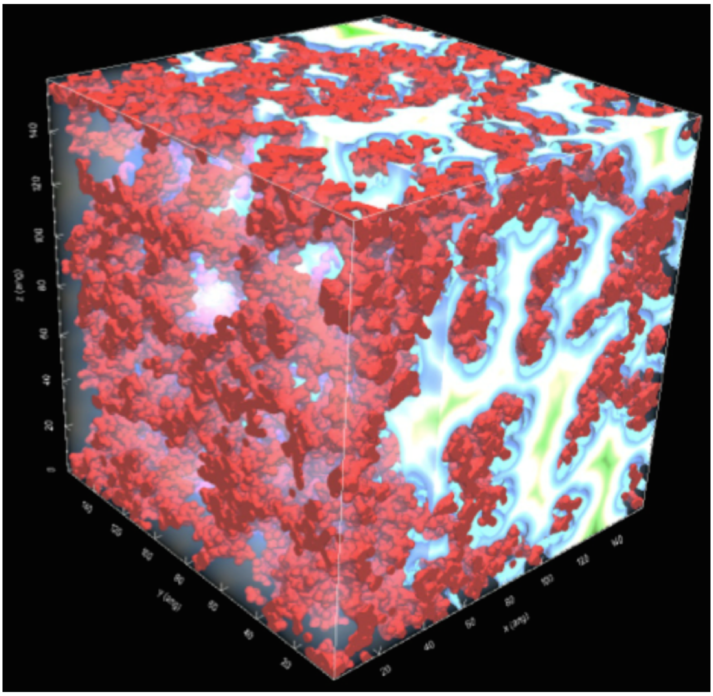

Fig. 1.1 Illustration of a porous material from a nanoporous silicate (SiO_2). The colors inside the pores illustrates the distance to the nearest part of the solid.

We will here introduce a simplified model for a random porous material. We divide the material into cubes (*sites*) of size d. Each site can be either filled or empty. We can use this method to characterize an actual porous medium, as illustrated in Fig. 1.1, or we can use it as a model for a *random porous medium* if we fill each voxel with a probability p. On average, the volume of the solid part of the material will be $V_s = pV$, where V is the volume of the system, and the volume of the pores will be $V_p = (1-p)V$. We usually call the relative volume of the pores, the **porosity**, $\phi = V_p/V$, of the material. The solid is called **the matrix** and the relative volume of the matrix, V_s/V is called the solid fraction, $c = V_s/V$. In this case, we see that p corresponds to the solid fraction. Initially, we will assume that on the scale of lattice cells, the fill probabilities are statistically independent – we will study an *uncorrelated random medium*.

Fig. 1.2 illustrates a two-dimensional system of 4 × 4 cells filled with a probability p. We will call the filled cells occupied or set, and they are colored black. This system is a 4 × 4 matrix, where each cell is filled with probability p. We can generate such a matrix, `m`, in python using

```
p = 0.25
z = rand(4,4)
m = z<p
imagesc(m)
```

The resulting matrices are shown in the Fig. 1.2 for various values of p. The left figure illustrates the matrix, m with its various values. A site i is set as p reaches the value m_i in the matrix. (This is similar to changing the water level and observing what parts of a landscape is above water).

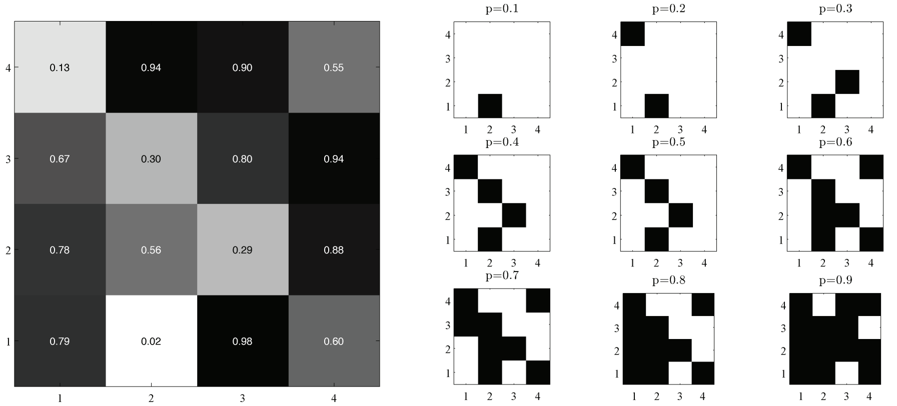

Fig. 1.2 Illustration of an array of 4 × 4 random numbers, and the various sites set for different values of p.

Percolation is the study of connectivity. The simplest question we can ask is when does a path form from one side of the sample to the other? By when, we mean at what value of p. For the particular realization of the matrix m shown in Fig. 1.2 we see that the answer depends on how we define connectivity. If we want to make a path along the set (black) sites from one side to another, we must decide on when two sites are connected. Here, we will typically use nearest neighbor connectivity: Two sites in a square (cubic) lattice are connected if they are nearest neighbors. In the square lattice in Fig. 1.2 each site has $Z = 4$ nearest neighbors and $Z = 8$ next-nearest neighbors, where the number Z is called the connectivity. We see that with nearest-neighbor connectivity, we get a path from the bottom to the top when $p = 0.7$, but with next-nearest neighbor connectivity we would get a path from the bottom to the top already at $p = 0.4$. We call the value p_c, when we first get a path from one side to another (from the top to the bottom, from the left to the right, or both) the *percolation threshold*. For a given realization of the matrix, there is well-defined value for p_c, but for another realization, there would be another p_c. We therefore need to either use statistical averages to characterize the properties of the percolation system, or we need to refer to a theoretical – thermodynamic – limit, such as the value for p_c in an infinitely large system. When we use p_c here, we will refer to the thermodynamic value.

In this book, we will develop theories describing various physical properties of the percolation system as a function of p. We will characterize the sizes of connected regions, the size of the region connecting one side to another, the size of the region that contributes to transport (fluid, thermal or electrical transport), and other geometrical properties of the system. Most of the features we study will be universal, independent of many of the details of the system. From Fig. 1.2 we see that p_c depends on the details: It depens on the rule for connectivity. It would also depend on the type of lattice used: square, trianglar, hexagonal, etc. The value of p_c is specific. However, many other properties are general. For example, how the conductivity of the porous medium depends on p near p_c does not depend on the type of lattice or the choice of connectivity rule. It is universal. This means that we can choose a system which is simple to study in order to gain intuition about the general features, and then apply that intuition to the special cases afterwards. While the connectivity or type of lattice does not matter, some things do matter. For example, the dimensionality matters: The behavior of a percolation system is different in one, two and three dimensions. However, the most important differences occur between one and two dimensions, where the difference is dramatic, whereas the difference between two and three dimensions is more of a degree that we can easily handle. Actually, the percolation problem becomes simpler again in higher dimensions. In two dimensions, it is possible to go around a hole, and still have connectivity. But it is not possible to have connectivity of both the pores and the solid in the same direction at the same time. This is possible in three dimensions: A two-dimensional creature would have problems with having a digestive tract, as it would divide the creature in two, but in three dimensions this is fully possible. Here, we will therefore focus on two and three-dimensional systems.

In this book, we will first address percolation in one and infinite dimensions, since we can solve the problems exactly in these cases. We will then address percolation in two dimensions, where there is no exact solutions. However, we will see that if we assume that the cluster density function has a particular scaling form, we can still address the problem in two dimensions and make powerful predictions. We will also see that close to the percolation threshold the porous medium has a self-affine scaling structure — it is a fractal. This property has important consequences for the physical properties of random systems. We will also see how this is reflected in a systematic change of scales, a renormalization procedure, which is a general tool that can applied to rescaling in many areas.

1.1 Basic concepts in percolation

Let us initially study a specific example of a random medium. We will generate an $L \times L$ lattice of points that are occupied with probability p. This corresponds to a coarse-grained porous medium with a porosity $\phi = p$, if we assume that the occupied sites are considered to be holes in the porous material.

We can generate a realization of a square $L \times L$ system in python using

```
from pylab import *
L = 20
p = 0.5
z = rand(L,L)
m = z<p
imshow(m, origin=’lower’)
show()
```

The resulting matrix is illustrated in Fig. 1.3. However, this visualization does not provide us with any insight into the connectivity of the sites in this system. Let us instead analyze the connected regions in the system.

Definitions

- two sites are **connected** if they are nearest neighbors (4 neighbors on square lattice)
- a **cluster** is a set of connected sites
- a cluster is **spanning** if it spans from one side to the opposite side

- a cluster that is spanning is called the **spanning cluster**
- a system is **percolating** if there is a spanning cluster in the system

Fortunately, there are built-in functions in python that finds connected regions in an image. The function `measurements.label` finds clusters based on a given connectivity. For example, with a connectivity corresponding to 4 we find

```
from scipy.ndimage import measurements
lw, num = measurements.label(m)
```

This function returns the matrix `lw`, which for each site in the original array tells what cluster it belongs to. Clusters are numbered sequentially, and each cluster is given an index. All the sites with the same index belong to the same cluster. The resulting array is shown in Fig. 1.3, where the index for each site is shown and a color is used to indicate the various clusters. Notice that there is a distribution of cluster sizes, but no cluster is large enough to reach from one side to another, and as a result the system does not percolate.

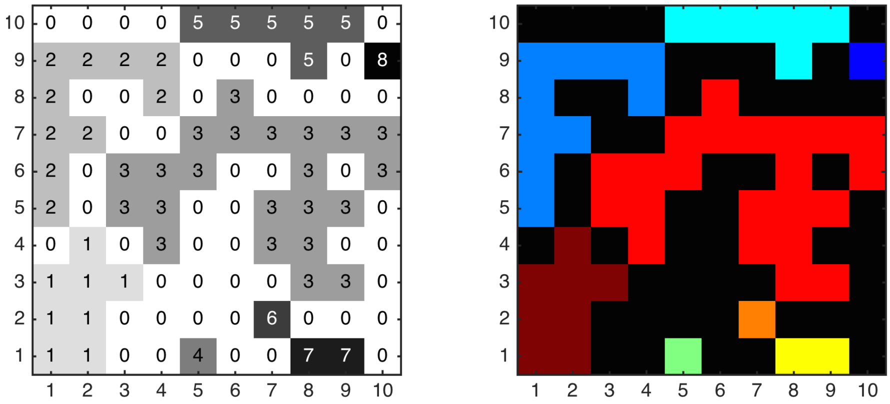

	1	2	3	4	5	6	7	8	9	10
10	0	0	0	0	5	5	5	5	5	0
9	2	2	2	2	0	0	0	5	0	8
8	2	0	0	2	0	3	0	0	0	0
7	2	2	0	0	3	3	3	3	3	3
6	2	0	3	3	3	0	0	3	0	3
5	2	0	3	3	0	0	3	3	3	0
4	0	1	0	3	0	0	3	3	0	0
3	1	1	1	0	0	0	0	3	3	0
2	1	1	0	0	0	0	6	0	0	0
1	1	1	0	0	4	0	0	7	7	0

Fig. 1.3 Illustration of the index array for a 10×10 system for $p = 0.45$.

In order to visualize the clusters effectively, we give the various clusters different colors.

```
imshow(lw, origin='lower')
```

Unfortunately, this colors the clusters gradually from the bottom up. This is a property of the underlying algorithm: Clusters are indexed starting from the bottom-left of the matrix. Hence, clusters that are close to each other will get similar colors and therefore be difficult to discern unless we shuffle the colormap. We can fix this by shuffling the labeling:

```
b = arange(lw.max() + 1)
shuffle(b)
shuffledLw = b[lw]
imshow(shuffledLw, origin=’lower’)
```

The resulting image is shown to the right in Fig. 1.3. (Notice that in these figures we have reversed the ordering of the y-axis. Usually, the first row is in the top-right corner in your plots – and this will also be the case in most of the following plots).

It may also be useful to color the clusters based on the size of the clusters, where size refers to the number of sites in a cluster. We can do this using

```
area = measurements.sum(m, lw, index=arange(lw.max() + 1))
areaImg = area[lw]
imshow(areaImg, origin=’lower’)
colorbar()
```

Let us now study the effect p on the set of connected clusters. We vary the value of p for the same underlying random matrix, and plot the resulting images:

```
from pylab import *
from scipy.ndimage import measurements
L = 100
pv = [0.2,0.3,0.4,0.5,0.6,0.7]
z = rand(L,L)
for i in range(len(pv)):
    p = pv[i]
    m = z<p
    lw, num = measurements.label(m)
    area = measurements.sum(m, lw, index=arange(lw.max() + 1))
    areaImg = area[lw]
    subplot(2,3,i+1)
    tit = ’p=’+str(p)
    imshow(areaImg, origin=’lower’)
    title(tit)
    axis()
```

Fig. 1.4 shows the clusters for a 100×100 system for p ranging from 0.2 to 0.7 in steps of 0.1. We see that the clusters increase in size as p increases, but at $p = 0.6$, there is just one large cluster spanning the entire region. We have a *percolating cluster*, and we call this cluster that spans the system the **spanning cluster**. However, the transition is very rapid from $p = 0.5$ to $p = 0.6$. We therefore look at this region in more detail in Fig. 1.5. We see that the size of the largest cluster increases rapidly as p reaches a value around 0.6, which corresponds to p_c for this system. At this point, the largest cluster spans the entire system. For the two-dimensional system illustrated here we know that in an infinite lattice the percolation threshold is $p_c \simeq 0.5927$.

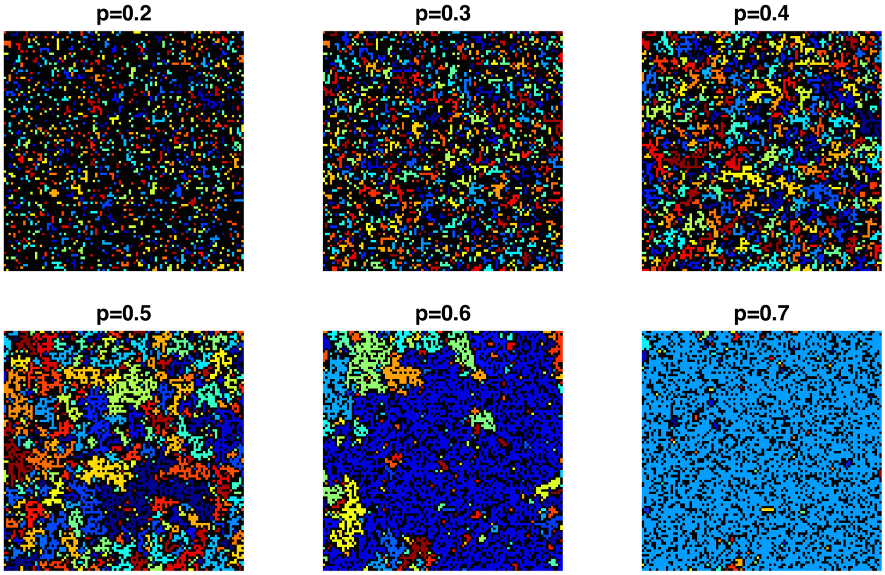

Fig. 1.4 Plot of the clusters in a 100×100 system for various values of p.

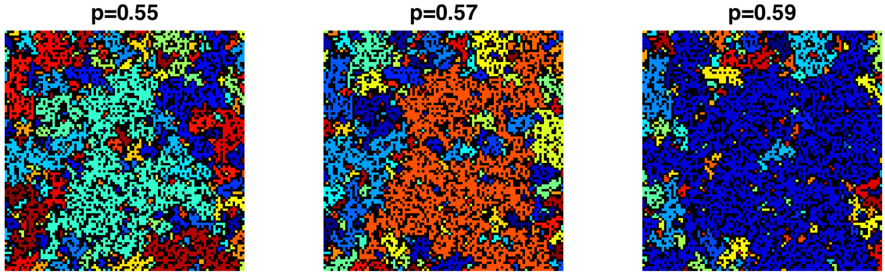

Fig. 1.5 Plot of the clusters in a 100×100 system for various values of p.

The aim of this book is to develop a theory to describe how this random porous medium behaves close to p_c. We will characterize properties such as the density of the spanning cluster, the geometry of the spanning cluster, and the conductivity and elastic properties of the spanning cluster. We will address the distribution of cluster sizes and how various parts of the clusters are important for particular physical processes. We start by characterizing the behavior of the spanning cluster near p_c.

1.2 Percolation probability

When does the system percolate? When there exists a path connecting one side to another. This occurs at some value $p = p_c$. However, in a finite system, like the system we simulated above, the value of p_c for a given realization will vary with each realization. It may be slightly above or slightly below the p_c we find in an infinite sample. Later, we will develop a theory to understand how the effective p_c in a finite system varies from the thermodynamic p_c in an infinitely large system. But already now, we realize that as we perform different experiments, we will measure various values of p_c. We can characterize this behavior by introducing a probability $\Pi(p, L)$:

Percolation probability

The percolation probability $\Pi(p, L)$ is the probability for there to be a connected path from one side to another side as a function of p in a system of size L.

We can measure $\Pi(p, L)$ in a finite sample of size $L \times L$, by generating many random matrices. For each matrix, we perform a cluster analysis for a sequence of p_i values. For each p_i we find all the clusters. We then check if any of the clusters are present both on the left- and on the right-hand side of the lattice. In that case, they are spanning. (We could also have included a test for clusters spanning from the top to the bottom, but this does not change the statistics significantly). In this case, there is a spanning cluster — the system percolates — and we count up how many times a system percolates for a given p_i, N_i, and then divide by the total number of experiment, N to estimate the probability for percolation for a given p_i, $\Pi(p_i, L) \simeq N_i/N$. We implement this as follows. First, we generate a sequence of 100 p_i values from 0.35 to 1.0:

```
p = linspace(0.35,1.0,100)
```

Then we prepare an array for N_i with the same number of elements as p_i:

```
nx = len(p)
Pi = zeros(nx)
```

We will generate $N = 1000$ samples:

```
N = 100
```

We will then loop over all samples, and for each sample we generate a new random matrix. The for each value of p_i we perform the cluster analysis as we did above. We use the function `measurements.label` to label the clusters. Then we check if the set of labels on the left side and the set of labels on the right side have any intersection. If the length of the set of intersections is larger than zero, there is at least one percolating cluster:

```
lw,num = measurements.label(z)
perc_x = intersect1d(lw[0,:],lw[-1,:})
perc = perc_x[where(perc_x>0)]
```

Now, we are ready to implement this into a complete program. For a given value of p, we count in how many simulations $N_p(p)$ there is a path spanning from one side to another and estimate $\bar{\Pi}(p) \simeq N_p(p)/N$, where N is the total number of simulations/samples. This is implemented in the following program:

```
from pylab import *
from scipy.ndimage import measurements
p = linspace(0.4,1.0,100)
nx = len(p)
Ni = zeros(nx)
P = zeros(nx)
N = 1000
L = 100
for i in range(N):
    z = rand(L,L)
    for ip in range(nx):
        m = z<p[ip]
        lw, num = measurements.label(m)
        perc_x = intersect1d(lw[0,:],lw[-1,:])
        perc = perc_x[where(perc_x>0)]
        if (len(perc)>0):
            Ni[ip] = Ni[ip] + 1
Pi = Ni/N
plot(p,Pi)
xlabel('$p$')
ylabel('$\Pi$')
```

The resulting plot of $\Pi(p, L)$ is seen in Fig. 1.7. The figure shows the resulting plots as a function of system size L. We see that as the system size increases, $\Pi(p, L)$ approaches a step function at $p = p_c$.

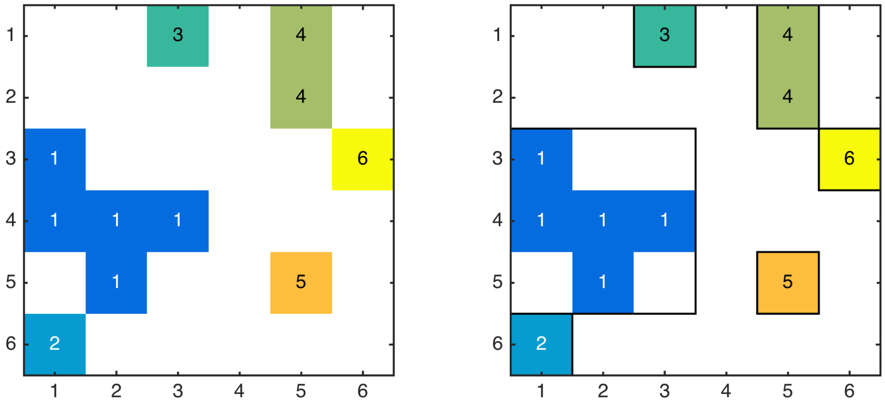

Fig. 1.6 Illustration of the BoundingBox for the clusters in a 6 × 6 simulation.

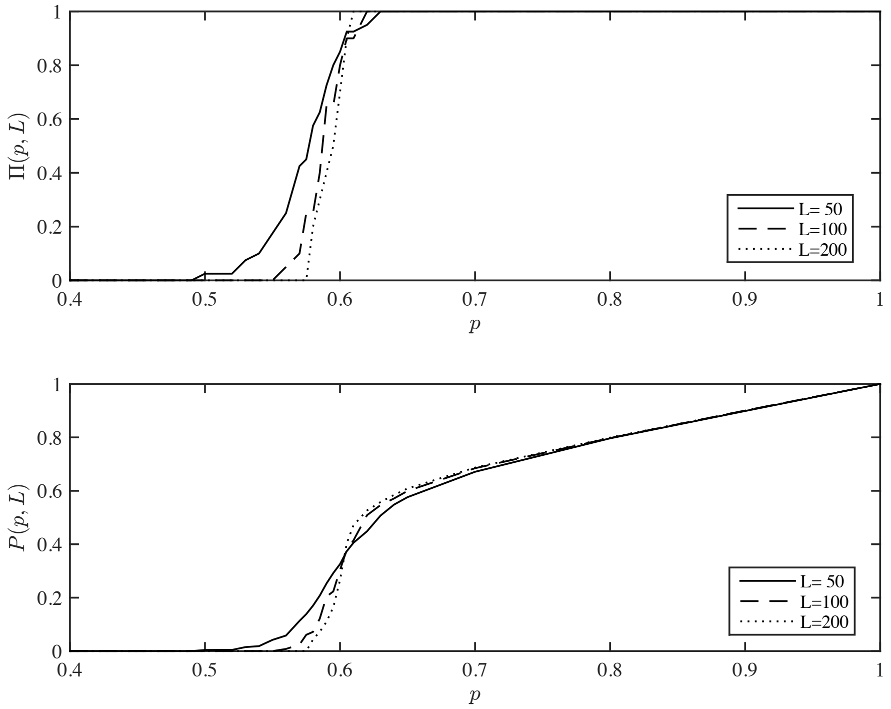

Fig. 1.7 Plot of $\Pi(p,L)$, the probability for there to be a connected path from one side to anther, as a function of p for various system sizes L.

1.3 Spanning cluster

The probability $\Pi(p,L)$ described the probability for there to be a spanning cluster, but what about the spanning cluster itself, how can we characterize it? We see from Fig. 1.4 that the spanning cluster grows quickly around $p = p_c$. Let us therefore characterize the cluster by its size, M_S, or by its density, $P(p,L) = M_S/L^2$, which corresponds to the probability for a site to belong the spanning cluster.

Density of the spanning cluster

The probability $P(p,L)$ for a site to belong to a spanning cluster is called the *density of the spanning cluster*, or the order parameter for the percolation problem.

We can measure $P(p, L)$ by counting the mass M_i of the spanning cluster as a function of p_i for various values of p_i. We can find the mass of the spanning cluster, by finding a cluster that spans the system (there may be more than one) as we did above, and then measuring the number of sites in the cluster using the area = measurements.sum(m, lw, perc)

We do this in the same program as we developed above. For each p_i, we see if a cluster is spanning from one side to another, and if it is, we add the mass of this cluster to $M_S(p_i)$. We implement these features in the following program, which measures both $\Pi(p, L)$ and $P(p, L)$ for a given value of L:

```
from pylab import *
from scipy.ndimage import measurements
p = linspace(0.4,1.0,100)
nx = len(p)
Ni = zeros(nx)
P = zeros(nx)
N = 1000
L = 100
for i in range(N):
    z = rand(L,L)
    for ip in range(nx):
        m = z<p[ip]
        lw, num = measurements.label(m)
        perc_x = intersect1d(lw[0,:],lw[-1,:])
        perc = perc_x[where(perc_x>0)]
        if (len(perc)>0):
            Ni[ip] = Ni[ip] + 1
            area = measurements.sum(m, lw, perc[0])
            P[ip] = P[ip] + area
Pi = Ni/N
P = P/(N*L*L)
subplot(2,1,1)
plot(p,Pi)
subplot(2,1,1)
plot(p,Pi)
subplot(2,1,2)
plot(p,P)
```

The resulting plot of $P(p, L)$ is shown in the bottom of Fig. 1.7. We see that $P(p, L)$ changes rapidly around $p = p_c$ and that it grows slowly – approximately linearly – as $p \to 1$. We can understand this linear behavior: When p is near 1 all the set sites are connected and part of the spanning cluster. The density of the spanning cluster is therefore proportional to p in this limit. We will now develop a theory for the observations of $\Pi(p, L)$, $P(p, L)$ and other features of the percolation system. First, we see what insights we can gain from small, finite systems.

1.4 Percolation in small systems

First, we will address the two-dimensional system directly. We will study a $L \times L$ system, and the various physical properties of it. We will start with $L = 1$, $L = 2$, and $L = 3$, and then try to generalize.

First, let us address $L = 1$. In this case, the system percolates if the site is present, which has a probability p, hence the percolation probability is $\Pi(p, 1) = p$. The probability for a site to belong to the spanning cluster is p, therefore $P(p, 1) = 1$.

Then, let us examine $L = 2$. This is still simple, but we now have to develop a more advanced strategy than for $L = 1$. Our strategy will be to list all possible outcomes, find the probability for each outcome, and then use this to find the probability for the various physical properties we are interested in. The possible configurations are listed in Fig. 1.8.

The strategy is to use a basic result from probability theory: If we want to calculate the probability of an event A, we can do this by summing the probability of A given B multiplied by the probability for B over all possible outcomes B.

$$P(A) = \sum_B P(A|B)P(B) \ , \tag{1.1}$$

where we have used the notation $P(A|B)$ to denote the probability of A given that B occurs . We can use this to calculate properties such as Π and $P(p, L)$ by summing over all possible configurations c:

$$\Pi(p, L) = \sum_c \Pi(p, L|c)P(c) \ , \tag{1.2}$$

where $\Pi(p, L|c)$ is the value of Π for the particular configuration c, and $P(c)$ is the probability of this configuration.

The configurations for $L = 2$ have been numbered from $c = 1$ to $c = 16$ in Fig. 1.8. However, configurations that are either mirror images or rotations of each other will have the same probability and the same physical properties since percolation can take place both in the x and the y directions. It is therefore only necessary to group the configurations into 6 different classes as illustrated in the bottom of Fig. 1.8, but we then need to remember the multiplicity, g_c, for each class when we calculate probabilities. Let us make table of the configurations, the number of such configurations, the probability of *one* such configuration, and the value of $\Pi(p, L|c)$ for this configuration.

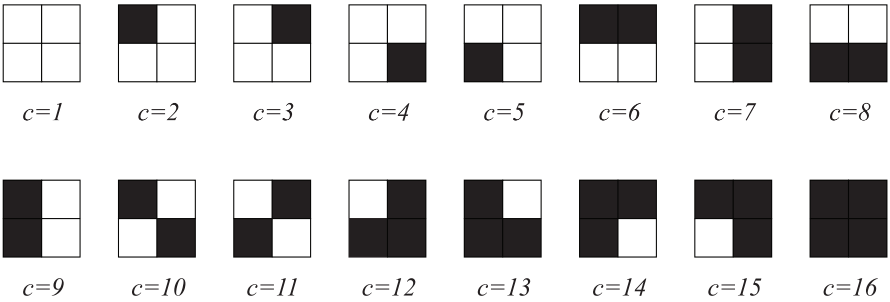

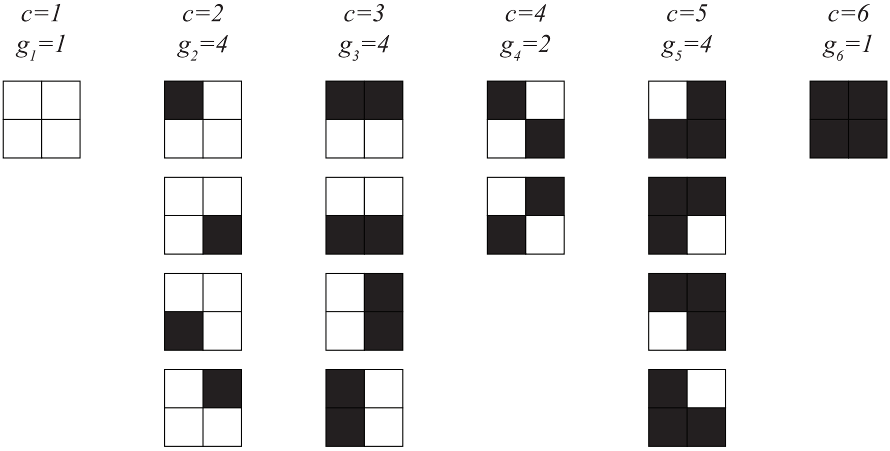

Fig. 1.8 The possible configurations for a $L = 2$ site percolation lattice in two-dimensions. The configurations are indexed using the cluster configuration number c.

c	g_c	$P(c)$	$\Pi(p, L \mid c)$
1	1	$p^0(1-p)^4$	0
2	4	$p^1(1-p)^3$	0
3	4	$p^2(1-p)^2$	1
4	2	$p^2(1-p)^2$	0
5	4	$p^3(1-p)^1$	1
6	1	$p^4(1-p)^0$	1

We should check that we have actually listed all possible configurations. The total number of configurations is $2^4 = 16 = 1 + 4 + 2 + 4 + 4 + 1$, which is ok.

We can then find the probability for Π directly:

$$\Pi = 0 \cdot 1 \cdot p^0(1-p)^4 + 0 \cdot 4 \cdot p^1(1-p)^3 + 1 \cdot 4 \cdot p^2(1-p)^2 \tag{1.3}$$
$$+ 0 \cdot 2 \cdot p^2(1-p)^2 + 1 \cdot 4 \cdot p^3(1-p)^1 + 1 \cdot 1 \cdot p^4(1-p)^0 \; . \tag{1.4}$$

We therefore find the exact value for $\Pi(p, L = 2)$:

$$\Pi(p, L = 2) = 4p^2(1-p)^2 + 4p^3(1-p)^1 + p^4(1-p)^0 \; , \tag{1.5}$$

which we can simplify further if we want. The shape of $\Pi(p, L)$ for $L = 1$, and$L = 2$ is shown in Fig. 1.9.

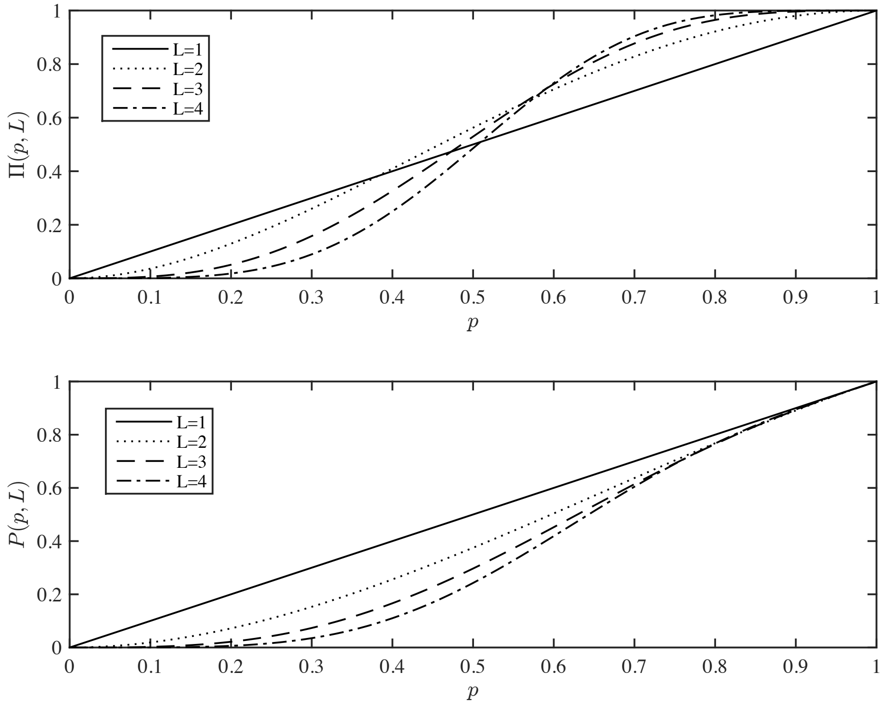

Fig. 1.9 Plot of $\Pi(p, L)$ for $L = 1$ and $L = 2$ as a function of p.

We could characterize $p = p_c$ as the number for which $\Pi = 1/2$, which would give $p_c(L = 2) =$, which is better than for $L = 1$, for which we got $p_c(L = 1) = 1/2$. Maybe we can just continue doing this type of calculation for higher and higher L and we will get a better and better approximation for p_c?

We notice that for finite L, $\Pi(p, L)$ will be a polynomial of order $o = L^2$ - it is in principle a function we can calculate. However, the number of possible configurations is 2^{L^2} which increases very rapidly with L. It is therefore not realistic to use this technique for calculating the percolation probabilities. We will need to have more powerful techniques, or simpler problems, in order to perform exact calculations.

However, we can still learn much from a discussion of finite L. For example, we notice that

$$\Pi(p,L) \simeq Lp^L + c_1 p^{L+1} + \ldots + c_n p^{L^2} \ , \tag{1.6}$$

in the limit of $p \ll 1$. The leading order term when $p \to 0$ is therefore Lp^L.

Similarly, we find that for $p \to 1$, the leading order term is approximately

$$\Pi(p,L) \simeq 1 - (1-p)^L \ . \tag{1.7}$$

These two results gives us an indication about how the percolation probability $\Pi(p,L)$ is approaching the step function when $L \to \infty$.

Similarly, we can calculate $P(p,L)$ for $L = 2$. However, we leave the calculation of the $L = 3$ and the $P(p,L)$ system to the exercises.

1.5 Further reading

There are good general introduction texts to percolation theory such as the popular books by Stauffer and Aharony [37], by Sahimi [30], by Christensen and Moloney [7], and the classical book by Grimmet [14]. Mathematical aspects are addressed by Kesten [21] and phase transitions in general are introduced by e.g. Stanley [35]. Applications of percolation theory are found in many fields such as in geoscience [22], porous media [18] or social networks [33] and many more. We enourage you to explore

1.6 Exercises

Exercise 1.1: Percolation for $L = 3$

a) Find $P(p,L)$ for $L = 1$ and $L = 2$.

b) Categorize all possible configurations for $L = 3$.

c) Find $\Pi(p,L)$ and $P(p,L)$ for $L = 3$.

Exercise 1.2: Counting configurations in small systems

a) Write a program to find all the configurations for $L = 2$.

b) Use this program to find $\Pi(p, L = 2)$ and $P(p, L = 2)$. Compare with the exact results from the previous exercise.

c) Use you program to find $\Pi(p, L)$ and $P(p, L)$ for $L = 3, 4$ and 5.

Exercise 1.3: Percolation in small systems in 3d

In this exercise we will study the three-dimensional site percolation system for small system sizes.

a) How many configurations are there for $L = 2$?

b) Categorize all possible configurations for $L = 2$.

c) Find $\Pi(p, L)$ and $P(p, L)$ for $L = 2$.

d) Compare your results with your result for the two-dimensional system. Comment on similarities and differences.

One-dimensional percolation 2

The percolation problem can be solved exactly in two limits: in the one-dimensional and the infinite dimensional cases. Here, we will first address the one-dimensional system. While the one-dimensional system does not allow us to study the full complexity of the percolation problem, many of the concepts and measures introduced to study the one-dimensional problem can generalized to higher dimensions.

2.1 Percolation probability

Let us first address a one-dimensional lattice of L sites. In this case, there is a spanning cluster if and only if all the sites are occupied. If only a single site is empty, there will not be any connecting path from one side to the other. The percolation probability is therefore

$$\Pi(p, L) = p^L \tag{2.1}$$

This has a trivial behavior when $L \rightarrow \infty$

$$\Pi(p, \infty) = \begin{cases} 0 \; p < 1 \\ 1 \; p = 1 \end{cases} . \tag{2.2}$$

This shows that the percolation threshold is $p_c = 1$ in one dimension. However, the one-dimensional system is anomalous, and higher dimensions, we will always have $p_c < 1$, so that we can study the system both above and below p_c. Unfortunately, for the one-dimensional system we can only study the system below p_c.

2.2 Cluster number density

2.2.1 Definition of cluster number density

In the simulations in Fig. 1.4 we saw that the percolation system was characterized by a wide distribution of clusters – regions of connected sites. The clusters have varying shape and size. If we increase p to approach p_c we saw that the clusters increased in size until they reached the system size. We can use the one-dimensional system to learn more about the behavior of clusters as p approaches p_c.

Fig. 2.1 illustrates a realization of an $L = 16$ percolation system in one dimension below $p_c = 1$. In this case there are 5 clusters of sizes 1,1,4,2,1 measured in the number of sites in each cluster. The clusters are numbered - indexed - from 1 to 5 as we did for the numerical simulations in two dimensions. How can we characterize the clusters in a system? In percolation theory we characterize cluster sizes by asking a particular question: If you point at a (random) site in the lattice, what is the probability for this site to belong to a cluster of size s?

$$P(\text{site is part of cluster of size } s) = sn(s,p) \ . \tag{2.3}$$

It is common to use the notation $sn(s,p)$ for this probability for a given site to belong to a cluster of size s. Why is it divided into two parts, s and $n(s,p)$? Because we must divide the question into two parts: (1) What is the probability for a given site to be a *specific site* in a cluster of size s, and (2) how many such specific sites are there? What do we mean by a specific site? For cluster number 3 in Fig. 2.1 there are 4 sites. We could therefore ask the question, what is the probability for a site to be the left-most site in a cluster of size s. This is what we mean with a specific site. We could ask the same question about the second left-most, the third left-most and so on. We call the probability for a site to belong to a specific site in a cluster of size s (such as the left-most site in the cluster) the **cluster number density**, and we use the notation $n(s,p)$ for this. To find the probability $sn(s,p)$ for a site to belong to any of the s sites in a cluster of size s we must sum the probabilities for each of the specific sites. This is illustrated for the case of a cluster of size 4:

$$
\begin{aligned}
&P(\text{site to be in cluster of size } 4) \\
&\quad = P(\text{site to be left-most site in cluster of size } 4) \\
&\quad + P(\text{site to be second left-most site in cluster of size } 4) \\
&\quad + P(\text{site to be third left-most site in cluster of size } 4) \\
&\quad + P(\text{site to be fourth left-most site in cluster of size } 4) \\
&\quad = 4P(\text{site to be left-most site in cluster of size } 4) \\
&;.
\end{aligned}
$$

Because each of these probabilities are the same. What is the probability for a site to be the left-most site in a cluster of size s in one dimension? In order for it to be in a cluster of size s, the site must be present, which has probability p, and then $s-1$ sites must also be present to the right of it, which has probability p^{s-1}. In addition, the site to the left must be empty (illustrated by an X in Fig. 2.1 bottom part), which has probability $(1-p)$ and the site to the right of the fourth site (illustrated by an X in Fig. 2.1 bottom part), which also has probability $(1-p)$. Since the occupation probabilities for each site are independent, the probability for the site to be the left-most site in a cluster of size s is:

$$
n(s,p) = (1-p)^2 p^s \ . \tag{2.4}
$$

This is the cluster number density in one dimension.

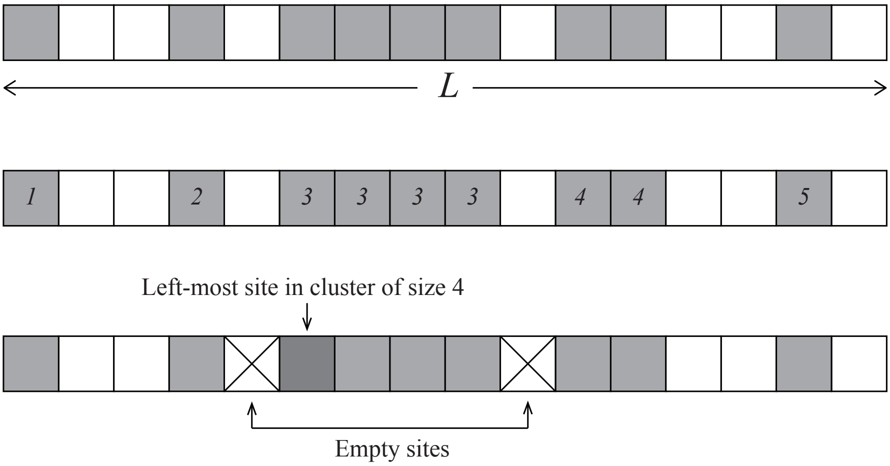

Fig. 2.1 Realization of a $L = 16$ percolation system in one dimension. Occupied sites are marked with black squares.

Cluster number density

The cluster number density $n(s,p)$ is the probability for a site to be a particular site in a cluster of size s. For example, in 1d, $n(s,p)$ is the probability for a site to be the left-most site in a cluster of size s.

We should check that $sn(s,p)$ really is a normalized probability. How should it be normalized? We know that if we point at a random site in the system, the probability for that site to be occupied is p. An occupied site is then either a part of a finite cluster of some size s or it is part of the infinite cluster. The probability for a site to be a part of the infinite cluster is P. This means that we have the following normalization condition:

Normalization of the cluster number density

A site is occupied with probability p. An occupied site is either part of a finite cluster of size s with probability $sn(s,p)$ or it is part of the infinite (spanning) cluster with probability P:

$$p = \sum_{s=1}^{\infty} sn(s,p) + P \ . \tag{2.5}$$

Let us check that this is indeed the case for the one-dimensional result we have found by calculating the sum:

$$\sum_{s=1}^{\infty} sn(s,p) = \sum_{s=1}^{\infty} sp^s(1-p)^2 = (1-p)^2 p \sum_{s=1}^{\infty} sp^{s-1} \ , \tag{2.6}$$

where we will now employ a common trick:

$$\sum_{s=1}^{\infty} sp^{s-1} = \frac{d}{dp}\sum_{s=0}^{\infty} p^s = \frac{d}{dp}\frac{1}{1-p} = (1-p)^{-2} \ , \tag{2.7}$$

which gives

$$\sum_{s=1}^{\infty} sn(s,p) = (1-p)^2\, p \sum_{s=1}^{\infty} sp^{s-1} = (1-p)\, p\, (1-p)^{-2} = p \ . \tag{2.8}$$

Since $P = 0$ when $p < 0$ we see that the probability is normalized. We can use similar tricks to calculate moments of any order.

2.2.2 Measuring the cluster number density

In order to gain further insight into the distribution of cluster sizes, let us look study Fig. 2.1 in more detail. There are 3 clusters of size $s = 1$, one cluster of size $s = 2$, and one cluster of size $s = 4$. We could therefore introduce a histogram of cluster sizes, which is what we would do if we studied the cluster distribution numerically. Let us write N_s as the number of clusters of size s.

s	N_s	$n(s,p)$
1	3	3/16
2	1	1/16
3	0	0/16
4	1	1/16

How can we now estimate $sn(s,p)$, the probability for a given site to be part of a cluster of size s, from N_s? The probability for a site to belong to cluster of size s can be estimated by the number of sites belonging to a cluster of size s divided by the total number of sites. The number of sites belonging to a cluster of size s is sN_s, and the total number of sites is L^d, where L is the system size and d is the dimensionality. (Here, $d = 1$). This means that we can estimate the probability $sn(s,p)$ from

$$\overline{sn(s,p)} = \frac{sN_s}{L^d} \ , \tag{2.9}$$

where we use a bar to show that this is an estimated quantity and not the actual probability. We divide by s on both sides, and find

$$\overline{n(s,p)} = \frac{N_s}{L^d} \ . \tag{2.10}$$

This argument and the result are valid in any dimension, not only for $d = 1$. We have therefore found a method to estimate the cluster number density:

Measuring the cluster number density

We can measure $n(s,p)$ in a simulation by measuring N_s, the number of clusters of size s, and then calculate $n(s,p)$ from

$$\overline{n(s,p)} = \frac{N_s}{L^d} \ . \tag{2.11}$$

For the clusters in Fig. 1.8 we find that

$$\overline{n(1,p)} = \frac{N_1}{L^1} = \frac{3}{16} \ , \tag{2.12}$$

$$\overline{n(2,p)} = \frac{N_2}{L^1} = \frac{1}{16} \ , \tag{2.13}$$

$$\overline{n(3,p)} = \frac{N_3}{L^1} = \frac{0}{16} \ , \tag{2.14}$$

$$\overline{n(4,p)} = \frac{N_4}{L^1} = \frac{1}{16} \ , \tag{2.15}$$

which is our estimate of $n(s,p)$ based on this single realization.

We check the consistency of the result by ensuring that the estimated probabilities also are normalized:

$$\sum_s \overline{sn(s,p)} = 1 \cdot \frac{3}{16} + 2 \cdot \frac{1}{16} + 3 \cdot 0 + 4 \cdot \frac{1}{16} = \frac{9}{16} = \overline{p} \ , \tag{2.16}$$

where $\overline{p}$ is estimated from number of present sites divided by the total number of sites.

In order to produce good statistical estimates for $n(s,p)$ we must sample from many random realization of the system. If we sample from M realizations, and then measure the total number of clusters of size s, $N_s(M)$, summed over all the realizations, we estimate the cluster number density from

$$\overline{n(s,p)} = \frac{N_s(M)}{ML^d} \ . \tag{2.17}$$

Notice that all simulations are for finite L, and we would therefore expect deviations due to L as well as randomness due to the finite number of samples. However, we expect the estimated $\overline{n(s,p;L)}$ to approach the underlying $n(s,p)$ as M and L approaches infinity.

2.2.3 Shape of the cluster number density

We found that the cluster number density in one dimension is

$$n(s,p) = (1-p)^2 p^s \ . \tag{2.18}$$

In Fig. 2.2 we have plotted $n(s,p)$ for various values of p. In order to compare see the s-dependence of the plot directly for various p-values we plot

$$G(s) = (1-p)^2 \, n(s,p) = p^s \ , \tag{2.19}$$

as a function of s. We notice that $(1-p)^2 n(s,p)$ is approximately constant for a wide range of s, and then falls off rapidly for some characteristic value s_ξ which increases as p approaches $p_c = 1$. We can understand this behavior better by rewriting $n(s,p)$ as

$$n(s,p) = (1-p)^2 e^{s \ln p} = (1-p)^2 e^{-s/s_\xi} \ , \tag{2.20}$$

where we have introduced the cut-off cluster size

$$s_\xi = \frac{-1}{\ln p} \ . \tag{2.21}$$

What we are seeing in Fig. 2.2 is therefore the exponential cut-off curve, where the cut-off $s_\xi(p)$ increases as $p \to 1$. We call it a *cut-off* because the value of $n(s,p)$ decays very rapidly (exponentially) when s is larger than s_ξ.

How does s_ξ depend on p?. We see from (2.21) that as p approaches $p_c = 1$, the characteristic cluster size s_ξ will diverge. The form of the divergence can be determined in more detail through a Taylor expansion:

$$s_\xi = -\frac{1}{\ln p} \tag{2.22}$$

when p is close to 1, $1 - p \ll 1$ and we can write

$$\ln p = \ln(1 - (1-p)) \simeq -(1-p) \ , \tag{2.23}$$

where we have used that $\ln(1-x) = -x + o(x^2)$, which is simply the Taylor expansion of the logarithm. As a result

$$s_\xi \simeq \frac{1}{1-p} = \frac{1}{p_c - p} = |p - p_c|^{-1/\sigma} \ . \tag{2.24}$$

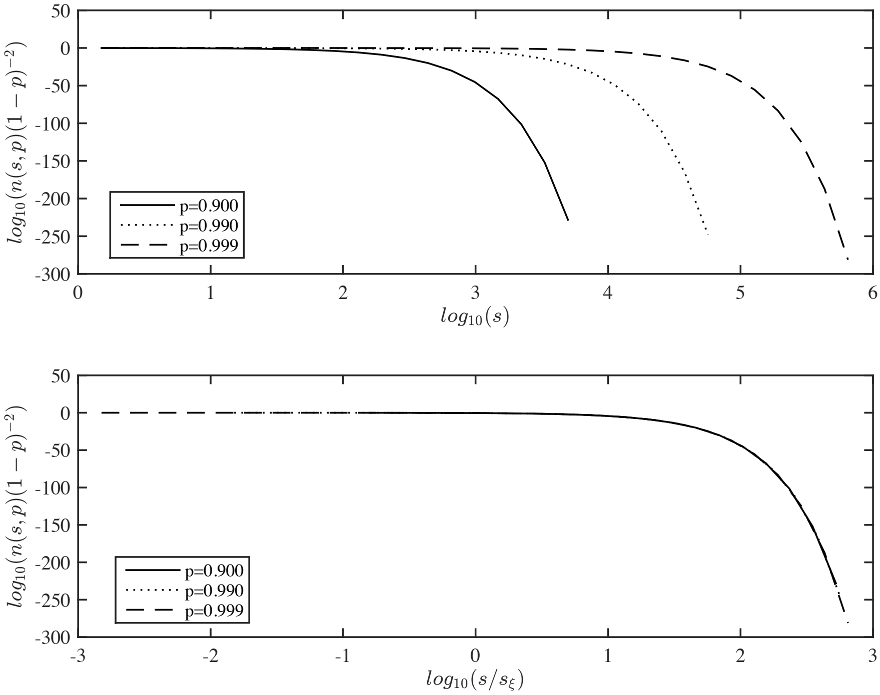

Fig. 2.2 (Top) A plot of $n(s,p)(1-p)^2$ as a function of s for various values of p for a one-dimensional percolation system shows that the cut-off increases as a function of s. (Bottom) When the s axis is rescaled by s/s_ξ all the curves fall onto a common scaling function, that is, $n(s,p) = (1-p)^2 F(s/s_\xi)$.

This shows that the divergence of s_ξ as p approaches p_c is a power-law with exponent -1. This is a feature which is general in percolation theory.

Scaling behavior of the characteristic cluster size The characteristic clustes size s_ξ diverges as

$$s_\xi \propto |p - p_c|^{-1/\sigma} \ , \tag{2.25}$$

when $p \to p_c$. In one dimension, $\sigma = 1$.

The value of the exponent σ depends on the lattice dimensionality, but it does not depend on the details of the lattice. It would, for example, be the same also for next-nearest neighbor connectivity — a problem we leave for the reader to solve as an exercise.

The functional form we have found is also an example of a **data collapse**. We see that if we plot $(1-p)^{-2}n(s,p)$ as a function of s/s_ξ, all data-points for various values of p should fall onto a single curve, as illustrated in Fig. 2.2:

$$n(s,p) = (1-p)^2 e^{-s/s_\xi} \ , \tag{2.26}$$

This is what we call a data-collapse. We have one behavior for small s and then a rapid cut-off when s reaches s_ξ. We can rewrite $n(s,p)$ so that all the s_ξ dependence is in the cut-off function by realizing that since $s_\xi \simeq (1-p)^{-1}$ we have that $(1-p)^2 = s_\xi^{-2}$. This gives

$$n(s,p) = s_\xi^{-2} e^{-s/s_\xi} = s^{-2}\left(\frac{s}{s_\xi}\right)^2 e^{-\frac{s}{s_\xi}} = s^{-2} F\left(\frac{s}{s_\xi}\right) \ . \tag{2.27}$$

where $F(u) = u^2 e^{-u}$. We will see later that this form is general – it is valid for percolation in any dimension, although with other values for the exponent -2. In percolation theory, we call this exponent τ:

$$n(s,p) = s^{-\tau} F(s/s_{xi}) \ , \tag{2.28}$$

where $\tau = 2$ in two dimensions. The exponent τ is another example of a universal exponent that does not depend on details such as the connectivity rule, but it does depend on the dimensionality of the system.

2.2.4 Numerical measurement of the cluster number density

Let us now test the measurement method and the theory through a numerical study of the cluster number density. According to the theory developed above we can estimate the cluster number density $n(s,p)$ from

$$\overline{n(s,p)} = \frac{N_s(M)}{L^2 \cdot M} \ , \tag{2.29}$$

where $N_s(M)$ is the number of clusters of size s measured in M realizations of the percolation system. We generate a one-dimensional percolation system and index the clusters using

```
from pylab import *
from scipy.ndimage import measurements
L = 20
p = 0.90
z = rand(L)
```

```
m = z<p
lw, num = measurements.label(m)
```

Now, `lw` contains the indices for all the clusters. We can extract the size of the clusters by summing the number of elements for each label:

```
labelList = arange(lw.max() + 1)
area = measurements.sum(m, lw, labelList)
```

The resulting list of areas for one sample is

```
>> lw
array([1, 1, 1, 0, 2, 2, 2, 2, 2, 2, 2, 2, 2, 0, 3, 0, 4, 4, 4, 4],
      dtype=int32)
>> area
array([0., 3., 9., 1., 4.])
```

We need to collect all the areas of all the clusters for many realizations, and then calculate the number of clusters of each size s based on this long list of areas. This is all brought together by continuously appending the `area`-array to the end of an array `allarea` that contains the areas of all the clusters.

```
from pylab import *
from scipy.ndimage import measurements
nsamp = 1000
L = 1000
p = 0.90
allarea = array([])
for i in range(nsamp):
    z = rand(L)
    m = z<p
    lw, num = measurements.label(m)
    labelList = arange(lw.max() + 1)
    area = measurements.sum(m, lw, labelList)
    allarea = append(allarea,area)
n,sbins = histogram(allarea,bins=int(max(allarea)))
s = 0.5*(sbins[1:]+sbins[:-1])
nsp = n/(L*nsamp)
sxi = -1.0/log(p)
nsptheory = (1-p)**2*exp(-s/sxi)
plot(s,nsp,’o’,s,nsptheory,’-’)
xlabel(’$s$’)
ylabel(’$n(s,p)$’)
```

This script also calculates N_s using the histogram function with L bins to ensure that there is at least one bin for each value of s:

```
n,sbins = histogram(allarea,bins=int(max(allarea)))
s = 0.5*(sbins[1:]+sbins[:-1])
```

where we find s as the midpoints of the bins returned by the `histogram`-function.

We estimate $\overline{n(s,p)}$ from

```
nsp = n/(L*nsamp)
```

We find the theoretically predicted form for $n(s,p)$, which is $n(s,p) = (1-p)^2 \exp(-s/s_\xi)$, where $s_\xi = -1/lnp$. This is calculated for the same values of s as found from the histogram using:

```
sxi = -1.0/log(p)
nsptheory = (1-p)**2*exp(-s/sxi)
```

When we use the histogram function with many bins, we risk that many of the bins contain zero elements. To remove these elements from the plot, we can use the `nonzero` function to find the indices of the elements of `n` that are non-zero:

```
i = nonzero(n)
```

And then we only plot the values of $\overline{n(s,p)}$ at these indices. The values for the theoretical $n(s,p)$ are calculated for all values of s:

```
plot(s[i],nsp[i],'o',s,nsptheory,'-')
```

The resulting plot is shown in Fig. 2.3. We see that the measured results and the theoretical values fit nicely, even though the theory is for infinite system sizes, and the simulations where performed at $L = 1000$. We also see that for larger values of s there are fewer observed values. It may therefore be a good idea to make the bins used for the histogram larger for larger values of s. We will return to this when we measure the cluster number density in two-dimensional systems in chapter 4.

2.2.5 Average cluster size

Since we have a precise form of the cluster number density, $n(s,p)$ we can use it to calculate the average cluster size. However, what do we mean by the average cluster size in this case? In percolation theory it is common to define the average cluster size as the average size of a cluster connected to a given (random) site in our system. That is, we will use the cluster number density, $n(s,p)$, as the basic distribution for calculating the moments.

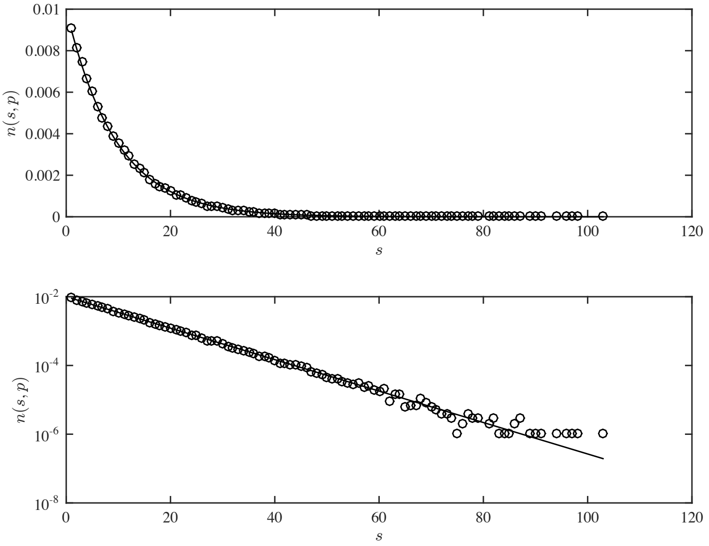

Fig. 2.3 Plot of the predicted $\overline{n(s,p)}$, based on $M = 1000$ samples of a $L = 1000$ system with $p = 0.9$, and the theoretical $n(s,p)$ curve on a linear scale (top) and a semilogarithmic scale (bottom). The semilogarithmic plot clearly shows that $\overline{n(s,p)}$ follows an exponential curve.

Average cluster size

The average cluster size $S(p)$ is defined as

$$S(p) = \langle s \rangle = \sum_s s(\frac{sn(s,p)}{\sum_s sn(s,p)}) \, , \tag{2.30}$$

The normalization sum in the denominator is equal to p when $p < p_c$. We can therefore write this as

$$S(p) = \sum_s s(\frac{sn(s,p)}{p}) \, . \tag{2.31}$$

Similarly, we can define the k-th moment to be

$$S_k = \langle s^k \rangle = \sum s^k(\frac{sn(s,p)}{p}) \, . \tag{2.32}$$

Let us calculate the first moment, corresponding to $k = 1$, the average cluster size.

$$S = \frac{1}{p}\sum_s s^2 n(s,p) \tag{2.33}$$

$$= \frac{(1-p)^2}{p}\sum_s s^2 p^s \tag{2.34}$$

$$= \frac{(1-p)^2}{p}\sum_s p\frac{\partial}{\partial p}p\frac{\partial}{\partial p}p^s \tag{2.35}$$

$$= \frac{(1-p)^2}{p}p\frac{\partial}{\partial p}p\frac{\partial}{\partial p}\sum_s p^s \tag{2.36}$$

$$= \frac{(1-p)^2}{p}p\frac{\partial}{\partial p}\frac{p}{(1-p)^2} \text{ (from } \sum_s sn(s,p) \text{)} \tag{2.37}$$

$$= (1-p)^2\frac{\partial}{\partial p}\frac{p}{(1-p)^2} \tag{2.38}$$

$$= (1-p)^2(\frac{1}{(1-p)^2} + \frac{2p}{(1-p)^3}) \tag{2.39}$$

$$= \frac{1+p}{1-p} \tag{2.40}$$

where we have used the trick introduced in (2.7) to move the derivation out through the sum. In addition, we have also used our previous result from $\sum_s sn(s,p)$ directly.

This shows that we can write

$$S = \frac{1+p}{1-p} = \frac{\Gamma}{|p-p_c|^\gamma} , \tag{2.41}$$

with $\gamma = 1$ and $\Gamma(p) = 1 + p$. That is, the average cluster size also diverges as a power-law when p approaches p_c. The exponent $\gamma = 1$ of the power-law is again universal. That is, it depends on features such as dimensionality, but not on details such as the lattice structure.

Later, we will observe that we have a similar behavior for percolation in any dimension, although with other values of γ.

We will leave it as an exercise for our reader to find the behavior for higher moments, S_k, using a similar argument.

2.3 Spanning cluster

The density of the spanning cluster, $P(p;L)$, is similarly simple to find and discuss. The spanning cluster only exists for $p \geq p_c$. The discussion for $P(p; L)$ is therefore not that interesting for the one-dimensional case. However, we can still introduce some of the general notions.

The behavior of $P(p; \infty)$ in one dimension is given as

$$P(p; \infty) = \begin{cases} 0 \; p < 1 \\ 1 \; p = 1 \end{cases} . \tag{2.42}$$

We could introduce a similar finite size scaling discussion also for $P(p; L)$. However, we will here concentrate on the relation between $P(p; L)$ and the distribution of cluster sizes. The distribution of the size of a finite cluster is described by $sn(s, p)$, which is the probability that a given site belongs to a cluster of size s. If we look at a given site, that site is occupied with probability p. If a site is occupied it is either part of a finite cluster of size s or it is part of the spanning cluster. Since these two events cannot occur at the same time, the probability for a site to be set must be the sum of the probability to belong to a finite cluster and to belong to the infinite cluster. The probability to belong to a finite cluster is the sum of the probability to belong to a cluster of s for all s. We therefore have the equality:

$$p = P(p; L) + \sum_s sn(s, p; L) \ , \tag{2.43}$$

which is not only valid in the one-dimensional case, but also for percolation problems in general.

We can use this relation to find the density of the spanning cluster from the cluster number density $n(s, p)$ through

$$P(p) = p - \sum_s sn(s, p) \ . \tag{2.44}$$

This illustrates that the cluster number density $n(s, p)$ is a fundamental property, which can be used to deduce many of the other properties of the percolation system.

2.4 Correlation length

From the simulations in Fig. 1.4 we see that the size of the clusters increases as $p \to p_c$. We expect a similar behavior for the one-dimensional system. We have already seen that the mass (or area) of the clusters diverges as $p \to p_c$. However, the characteristic cluster size s_ξ characterizes the mass (or area) of a cluster. How can we characterize the extent of a cluster?

To characterize the linear extent of a cluster, we find the probability for two sites at a distance r to be part of the same cluster. This probability is called the **correlation function**, $g(r)$:

> The correlation function $g(r)$ describes the conditional probability that two sites a and b, which both are occupied and are separated by a distance r belong to the same cluster.

For one-dimensional percolation, two sites a and b only can be part of the same cluster if all the points in between a and b are occupied. If r denotes the number of points between a and b (not counting the start and end positions) as illustrated in Fig. 2.4, we find that the correlation function is

$$g(r) = p^r = e^{-r/\xi} , \tag{2.45}$$

where $\xi = -\frac{1}{\ln p}$ is called the correlation length. The correlation length diverges as $p \to p_c = 1$. We can again find the way in which it diverges through by using that when $p \to 1$

$$\ln p = \ln(1 - (1 - p)) \simeq -(1 - p) . \tag{2.46}$$

We find that the correlation length is

$$\xi = \xi_0 (p_c - p)^{-\nu} , \tag{2.47}$$

with $\nu = 1$. The correlation length therefore diverges as a power-law when $p \to p_c = 1$. This behavior is general for percolation theory, although the particular value of the exponent ν depends on the dimensionality.

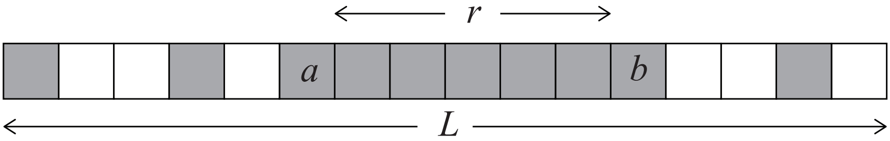

Fig. 2.4 An illustration of the distance r between two sites a and b. The two sites a and b are connected if and only if all the sites between a and b are occupied.

We can use the correlation function to strengthen our interpretation of when a finite system size becomes relevant. As long as $\xi \ll L$, we will not notice the effect of a finite system, because no cluster is large enough to notice the finite system size. However, when $\xi \gg L$, the behavior is dominated by the system size L, and we are no longer able to determine how close we are to percolation.

2.5 (Advanced) Finite size effects

We have so far not discussed the effects of a finite lattice size L. We have implicitly assumed that the lattice size L is so large that the corrections will be small and can be ignored. However, we have now observed that the average cluster size S, the characteristic cluster size s_ξ, and the correlation length ξ diverges when p approaches p_c. We will therefore eventually start observing effects of the finite system size as p approaches p_c.

We have essentially ignored two effects:

- **(a)** the upper limit for cluster sizes is L and not ∞
- **(b)** there are corrections to $n(s, p; L)$ due to the finite lattice size

The effect of (b) becomes clear as p approaches p_c: As s_ξ increases it will eventually be larger than L, which in one dimension also provides an upper limit for s. This is indeed observed in the scaling collapse plot for $n(s, p)$, where we for finite lattice sizes will find a cross-over cluster size s_L, which depends on the lattice size L.

What will be the effect of including a finite upper limit L for all the sums? This will imply that the result of the sum $\sum_s p^s$ will be

$$\sum_{s=1}^{L} p^s = \frac{1 - p^L}{1 - p} \ , \tag{2.48}$$

instead of $1/(1 - p)$ when L is infinite. Indeed, this sum approaches $1/(1 - p)$ as $L \to \infty$. This implies that S will approach L when $p \to p_c$, as can be seen by applying l'Hopital's rule to find the limit as $p \to p_c$. However, as long as $\xi \ll L$, we will still observe that $S \propto 1/(1 - p)$. We will make these types of arguments more precise when we discuss finite size scaling further on.

2.5.1 Finite size effects in $\Pi(p, L)$ and p_c

So far we have only addressed the behavior of an infinite system, We have found that $\Pi(p, L) = p^L$. From this, we find that

$$\Pi' = \frac{d\Pi}{dp} = Lp^{L-1} \ . \tag{2.49}$$

What is the interpretation of Π'? We can write

$$\Pi'(p, L)dp = \Pi(p + dp, L) - \Pi(p, L) \ , \tag{2.50}$$

where the right-hand term is the probability that the system became spanning when p increased from p to $p + dp$. That is, it is the probability that the spanning cluster appeared for the first time for p between p and $p + dp$. We can therefore interpret Π' as the probability density for p', which is the p when a spanning cluster appears.

What can we learn from the form of Π'? If we perform numerical experiments to find p_c, we see that for finite system sizes L, we might observe a p_c which is lower than 1. We can use Π' to find the average p' found - this will be done generally further on. Here, we will only study the width of the distribution Π', which will give us an idea about the possible deviation when we measure p_c by a measurement of p'. We define the width as the value p_x for which Π' has reached 1/2 (or some other value you like).

$$\Pi'(p_x, L) = Lp_x^{L-1} = 1/2 \ . \tag{2.51}$$

This gives

$$\ln p_x = -\frac{\ln 2}{L-1} \ , \tag{2.52}$$

We will now use a standard approximation for $\ln x$, when x is close to 1, by writing

$$\ln p_x = \ln(1 - (1 - p_x)) \simeq -(1 - p_x) \ , \tag{2.53}$$

where we have used that $\ln(1 - x) \simeq -x$, when $x \ll 1$. This gives us that

$$(1 - p_x) \simeq \frac{\ln 2}{L-1} \ , \tag{2.54}$$

and consequently,

$$p_x = p_c - \frac{\ln 2}{L-1} \ . \tag{2.55}$$

We will therefore have an L dependence in the effective p_c which is measured for a finite system. We will address this topic in much more depth later on under finite size scaling in chap. 6.

We can also find a similar scaling for $\Pi(p,L)$, because

$$\Pi(p,L) = p^L = e^{L\ln p} = e^{-L/\xi} \ , \tag{2.56}$$

where we have defined $\xi = -1/\ln p$. We notice that $\xi \to \infty$ when $p \to p_c = 1$. We can therefore classify the behavior of Π according to the relative sizes of the length ξ and L:

$$\Pi(p,L) = \begin{cases} 1 & L \ll \xi \\ 0 & L \gg \xi \end{cases} \ , \tag{2.57}$$

We have therefore found an important length scale ξ in our problem that appears whenever the length L appears.

2.6 Exercises

Exercise 2.1: Next-nearest neighbor connectivity in 1d

Assume that connectivity is to the next-nearest neighbors for an infinite one-dimensional percolation system.

a) Find $\Pi(p,L)$ for a system of length L.

b) What is p_c for this system?

c) Find $n(s,p)$ for an infinite system.

Exercise 2.2: Higher moments of s

The k'th moment of s is defined as

$$\langle s^k \rangle = \sum_s s^k (\frac{sn(s,p)}{p}) \ . \tag{2.58}$$

a) Find the second moment of s as a function of p.

b) Calculate the first moment of s numerically from $M = 1000$ samples for $p = 0.90$, 0.95, 0.975 and 0.99. Compare with the theoretical result.

c) Calculate the second moment of s numerically from $M = 1000$ samples for $p = 0.90$, 0.95, 0.975 and 0.99. Compare with the theoretical result.

3 Infinite-dimensional percolation

We have now seen how the percolation problem can be solved exactly for a one-dimensional system. However, in this case the percolation threshold is $p_c = 1$, and we were not able to address the behavior of the system for $p > p_c$. There is, however, another system in which many features of the percolation problem can be solved exactly, and this is percolation on a regular tree structure on which there are no loops. The condition of no loops is essential. This is also why we call this system a system of infinite dimensions, because we need an infinite number of dimensions in Euclidean space in order to embed a tree without loops. In this section, we will provide explicit solution to the percolation lattice on a particular tree structure called the Bethe lattice.

The Bethe lattice, which is also called the Cayley tree, is a tree structure in which each node has Z neighbors. This structure has no loops. If we start from the central point and draw the lattice, the perimeter grows as fast as the bulk. Generally, we will call Z the coordination number. The Bethe lattice is illustrated in Fig. 3.1.

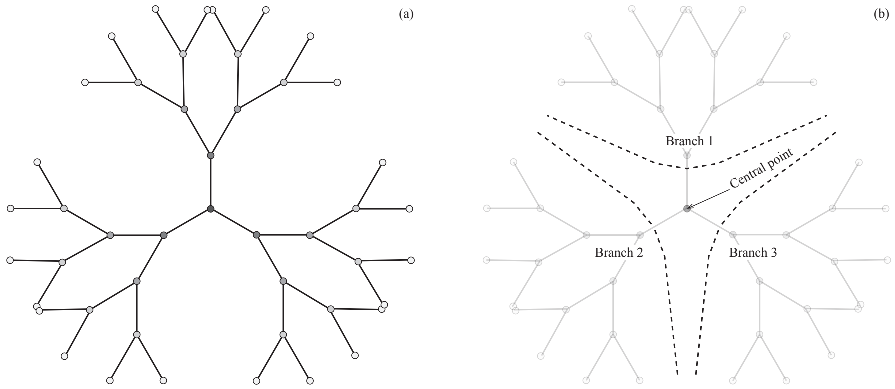

Fig. 3.1 Illustration of four generations of the Bethe lattice with number of neighbors $Z = 3$.

3.1 Percolation threshold

If we start from the center and move along a branch, we will generate $(Z - 1)$ new neighbors from each of the branches. To get a spanning cluster, we need to ensure that at least one of the $Z - 1$ sites are occupied on average. That is, the occupation probability, p, must be:

$$p(Z - 1) \geq 1 \; , \tag{3.1}$$

in order for this process to continue indefinitely.

We associate p_c with the value for p where the cluster is on the verge of dying out, that is

$$p_c = \frac{1}{Z - 1} \; . \tag{3.2}$$

For $Z = 2$ we regain the one-dimensional system, with percolation threshold $p_c = 1$. However, when $Z > 2$, we obtain a finite percolation threshold, that is, $p_c < 1$, which means that we can observe the behavior both above and below p_c.

In the following, we will use a set of standard techniques to find the density of the spanning cluster, $P(p)$, the average cluster size S, before we address the full scaling behavior of the cluster density $n(s, p)$.

3.2 Spanning cluster

We will use a standard approach to find the density $P(p)$ of the spanning cluster when $p > p_c$. The technique is based on starting from a "central" site, and then address the probability that a given branch is connected to infinity.

We can use a strictly technical approach to find P by noting that P can be found from

$$p = P + \sum_s sn(s,p) \ , \tag{3.3}$$

where the sum is the probability that the site is part of a finite cluster, that is, it is the probability that the site is not connected to infinity. Let us use Q to denote the probability that a branch does not lead to infinity. The concept of a central point and a branch is illustrated in Fig. 3.1.

We can arrive at this result by noticing that the probability that at site is not connected to infinity in a particular direction is Q. The probability that the site is not connected to infinity in any direction is therefore Q^Z. The probability that the site *is* connected to infinity is therefore $1 - Q^Z$. In addition, we need to include the probability p that the site is occupied. The probability that a given site is connected to infinity, that is, that it is part of the spanning cluster, is therefore

$$P = p(1 - Q^Z) \ . \tag{3.4}$$

It now remains to find an expression for $Q(p)$. We will determine Q through a consistency equation. Let us assume that we are moving along a branch, and that we have come to a point k. Then, Q gives the probability that this branch does not lead to infinity. This can occur by either the site k not being occupied, with probability $(1-p)$, or by site k being occupied with probability p, and all of the $Z-1$ branches leading out of k not being connected to infinity, with probability Q^{Z-1}. The probability Q for the branch not to be connected to infinity is therefore

$$Q = (1-p) + pQ^{Z-1} \ . \tag{3.5}$$

We can check this equation by looking at the case when $Z = 2$, which should correspond to the one-dimensional system. In this case we have $Q = 1 - p + pQ$, which gives, $(1-p)Q = (1-p)$, where we see that when $p \neq 1$, $Q = 1$. That is, when $p < 1$ all branches are not connected to infinity, implying that there is no spanning cluster. We regain the results from one-dimensional percolation theory.

We could solve this equation for general Z. However, for simplicity we will restrict ourselves to $Z = 3$, which is the smallest Z that gives a behavior different from the one-dimensional system. In this case

$$Q = 1 - p + pQ^2 \ , \tag{3.6}$$

$$pQ^2 - Q + 1 - p = 0 \ . \tag{3.7}$$

The solution of this second order equation is

$$Q = \frac{1 \pm \sqrt{(2p-1)^2}}{2p} = \begin{cases} 1 & p < p_c \\ \frac{1-p}{p} & p > p_c \end{cases} \ . \tag{3.8}$$

There are two possible solutions. We recognize that the solution $(1-p)/p$ is 1 for $p = p_c = 1/2$, and is larger than 1 for smaller values of p, we must therefore use the other solution of $Q = 1$ for $p < p_c = 1/2$. These results confirm the value $p_c = 1/2$ as the percolation threshold. When $p \leq p_c$, we find that $Q = 1$, that is, no branch propagates to infinity. Whereas, when $p > p_c$, Q becomes smaller than 1, and there is a finite probability for a branch to continue to infinity.

We insert this back into the equation for $P(p)$ and find that for $p > p_c$:

$$\begin{aligned} P &= p(1 - Q^3) && (3.9) \\ &= p(1 - (\frac{1-p}{p})^3) && (3.10) \\ &= p(1 - \frac{1-p}{p})(1 + \frac{1-p}{p} + (\frac{1-p}{p})^2) \ . && (3.11) \end{aligned}$$

This result is illustrated in Fig. 3.2.

From this we observe the expected result that when $p \to 1$, $P(p) \propto p$. We can rewrite the equation as

$$P = 2(p - \frac{1}{2})(1 + \frac{1-p}{p} + (\frac{1-p}{p})^2) \ , \tag{3.12}$$

From this we can immediately find the leading order behavior when $p \to p_c = 1/2$. In this case we have

$$P \simeq 6(p - p_c) + o((p-p_c)^2) \ . \tag{3.13}$$

We have therefore found that for $p > p_c$

$$P(p) \simeq B(p - p_c)^{\beta} \ , \tag{3.14}$$

where $B = 6$, and the exponent $\beta = 1$. The density of the spanning cluster is therefore a power-law in $(p - p_c)$ with exponent β. The exponent depends on the dimensionality of the lattice, but should not depend on

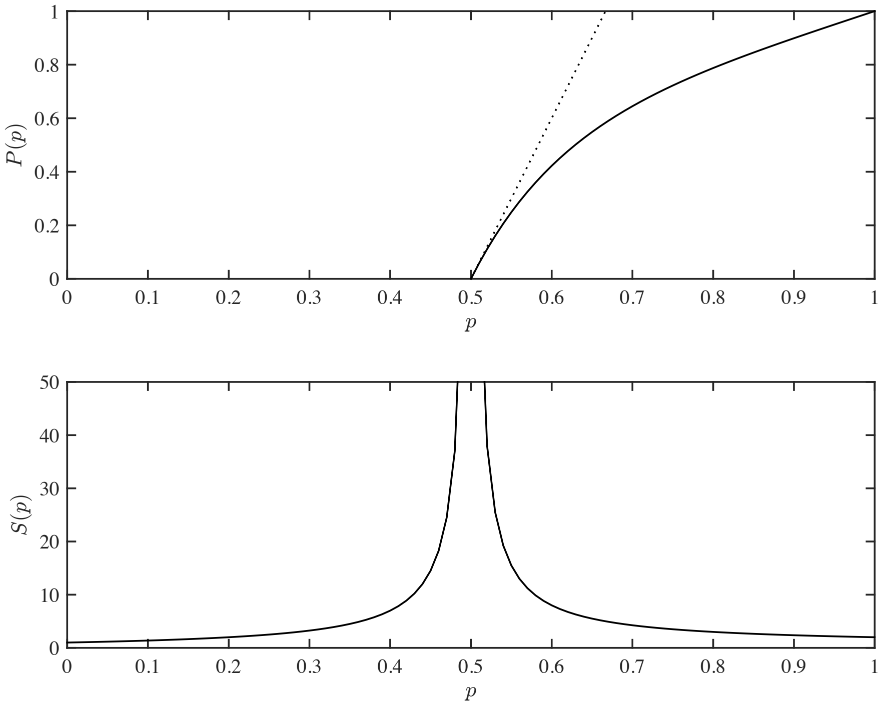

Fig. 3.2 (Top) A plot of $P(p)$ as a function of p for the Bethe lattice with $Z = 3$. The tangent at $p = p_c$ is illustrated by a straight line. (Bottom) A plot of the average cluster size, $S(p)$, as a function of p for the Bethe lattice with $Z = 3$. The average cluster size diverges when $p \to p_c = 1/2$ both from below and above.

lattice details, such as the number of neighbors Z. We will leave it to the reader as an exercise to show that β is the same for $Z = 4$.

We notice in passing that our approach is an example of a mean field solution, or a self-consistency solution: We assume that we know Q, and then solve to find Q. We will use similar methods further on in this course.

3.3 Average cluster size

We will use a similar method to find the average cluster size, $S(p)$. Let us introduce $T(p)$ as the average number of sites connected to a given site on a specific branch, such as in branch 1 in Fig. 3.1. The average cluster size S is then given as

$$S = 1 + ZT \ , \tag{3.15}$$

where the 1 represents the central point, and T is the average number of sites on each branch. We will again find a self-consistent equation for T, starting from a center site. The average cluster size T is found from summing the probability that the next site k is empty, $1-p$, multiplied with the contribution to the average in this case (0), plus the probability that the next site is occupied, p, multiplied with the contribution in this case, which is the contribution from the site (1) and the contribution of the remaining $Z-1$ subbranches. In total:

$$T = (1-p)0 + p(1 + (Z-1)T) \ , \tag{3.16}$$

We can solve this directly for T, finding

$$T = \frac{p}{1 - p(Z-1)} \ , \tag{3.17}$$

where we recognize that the value $p_c = 1/(Z-1)$ plays a special role because the average size of the branch diverges when $p \to p_c$. We find the average cluster size S to be:

$$S = 1 + ZT = \frac{1+p}{1-(Z-1)p} = \frac{p_c(1+p)}{p_c - p} \ , \tag{3.18}$$

which is illustrated in Fig. 3.2. The expression for $S(p)$ can therefore be written on the general form

$$S = \frac{\Gamma}{(p_c - p)^{\gamma}} \ , \tag{3.19}$$

where our argument determines $p_c = 1/(Z-1)$, and the exponent $\gamma = 1$. The average cluster size S therefore diverges as a power-law when p approaches p_c. The exponent γ characterizes the behavior, and the value of γ depends on the dimensionality, but not on the details of the lattice. Here, we notice in particular that γ does not depend on Z.

3.4 Cluster number density

In order to find the cluster number density for the Bethe lattice, we need to address how we in general can find the cluster number density. In general, in order to find the cluster number density for a given s, we need to find all possible configurations of clusters of size s, and sum up their probability:

$$n(s,p) = \sum_{c(s)} p^s (1-p)^{t(c)} \tag{3.20}$$

Here we have included the term p^s, because we know that we must have all the s sites of the cluster present, and we have included the term $(1-p)^t$, because all the neighboring sites must be unoccupied, and there are $t(c)$ neighbors for configuration c. Based on this, we realize that we could instead make a sum over all t, but then we need to include the effect that there are several clusters that can have the same t. We will then have to introduce the degeneracy factor $g_{s,t}$ which gives the number of different clusters that have size s and a number of neighbors equal to t. The cluster number density can then be written as

$$n(s,p) = p^s \sum_{t} g_{s,t} (1-p)^t \ . \tag{3.21}$$

This can be illustrated for two-dimensional percolation. Let us study the case when $s = 3$. In this case there are 6 possible clusters for size $s = 3$, as illustrated in Fig. 3.3.

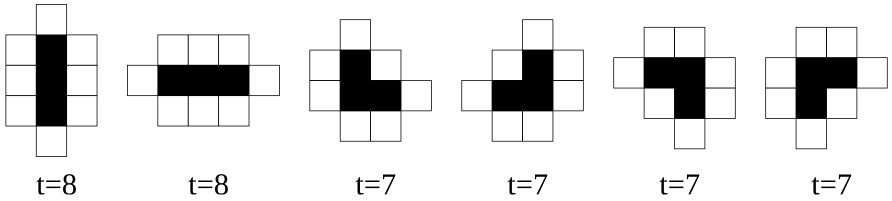

Fig. 3.3 Illustration of the 6 possible configurations for a two-dimensional cluster of size $s = 3$.

There are two clusters with $t = 8$, and four clusters with $t = 7$. There are no other clusters of size $s = 3$. We can therefore conclude that for the two-dimensional lattice, we have $g_{3,8} = 2$, and $g_{3,7} = 4$, and $g_{3,t} = 0$ for all other values of t.

For the Bethe lattice, there is a particularly simple relation between the number of sites, and the number of neighbors. We can see this by looking at the first few generations of a Bethe lattice grown from a central seed. For $s = 1$, the number of neighbors is $t_1 = Z$. When we add one more site, we remove one neighbor from what we had previously, in order to add a new site, and then we add $Z-1$ new neighbors: $s = 2$, and $t_2 = t_1 + (Z-2)$. Consequently,

$$t_k = t_{k-1} + (Z-2) \ , \tag{3.22}$$

and therefore:

$$t_s = s(Z-2)+2 \; . \tag{3.23}$$

The cluster number density, given by the sum over all t, is therefore reduced to only a single term for the Bethe lattice

$$n(s,p) = g_{s,t_s} p^s (1-p)^{t_s} \; , \tag{3.24}$$

For simplicity, we will write $g_s = g_{s,t_s}$. In general, we do not know g_s, but we will show that we still can learn quite a lot about the behavior of $n(s,p)$.

The cluster density can therefore be written as

$$n(s,p) = g_s p^s (1-p)^{2+(Z-2)s} \; . \tag{3.25}$$

We rewrite this as a common factor to the power s:

$$n(s,p) = g_s [p(1-p)^{Z-2}]^s (1-p)^2 \; , \tag{3.26}$$

which, for $Z=3$ becomes

$$n(s,p) = g_s [p(1-p)]^s (1-p)^2 \; . \tag{3.27}$$

However, we can use a general Z for our argument. We will study $n(s,p)$ for p close to p_c. In this range, we will do a Taylor expansion of the term $f(p) = p(1-p)^{Z-2}$, which is raised to the power s in the equation for $n(s,p)$. The shape of $f(p)$ as a function of p is shown in Fig. 3.4. The maximum of $f(p)$ occurs for $p = p_c = 1/(Z-1)$. This is also easily seen from the first derivative of $f(p)$.

$$\begin{aligned} f'(p) &= (1-p)^{Z-2} - p(Z-2)(1-p)^{Z-3} = \qquad (3.28)\\ &= (1-p)^{Z-3}(1-p-p(Z-2)) = \qquad (3.29)\\ &= (1-p)^{Z-3}(1-(Z-1)p) \qquad (3.30) \end{aligned}$$

which shows that $f'(p_c) = 0$. We leave it to the reader to show that $f''(p_c) < 0$.

The Taylor expansion can be written as

$$f(p) = f(p_c) + f'(p_c)(p-p_c) + \frac{1}{2} f''(p_c)(p-p_c)^2 + o((p-p_c)^3) \; , \tag{3.31}$$

where we already have found the the first order term, $f'(p_c) = 0$. We can therefore write

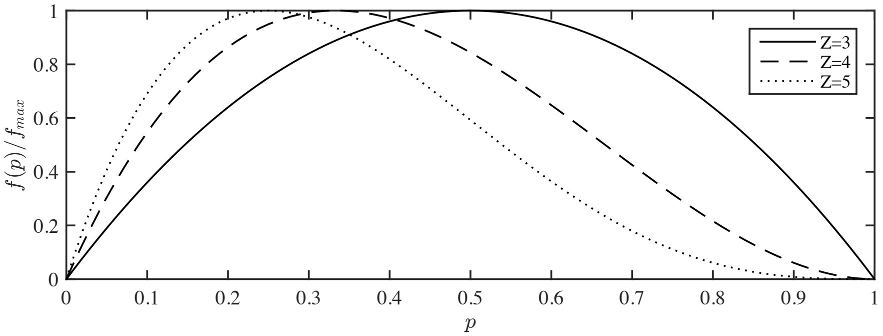

Fig. 3.4 A plot $f(p) = p(1-p)^{Z-2}$, which is a term in the cluster number density $n(s,p) = g_s[p(1-p)^{Z-2}]^s(1-p)^2$ for the Bethe lattice. We notice that $f(p)$ has a maximum at $p = p_c$, and that the second derivative, $f''(p)$, is zero in this point. A Taylor expansion of $f(p)$ around $p = p_c$ will therefore have a second order term in $(p - p_c)$ as the lowest-order term - to lowest order it is a parabola at $p = p_c$. It is this second order term which determines the exponent σ, which consequently is independent of Z.

$$f(p) \simeq f(p_c) - \frac{1}{2}f''(p_c)(p-p_c)^2 = A(1 - B(p-p_c)^2)\,. \tag{3.32}$$

The cluster number density is

$$n(s,p) = g_s[f(p)]^s(1-p)^2 = g_s e^{s\ln f(p)}(1-p)^2\,, \tag{3.33}$$

where we now insert $f(p) \simeq A(1 - B(p-p_c)^2)$ to get

$$n(s,p) \simeq g_s A^s e^{s\ln(1-B(p-p_c)^2)}(1-p)^2\,. \tag{3.34}$$

We use the first order of the Taylor expansion of $\ln(1-x) \simeq -x$, to get

$$n(s,p) \simeq g_s A^s e^{-sB(p-p_c)^2}(1-p)^2\,. \tag{3.35}$$

Consequently, for $p = p_c$ we get

$$n(s,p_c) = g_s A^s (1-p)^2\,. \tag{3.36}$$

As a result, we can rewrite the cluster density in terms of $n(s,p_c)$, giving

$$n(s,p) = n(s,p_c)e^{-sB(p-p_c)^2}\,, \tag{3.37}$$

when p is close to p_c. The exponential term we could again rewrite as

$$n(s,p) = n(s,p_c)e^{-s/s_\xi}\,, \tag{3.38}$$

where the characteristic cluster size s_ξ is

$$s_\xi = B^{-1}(p-p_c)^{-2} \; , \tag{3.39}$$

which implies that the characteristic cluster size diverges as a power-law with exponent $1/\sigma = 2$. The general scaling form for the characteristic cluster size s_ξ is

$$s_\xi \propto |p-p_c|^{-1/\sigma} \; , \tag{3.40}$$

where the exponent σ is universal, meaning that is does not depend on lattice details such a Z, as we have demonstrated here, but it does depend on lattice dimensionality. It will therefore be a different value for two-dimensional percolation.

Behavior at $p = p_c$. The next step is to address the behavior at $p = p_c$, when the characteristic cluster size is diverging.

We have already found some limits on the behavior of the cluster density $n(s,p)$, because we have found S and $P(p)$, which can be related to the cluster number density. We will use these relations two find limits on the behavior of $n(s,p_c)$.

The average cluster size at $p = p_c$ is

$$S = \frac{\Gamma}{p_c - p} \; , \tag{3.41}$$

which should diverge, that is

$$S = \sum s^2 n(s,p_c) \to \infty \; , \tag{3.42}$$

if we go the the limit of a continuous $n(s,p_c)$, the integral

$$S = \int_0^\infty s^2 n(s,p_c) ds \to \infty \; , \tag{3.43}$$

should diverge. We can therefore conclude that $n(s,p_c)$ is not an exponential, since that would lead to convergence. We can make a scaling ansatz

$$n(s,p_c) \simeq C s^{-\tau} \; , \tag{3.44}$$

for $s \gg 1$. We can include this into the restrictions that

$$\sum_s s n(s,p) = p - P \; , \tag{3.45}$$

which should converge, and

$$\sum_s s^2 n(s,p_c) \to \infty \; , \tag{3.46}$$

which should not converge. This provides a set of limits on the possible values of τ, because

$$\sum_s sn(s,p_c) \simeq \sum_s s^{1-\tau} < \infty \;\Rightarrow\; \tau - 1 > 1 \;, \tag{3.47}$$

and

$$\sum s^2 n(s,p_c) \simeq \sum_s s^{2-\tau} > \infty \;\Rightarrow\; \tau - 2 \leq 1 \;, \tag{3.48}$$

which therefore implies that

$$2 < \tau \leq 3 \;. \tag{3.49}$$

Summary of arguments. We can therefore sum up our arguments so far in the relation

$$n(s,p) = n(s,p_c)e^{-B(p-p_c)^2 s} = Cs^{-\tau}e^{-B(p-p_c)^2 s} = Cs^{-\tau}e^{-s/s_\xi} \;. \tag{3.50}$$

We will now use this expression to calculate S, for which we know the exact scaling behavior, and then again use this to find the value for τ

$$S = C\sum_s s^{2-\tau}e^{-s/s_\xi} \to C\int_1^\infty s^{2-\tau}e^{-s/s_\xi}ds \;. \tag{3.51}$$

We could now make a very rough estimate. This is useful, since it is in the spirit of this course, and it also provides the correct behavior. We could assume that

$$S = C\int_1^\infty s^{2-\tau}e^{-s/s_\xi}ds \sim C\int_1^{s_\xi} s^{2-\tau}ds \sim s_\xi^{3-\tau} \;, \tag{3.52}$$

which actually provides the correct result. We can do it slightly more elaborately:

$$S \simeq C\int_1^\infty s^{2-\tau}e^{-s/s_\xi}ds \;, \tag{3.53}$$

we change variables by introducing, $u = s/s_\xi$, which gives

$$S \simeq s_\xi^{3-\tau}\int_{1/s_\xi}^\infty u^{2-\tau}e^{-u}du \;. \tag{3.54}$$

Where the integral is now a number, since $1/s_\xi \to 0$, when $p \to p_c$. The asymptotic scaling behavior in the limit $p \to p_c$ is therefore

$$S \sim s_\xi^{3-\tau} \sim (p-p_c)^{-2(3-\tau)} \sim (p-p_c)^{-1} \;, \tag{3.55}$$

where we have used that

$$s_\xi \sim (p - p_c)^{-2} \ , \tag{3.56}$$

and that

$$S \sim (p - p_c)^{-1} \ . \tag{3.57}$$

Direct solution therefore shows that

$$\tau = \frac{5}{2} \ . \tag{3.58}$$

This relation also satisfies the exponent relations we found above, since $2 < 5/2 \leq 3$. A plot of the scaling form is shown in Fig. 3.5.

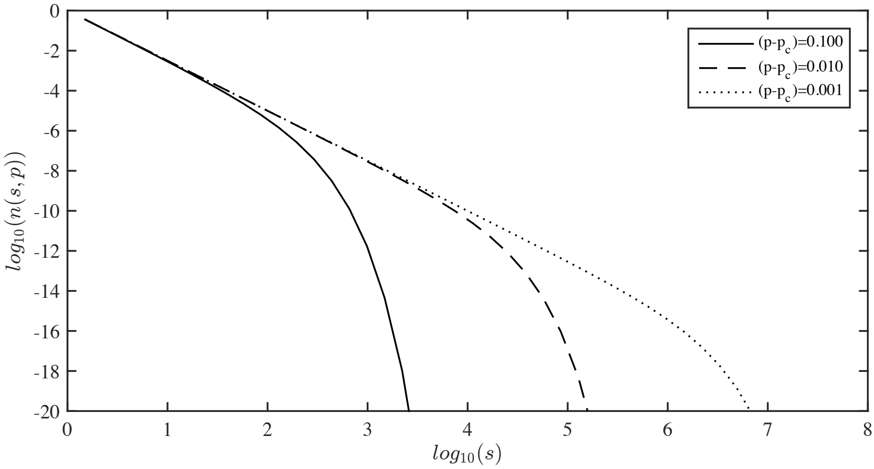

Fig. 3.5 A plot of $n(s,p) = s^{-\tau} \exp(-s(p-p_c)^2)$ as a function of s for various values of p illustrates how the characteristic cluster size s_ξ appears as a cut-off in the cluster number density that scales with $p - p_c$.

Preliminary scaling theory for cluster number density. This provides us with a preliminary scaling theory for the cluster number density. We will spend time now trying to verify this scaling relation for percolation in other dimensionalities. We have found that in the vicinity of p_c, we do not expect deviations until we reach large s, that is, before we reach a characteristic cluster size s_ξ that increases as $p \to p_c$. We therefore expect a general form of the cluster density

$$n(s,p) = n(s,p_c) F(\frac{s}{s_\xi}) \ , \tag{3.59}$$

where

$$n(s, p_c) = Cs^{-\tau} \ , \tag{3.60}$$

and

$$s_\xi = s_0 |p - p_c|^{-1/\sigma} \ . \tag{3.61}$$

In addition, we have the following scaling relations:

$$P(p) \sim (p - p_c)^\beta \ , \tag{3.62}$$

$$\xi \sim |p - p_c|^{-\nu} \ , \tag{3.63}$$

and

$$S \sim |p - p_c|^{-\gamma} \ , \tag{3.64}$$

with a possible non-trivial behavior for higher moments of the cluster density.

3.5 (Advanced) Embedding dimension

Why is it difficult to embed such a structure in a $d+1$-dimensional space? Because for a Euclidean structure of dimension d, the volume, V grows as

$$V \propto L^d \ , \tag{3.65}$$

and the surface, S, grows as

$$S \propto L^{d-1} \ , \tag{3.66}$$

where L is the linear dimension of the system. This means that

$$S \propto V^{1-\frac{1}{d}} \ . \tag{3.67}$$

However, for the Bethe lattice, the surface is proportional to the volume, $S \propto V$, which would imply that $d \to \infty$.

3.6 Exercises

Exercise 3.1: $P(p)$ for $Z = 4$

Find $P(p)$ for $Z = 4$ and determine β for this value of Z.

4 Finite-dimensional percolation

For the one-dimensional and the infinite-dimensional systems we have been able to find exact results for the percolation probability, $\Pi(p)$, for $P(p)$, the probability for a site to belong to an infinite cluster, and we have characterized the behavior using the distribution of cluster sizes, $n(s,p)$ and its cut-off, s_ξ. In both one and infinite dimensions we have been able to calculate these functions exactly. However, in two and three dimensions – which are the most relevant for our world – we are unfortunately not able to find exact solutions. We saw above that the number of configurations in a L^d system in d-dimensions increases very rapidly with L – so rapidly that a complete enumeration is impossible. But can we still use what we learned from the one and infinite-dimensional systems?

In the one-dimensional case it was simple to find $\Pi(p,L)$ because there is only one possible path from one side to another. We cannot generalize this to two dimensions, since in two-dimensions there are many paths from one side to another – and we need to include all to estimate the probability for percolation. Similarly, it was simple to find $n(s,p)$, because all clusters only have two neighboring sites – the surface is always of size 2. This is also not generalizable to higher dimensions.

In the infinite-dimensional system, we were able to find $P(p)$ because we could separate the cluster into different paths that never can intersect expect in a single point, because there are no loops in the Bethe lattice. This is not the case in two and three dimensions, where there will always be the possibility for loops. When there are loops present, we cannot use the arguments we used for the Bethe lattice, because a branch cut off at one point may be connected again further out. For the Bethe lattice, we could also estimate the multiplicity $g(s,t)$ of the clusters, the number of possible clusters of size s and surface t, since t was a function of s. In a two- or three-dimensional system this is not similarly simple, because the multiplicity $g(s,t)$ is not simple even in two dimensions, as illustrated in Fig. 4.1.

This means that the solution methods used for the one and the infinite dimensional systems cannot be extended to address two- or three-dimensional systems. However, several of the techniques and observations we have made for the one-dimensional and the Bethe lattice systems, can be used as the basis for a generalized theory that can be applied in any dimension. Here, we will therefore pursue the more general features of the percolation system, starting with the cluster number density, $n(s,p)$.

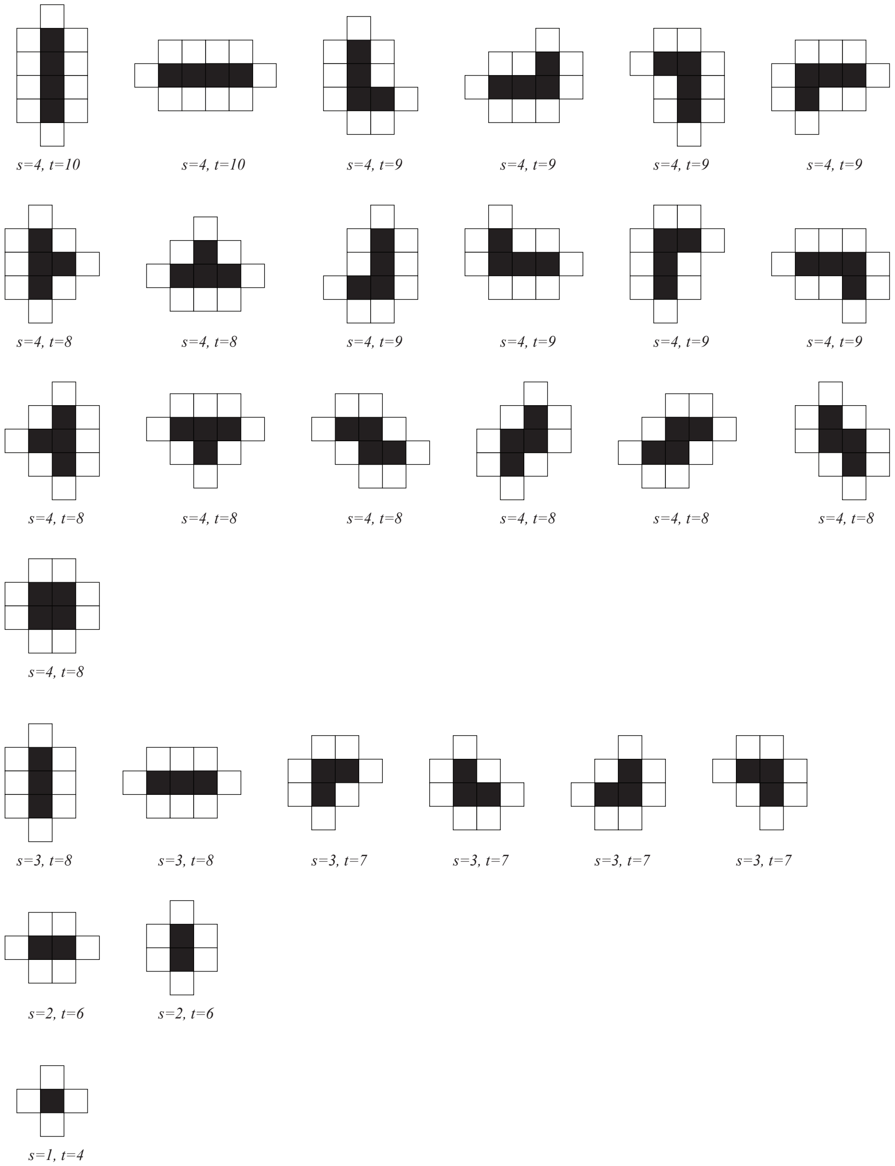

Fig. 4.1 Illustration of the possible configurations for two-dimensional clusters of size $s = 1, 2, 3, 4$.

4.1 Cluster number density

We have found that the cluster number density plays a fundamental role in our understanding of the percolation problem, and we will use it here as our basis for the scaling theory for percolation.

When we discussed the Bethe lattice, we found that we could write the cluster number density as a sum over all possible configurations of cluster size, s:

$$n(s,p) = \sum_j p^s (1-p)^{t_j} \ , \tag{4.1}$$

where j runs over all different configurations, and t_j denotes the number of neighbors for this particular configuration. We can simplify this by rewrite the sum to be over all possible number of neighbors, t, and include the degeneracy $g_{s,t}$, the number of configurations with t neighbors:

$$n(s,p) = \sum_t g_{s,t} p^s (1-p)^t \ . \tag{4.2}$$

The values of $g_{s,t}$ have been tabulated up to $s = 40$. However, while this may give us interesting information about the smaller cluster, and therefore for smaller values of p, it does not help us to develop a theory for the behavior for p close to p_c.

In order to address the cluster number density, we will need to study the characteristics of $n(s,p)$, for example by generating numerical estimates for its scaling behavior, and then propose a general scaling form which will be tested in various settings.

4.1.1 Numerical estimation of $n(s,p)$

We discussed how to measure $n(s,p)$ from a set of numerical simulations in chap. 2. We can use the same method in two and higher dimensions. We estimate $n(s,p;L)$ using

$$\overline{n(s,p;L)} = \frac{N_s}{M \cdot L^d} \ , \tag{4.3}$$

where N_s is the total number of clusters of size s measured for M simulations in a system of size L^d and for a given value of p. We perform these simulations just as we did in one dimension, using the following program:

```
from pylab import *
from scipy.ndimage import measurements
nsamp = 2000
L = 200
p = 0.58
allarea = array([])
for i in range(nsamp):
    z = rand(L)
    m = z<p
    lw, num = measurements.label(m)
    labelList = arange(lw.max() + 1)
    area = measurements.sum(m, lw, labelList)
    allarea = append(allarea,area)
n,sbins = histogram(allarea,bins=int(max(allarea)))
s = 0.5*(sbins[1:]+sbins[:-1])
nsp = n/(L*nsamp)
i = nonzero(n)
subplot(2,1,1)
plot(s[i],nsp[i],’o’)
xlabel(’$s$’)
ylabel(’$n(s,p)$’)
subplot(2,1,2)
loglog(s[i],nsp[i],’o’)
xlabel(’$s$’)
ylabel(’$n(s,p)$’)
```

The resulting plot of $\overline{n(s,p;L)}$ for $L = 200$ is shown in Fig. 4.2a,b. Unfortunately, this plot is not very useful. The problem is that there are many values of s for which we have little or no data at all! For small values of s we have many clusters for each value of s and the statistics is good. But for large values of s, such as for clusters of size $s = 10^4$ and above, we have less than one data point for each value of s. Our measured distribution $\overline{n(s,p;L)}$ is therefore a poor representation of the real $n(s,p;L)$ in this range.

4.1.2 Measuring probabilty densities of rare events

The problem with the measured results in Fig. 4.2 occur because we have chosen a very small bin size for the histogram. However, we see that for small values of s we want to have a small bin size, since the statistics here is good, but for large values of s we want to have larger bin sizes. This is often solved by using logarithmic binning: We make the bin edges a^i, where a is the basis for the bins and i is bin number. If we chose $a = 2$ as the basis for the bins, the bin edges will be $2^0, 2^1, 2^2, 2^3, \ldots$, that is $1, 2, 4, 8, \ldots$. (Maybe we should instead have called the method *exponential binning*). We then count how many events occur in each such bin. If we number the bins by i, then the edges of the bins are $s_i = a^i$, and the width of bin i is $\Delta s_i = s_{i+1} - s_i$. We then count how many events, N_i, occur in the range from s_i to $s_i + \Delta s_i$, and we use this to find the cluster number density $n(s,p;L)$. However, since we now look at ranges of s values, we need to be precise: We want to measure the probability for a cluster to belong to a specific site of a cluster in the range from s to $s + \Delta s$, that is, we want to measure $n(s,p;L)\Delta s$, which we estimate from

$$\overline{n(s_i,p;L)}\Delta s_i = \frac{N_i}{ML^d} \ , \tag{4.4}$$

and we find $n(s,p;L)$ from

$$\overline{n(s_i,p;L)} = \frac{N_i}{ML^d \Delta s_i} \ . \tag{4.5}$$

It is important to remember to divide by Δs_i when the bin sizes are not all the same! We implement this by generating an array of all the bin edges. First, we find an upper limit to the bins, that is, we find an i_m so that

$$a^{i_m} > \max(s) \ \Rightarrow \ \log_a a^{i_m} > \log_a \max(s) \ , \tag{4.6}$$

$$i_m > \log_a \max(s) \ . \tag{4.7}$$

We can for example round the right hand side up to the nearest integer

```
a = 1.2
logamax = ceil(log(max(allarea))/log(a));
```

where `allarea` corresponds to all the s-values. We can then generate an array of indices from 1 to this maximum value

```
logbins = a**arange(0,logamax)
```

And we can further generate the histogram with this set of bin edges

```
nl,nlbins = histogram(allarea,bins=logbins)
```

And we must then find the bin sizes and the bin centers

```
nl,nlbins = histogram(allarea,bins=logbins)
```

And we calculate the estimated value for $\overline{n(s,p;L)}$:

```
nsl = nl/(nsamp*L**2*ds)
```

Finally we plot the results. The complete code for this analysis is found in the following script

```
a = 1.2
```

```
logamax = ceil(log(max(s))/log(a))
logbins = a**arange(0,logamax)
nl,nlbins = histogram(allarea,bins=logbins)
ds = diff(logbins)
sl = 0.5*(logbins[1:]+logbins[:-1])
nsl = nl/(M*L**2*ds)
loglog(sl,nsl,'.b')
```

The resulting plot for $a = 1.2$ is shown in Fig. 4.2c. Notice that the resulting plot now is much easier to interpret than the linearly binned plot. (You should, however, always reflect on whether your binning method may influence the resulting plot in some way, since there may be cases where your choice of binning method may affect the results you get. Although this is not expected to play any role in your measurements in this book.) We will therefore in the following adapt logarithmic binning strategies whenever we measure a dataset which is sparse.

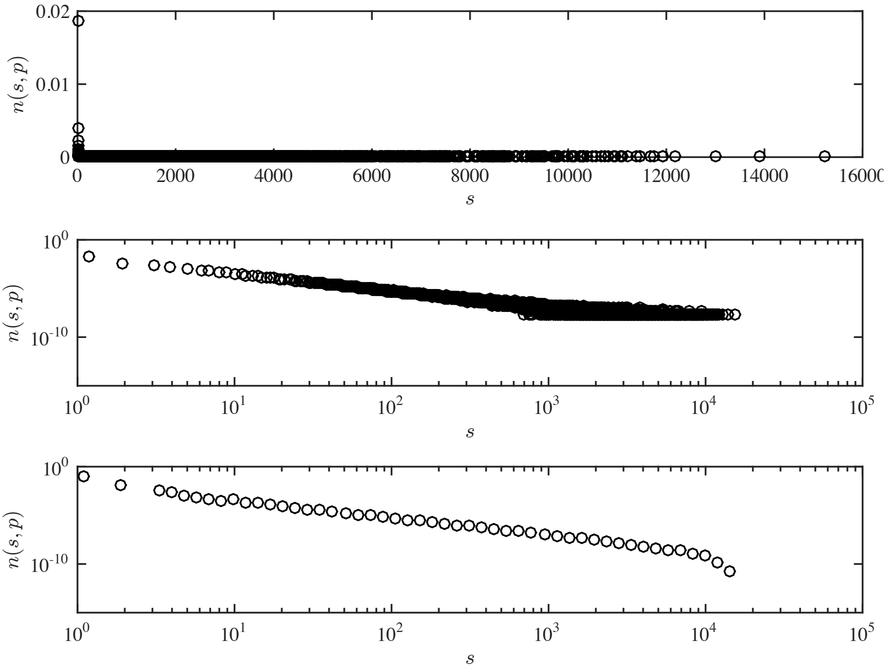

Fig. 4.2 Plot of $n(s, p; L)$ estimated from $M = 1000$ samples for $p = 0.58$ and $L = 200$. (a) Direct plot. (b) Log-log plot. (c) Plot of the logarithmically binned distribution.

4.1.3 Measurements of $n(s,p)$ when $p \to p_c$

What happens to $n(s,p:L)$ when we change p so that it approaches p_c. We perform a sequence of simulations for various values of p_c and plot the resulting values for $\overline{n(s,p;L)}$. The resulting plot is shown in Fig. 4.3.

Since the plot is double-logarithmic, a straight line corresponds to a power-law type behavior, $n(s,p) \propto s^{-\tau}$. We see that as p approaches p_c the cluster number density $n(s,p)$ more and more approaches a power-law behavior. For a value of p which is away from p_c, the $n(s,p)$ curve follows the power-law behavior for some time, but then deviates by dropping rapidly. This is an effect of the characteristic cluster size, which also can be visually observed in Fig. 1.4 and Fig. 1.5, where we see that the characteristic cluster size increases as p approaches p_c. How can we characterize the characteristic cluster size based on this measurement of $n(s,p)$? When s reaches s_ξ, it falls off from the power-law type behavior observed as $p \to p_c$. So, we could measure s_ξ directly from the lot, by drawing a straight line parallel to the behavior of $n(s,p_c)$, but below the $n(s,p_c)$ line, as illustrated in Fig. 4.3. When the measured, $\overline{n(s,p)}$ intersects this drawn line, $n(s,p)$ has fallen by a constant factor below $n(s,p_c)$ and we *define* this as s_ξ, and we measure it by reading the values from the s-axis. The resulting set of s_ξ values are plotted as a function of p in Fig. 4.3. We see that s_ξ increases and possibly diverges as p approaches p_c. This is an effect we also found in the one-dimensional and the infinite-dimensional case, where we found that

$$s_\xi \propto |p-p_c|^{-1/\sigma} \tag{4.8}$$

where σ was 1 is one dimension. We will now use this to develop a theory for both $n(s,p;L)$ and s_ξ based on our experience from one and infinite dimensional percolation.

4.1.4 Scaling theory for $n(s,p)$

When we develop a theory, we realize that we are only interested in the limit $p \to p_c$, that is $|p-p_c| \ll 1$, and $s \gg 1$. In this limit, we expect that s_ξ marks the cross-over between two different behaviors. There is a common behavior for small s, up to a cut-off, s_ξ, as we also observe in Fig. 4.3: The curves for all p are approximately equal for small s.

Based on what we observed in one-dimension and infinite-dimensions, we expect and propose the following form for $n(s,p)$:

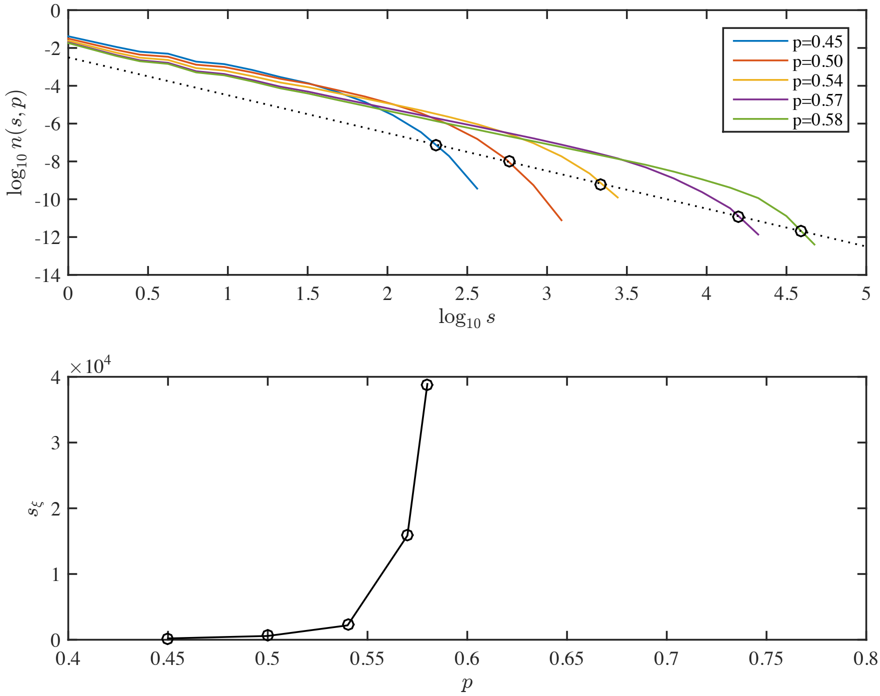

Fig. 4.3 (a) Plot of $n(s, p; L)$ as a function of s for various values of p for a 512 × 512 lattice. (b) Plot of $s_\xi(p)$ measured from the plot of $n(s, p)$ corresponding to the points shown in circles in (a).

$$n(s,p) = n(s,p_c)F(\frac{s}{s_\xi}) \ , \tag{4.9}$$

$$n(s,p_c) = Cs^{-\tau} \ , \tag{4.10}$$

$$s_\xi = s_0|p-p_c|^{-1/\sigma} \ . \tag{4.11}$$

The best estimates for the exponents for various systems are listed in the following table [37, 7] .

d	β	τ	σ	γ	ν	D	μ	D_{min}	D_{max}	D_B
1		2	1	1	1					
2	5/36	187/91	36/91	43/18	4/3	91/48	1.30	1.13	1.4	1.6
3	0.41	2.18	0.45	1.80	0.88	2.53	2.0	1.34	1.6	1.7
4	0.64	2.31	0.48	1.44	0.68	3.06	2.4	1.5	1.7	1.9
Bethe	1	5/2	1/2	1	1/2	4	3	2	2	2

We will often simplify the scaling form by writing it on the form:

$$n(s,p) = s^{-\tau}F(s/s_\xi) = s^{-\tau}F((p-p_c)^{1/\sigma}s) \ . \tag{4.12}$$

What can we expect from the scaling function $F(x)$?

This is essentially the prediction of a data-collapse. If we plot $s^{\tau}n(s,p)$ as a function of $s|p-p_c|^{1/\sigma}$ we would expect to get the scaling function $F(x)$, which should be a universal curve, as illustrated in Fig. 4.4.

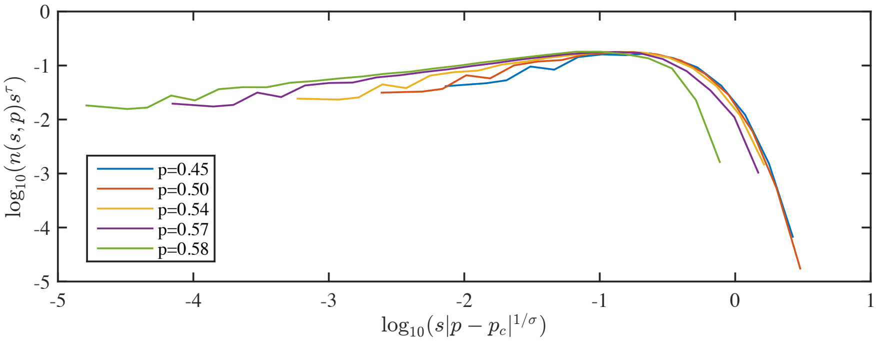

Fig. 4.4 A plot of $n(s,p)s^{\tau}$ as a function of $|p-p_c|^{1/\sigma}s$ shows that the cluster number density satisfies the scaling ansatz of (4.12).

An alternative scaling form is

$$n(s,p) = s^{-\tau}\hat{F}((p-p_c)s^{\sigma}) \ , \tag{4.13}$$

where we have introduced the function $\hat{F}(u) = F(u^{\sigma})$. These forms are equivalent, but in some cases this form produces simpler calculations.

This scaling form should in particular be valid for both the 1d and the Bethe lattice cases - let us check this in detail.

4.1.5 Scaling ansatz for 1d percolation

In the case of one-dimensional percolation, we know that we can write the cluster density exactly as

$$n(s,p) = (1-p)^2 e^{-s/s_{\xi}} \ . \tag{4.14}$$

We showed that we could rewrite this as

$$n(s,p) = s^{-2}F(\frac{s}{s_{\xi}}) \ , \tag{4.15}$$

where $F(u) = u^2e^{-u}$. This is indeed in the general scaling form with $\tau = 2$.

4.1.6 Scaling ansatz for Bethe lattice

For the Bethe lattice we found that the cluster density was approximately on the form

$$n(s,p) \propto s^{-\tau} e^{-s/s_\xi} \ , \tag{4.16}$$

which is already on the wanted form, so that

$$n(s,p) = s^{-\tau} F(s/s_\xi) \ . \tag{4.17}$$

4.2 Consequences of the scaling ansatz

The scaling ansatz is simple, but it has powerful consequences. Here, we address the theoretical consequences of the scaling ansatz, and demonstrate how we can use the scaling ansatz in theoretical arguments. The methods we introduce here are important methods in scaling theories, and we will use them in theoretical arguments throughout this text.

4.2.1 Average cluster size

Let us demonstrate how we can use the scaling ansatz to calculate the scaling of the average cluster size, and how this can be used to provide limits for the exponent τ.

Definition of average cluster size S. The average cluster size is defined as follows: We point to a random point in the percolation system. What is the average size of the cluster connected to that point? The probability that a random point is part of the cluster of size s is $sn(s,p)$ and the size of that cluster is s. We find the average cluster by summing over all (finite) clusters, that is from $s = 1$ to infinity:

$$S(p) = \sum_{s=1}^{\infty} s s n(s,p) = \sum_{s=1}^{infty} s^2 n(s,p) \ . \tag{4.18}$$

We assume that we are study systems where p is close to p_c so that the cluster number density $n(s,p)$ is wide and that its drop-off (crossover) s_ξ is large. The sum over s will then be a sum with many non-negligible terms and we can approximate this sum by an integral over s instead:

$$S(p) = \sum_{s=1}^{infty} s^2 n(s,p) \simeq \int_1^{\infty} s^2 n(s,p)\, ds \ . \tag{4.19}$$

We can now insert the scaling ansatz $n(s,p) = s^{-\tau}F(s/s_\xi)$, getting:

$$S(p) = \int_1^\infty s^{2-\tau}F(s/s_\xi)ds \ , \tag{4.20}$$

We know that the function $F(s/s_\xi)$ goes very rapidly to zero when s is larger than s_ξ, and that it is approximately a constant when s is smaller than s_ξ. We will therefore approximately $F(u)$ by a step function which is constant up to 1 and then 0 afterwards. We therefore only integrate up to s_ξ, where $F(s/s_\xi)$ is constant:

$$S(p) = \int_1^\infty s^{2-\tau}F(s/s_\xi)ds \simeq \int_1^{s_\xi} Cs^{2-\tau}ds \tag{4.21}$$

We solve this integral, finding that

$$S(p) = C' s_\xi^{3-\tau} \ . \tag{4.22}$$

We can now insert the behavior of s_ξ, $s_\xi = |p-p_c|^{-1/\sigma}$, giving:

$$S(p) \propto \left(|p-p_c|^{-1/\sigma}\right)^{3-\tau} \propto |p-p_c|^{\frac{3-\tau}{\sigma}} \ . \tag{4.23}$$

We recall that we called the scaling exponent of $S(p)$ γ: $S(p) \propto |p - p_c|^{-\gamma}$. We have therefore found what we call a relation between scaling exponents:

$$\gamma = \frac{3-\tau}{\sigma} \ . \tag{4.24}$$

Consequences for τ. We know that the average cluster size diverges as $p \to p_c$. This implies that the exponent γ must be positive, which again implies that

$$\gamma > 0 \ \Rightarrow \ \frac{3-\tau}{\sigma} > 0 \ \Rightarrow \ 3 > \tau \ . \tag{4.25}$$

We have therefore found a first bound for τ: $\tau < 3$. As an exercise, you can check that this relation holds for the one-dimensional system and the Bethe lattice.

4.2.2 Density of spanning cluster

We can use a similar argument to find the behavior of $P(p)$ from the cluster number density, which will give us further scaling relations —

relations between scaling exponent — and another bound on the exponent τ.

Relation between $P(p)$ and $n(s,p)$. We recall the general relation

$$\sum_s sn(s,p) + P(p) = p \; . \tag{4.26}$$

We interpret this equation as a way of formulating that a site picked at random is occupied with probability p (right hand side), and this site must either be in a finite cluster, with a probability corresponding to the sum $\sum_s sn(s,p)$, or in the infinite cluster with probability $P(p)$.

We can therefore find $P(p)$ from

$$P(p) = p - \sum_s sn(s,p) \; . \tag{4.27}$$

We can therefore find $P(p)$ by calculating the sum.

Finding $\sum_s sn(s,p)$. We can find the sum over $sn(s,p)$ when p is close to p_c in the same way as we did above. We realize that we can replace $n(s,p)$ with its scaling form: $n(s,p) = s^{-\tau}F(s/s_\xi)$:

$$\sum_{s=1}^{\infty} sn(s,p) = \sum_{s=1}^{\infty} ss^{-\tau}F(s/s_\xi) \; . \tag{4.28}$$

And we realize that the sum can be approximated by an integral over s since there is a wide range of s-values when p is close to p_c:

$$\sum_{s=1}^{\infty} s^{1-\tau}F(s/s_\xi) \simeq \int_1^{\infty} s^{1-\tau}F(s/s_\xi)ds \; . \tag{4.29}$$

And we recall that $F(s/s_\xi)$ is approximately a constant when $s < s_\xi$ and goes very rapidly to zero when $s > s_\xi$, so we integrate up to s_ξ assuming that $F(s/s_\xi)$ is a constant C up to s_ξ, giving

$$\int_1^{\infty} s^{1-\tau}F(s/s_\xi)ds \simeq \int_1^{s_\xi} s^{1-\tau}ds = c_1 + c_2 s_\xi^{2-\tau} \; . \tag{4.30}$$

We insert this back into the expression for $P(p)$, getting:

$$P(p) = p - \sum_s sn(s,p) \simeq p - c_1 - c_2 s_\xi^{2-\tau} \; . \tag{4.31}$$

Consequences for τ. First, we realize that $P(p)$ cannot diverge when $p \to p_c$. Since s_ξ diverges, this means that the exponent $2 - \tau$ must be smaller than or equal to zero, otherwise $P(p)$ will diverge. This gives us a new boundary for τ:

$$2-\tau \leq 0 \;\Rightarrow\; 2 \leq \tau \,. \tag{4.32}$$

The two boundaries we have for τ are then $2 \leq \tau < 3$. We have therefore bounded τ between 2 and 3! This is a nice result from the scaling ansatz.

Relating β and τ. We can rewrite the expression in (4.31) for $P(p)$ and insert $s_\xi = s_0|p-p_c|^{-1/\sigma}$, getting:

$$P(p) \simeq p - c_1 - c_2 s_\xi^{2-\tau} \simeq (p-p_c) + c_2\left(|p-p_c|^{-1/\sigma}\right)^{2-\tau} \tag{4.33}$$

We realize that when $p \to p_c$ the linear term $(p-p_c)$ will be smaller than the term $|p-p_c|^{(\tau-2)/\sigma}$. And we remember that $P(p) \propto (p-p_c)^\beta$. This gives us a new scaling relation for β:

$$\beta = \frac{\tau-2}{\sigma} \,. \tag{4.34}$$

We have therefore again demonstrated the power of the scaling ansatz by both calculating bounds for τ and finding relations between the scaling exponents.

4.3 Percolation thresholds

While the exponents are universal — independent of the details of the lattice but dependent on the dimensionality — the percolation threshold, p_c, depends on all the details of the system. The percolation threshold depends on the lattice type and the type of percolation. We typically discern between site percolation, where percolation is on the sites of a lattice, and bond percolation, where the bonds between the sites determines the connectivity. The following table provides established values for the percolation thresholds for various dimensions and lattice types [37, 7]. (For $d = 1$, the percolation threshold is $p_c = 1$ for all lattice types.)

Lattice type	Site	Bond
$d = 2$		
Square	0.592746	0.50000
Triangular	0.500000	0.34729
$d = 3$		
Cubic	0.3116	0.2488
FCC	0.198	0.119
BCC	0.246	0.1803
$d = 4$		
Cubic	0.197	0.1601
$d = 5$		
Cubic	0.141	0.1182
$d = 6$		
Cubic	0.107	0.0942
$d = 7$		
Cubic	0.089	0.0787

4.4 Exercises

Exercise 4.1: Alternative way to analyze percolation clusters

In this exercise we will use python to generate and visualize percolation clusters. We generate a $L \times L$ matrix of random numbers, and will examine clusters for a occupation probability p.

We generate the percolation matrix consisting of occupied (1) and unoccupied (0) sites, using

```
from pylab import *
from scipy.ndimage import measurements
L = 100
r = rand(L,L)
p = 0.6
z = r<p # This generates the binary array
lw, num = measurements.label(m)
```

We have then produced the array `lw` that contains labels for each of the connected clusters.

a) Familiarize yourself with labeling by looking at `lw`, and by studying the second example in the python help system on the image analysis toolbox.

We can examine the array directly by mapping the labels onto a color-map, using `imshow`.

```
imshow(lw)
```

We can extract information about the labeled image using `measurements`, for example, we can extract an array of the areas of the clusters using

```
labelList = arange(lw.max() + 1)
area = measurements.sum(m, lw, labelList)
```

You can also extract information about the clusters using the `skimage.measure` module. This provides a powerful set of tools that can be used to characterize the clusters in the system. For example, you can determine if a system is percolating by looking at the extent of a cluster. If the extent in any direction is equal to L, then the cluster is spanning the system. We can use this to find the area of the spanning cluster or to mark if there is a spanning cluster:

```
import skimage
props = skimage.measure.regionprops(lw)
spanning = False
for prop in props:
    if (prop.bbox[2]-prop.bbox[0]==L or prop.bbox[3]-prop.bbox[1]==L):
        # This cluster is percolating
    area = prop.area
    spanning = True
        break
```

b) Using these features, write a program to calculate $P(p, L)$ for various p for the two-dimensional system.

c) How robust is your algorithm to changes in boundary conditions? Could you do a rectangular grid where $L_x \gg L_y$? Could you do a more complicated set of boundaries? Can you think of a simple method to ensure that you can calculate P for any boundary geometry?

Exercise 4.2: Finding $\Pi(p, L)$ and $P(p, L)$

a) Write a program to find $P(p, L)$ and $\Pi(p, L)$ for $L = 2, 4, 8, 16, 32, 64, 128$. Comment on the number of samples you need to make to det a good estimate for P and Π.

b) Test the program for small L by comparing with the exact results from above. Comment on the results?

Exercise 4.3: Determining β

We know that when $p > p_c$, the probability $P(p, L)$ for a given site to belong to the percolation cluster, has the form

$$P(p, L) \sim (p - p_c)^{\beta} \ . \tag{4.35}$$

Use the data from above to find an expression for β. For this you may need that $p_c = 0.59275$.

Exercise 4.4: Determining the exponent of power-law distributions

In this exercise you will build tools to analyse power-law type probability densities.

Generate the following set of data-points in python:

```
from pylab import *
z = rand(1e6)**(-3+1)
```

Your task is to determine the distribution function $f_Z(z)$ for this distribution. Hint: the distribution is on the form $f(u) \propto u^{\alpha}$.

a) Find the cumulative distribution, that is, $P(Z > z)$. You can then find the actual distribution from

$$f_Z(z) = \frac{dP(Z > z)}{dz} \ . \tag{4.36}$$

b) Generate a method to do logarithmic binning in python. That is, you estimate the density by doing a histogram with bin-sizes that increase exponentially in size.

Hint. Remember to divide by the correct bin-size.

Exercise 4.5: Cluster number density $n(s, p)$

We will generate the cluster number density $n(s, p)$ from the two-dimensional data-set.

Hint 1. The cluster sizes are extracted using `area = measurements.sum(m, lw, labelList)` as described in a previous exercise.

Hint 2. Remember to remove the percolating cluster.

Hint 3. Use logarithmic binning.

a) Estimate $n(s, p)$ for a sequence of p values approaching $p_c = 0.59275$ from above and below.

b) Estimate $n(s, p_c; L)$ for $L = 2^k$ for $k = 4, \dots, 9$. Use this plot to estimate τ.

c) Can you estimate the scaling of $s_\xi \sim |p - p_c|^{-1/\sigma}$ using this data-set?
Hint 1: Use $n(s, p)/n(s, p_c) = F(s/s_\xi) = 0.5$ as the definition of s_ξ.

Exercise 4.6: Average cluster size

a) Find the average (finite) cluster size $S(p)$ for p close to p_c, for p above and below p_c.

b) Determine the scaling exponent $S(p) \sim |p - p_c|^{-\gamma}$.

c) In what ways can you generate $S^{(k)}(p)$? What do you think is the best way?

5 Geometry of clusters

We have seen how we can characterize clusters by their mass, s.

As p approaches p_c, the typical cluster size s increases. From this figure we also see that the characteristic diameter of the clusters increases. In this chapter we will discuss the geometry of clusters, and by geometry we will mean how the number of sites in a cluster is related to the linear size of the cluster. We will introduce a measure to characterize the spatial extent, the characteristic diameter, of clusters; how the characteristic length behaves as p approaches p_c; and how the characteristic length is related to the characteristic mass, s, of a cluster.

5.1 Characteristic cluster size

We have so far studied the clusters in our model porous material, the percolation system, through the distribution of cluster sizes, $n(s,p)$, and derivatives of this, such as the average cluster size, S and the characteristic cluster size, s_ξ. However, clusters with the same mass, s, can have very different shapes. Fig. 5.1 illustrates three clusters all with $s = 20$ sites. (The linear and the compact clusters are unlikely, but possible realizations). How can we characterize the diameter or radius of these clusters?

There are many ways to define the extent of a cluster. We could, for example, define the maximum distance between any two points in the cluster ($R_{\max}$) to be the extent of the cluster, or we could use the average

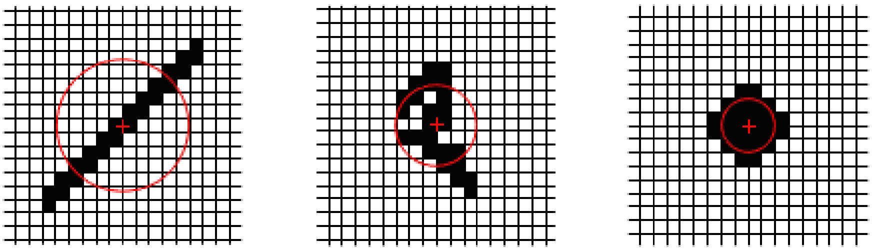

Fig. 5.1 Illustrations of three clusters all with $s = 24$.

distance between two points in the cluster. However, we usually introduce a measure which is similar to the standard deviation used to characterize the spread in a random variable: We use the standard deviation in the position, which is also known as the radius of gyration of a cluster:

The radius of gyration, R_i for a particular cluster i of size s_i, with sites $\mathbf{r}_j$ for $j = 1, \ldots, s_i$, is defined as

$$R_i^2 = \frac{1}{s_i} \sum_{j=1}^{s_i} \left(\mathbf{r}_j - \mathbf{r}_{cm,i}\right)^2 \ , \tag{5.1}$$

where $\mathbf{r}_{cm,j}$ is the center of mass of cluster i. An equivalent definition is

$$R_i^2 = \frac{1}{2 s_i^2} \sum_{n,m} (\mathbf{r}_n - \mathbf{r}_m)^2 \ , \tag{5.2}$$

where the sum is over all sites n and m in cluster i, and we have divided by $2s_i^2$ because each site is counted twice and the number of components in the sum is s_i^2. The radius of gyration of the clusters in Fig. 5.1 is illustrated by the circles in the figures[1].

This provides a measure of the radius of a cluster i. As we see from Fig. 5.1, clusters of the same size s can have different radii. How can we then find a characteristic size for a given cluster size s? We find that by averaging over all clusters of the same size s.

$$R_s^2 = \langle R_i^2 \rangle_i \ . \tag{5.3}$$

where the average is over all clusters of the same size.

[1] Notice that we could have used another moment q to define the radius. Higher moments will put more emphasis on the sites that are far from the center of mass. As the order q approaches infinity, the radius will approach the maximum size of the cluster, $R_{\max}$.

5.1.1 Analytical results in one dimension

We can use the one-dimensional percolation system to gain insight into how we expect R_s to depend on s. For the one-dimensional system, there is just one cluster for a given size s corresponding to a line of length s. If the cluster runs from 1 to s, the center of mass is at $s/2$, and the sum over all sites runs from 1 to s:

$$R_s^2 = \frac{1}{s}\sum_{i=1}^{s}(i - s/2)^2 \ , \tag{5.4}$$

where we assume that s is so large that we only need to address the leading term in s, and we do not have to treat even and odd s separately. This can be expanded to

$$\begin{aligned} R_s^2 &= \frac{1}{s}[\sum_{i=1}^{s} i^2 - is + \frac{s^2}{4}] \qquad &(5.5)\\ &= \frac{1}{s}[\frac{s^3}{3} - s\frac{s(s+1)}{2} + s\frac{s^2}{4} \qquad &(5.6)\\ &\propto \qquad s^2 \qquad &(5.7) \end{aligned}$$

We have therefore found the result that $s \propto R_s$ in one dimension — which is what we expected.

5.1.2 Numerical results in two dimensions

For the one-dimensional system we found that $s \propto R_s$. How does this generalize to higher dimensions? We start by measuring the behavior for a finite system of size L and with a percolation threshold p. Our strategy is to generate clusters on a $L \times L$ lattice, analyze the clusters, for each cluster, i, of size s_i we will find the center of mass and the radius of gyration, R_i^2. For each value of s we will find the average radius, R_i^2, by a linear average. However, for larger values of s we will collect the data in bins, following the same approach we used to determine $n(s,p)$ — using logarithmic binning.

First, we introduce a function to calculate the radius of gyration of all the clusters in a lattice. This is done in two steps, first we find the center of mass of all clusters, and then we find the radius of gyration. The center of mass for a cluster i with positions $\mathbf{r}_{i,j}$ for $j = 1, \dots, s_i$, is

$$\mathbf{r}_{cm,i} = \frac{1}{s_i}\sum_{j=1}^{s_i} \mathbf{r}_{i,j} \ , \tag{5.8}$$

We assume that the clusters are numbered and marked in the lattice with their index, as done by the `lw, num = measurements.label(m)` command. We can find the center of mass by a built-in function, such as `cm = measurements.center_of_mass(m, lw, labelList)` or we can calculate the center-of-mass explicitly. This is done by running through all the sites `ix,iy`, in the lattice. For each site, we find what cluster i the site belongs to: `i = lw[ix,iy]`. If the site belongs to a cluster, that is if `i>0`, we add the coordinates for this part of the cluster to the sum for the center of mass of the cluster

```
rcm[ilw] = rcm[ilw] + array([ix,iy])
```

Finally, we find the center of mass for each of cluster by dividing `rcm` by the corresponding area for each of the clusters:

```
rcm[:,0] = rcm[:,0]/area
rcm[:,1] = rcm[:,1]/area
```

Second, we follow a similar approach to find the radius of gyration. We run through all the sites in the cluster, and for each site, we find the cluster number i it belongs to, and add the sum of the square of the distance from the site to the center of mass:

```
dr = array([ix,iy])-cm[ilw]
rad2[ilw] = rad2[ilw] + dot(dr,dr)
```

After running through all the sites, we divide by the area, s_i, to find the radius of gyration according to the formula

$$R_i^2 = \frac{1}{s_i}\sum_{j=1}^{s_i} \left(\mathbf{r}_{i,j} - \mathbf{r}_{cm,i}\right)^2 \ , \tag{5.9}$$

This is implemented in the following function:

```
from pylab import *
from scipy.ndimage import measurements

import numba

@numba.njit(cache=True)
def radiusofgyration(m,lw):
    labelList = arange(lw.max() + 1)
    area = measurements.sum(m, lw, labelList)
    cm = measurements.center_of_mass(m, lw, labelList)
    nx = shape(lw)[0]
    ny = shape(lw)[1]
    rad2 = zeros(int(lw.max()+1))
    for ix in range(nx):
        for iy in range(ny):
            ilw = lw[ix,iy];
            if (ilw>0):
                dr = array([ix,iy])-cm[ilw]
                dr2 = dot(dr,dr)
                rad2[ilw] = rad2[ilw] + dr2
    rad = sqrt(rad2/area)
```

We use this function to calculate the average radius of gyration for each cluster size s and plot the results using the following script:

```
M = 20   # Nr of samples
L = 400  # System size
p = 0.58 # p-value
allr2 = array([])
allarea = array([])
for i in range(M):
    z = rand(L,L)
    m = z<p
    lw, num = measurements.label(m)
    area,rcm,rad2 = radiusofgyration(m,lw)
    allr2 = append(allr2,rad2)
    allarea = append(allarea,area)
```

The resulting plots for several different values of p are shown in Fig. 5.2. We see that that there is an approximately linear relation between R_s^2 and s in this double-logarithmic plot, which indicates that there is a power-law relationship between the two:

$$R_s^2 \propto s^x \ . \tag{5.10}$$

How can we interpret this relation? Equation (5.10) relates the radius R_s and the area (or mass) of the cluster. We are more used to the inverse relation:

$$s \propto R_s^D \ , \tag{5.11}$$

where $D = 2/x$ is the exponent relating the radius to the mass of a cluster. This corresponds to our intuition from geometry. We know that for a cube of size L, the mass (or volume) of the cube is $M = L^3$. For a square of length L, the mass (or area) is $M = L^2$, and similarly for a circle $M = \pi R^2$, where R is the radius of the circle. For a line of length L, the mass is $M = L^1$. We see a general trend, $M \propto R^d$, where R is a characteristic length for the object, and d describes the dimensionality of the object. If we extend this intuition to the relation in (5.11), which is an observation based on Fig. 5.2, we see that we may interpret D as the dimension of the cluster. However, the value of D is not an integer. We have indicated the value of $D = 1.89$ with a dotted line in Fig. 5.2. (The value of D is well know for the two-dimensional percolation problem). This non-integer value of D may seem strange, but it is fully possible, mathematically, to have non-integer dimensions. This is a feature frequently found in fractal structures, and the percolation clusters as p approaches p_c is indeed a good example of a self-similar fractal. We will return to this aspect of the geometry of the percolation system in Sect. 5.5.

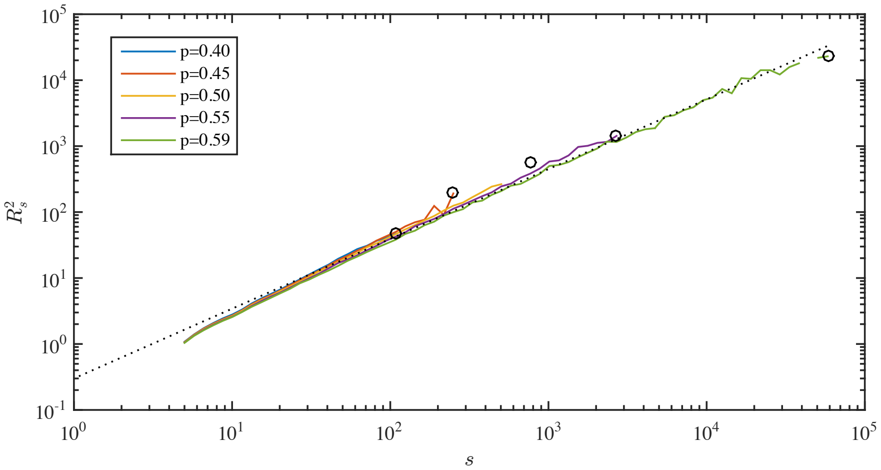

Fig. 5.2 Plot of R_s^2 as function of s for simulations on two-dimensional percolation system with $L = 400$. The largest cluster for each value of p is illustrated by a circle. The dotted line shows the curve $R_s^2 \propto s^{2/D}$ for $D = 1.89$.

The largest cluster and its corresponding radius of gyration is indicated by a circle for each p value in Fig. 5.2. We see that as p approaches p_c, both the area and the radius of the largest cluster increases. Indeed, this corresponds to the observation we have previously made for the characteristic cluster size, s_ξ. We may define a corresponding characteristic cluster radius, R_{s_ξ}. This gives:

$$s_\xi \propto R_{s_\xi}^D \ . \tag{5.12}$$

This length is a characteristic length for the system at a given value of p, corresponding to the largest cluster size or the typical cluster size in the system. In Sect. 5.2 we see how we can relate this length directly to the cluster size distribution.

5.1.3 Scaling behavior in two dimensions

We have already found that the characteristic cluster size s_ξ diverges as a power law as p approaches p_c:

$$s_\xi \simeq s_0 \left(p - p_c\right)^{-1/\sigma} \ , \tag{5.13}$$

when $p < p_c$. The behavior is similar when $p > p_c$, but the prefactor s_0 may have a different value. How does R_{s_ξ} behave when p approaches p_c? We can find this by combining the scaling relations for s_ξ and R_{s_ξ}. We remember that $R_{s_\xi} \propto s_\xi^{1/D}$. Therefore

$$R_{s_\xi} \propto s_\xi^{1/D} \propto \left(\left(p - p_c\right)^{-1/\sigma}\right)^{1/D} \propto \left(p - p_c\right)^{-1/\sigma D} \ , \tag{5.14}$$

where we introduce the symbol $\nu = 1/(\sigma D)$. For two-dimensional percolation the exponent ν is a universal number, just like σ and D. This means that it does not depend on details such as the lattice type or the connectivity of the lattice, although it does depend on the dimensionality of the system. We know the value of ν reasonably well in two dimensions, $\nu = 4/3$.

The arguments we have provided here is again an example of scaling argument. In these arguments we are only interested in the exponent in the scaling relation, the functional form, and not in the values of the constant prefactors.

5.2 Geometry of finite clusters

We have defined the characteristic length R_{s_ξ} through the definition of the characteristic cluster size, s_ξ, and the scaling relation $s \propto R_s^D$. However, it may be more natural to define the characteristic length of the system as the *average* radius and not the *cut-off* radius. We have introduced several averages for the radius of gyration. For each cluster i we can calculate the radius of gyration, R_i. We can then find the average radius of gyration for a cluster of size s by averaging over all clusters i of size s:

$$R_s^2 = \langle R_i^2 \rangle_i \ , \tag{5.15}$$

where the average is over all clusters i of the same size s. This gives us the radius of curvature R_s which we found to scale with cluster mass s as $s \propto R_s^D$.

For the cluster sizes, we introduced an average cluster size S, which is

$$S = \frac{1}{Z_S} \sum_s s \, sn(s,p) \; , \; Z_S = \sum_s sn(s,p) \; . \tag{5.16}$$

We can also similarly introduce an average radius of gyration, R, by averaging R_s over all cluster sizes:

$$R = \frac{1}{Z_R} \sum_s R_s^2 s^k sn(s,p) \; , \; Z_R = \sum_s s^k sn(s,p) \; . \tag{5.17}$$

Here, we have purposely introduced an unknown exponent k. We are to some extent free to choose this exponent, although the average needs to be finite, and the exponent will determine how we small and large clusters are weighed in the sum. A natural choise may be to choose $k = 1$ so that we get terms $R_s^2 s^2 n(s,p)$ in the sum. However, the results we present here will not change in any significant way, expect for different prefactors to the scaling relations, if you choose a larger value of k. Our definition of the average radius of gyration is therefore:

$$R = \frac{1}{Z_R} \sum_s R_s^2 s^2 n(s,p) \; , \; Z_R = \sum_s s^2 n(s,p) \; , \tag{5.18}$$

where we notice that the normalization sum $Z_R = S$ is the average cluster size.

Fig. 5.3 shows a plot of the average R as a function of p for various systems sizes L. We see that R diverges as p approaches p_c. How can we develop a theory for this behavior?

We know that the cluster number density $n(s,p)$ has the approximate scaling form

$$n(s,p) = s^{-\tau} F\left(s/s_\xi\right) \; , \; s_\xi \propto |p - p_c|^{-1/\sigma} \; . \tag{5.19}$$

We can use this to calculate the average radius of gyration, R, when p is close to p_c.

The average radius of gyration is

$$R^2 = \frac{\sum_s R_s^2 s^2 n(s,p)}{\sum_s s^2 n(s,p)} = \frac{\int_1^\infty R_s^2 s^{2-\tau} F(s/s_\xi) ds}{\int_1^\infty s^{2-\tau} F(s/s_\xi) ds} \tag{5.20}$$

$$\propto \frac{\int_1^\infty s^{2/D} s^{2-\tau} F(s/s_\xi) ds}{\int_1^\infty s^{2-\tau} F(s/s_\xi) ds} \; , \tag{5.21}$$

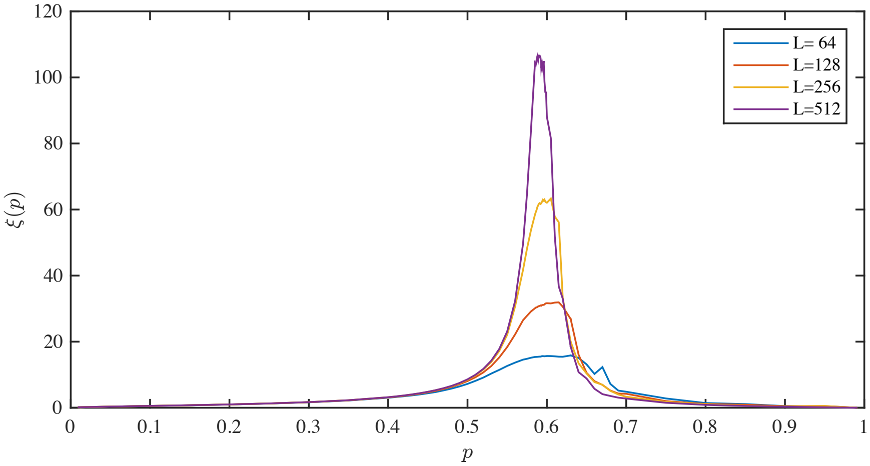

Fig. 5.3 A plot of ξ as a function of p for a $L = 64$, 128, 256 and 512 system as a function of p. We observe that ξ diverges when $p \to p_c$. We notice that the correlation length does not diverge, but crosses over as a result of the finite system size.

where we have inserted $R_s^2 \propto s^{2/D}$. This expression is valid when $s < s_\xi$. We insert it here since $F(s/s_\xi)$ goes rapidly to zero when $s > s_\xi$, and therefore only the $s < s_\xi$ values will contribute significantly to the integral. We change variables to $u = s/s_\xi$, getting:

$$R^2 \propto \frac{s_\xi^{2/D+3-\tau} \int_{1/s_\xi}^{\infty} u^{2/D+2-\tau} F(u) du}{s_\xi^{3-\tau} \int_{1/s_\xi}^{\infty} u^{2-\tau} F(u) du} \tag{5.22}$$

$$\propto s_\xi^{2/D} \frac{\int_0^\infty u^{2/D+2-\tau} F(u) du}{\int_0^\infty u^{2-\tau} F(u) du} \propto s_\xi^{2/D} \ , \tag{5.23}$$

where the two integrals over $F(u)$ simply are numbers, and therefore have been included in the constant of proportionality.

This shows that $R^2 \propto s_\xi^{2/D}$. We found above that $R_{s_\xi} \propto s_\xi^{2/D}$. Therefore, $R \propto R_{s_\xi}$! These two characteristic lengths therefore have the same behavior. They are only different by a constant of proportionality, $R = c\,R_{s_\xi}$. We can therefore use either length to characterize the system — they are effectively the same.

Fig. 5.4 illustrates the radius of gyration of the largest cluster with a circle and the average radius of gyration, R, indicated by the length of the side of the square. As p increases, both the maximum cluster size and the average cluster size increases — according to the theory they are indeed proportional to each other and therefore increase in concert.

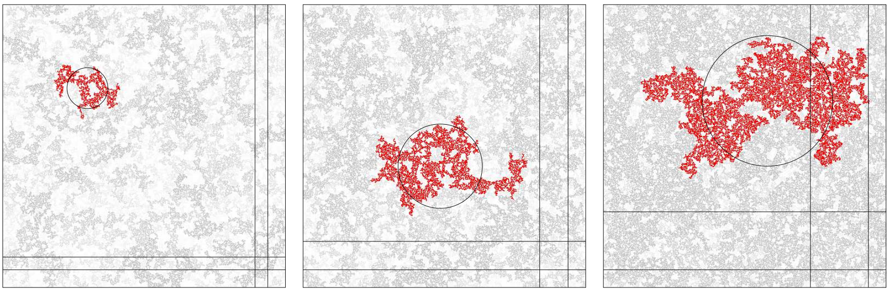

Fig. 5.4 Illustration of the largest cluster in 512×512 systems for $p = 0.55$, $p = 0.57$, and $p = 0.59$. The circles illustrate the radius of gyration of the largest cluster, and the boxes show the size of the average radius of gyration, $R = \langle R_s \rangle$. We observe that both lengths increase approximately proportionally as p approaches p_c.

5.2.1 Correlation length

We can also measure the typical size of a cluster from the correlation function. The correlation function $g(r, p)$, which is the probability that two sites, which are a distance r apart, are connected and part of the same cluster for a system with occupation probability p. We can use this to define the average squared distance between two sites i and j belonging to the same cluster as

$$\xi = \langle \frac{\sum_j r_{ij}^2 g(r_{ij}; p)}{\sum_j g(r_{ij}; p)} \rangle_i \ . \tag{5.24}$$

where the sum is over all sites j and the average is also over all sites i. The denominator is a normalization sum, which corresponds to the average cluster size, S. You can think of this sum in the following way: For a site i, we sum over all other sites j in the system. The probability that site j belongs to the same cluster as site i is $g(r_{ij}; p)$, and the mass of the site at j is 1. The average number of sites connected to site at i is therefore:

$$S(p) = \langle \sum_j g(r_{ij}; p) \ = \sum_j g(r_{ij}; p) \rangle_i \ , \tag{5.25}$$

where we average over all the the sites i in the system.

This means that we can connect $g(r; p)$ and ξ to the average cluster size S. Let us now see if we can calculate the behavior of $g(r; p)$ in a one-dimensional system, how to measure it in a two-dimensional system, and how to develop a theory for it for any dimension.

One-dimensional system. In chapter 2 we found that for the one-dimensional system the correlation function $g(r)$ is

$$g(r) = p^r = e^{-r/\xi} \ , \tag{5.26}$$

where $\xi = -\frac{1}{\ln p} = \simeq 1/(1-p_c)$ is called the correlation length. The correlation length diverges as $p \to p_c = 1$, $\xi \simeq (1-p_c)^{-\nu}$, where $\nu = 1$.

We can generalize this behavior by writing the correlation function in a more general scaling form for the one-dimensional system

$$g(r) = r^0 f(r/\xi) \ , \tag{5.27}$$

where $f(u)$ decays rapidly when u is larger than 1. We will assume that this behavior is general. Also for other dimensions, we expect the correlation function to decay rapidly beyond a length, which corresponds to the typical extent of clusters in the system.

Measuring the correlation function. For the two- or three-dimensional system, we cannot find an exact solution for the correlation function. However, we can still measure it from our simulations, although such measurements typically are computationally intensive. How can we measure it? We can loop through all sites i and j and find their distance r_{ij}. We estimate the probability for two sites at a distance r_{ij} to be connected to count how many of the sites that are a distance r_{ij} apart are connected, compared to how many sites in total are a distance r_{ij} apart. This is done through the following implementation, which returns the correlation function `g(r)` estimated for a lattice `lw` which contains the cluster indexes for each site, similar to what is returned by the `lw, num = measurements.label(m)` command. We write a subroutine `perccorrfunc` to find the correlation function for a given lattice `lw`, and then we use this function to find the correlation function for several values of p and for several values of L:

```python
from pylab import *
from scipy.ndimage import measurements
from numba import jit
@jit
def perccorrfunc(m,lw):
    nx = shape(lw)[0]
    ny = shape(lw)[1]
    L = max([nx,ny])
    r = arange(2*L) # Positions
    pr = zeros(2*L)   # Correlation function
    npr = zeros(2*L)  # Nr of elements
    for ix1 in range(nx):
        for iy1 in range(ny):
            lw1 = lw[ix1,iy1]
            if (lw1>0):
                for ix2 in range(nx):
                    for iy2 in range(ny):
                        lw2 = lw[ix2,iy2]
                        if (lw2>0):
                            dx = (ix2-ix1)
                            dy = (iy2-iy1)
                            rr = hypot(dx,dy)
                            nr = int(ceil(rr)+1) # Corresponding box
                            pr[nr] = pr[nr] + (lw1==lw2)
                        npr[nr] = npr[nr] + 1
    pr = pr/npr
    return r,pr
# Calculate correlation function
M = 10 # Nr of samples
L = 200 # System size
pp = [0.5,0.52,0.54,0.55,0.56] # p-value
lenpp = len(pp)
pr = zeros((2*L,lenpp),float)
rr = zeros((2*L,lenpp),float)
for i in range(M):
    print("i = ",i)
    z = rand(L,L)
    for ip in range(lenpp):
        p = pp[ip]
        m = z<p
        lw, num = measurements.label(m)
        r,g = perccorrfunc(m,lw)
        pr[:,ip] = pr[:,ip] + g
        rr[:,ip] = rr[:,ip] + r
pr = pr/M
r = r/M
# Plot data - linearly binned
for ip in range(lenpp):
    loglog(rr[:,ip],pr[:,ip],’.’,label="p="+str(pp[ip]))
legend()
```

Fig. 5.5 shows the resulting plots of the correlation function $g(r;p)$ for various values of p for an $L = 200$ system. First, we notice that the scaling is rather poor. We will understand this as we develop a theory for $g(r;p)$ below. The plot shows that there is indeed a cross-over length ξ, beyond which the correlation function falls rapidly to zero. And there appears to be a scaling regime for $r > \xi$ where the correlation function is approximately a power-law, although it is unclear how wide that scaling regime is in this plot. The plot suggests the following functional form

$$g(r;p) = r^x f(r/\xi) , \tag{5.28}$$

where the cross-over function $f(u)$ falls rapdily to zero when $u > 1$ and is approximately constant when $u < 1$. When p approaches p_c, the correlation length ξ grows to infinity, and the correlation function $g(r;p_c)$ approaches a power-law r^x for all values of r.

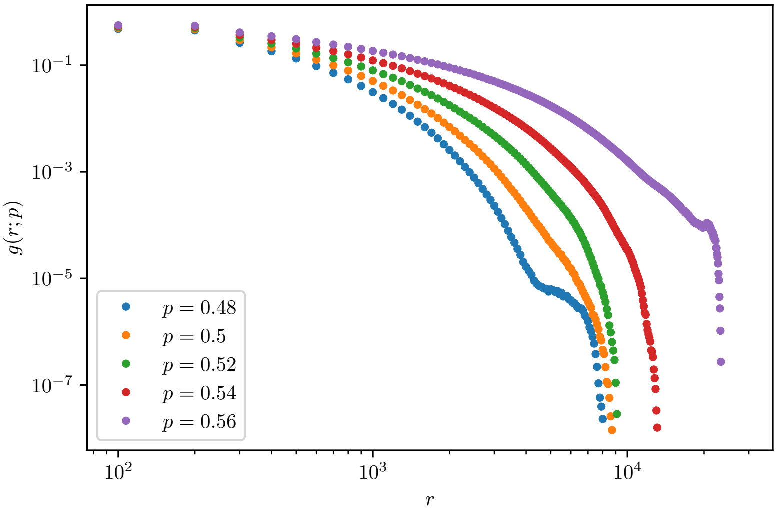

Fig. 5.5 A plot of $g(r;p)$ as a function of r for various values of p. The function approaches a power-law behavior $g(r) \propto r^x$ when p approaches p_c.

Theory for the correlation function. Based on these observations, we are motivated to develop a theory for the behavior of the correlation function. First, we know that when $p = p_c$, the average cluster size, S diverges. We can express S using the correlation function as

$$S = \sum_j g(r, p_c) = \int g(r)\, dr^d = \iint g(r) r^{d-1} dr d\Omega \ , \tag{5.29}$$

where the integral is written in spherical coordinates in a d-dimensional space, and the integration over Ω indicates an integration over all angles. For this integral to diverge, the function $g(r)$ cannot have an exponential cut-off, and it needs to diverge slower than a power-law with exponent $-d$. That is, in order for S to diverge at $p = p_c$, we know that at $p = p_c$:

$$g(r;p_c) \propto r^{-(d-2+\eta)} \ , \tag{5.30}$$

where η is a positive number, ranging from $\eta = 0$ for the Bethe lattice (infinite dimensions) to $\eta = 1$ for one-dimensional percolation, as we found above.

This corresponds both to the results we found for the one-dimensional system, and to the results we found from numerical measurements for the two-dimensional system. In addition, we know that for $p \neq p_c$, the correlation function should have a cut-off proportional to ξ, because the probability for two sites to be connected goes exponentially to zero with distance when the distance is significantly larger than ξ. These features indicates that $g(r, p)$ has a scaling form, and we propose the following scaling ansatz for $g(r, p)$:

$$g(r, p) = r^{-(d-2+\eta)} f(\frac{r}{\xi}) \; . \tag{5.31}$$

The scaling function $f(r/\xi)$ should be a constant when $r \ll \xi$, and in this range we cannot discern the behavior from the behavior of a system at p_c. For $r \gg \xi$, we expect the function to have an exponential form. The scaling function will therefore have the following behavior:

$$f(u) = \begin{cases} \text{constant} & \text{when } u \ll 1 \\ \exp(-u) & \text{when} u \gg 1 \end{cases} \; . \tag{5.32}$$

We can use this scaling form to determine the exponent η. We know that the average cluster size S is given as an integral over $g(r; p)$, that is

$$S = \sum_j g(r; p) = \int g(r; p) dr \; . \tag{5.33}$$

Let us use the scaling form for $g(r; p)$ to calculate this integral when p approaches p_c, but is not equal to p_c.

$$S = \int g(r; p) dr = \int_1^{\infty} r^{-(d-2+\eta)} f(r/\xi) dr^d \tag{5.34}$$

$$= \int_1^{\infty} r^{-(d-2+\eta} r^{d+1} \exp(-r/\xi) dr d\Omega \propto \int_1^{\infty} r^{1-\eta} \exp(-r/\xi) dr \tag{5.35}$$

$$= \xi^{2-\eta} \int (\frac{r}{\xi})^{1-\eta} \exp(-r/\xi) \frac{dr}{\xi} = \xi^{2-\eta} \int u^{1-\eta} \exp(-u) du \propto \xi^{2-\eta} \tag{5.36}$$

We already know the scaling behavior of S when $p \to p_c$:

$$S \propto |p - p_c|^{-\gamma} \propto \xi^{2-\eta} \; , \tag{5.37}$$

Consequently, we now know the behavior of ξ:

$$\xi \propto |p - p_c|^{-\gamma/(2-\eta)} , \tag{5.38}$$

where η is a number between 0 (for the infinite-dimensional system) and 1 (for the one-dimensional system). Indeed we remember that for the one-dimensional system we found that $\xi \propto |p - p_c|^{-1}$ and that $\gamma = 1$, which is indeed consistent with $\eta = 1$.

What does this teach us about the two- and three-dimensional system? For these systems, we already have related the average cluster size to the average radius of gyration, R:

$$S \propto s_\xi^{3-\tau} \propto R^{(3-\tau)/D} , \tag{5.39}$$

and we know that the average radius of gyration behaves as

$$R \propto R_{s_\xi} \propto s_\xi^{1/D} \propto |p - p_c|^{-1/\sigma D} . \tag{5.40}$$

We interpret both ξ and R (and R_{s_ξ}) as characteristic lengths. Let us now make a daring assumption! Let us assume that ξ and R are proportional — that there is only one characteristic length in the system. This allows us to write:

$$R \propto |p - p_c|^{-1/\sigma D} \propto |p - p_c|^{-\gamma/(2-\eta)} . \tag{5.41}$$

We can use this relation to find η, given that the assumption of $\xi \propto R$ is correct, or to demonstrate that $\xi \propto R$ by measuring η and checking for consistency with this equation.

We have already done this for the one-dimensional system, where $\sigma = D = 1$ and $\gamma = 1$, and therefore $\eta = 1$, which is indeed what we found above. Similarly, we can check this result for the Bethe-lattice, where we also find that the assumption holds. Simulations and theoretical arguments indeed support the assumption. We will therefore in the following only use one symbol for all the characteristic lengths since they are proportional to each other and therefore only differ (scaling-wise) by a constant of proportionality:

$$\xi \propto R \propto R_{s_\xi} \propto |p - p_c|^{-\nu} . \tag{5.42}$$

We will typically only use the symbol ξ for this characteristic length of the system, and the exponent ν characterizes how ξ diverges as p approaches p_c:

Correlation length

The correlation length ξ scales as

$$\xi \propto |p - p_c|^{-\nu} \quad \text{when} \quad p \to p_c \; . \tag{5.43}$$

The exponent $\nu = -1/(\sigma D) = -\gamma/(2 - \eta)$. For $d = 2$, $\nu = 4/3$.

The characteristic length ξ and system size L. The introduction of a single characteristic length ξ, corresponding to the characteristic cluster size s_ξ through $s_\xi \propto \xi^D$, allows us to discuss what happens to a system that is close to, but not exactly at, p_c. Fig. 5.6 shows a plot of $\xi(p)$ for two-dimensional systems with $L = 100$, 200, and 400. Notice that since ξ diverges as p approaches p_c, and we are in a finite system of size L, we will not observe clusters that are larger than L. This means that if we measure $\xi(p)$ and we try to estimate p_c we only know that it is somewhere in the region where $\xi(p) > L$, but we do not really know where. This also means that if we are studying a system where p is different from, but close to p_c, we need to study clusters that are at least of the size of ξ in order to notice that we are not at $p = p_c$.

If we study a system of size $L \ll \xi$, we will typically observe a cluster that spans the system, since the typical cluster size, ξ, is larger than the system size. We are therefore not able to determine if we observe a spanning cluster because we are at p_c or only because we are sufficiently close to p_c. We will start to observe a spanning cluster when $\xi \simeq L$, which corresponds to

$$\xi_-(p_c - p)^{-\nu} = \xi \simeq L \; , \tag{5.44}$$

and therefore that

$$(p_c - p) \simeq (L/\xi_-)^{-(1/\nu)} \; , \tag{5.45}$$

when $p < p_c$, and a similar expression for $p > p_c$. This means that when we observe spanning we can only be sure that p is within a certain range of p_c:

$$|p - p_c| = cL^{-1/\nu} \; . \tag{5.46}$$

The correlation length ξ is therefore the natural length characterizing the geometry of the cluster. At distances smaller than ξ, the system behaves as if it is at $p = p_c$. However, at distances much larger than ξ, the system is essentially homogeneous.

As we can observe in Fig. 5.6 the system becomes more and more homogeneous when p goes away from p_c. We will now address this feature in more detail when $p > p_c$.

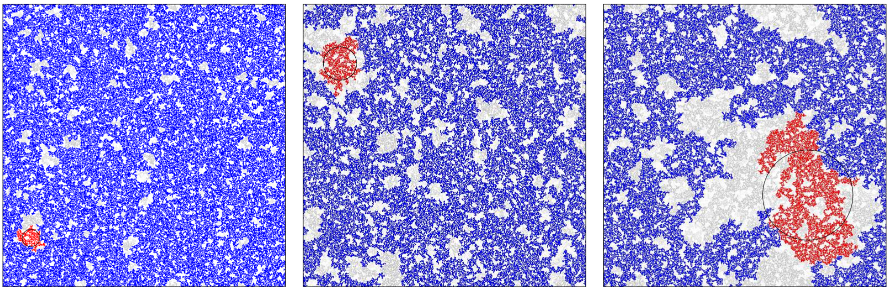

Fig. 5.6 Illustration of the largest cluster in 512×512 systems with $p > p_c$, for $p = 0.593$, $p = 0.596$, and $p = 0.610$. The circles illustrate the radius of gyration of the largest cluster. We observe that the radius of gyration increases as p approaches p_c.

5.3 Geometry of the spanning cluster

How can we develop a scaling theory for the spanning cluster? As p is increased from below towards p_c, the characteristic cluster size ξ diverges. However, the size of a characteristic cluster of size ξ is expected to follow the scaling relation $s_\xi \propto \xi^D$. For a given value of p we can therefore choose the system size L to be equal to ξ, $L = \xi(p)$. In this case, a cluster of size ξ would correspond to a cluster of size L, which is a spanning cluster in this system. For this system of size $L = \xi$, we therefore expect the mass of the spanning cluster to be $M(p, L) \propto \xi^D \propto L^D$. This suggests (but does not really prove) that the mass of the spanning cluster in a system close to or at p_c scales as $M(p, L) \propto L^D$.

The density of the spanning cluster at $p = p_c$ therefore has the following behavior:

$$P(p, L) = \frac{M(p, L)}{L^d} \propto L^D / L^d \propto L^{D-d} \, . \tag{5.47}$$

Because we know that $P(p, L) \to 0$ when $L \to \infty$, we deduce that $D < d$. The value of D in two-dimensional percolation is $D = 91/48 \simeq 1.90$.

Fractal geometry of the spanning cluster. What does this result tell us about the geometry of the percolation cluster? First, we observe that the density of the cluster depends on the system size, L, on which we are observing it. This is a general feature of a fractal with a dimension different from the Euclidean dimension in which it is embedded. For any object that obeys the scaling relation

$$M \propto L^D \ , \tag{5.48}$$

where $D < d$, and d is the dimension of the Euclidean dimension, we have that the density ρ is

$$\rho \propto \frac{M}{L^d} \propto L^{D-d} \ , \tag{5.49}$$

which depends on system size L. We also notice that the density decreases as the system size increases.

Notice that these features do not represent something new, but are simply extensions of features we are very well familiar with. For example, consider a thin, flat sheet of thickness h, and dimensions $\mathcal{L} \times \mathcal{L}$, placed in a three-dimensional space. If we cut out a volume of size $L \times L \times L$, so that $L \ll \mathcal{L}$, the mass of the sheet inside that volume is

$$M = hL^2 \ , \tag{5.50}$$

which implies that the density of the sheet is

$$\rho = \frac{hL^2}{L^3} = hL^{-1} \ . \tag{5.51}$$

It is only in the case when we use a two-dimensional volume $L \times L$ with a third dimension of constant thickness H larger than h, that we recover a constant density ρ independent of system size.

5.4 Spanning cluster above p_c

Let us now return to the discussion of the mass $M(p, L)$ of the spanning cluster for $p > p_c$ in a finite system of size L. The behavior of the percolation system for $p > p_c$ is illustrated in Fig. 5.6. We notice that the correlation length ξ diverges when p approaches p_c. At lengths larger than ξ, the system is effectively homogeneous because there are no holes significantly larger than ξ. There are two types of behavior, depending on whether L is larger than or smaller than the correlation length ξ.

When $L \ll \xi$, we are again in the situation where we cannot discern p from p_c because the size of the holes (empty regions described by ξ when

$p > p_c$) in the percolation cluster is much larger than the system size. In this case, the mass of the percolation cluster will follow the scaling relation $s \propto R_s^D$, and the finite section of size L of the cluster will follow the same scaling if we assume that the radius of gyration of the cluster inside a region of size L is proportional to L:

$$M(p, L) \propto L^D \text{ when } L \ll \xi \; . \tag{5.52}$$

In the other case, when $L \gg \xi$, and $p > p_c$, the typical size of a hole in the percolation cluster is ξ, as illustrated in Fig. 5.6. This means that on lengths much larger than ξ, the percolation cluster is effectively homogeneous. We can therefore divide the $L \times L$ system into $(L/\xi)^d$ regions of size ξ, so that for each such region, the mass if $m \propto \xi^D$. The total mass of the spanning cluster is therefore the mass of one such region multiplied with the number of regions:

$$M(p, L) \propto (\xi^D)(L/\xi)^d \propto \xi^{D-d} L^d \; . \tag{5.53}$$

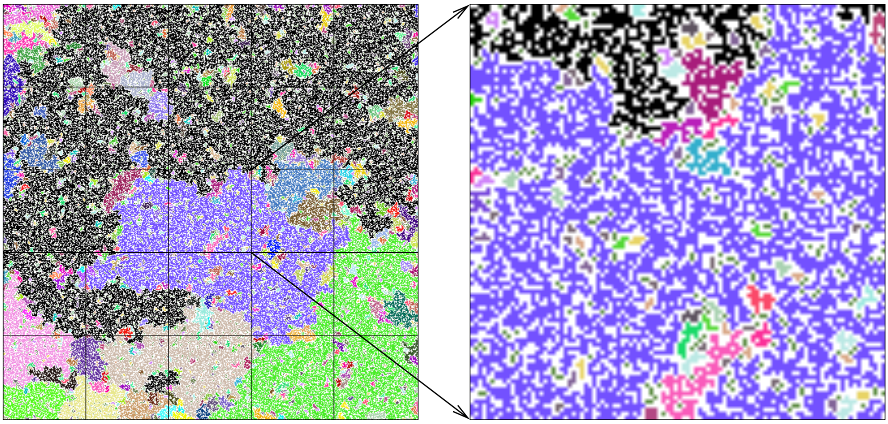

Fig. 5.7 Illustration of the spanning cluster in a 512×512 system at $p = 0.595 > p_c$. In this case, the correlation length is $\xi = 102$. The system is divided into regions of size ξ. Each such region has a mass $M(p, \xi) \propto \xi^D$, and there are $(L/\xi)^d \simeq 25$ such regions in the system.

We can now introduce the complete behavior of the mass, $M(p, L)$, of the spanning cluster for $p > p_c$:

$$M(p, L) \propto \begin{cases} L^D & L \ll \xi \\ \xi^{D-d} L^d & L \gg \xi \end{cases} \; . \tag{5.54}$$

This form can be rewritten in the standard scaling form as:

$$M(p,L) = L^D Y(\frac{L}{\xi}) \ , \tag{5.55}$$

where

$$Y(u) = \begin{cases} \text{constant} & u \ll 1 \\ u^{d-D} & u \gg 1 \end{cases} \ . \tag{5.56}$$

5.5 Fractal cluster geometry

What happens to the scaling behavior of the system if we change the effective length-scale by a factor b?. That is, what happens if we introduce a new set of variables $\xi' = \xi/b$, and $L' = L/b$.

We can use our scaling form $M(p,L) = L^D Y(L/\xi)$, to find that

$$M(p',L') = (L')^D Y(L'/\xi') = (L/b)^D Y(L/\xi) = b^{-D} M(p,L) \ , \tag{5.57}$$

where we have written p' to indicate that a rescaling of the correlation length corresponds to a change in p - reducing the correlation length corresponds to moving p further away from p_c.

This shows that the mass displays a simple rescaling when the system size is rescaled. Functions that display this simple form of rescaling are called homogeneous functions.

The change of length-scale results in a change of correlation length, except for the cases when the correlation length is either zero or infinity. The correlation length is zero for $p = 0$, and for $p = 1$. These two values of p therefore correspond to trivial fix-points for the rescaling: The scaling behavior does not change under this rescaling. The correlation length is infinite for $p = p_c$, which implies that the correlation length does not change when the system size is rescaled by a factor b. This is illustrated in Fig. 5.8, which shows that the structure of the percolation cluster at $p = p_c$ does not change significant.

Self-similar fractals. The spanning cluster shows a particular simple scaling behavior at $p = p_c$. That is when the correlation length increases to infinity — there is therefore no other length-scale in our system except the system size L and the lattice unit a. When $p = p_c$ we found that the mass of the spanning cluster displayed the scaling relation:

$$M(L) = b^{-D} M(bL) \ , \tag{5.58}$$

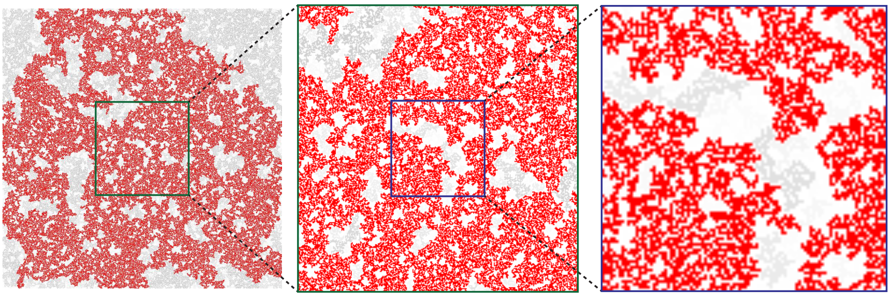

Fig. 5.8 Illustrations of the spanning cluster (shown in red), and the other clusters (shown in gray) at $p = p_c$ in a $L = 900$ site percolation system. **a** The 900 × 900 system. **b** The central 300 × 300, and part. **c** The central 100 × 100. Each step represents a rescaling by a factor 3. However, at $p = p_c$, the correlation length is infinite, so a rescaling of the length-scales should not influence the geometry of the cluster, which is evident from the pictures: The percolation clusters are indeed similar in a statistical manner.

corresponding to a rescaling by a factor b. This is an example of self-similar scaling.

Let us address self-similar scaling in more detail by addressing an example of a deterministic fractal, the Sierpinski gasket [32]. The Sierpinski gasket can be defined iteratively. We start with a unit equilateral triangle as illustrated in Fig. 5.9. We divide the triangle into 4 identical triangles, and remove the center triangle. For each of the remaining triangles, we continue this process. The result set of points after infinitely many iterations is called the Sierpinski gasket. This set contains a hierarchy of holes. We also notice that the structure is identical under (a specific) dilatational rescaling. If we take one of the tree triangles generated in the first step and rescale it to fit on top of the initial triangle, we see that it reproduces the original identically. This structure is therefore a fractal.

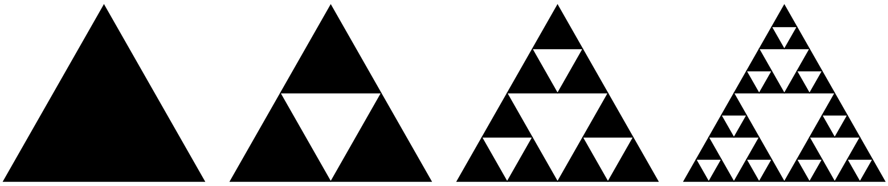

Fig. 5.9 Illustration of three generations of the Sierpinski gasket starting from an equilateral triangle.

The dimensionality of the structure is related to the relation between the rescaling of the mass and the length. If we take one of the three triangles from the first iteration, we need to rescale the x and the y axes by a factor 2. We can write this as a rescaling of the system size, L, by a factor 2

$$L' = 2L \; . \tag{5.59}$$

Through this rescaling we get three triangles, each with the same mass as the original triangle. The mass is therefore rescaled by a factor 3.

$$M' = 3M \; . \tag{5.60}$$

If we write the mass as a function of length, $M(L)$, we can formulate the scaling as

$$M(2L) = 3M(L) \; , \tag{5.61}$$

or, equivalently,

$$M(L) = 3^{-1}M(2L) \; . \tag{5.62}$$

If we compare this with the general relation,

$$M(L) = b^{-D}M(bL) \; , \tag{5.63}$$

we see that

$$2^{-D} = 3^{-1} \; , \tag{5.64}$$

giving

$$D = \frac{\ln 3}{\ln 2} \; . \tag{5.65}$$

We will use this rescaling relation as our definition of fractal dimension. The relation corresponds to the relation $M = L^D$ for the mass. Let us also show that this relation is indeed consistent with our notion of Euclidean dimension. For a cube of size L, the mass is L^3. If we look at a piece of size $(L/2)^3$, we see that we need to rescale it by a factor of 2 in all direction to get back to the original cube, but the mass must be rescaled by a factor 8. We will therefore find the dimension from

$$D = \frac{\ln 8}{\ln 2} = 3 \; , \tag{5.66}$$

which is, as expected, the Euclidean dimension of the cube.

Typically, the mass dimension is measured by box counting. The sample is divided into regular boxes where the size of each side of the box is δ. The number of boxes, $N(\delta)$, that contain the cluster are counted as a function of δ. For a uniform mass we expect

$$N(\delta) = (\frac{L}{\delta})^d \, , \tag{5.67}$$

and for a fractal structure we expect

$$N(\delta) = (\frac{L}{\delta})^D \, , \tag{5.68}$$

We leave it as an exercise for the reader to address what happens when $\delta \to 1$, and when $\delta \to L$.

5.6 Exercises

Exercise 5.1: Mass scaling of percolating cluster

a) Find the mass $M(L)$ of the percolating cluster at $p = p_c$ as a function of L, for $L = 2^k$, $k = 4, \ldots, 11$.

b) Plot $\log(M)$ as a function of $\log(L)$.

c) Determine the exponent D.

Exercise 5.2: Correlation function

a) Write a program to find the correlation function, $g(r, p, L)$ for $L = 256$.

b) Plot $g(r, p, L)$ for $p = 0.55$ to $p = 0.65$ for $L = 256$.

c) Find the correlation length $\xi(p, L)$ for $L = 256$ for the p-values used above.

d) Plot ξ as a fuction of $p - p_c$, and determine ν.

6 Finite size scaling

In this chapter we will learn how to utilize a disadvantage, such as a finite system size, to an advantage. Usually, we have found a finite system size to be a hassle in simulations. We would like to find the general behavior, but we are limited by the largest finite system size we can afford to simulate. It may be tempting to put all our resources into one attempt — to make one simulation in a really large system. However, this is usually not a good strategy. Because we will then know that our results are limited by the system size, but we do not know to what degree this affects our result.

Instead, we will follow a different strategy: the strategy of finite size scaling. We will systematically increase the system size, measure the quantities we are interested in, and then try to extrapolate to an infinite system size. This has several advantages: It allows us to understand and estimate the errors in our predictions, and it allows us to use simulations of smaller systems. Indeed, it turns out that it is more important to do simulations in smaller systems, than only to try to simulate that largest system possible. However, for this to be effective, we need to have a theoretical understanding of finite size scaling [6].

The methods we develop here are powerful and can be generalized to many other experimental and computational situations. In many experiments it is also tempting to try to perform the perfect experiment by reducing noise or measurement errors. For example, we may perform an experiment where we need to make the experimental system as horizontal as possible, because deviations from a horizontal system would introduce errors. Instead of trying to make the system as horizontal as possible, we may instead systematically vary the orientation, and then extrapolate to the case when the system is perfectly horizontal. This also allow us to control the uncertainty. Of course, we cannot vary all possible uncertainties in an experiment or a simulation, but this alternative mindset provides us with a new tool in our toolbox, and a new way to deal with uncertainties.

In practical situations, we will always be limited by finite system sizes. If you measure the size of earthquakes in the Earth's crust, your results are limited by the thickness of the crust or by the extent of a homogeneous region. If you simulate a molecular system, you are definitely limited by the number of atoms you can include in your simulation. Thus, better insight into how we can systematically vary the system size and use this to gain insight are general tools of great utility.

Here, you will learn how to systematically vary system size L in order to find much better estimates for exponents and percolation thresholds. Indeed, my hope is that you will see that finite size scaling is a powerful tool that can be used both theoretically and computationally. To introduce this tool, we need to address specific examples that can help build our intuition and shape our mindset. We will therefor start from a few examples, such as the finite size scaling for the density of the spanning cluster, $P(p, L)$, and then apply the method to a new case, the percolation probability $\Pi(p, L)$.

6.1 General aspects of finite size scaling

We have found that a percolation system is described by three length-scales: the size of a site, the system size L, and the correlation length ξ. Finite size scaling addresses the change in behavior of a system as we change the system size L. Typically, we divide the behavior into two categories:

- When the system size L is much smaller than the correlation length ξ, $L \ll \xi$, the system appears to be on the percolation threshold
- When L is much larger than ξ, $L \gg \xi$, the geometry is essentially homogeneous at lengths longer than ξ

We will then address the behavior close to p_c. In the case of percolation, we usually assume that the behavior is a power-law in $p - p_c$. For example, the mass $M(p; L)$ of the spanning cluster:

$$M(p) \propto (p - p_c)^{-x} \ , \tag{6.1}$$

where the exponent x determines the behavior close to p_c.

The general approach in finite size scaling is to make a scaling ansatz — an assumption about how the system behaves:

$$M(p, L) = L^{\frac{x}{\nu}} f\left(\frac{L}{\xi}\right) \ , \tag{6.2}$$

where $f(u)$ is an unknown function. (Sometimes we instead make the assumption $M(p, L) = \xi^{x/\nu} \tilde{f}(L/\xi)$ and we leave it to the reader to demonstrate that these assumptions are equivalent.)

We will then apply our insight into the particulars of the system to infer the behavior in the limits when $\xi \gg L$, and $\xi \ll L$ to determine the form of the scaling function $f(u)$, and use this functional form as a tool to study the behavior of the system. We will explain this reasoning through three examples: The case of $P(p, L)$, the case of $S(p, L)$ and the case of $\Pi(p, L)$.

6.2 Finite size scaling of $P(p, L)$

Measuring $P(p, L)$ for finite L. Let us now apply this methodology to study the behavior of the density of the spanning cluster, $P(p, L)$, for finite system sizes. First, we generate a plot of $P(p, L)$ for various values of L using the following program:

```
from pylab import *
from scipy.ndimage import measurements
LL = [25,50,100,200]
p = linspace(0.4,0.75,50)
nL = len(LL)
nx = len(p)
P = zeros((nx,nL),float)
for iL in range(nL):
    L = LL[iL]
    N = int(2000*25/L)
    for i in range(N):
        z = rand(L,L)
        for ip in range(nx):
            m = z<p[ip]
            lw, num = measurements.label(m)
            perc_x = intersect1d(lw[0,:],lw[-1,:])
            perc = perc_x[where(perc_x>0)]
            if (len(perc)>0):
                Ni[ip] = Ni[ip] + 1
                area = measurements.sum(m, lw, perc[0])
                P[ip] = P[ip] + area
    P[:,iL] = P[:,iL]/((L*L)*N)
for iL in range(nL):
    L = LL[iL]
    plot(p,P[:,iL])
    ylabel('P(p,L)')
    xlabel('p')
```

The resulting plot of $P(p, L)$ is shown in Fig. 6.1. We see that as L increases, $P(p, L)$ approaches the shape expected in the limit when $L \to \infty$. We can see how it approaches this limit by finding the value of $P(p_c, L)$ as a function of L. We expect this value to go to zero as L increases. Fig. 6.1b shows how $P(p_c, L)$ approaches zero. Let us see if we can develop a theoretical prediction for this behavior and check if our measured results confirm the prediction.

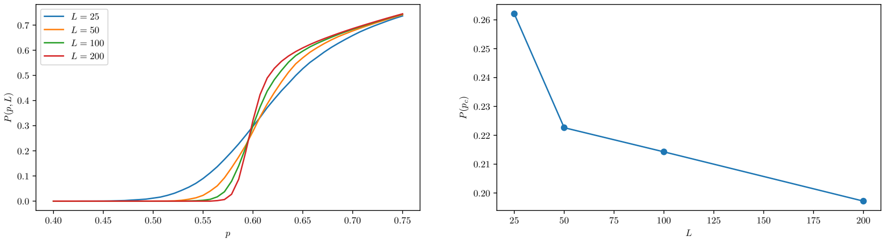

Fig. 6.1 (a) Plot of $P(p, L)$. (b) Plot of $P(p_c; L)$ as a function of L.

Finite size effects in $P(p, L)$. We expect

$$P(p) \propto (p - p_c)^{\beta} \propto \xi^{-\beta/\nu} , \tag{6.3}$$

in the limit when $L \to \infty$. The limit of large L corresponds to L being large compared to the characteristic length scale in the system, ξ: $L \gg \xi$.

The other limit, when L is small compared to ξ, $L \ll \xi$, that is when ξ is large, which again corresponds to $p \to p_c$. In this case, we see from Fig. 6.1 that $P(p_c, L)$ depends on L. In this case we found that

$$P(p, L) = \frac{M(p, L)}{L^2} \propto \frac{L^D}{L^d} \propto L^{D-d} \propto L^{-\beta/\nu} . \tag{6.4}$$

Finite size scaling ansatz. The fundamental idea of finite size scaling is then to *assume* a particular form of a function that encompasses the behavior both when $\xi \ll L$ and $\xi \gg L$, by rewriting the expression for $P(p, L)$ as

$$P(p, L) = L^{-\beta/\nu} f(L/\xi) \; . \tag{6.5}$$

Where we have assumed that the only length scales are L and ξ and that the function therefore only can depend on a ratio between these two length scales. How does the function $f(u)$ need to behave for this general form to reduce to eq.(6.3) and eq.(6.4)?

First, we see that when $\xi \gg L$ the function $f(L/\xi)$ should be a constant, that is, $f(u)$ is a constant when $u \ll 1$.

Second, we see that when $\xi \ll L$, we need the function $f(L/\xi)$ to cancel all the L-dependency in order to find the relation in eq.(6.3):

$$P(p, L) = L^{-\beta/\nu} f(L/\xi) = \xi^{-\beta/\nu} \; . \tag{6.6}$$

We assume that $f(u)$ is a power-law, $f(u) = u^a$. In order to cancel L we see that:

$$\begin{aligned} P(p, L) \; &= \; L^{-\beta/\nu}(L/\xi)^a = L^{-\beta/\nu+a}\xi^{-a} = \xi^{-\beta/\nu} & (6.7) \\ &\Rightarrow \; -\beta/\nu + a = 0 \; \Rightarrow \; a = \beta/\nu \; . & (6.8) \end{aligned}$$

Indeed, we could have used this in order to find the exponent in the relation $\xi^{-\beta/\nu}$ — it would simply have been enough to assume that $P(p, L) = \xi^x$ for some exponent x in the limit of $\xi \ll L$.

We have therefore found that in order to satisfy these conditions, the scaling form of $P(p, L)$ must be

$$P(p, L) = L^{-\beta/\nu} f(L/\xi) \; , \tag{6.9}$$

where

$$f(u) = \begin{cases} \text{const.} & u \ll 1 \\ u^{\beta/\nu} & u \gg 1 \end{cases} \tag{6.10}$$

Testing the scaling ansatz. We can now test the scaling ansatz by plotting $P(p, L)$ according to the ansatz, following a strategy similar to what we developed for $n(s, p)$. We rewrite the scaling function $P(p, L) = L^{-\beta/\nu} f(L/\xi)$ by inserting $\xi = \xi_0 |p - p_c|^{-\nu}$:

$$\begin{aligned} P(p, L) &= L^{-\beta/\nu} f(L/\xi) & (6.11) \\ &= L^{-\beta/\nu} f(L\xi_0 |p - p_c|^{\nu}) & (6.12) \\ &= L^{-\beta/\nu} f((\xi_0 L^{1/\nu}(p - p_c))^{\nu}) & (6.13) \\ &= L^{-\beta/\nu} \tilde{f}(L^{1/\nu}(p - p_c)) \; . & (6.14) \end{aligned}$$

We can again rewrite this as

$$L^{\beta/\nu} P(p,L) = \tilde{f}(L^{1/\nu}(p-p_c)) \; . \tag{6.15}$$

Therefore is we plot $L^{1/\nu}(p-p_c)$ along the x-axis and $L^{\beta/\nu}P(p,L)$ along the y-axis, we expect all the data to fall onto a common curve, the curve $f(u)$. This is done in Fig. 6.2, which shows that the measured data is consistent with the scaling ansatz. We call such as plot a *scaling data collapse* plot.

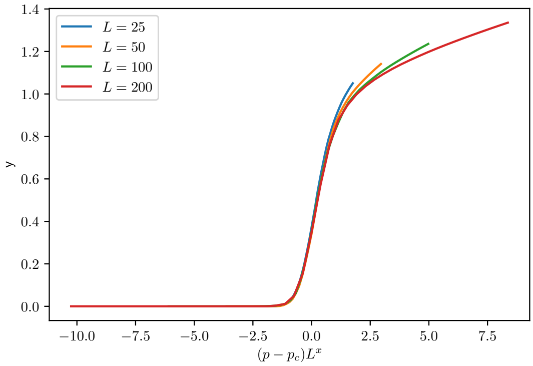

Fig. 6.2 Scaling data collapse plot of $P(p,L)$.

Comparing theory at $p = p_c$. Finally, we can now use this theory to understand the behavior for $P(p_c,L)$. In this case we find that $P(p_c,L) = cL^{-\beta/\nu}$. We can therefore measure $-\beta/\nu$ from the plot of $P(p_c,L)$ in Fig. 6.1. However, while the data in this figure is somewhat too poor to produce a reliable result, the figure demonstrates the principle.

Varying L to gain insight. The take-home message is that instead of trying to simulate one single simulation with as large L as possible, we should instead vary L systematically and then use this variation in order to estimate the relevant exponent ν and β. The methods demonstrated here usually provide much better results in term of precision of the exponents that a direct measurement for a large system size.

Alternative approaches. We could instead have started with a scaling ansatz of $P(p,L) = (p-p_c)^{\beta} g(L/\xi) = \xi^{-\beta/\nu} g(L/\xi)$. The whole derivation and, of course, the end result would have been the same. We leave this as an exercise for the eager reader.

6.3 Average cluster size

We can characterize the distribution of cluster sizes using *moments of the cluster number distribution*. The k-th moment $M_k(p,L)$ is defined as:

$$M_k(p,L) = \sum_{s=1}^{\infty} s^k n(s,p;L) \ . \tag{6.16}$$

We have already introduced the second moment, $M_2(p,L)$, which we called the average cluster size, $S(p,L)$.

$$S(p,L) = M_2(p,L) = \sum_{s=1}^{\infty} s^k n(s,p;L) \ . \tag{6.17}$$

Now, let us see if we can apply the finite-size scaling approach to develop a scaling theory for $S(p,L)$. First, we will measure $S(p,L)$, and then develop and test a scaling theory.

6.3.1 Measuring moments of the cluster number density

How would we measure $S(p,L)$? We recall that we measure the cluster number density from

$$\overline{n(s,p;L)} = \frac{N_s}{L^d} \ , \tag{6.18}$$

where N_s is the number of clusters of size s. Thus we can estimate $S(p,L)$ from:

$$\overline{S(p,L)} = \sum_{s=1}^{\infty} s^2 \frac{N_s}{L^d} \ . \tag{6.19}$$

We realize that we can perform this sum by summing over all possible s and then including how many clusters we have for a given s, or we can alternatively sum over all the observed clusters s_i. (Try to convince yourself that this is the same by looking at a sequence of clusters of sizes $1, 2, 1, 5, 1, 2.$). Thus, we can estimate the second moment from the sum:

$$\overline{S(p,L)} = \sum_i s_i^2/L^2 \ . \tag{6.20}$$

And similarly by summing over s_i^k for the k-th moment.

We implement this in the following program:

```
from pylab import *
from scipy.ndimage import measurements
LL = [25,50,100,200]
p = linspace(0.4,0.75,50)
nL = len(LL)
nx = len(p)
S = zeros((nx,nL),float)
for iL in range(nL):
    L = LL[iL]
    M = int(2000*25/L)
    for i in range(M):
        z = rand(L,L)
        for ip in range(nx):
            m = z<p[ip]
            lw, num = measurements.label(m)
            labelList = arange(lw.max() + 1)
            area = measurements.sum(m, lw, labelList)
            # Remove spanning cluster by setting its area to zero
            perc_x = intersect1d(lw[0,:],lw[-1,:])
            perc = perc_x[where(perc_x>0)]
            if (len(perc)>0):
                area[perc[0]] = 0
            S[ip,iL] = S[ip,iL] + sum(area*area)
    S[:,iL] = S[:,iL]/(L**2*M)
# Plotting the results
for iL in range(nL):
    L = LL[iL]
    lab = "$L="+str(L)+"$"
    plot(p,S[:,iL],label=lab)
    ylabel('$S(p,L)$')
    xlabel('$p$')
    legend()
```

The resulting plot of $S(p, L)$ as a function of $p$ for various values of L is shown in Fig. 6.3.

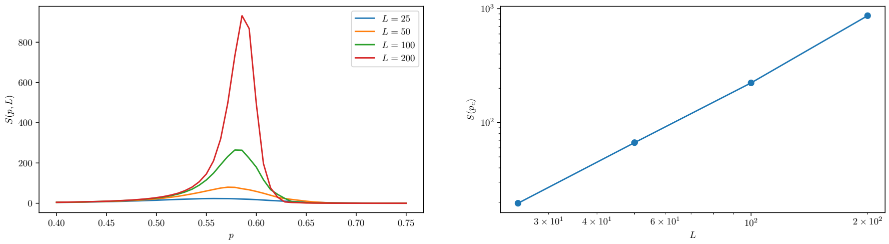

Fig. 6.3 (a) Plot of $S(p, L)$. (b) Plot of $S(p_c; L)$ as a function of L.

6.3.2 Scaling theory for $S(p, L)$

How can we understand these plots and how can we develop a theory for $S(p, L)$? We found previously that S diverges as p approaches p_c:

$$S(p) = S_0 |p - p_c|^{-\gamma} \ , \tag{6.21}$$

where the exponent $\gamma = 43/18$ for $d = 2$. Following the approach for finite-size scaling introduced above we introduce the finite size L through a scaling function $f(L/\xi)$, giving us a finite-size scaling ansatz (our hypothesis):

$$S(p, L) = S_0 |p - p_c|^{-\gamma} f\left(\frac{L}{\xi}\right) \ . \tag{6.22}$$

We rewrite the first expression by introducing $\xi = \xi_0 |p - p_c|^{-\nu}$ so that $S_0 |p - p_c|^{-\gamma} = \xi^{\gamma/\nu}$, giving:

$$S(p, L) = \xi^{\gamma/\nu} f\left(\frac{L}{\xi}\right) \ . \tag{6.23}$$

Now, we see from Fig. 6.3 that when $p = p_c$, $S(p_c, L)$ does not diverge, but depends on L — as we would expect for a finite system. Thus we know that in the limit when $p \to p_c$, $S(p, L)$ can only depend on L. This implies that the function $f(L/\xi)$ in this limit must be so that the ξ in $f(L/\xi)$ cancels the $\xi^{\gamma/\nu}$ in front of it. This can only happen if $f(L/\xi) \propto (L/\xi)^{\gamma/\nu}$:

$$S(p, L) \propto \xi^{\gamma/\nu} \left(\frac{L}{\xi}\right)^{\gamma/\nu} \propto L^{\gamma/\nu} \ . \tag{6.24}$$

Thus, we have found that $S(p_c, L) \propto L^{\gamma/\nu}$.

This allows us to write the scaling form of $S(p, L)$ in a different way:

$$S(p, L) = L^{\gamma/\nu} g\left(\frac{L}{\xi}\right) \ . \tag{6.25}$$

We can test this prediction by plotting $S(p, L) L^{-\gamma/\nu}$ as a function of L/ξ:

$$S(p, L) L^{-\gamma/\nu} = g\left(\frac{L}{\xi}\right) = g\left(L (p - p_c)^{-\nu}\right) \tag{6.26}$$

$$= g\left(\left(L^{1/\nu} (p - p_c)\right)^{\nu}\right) = \tilde{g}\left(L^{1/\nu} (p - p_c)\right) \ . \tag{6.27}$$

The resulting plot is shown in Fig. 6.4, which indeed demonstrates that the measured data is consistent with the scaling theory. Success!

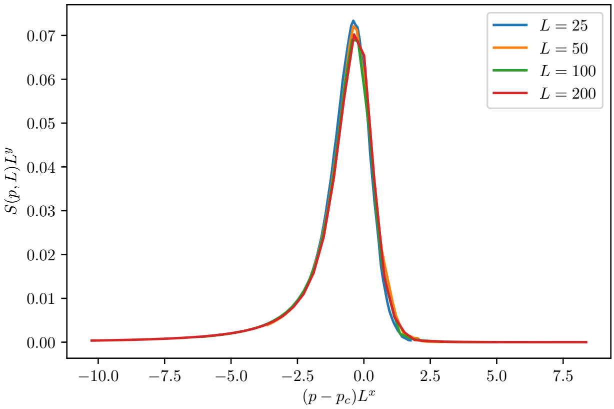

Fig. 6.4 A data-collapse plot of the rescaled average cluster size $L^{-\gamma/\nu}S(p,L)$ as a function of $L^{1/\nu}(p - p_c)$ for various L.

6.4 Percolation threshold

Finally, we will demonstrate one of the most elegant applications of finite-size scaling theory to the percolation probability $\Pi(p,L)$ and to see how a finite system size will affect the effective percolation threshold.

6.4.1 Measuring the percolation probability $\Pi(p,L)$

We can measure the percolation probability for a set of finite system sizes using the methods we developed previously. Here, we have implemented the measurement in the following program which is very similar to the program developed to measure $P(p,L)$

```
from pylab import *
from scipy.ndimage import measurements
LL = [25,50,100,200]
p = linspace(0.4,0.75,50)
nL = len(LL)
nx = len(p)
Ni = zeros((nx,nL),float)
Pi = zeros((nx,nL),float)
```

```
for iL in range(nL):
    L = LL[iL]
    N = int(2000*25/L)
    for i in range(N):
        z = rand(L,L)
        for ip in range(nx):
            m = z<p[ip]
            lw, num = measurements.label(m)
            perc_x = intersect1d(lw[0,:],lw[-1,:])
            perc = perc_x[where(perc_x>0)]
            if (len(perc)>0):
                Ni[ip,iL] = Ni[ip,iL] + 1
    Pi[:,iL] = Ni[:,iL]/N
for iL in range(nL):
    L = LL[iL]
    lab = "$L="+str(L)+"$"
    plot(p,Pi[:,iL],label=lab)
    ylabel('$\Pi(p,L)$')
    xlabel('$p$')
    legend()
```

The resulting plot of $\Pi(p, L)$ for various values of L is shown in Fig. 6.5.

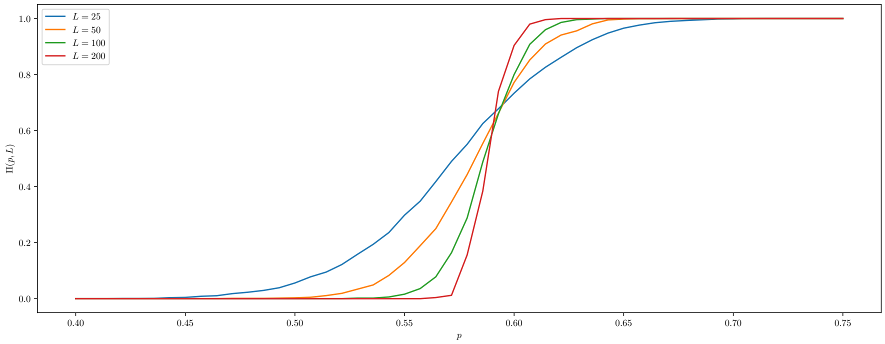

Fig. 6.5 Plot of $\Pi(p, L)$.

6.4.2 Measuring the percolation threshold p_c

Let us now assume that we do not a priori know p_c or any of the scaling exponents. How can we use this data-set to estimate the value for p_c?

The simplest approach may be to estimate p_c as the value for p that makes $\Pi(p, L) = 1/2$. This corresponds to intersection between the horizontal line $\Pi = 1/2$ and the curves in Fig. 6.5. This is illustrated in

Fig. 6.6. Here, we have also plotted $p_{1/2}$ as a function of $L$, where $p_{1/2}$ is the value for p so that $\Pi(p_{1/2}, L) = 1/2$. These values for $p_{1/2}$ are calculated by a simple interpolation as illustrated in the following program. (Notice that as usual in this book, we do not aim for high precision in this program. The simulations are for small system sizes and few samples, but are meant to illustrate the principle and be reproduceable for you.)

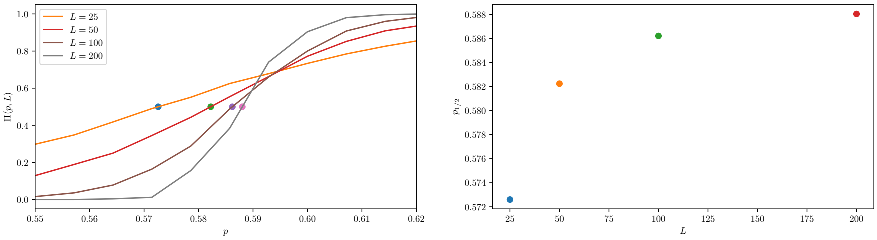

Fig. 6.6 (a) Plot of $\Pi(p, L)$. (b) Plot of $p_{1/2}$ as a function of $L$.

```
for iL in range(nL):
    ipc = argmax(Pi[:,iL]>0.5) # Find first value where Pi>0.5
    # Interpolate from ipc-1 to ipc to find intersection
    ppc = p[ipc-1] + (0.5-Pi[ipc-1,iL])*\
      (p[ipc]-p[ipc-1])/(Pi[ipc,iL]-Pi[ipc-1,iL])
    Pic = 0.5
    plot(L,ppc,'o')
xlabel('$L$')
ylabel('$p_{1/2}$')
```

From Fig. 6.6 we see that as $L$ increases the value for $p_{1/2}$ gradually approaches p_c. Well, we cannot really see that it is approaching p_c, but we guess that it will. However, in order extrapolate the curve to infinite $L$ we need to develop a theory for how $p_{1/2}$ behaves. We need to develop a finite size scaling theory for $\Pi(p, L)$.

6.4.3 Finite-size scaling theory for $\Pi(p, L)$

We apply the same method as before to develop a theory for $\Pi(p, L)$. First. we notice that at p_c $\Pi(p_c, L)$ does not either diverge or go to zero. This means that $\Pi(p, L)$ cannot be a function of ξ alone, but instead must have the scaling form:

$$\Pi(p, L) = \xi^0 f\left(\frac{L}{\xi}\right) . \tag{6.28}$$

We rewrite this in terms of $(p - p_c)$ by inserting $\xi = \xi_0 |p - p_c|^{-\nu}$:

$$\Pi(p, L) = f\left(L \xi_0 |p - p_c|^{\nu}\right) = f\left(\xi_0 \left(L^{1/\nu}(p - p_c)\right)^{\nu}\right) \ . \tag{6.29}$$

We introduce a new function $\Phi(u) = f\left(\xi_0 u^{1/\nu}\right)$:

$$\Pi(p, L) = \Phi\left(L^{1/\nu}(p - p_c)\right) \ . \tag{6.30}$$

This is our finite-size scaling ansatz (theory).

6.4.4 Estimating p_c using the scaling ansatz

How can we now use this to estimate p_c? We follow a technique similar to what we used above: We find the value p_x that makes $\Pi(p_x, L) = x$. Above we did this for $x = 1/2$, but we can do this more generally. Actually, as $L \to \infty$, we expect any such p_x to converge to p_c. We notice from above that p_x is a function of L: $p_x = p_x(L)$.

We insert this into the scaling ansatz:

$$x = \Phi\left(\left(p_x(L) - p_c\right) L^{1/\nu}\right) \ , \tag{6.31}$$

which can be solved as

$$(p_x - p_c) L^{1/\nu} = \Phi^{-1}(x) = C_x \ , \tag{6.32}$$

where it is important to realize that the right hand, C_x, side is a number which only depends on the x and not on L. We can therefore rewrite this as

$$p_x - p_c = C_x L^{-1/\nu} \ . \tag{6.33}$$

If we know ν, we see that this gives a method to estimate the value of p_c. Fig. 6.7 shows a plot of $p_{1/2} - p_c$ as a function of $L^{-1/\nu}$ for $\nu = 4/3$. We can use this plot to extrapolate to find p_c in the limit when $L \to \infty$ as indicated in the plot. The resulting value for p_c extrapolated from $L = 50, 100, 200$ is $p_c = 0.5914$, which is surprisingly good given the small system sizes and small sample sizes used for this estimate. This demonstrates the power of finite size scaling.

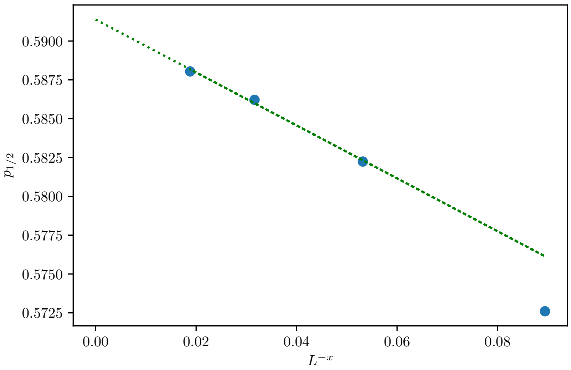

Fig. 6.7 Plot of $p_{1/2}$ as a function of $L^{-1/\nu}$. The dashed line indicates a linear fit to the data for $L = 50, 100, 200$. The extrapolated value for p_c at $L \to \infty$ is $p_c = 0.5914$.

6.4.5 Estimating p_c and ν using the scaling ansatz

However, this result depends on knowing the value for ν. What if we did not know neither ν nor p_c. How can we estimate both from the scaling ansatz? On alternative is to generate plots of p_x as a function of $L^{-1/\nu}$ for several values of x. Then we adjust the values of ν until we get a straight line, in that case we can read of the intersect with the p_x axis as the value for p_c.

However, we can do even better by noticing a trick: For two x values x_1 and x_2, we get

$$dp = p_{\Pi=x_1}(L) - p_{\Pi=x_2}(L) = (C_{x_1} - C_{x_2})L^{-\nu} \ , \tag{6.34}$$

and we can therefore plot $\log(dp)$ as a function of $\log(L)$ to get ν, and then use this to estimate p_c.

As an exercise, the reader is encouraged to demonstrate that this scaling ansatz is valid for $d = 1$, and in this case find C_x explicitly.

6.4.6 (Advanced) Finite-size scaling for $d\Pi(p, L)/dp$

We can make our theory even more elegant by looking at the derivative of Π instead of Π.

What is the interpretation of $\Pi' = d\Pi/dp$? Since we know that

$$\int_0^1 \Pi dp = p \ , \tag{6.35}$$

we find that Π' is normalized

$$\int_0^1 \Pi' dp = 1 \; . \tag{6.36}$$

Our interpretation of Π' is that $\Pi'(p)dp$ is the probability that the system percolates for the first time in the interval from p to $p+dp$. In an infinite system we know that Π is a step-function which goes abruptly from 0 to 1 at p_c. The derivative is the delta-function, which is zero everywhere, except in a small region around p_c.

We use our scaling ansatz to find the derivative:

$$\Pi' = L^{1/\nu}\Phi'[(p-p_c)L^{1/\nu}] \; . \tag{6.37}$$

In particular we find that

$$\Pi'(p_c) = L^{1/\nu}\Phi'[0] \; . \tag{6.38}$$

We also find that position of the maximum of Π' is given by the second derivative

$$\Pi'' = L^{2/\nu}\Phi''[(p-p_c)L^{1/\nu}] \; . \tag{6.39}$$

and we will be looking for where $\Pi'' = 0$. Let us suppose that the value x_0 makes the second derivate zero, that is, suppose that $\Phi'(x)$ has a maximum at $x = x_0$.

At the maximum of Φ' we have that

$$(p_{\max} - p_c)L^{1/\nu} = x_0 \; , \tag{6.40}$$

and therefore

$$p_{\max} = p_c + \frac{x_0}{L^{1/\nu}} \; . \tag{6.41}$$

In each numerical experiment we are really measuring an effective p_c, but as $L \to \infty$ we see that $p_{eff} \to p_c$. The way it goes to p_c tells us something about ν.

Average of the distribution. Because Π' is a probability density, we can also calculate the average p of this distribution, that is the average p at which we first get a percolation cluster in a system of size L. Let us call this quantity $\langle p \rangle$.

$$\langle p \rangle = \int_0^1 p\Pi'(p)dp \tag{6.42}$$

$$= L^{-1/\nu} \int_0^1 pL^{1/\nu}\Phi'[(p-p_c)L^{1/\nu}]dpL^{1/\nu} \tag{6.43}$$

$$= \int_0^1 (p-p_c)L^{1/\nu}\Phi'[(p-p_c)L^{1/\nu}]dp + p_c \int_0^1 \Pi' dp \tag{6.44}$$

where the last integral is the normalization integral, and is 1.

We therefore get the result that

$$\langle p \rangle = p_c + L^{-1/\nu} \int x\Phi'[x]dx \ , \tag{6.45}$$

where the last integral is simply a constant, so that we can write the average critical percolation threshold in a finite system size as

$$\langle p \rangle = p_c + CL^{-1/\nu} \tag{6.46}$$

Which is not located exactly at p_c but the shift decreases with L.

6.5 Exercises

Exercise 6.1: Finite-size scaling in one dimension

a) Show that the scaling ansatz for $\Pi(p, L)$ is valid for $d = 1$.

b) Find an explicit expression for C_x for $d = 1$.

Exercise 6.2: Finite-size scaling in two dimensions

In this exercise we will use the scaling ansatz to provide estimates of ν, p_c and the average percolation probability $\langle p \rangle$ in a system of size L.

We define p_x so that $\Pi(p_x, L) = x$. Notice that p_x is a function of system size L used for the simulation.

a) Find p_x for $x = 0.3$ and $x = 0.8$ for $L = 25, 50, 100, 200, 400, 800$. Plot p_x as a function of L.

According to the scaling theory we have

$$p_{x_1} - p_{x_2} = \left(C_{x_1} - C_{x_2}\right) L^{-1/\nu} \ . \tag{6.47}$$

b) Plot $\log(p_{0.8} - p_{0.3})$ as a function of $\log(L)$ to estimate the exponent ν. How does it compare to the exact result?

In the following, please use the exact value $\nu = 4/3$. The scaling theory also predicted that

$$p_x = p_c + C_x L^{-1/\nu} \ . \tag{6.48}$$

c) Plot p_x as a function of $L^{-1/\nu}$ to estimate p_c. Generate a data-collapse plot for $\Pi(p, L)$ to find the function $\Phi(u)$ described above.

d) Plot $\Pi'(p, L)$ as a function of p for the various L values used above. Generate a data-collapse plot of $\Pi'(p, L)$. Find $\langle p \rangle$ and plot $\langle p \rangle$ as a function of $L^{-1/\nu}$ to find p_c.

Exercise 6.3: Finite size scaling of $n(s, p_c, L)$

a) Develop a finite size scaling ansatz/theory for $n(s, p_c, L)$. You should provide arguments for the behavior in the various limits.

b) Plot $n(s, p_c, L)$ as a function of s for $L = 100, 200, 400, 800$.

c) Demonstrate the validity of the scaling theory by producing a data-collapse plot for $n(s, p_c, L)$.

7 Renormalization

We have now learned that when p approaches p_c, the correlation length grows to infinity, and the spanning cluster becomes a self-similar fractal structure. This implies that the spanning cluster has statistical self-similarity: if we cut out a piece of the spanning cluster, and rescale the lengths in the system, the rescaled system will have the same geometrical properties as the original system. In particular, the rescaled system will have the same mass scaling relation: it will also be a self-similar fractal with the same scaling properties.

What happens when $p \neq p_c$? In this case, there will be a finite correlation length, ξ, and a rescaling of the lengths in the system implies that the correlation length is also rescaled. A rescaling by a factor b corresponds to making an average over b^d sites in order to form the new lattice. Now, we will simply assume that this also implies that the correlation length is reduced by a factor b: $\xi' = \xi/b$. After a few iterations of this rescaling procedure, the correlation length will correspond to the lattice size, and the lattice is uniform.

We could have made this argument even simpler by initially stating that we divide the system into parts that are larger than the correlation length. Again, this would lead to a system that is homogeneous from the smallest lattice spacing an upwards. We can conclude that when $p < p_c$, the system behaves as a uniform, unconnected system. and when $p > p_c$, the system is uniform and connected.

The argument we have sketched above is the essence of the renormalization group argument. It is only exactly at $p = p_c$ that an iterative rescaling is a non-trivial fix point: the system iterates onto itself because it is a self-similar fractal. When p is away from p_c, rescaling iterations will make the system progressively more homogeneous, and effectively bring the rescaled p towards either 0 or 1.

In this section we will provide an introduction to the theoretical framework for renormalization. This is a powerful set of techniques, introduced for equilibrium critical phenomena by Kadanoff [19] in 1966 and by Wilson [40] in 1971. Wilson later received the Nobel prize for his work on critical phenomena.

7.1 The renormalization mapping

Let us return to our theoretical model for our study of disorder: the model porous medium with occupation probability p. We will study a system of size L with a correlation length ξ, which is a function of p. We will call the length of a side of a single site a, and we ensure that

$$L \gg \xi \gg a \ . \tag{7.1}$$

We will not address whether it is possible to average over some of the sites in such a way that the macroscopic behavior does not change significantly. That is, we want to replace cells of b^d sites with new, "renormalized" single sites. This averaging procedure is illustrated in Fig. 7.1.

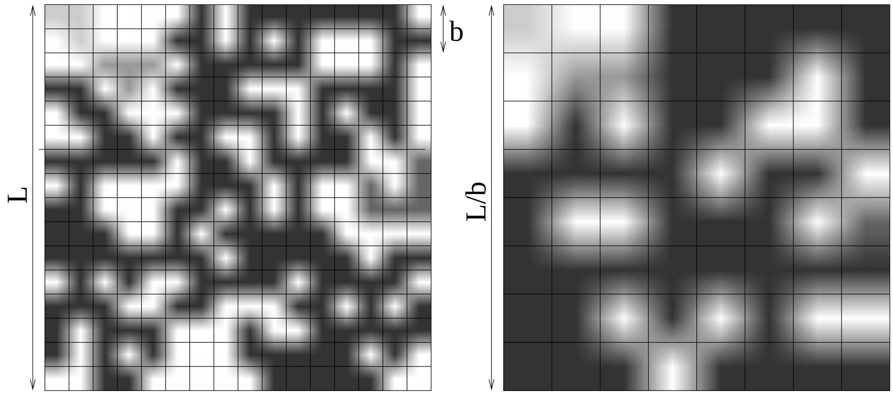

Fig. 7.1 Illustration of averaging using a rescaling $b = 2$, so that a cell of size $b \times b = 2 \times 2$ is reduced to a single site, producing a "renormalized" system of size $L/2$. The original pattern was generated with $p = 0.625$ for a $L = 16$ lattice.

In the original lattice the occupation probability is p. However, through our averaging procedure, we may change the occupation probability for the new, averaged sites. We will therefore call the new occupation probability p' - the probability to occupy a renormalized site. We write the mapping between the original and the new occupation probabilities as

$$p' = R(p) \; , \tag{7.2}$$

where the function $R(p)$, which provides the mapping, depends on the details of the rule used for renormalization. It is important to realize that the system size L and the correlation length ξ does not change in real terms, it is only in units of lattice constants they are changing.

There are many choices for the mapping between the original and the renormalized lattice. We have illustrated a particular rule for a mapping with a rescaling $b = 2$ in Fig. 7.2. For a site percolation problem with $b = 2$ there are b^d possible configurations. The different configurations are classified into the 6 categories c, where the number of configurations in each category is listed below. In Fig. 7.2 we have also illustrated a particular averaging rule. However, we could also have chosen different rules. Usually, we should ensure that the global information is preserved by the mapping. For example, we would want the mapping to conserve connectivity. That is, we would like to ensure that

$$\Pi(p, L) = \Pi(p', \frac{L}{b}) \; . \tag{7.3}$$

However, even though we may ensure this on the level of the mapping, this does not ensure that the mapping actually conserves connectivity when applied to a large cluster - it may, for example, connect clusters that were unconnected in the original lattice, or disconnect clusters that were connected, as illustrated in Fig. 7.3.

Currently, we will not consider the details of the renormalization mapping $p' = R(p)$, we will only assume that such a map exists and study its qualitative features. Then we will address the renormalization mapping through two worked examples. For any choice of mapping, the rescaling must result in a change in the correlation length ξ:

$$\xi' = \xi(p') = \frac{1}{b}\xi(p) \; . \tag{7.4}$$

We will use this relation to address the fixpoints of the mapping. A fixpoint is a point p^* that does not change when the mapping is applied. That is

$$p^* = R(p^*) \; . \tag{7.5}$$

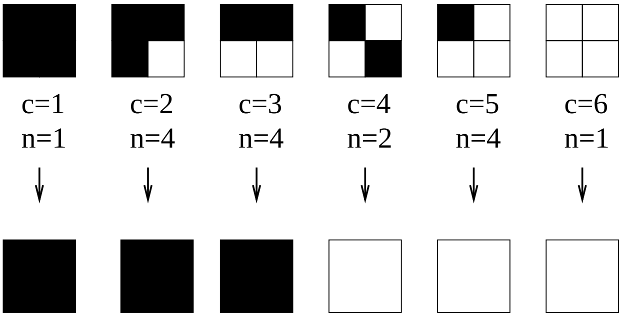

Fig. 7.2 Illustration of a renormalization rule for a site percolation problem with a rescaling $b = 2$. The top row indicates various clusters categorized into 6 classes c. The number of different configurations n in each class is also listed. The mapping ensures that connectivity is preserved. However, this renormalization mapping is not unique: we could have chosen many different averaging schemes.

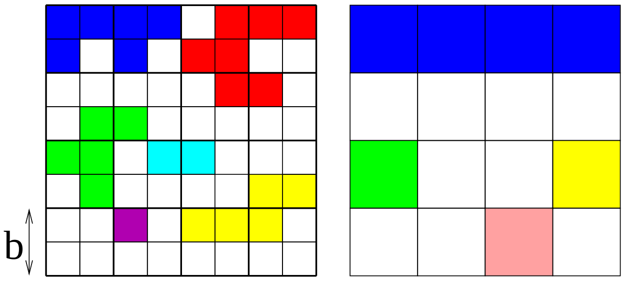

Fig. 7.3 Illustration of a single step of renormalization on an 8×8 lattice of sites. We see that the renormalization procedure introduces new connections: the blue cluster is now much larger than in the original. However, the procedure also removes previously existing connections: the original yellow cluster is split into two separate clusters.

There are two trivial fixpoints : $p = 0$ and $p = 1$. At a fixpoint, the iteration relation for the correlation length becomes:

$$\xi(p^*) = \frac{\xi(p^*)}{b} \; . \tag{7.6}$$

This relation is satisfied at the two trivial fixpoints, because the correlation length is zero here, $\xi(0) = \xi(1) = 0$. The only possible solutions for $\xi(p^*) = \xi(p^*)/b$ is for $\xi = 0$ or for $\xi = \infty$.

Let us assume that there exists a non-trivial fixpoint p^*, and let us address the behavior for p close to p^*. We notice that for any finite ξ, iterations by the renormalization relation will reduce ξ. That is, both for $p < p^*$ and for and for $p > p^*$ iterations will make ξ smaller. This implies that iterations will take the system further away from the non-trivial fixpoint, where the correlation length is infinite. The non-trivial fixpoint is therefore an unstable fixpoints. Similarly, for p close to a trivial fixpoint, where $\xi = 0$, iterations will decrease p, and the renormalized system will move closer to the fixpoint in each iteration. The trivial fixpoint is therefore stable.

Iterations by the renormalization relation $p' = R(p)$ may be studied through on the graph $R(p)$, as illustrated in Fig. 7.4. Consecutive iterations take the system along the arrows illustrated in the figure, as the reader should convince himself of by following the mapping. Notice that the line $p' = p$ is drawn as a dotted reference line. In the figure, the two end points, $p = 0$ and $p = 1$ are the only stable fixpoints, and the points p^* is the only unstable fixpoints. The actual shape of the function $R(p)$ depends on the renormalization rule, and the shape may be more complex than what is illustrated in Fig. 7.4.

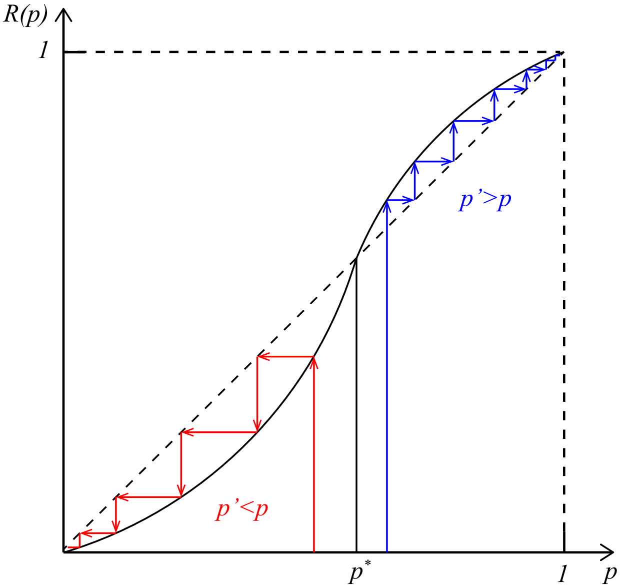

Fig. 7.4 Illustration the renormalization mapping $p' = R(p)$ as a function of p. The non-trivial fixpoint $p^* = R(p^*)$ is illustrated. Two iterations sequences are illustrated by the lines with arrows. Let us look at the path starting from $p > p^*$. Through the first application of the mapping, we read off the resulting value of p'. This value will then be the input value for the next application of the renormalization mapping. A fast way to find the corresponding position along the p axis is to reflect the p' value from the line $p' = p$ shown as a dotted line. This gives the new p value, and the mapping is applied again producing yet another p' which is even further from p^*. With the drawn shape of $R(p)$ there is only one non-trivial fixpoint, which is unstable.

7.1.1 (Advanced) Renormalization of correlation length

Let us make small diversion, and see what consequences the renormalization of the correlation length has if we know that there exists a percolation threshold p_c. In that case, we know that

$$\xi(p) = \xi_0(p - p_c)^{-\nu} \; , \tag{7.7}$$

and

$$\xi(p') = \xi_0(p' - p_c)^{-\nu} \; . \tag{7.8}$$

We can then use the renormalization condition for the correlation length from (7.4) to obtain:

$$\frac{1}{b}\xi_0(p - p_c)^{-\nu} = \xi_0(p' - p_c)^{-\nu} \; . \tag{7.9}$$

When $p \to p_c$, we see that both $\xi(p)$ and $\xi(p')$ approaches infinity, which implies that if $p = p_c$, then we must also have that $p' = p_c$. That is, we have found that p_c is a fixpoint of the mapping.

7.1.2 Iterating the renormalization mapping

We are now ready for a more quantitative argument for the effect of iterations through the renormalization mapping $R(p)$. We can argue that we have found that the non-trivial fixpoint corresponds to the percolation threshold, since the correlation length is diverging for this value of p, and we will indeed assume that we can identify p_c as the fixpoints, as we argued more quantitatively above.

We will now assume that $R(p)$ is an analytic function. This is not a strong assumption, since for any simple $R(p)$ based on polynomials of p and $1 - p$ this is trivially fulfilled. We will not Taylor expand the mapping $p' = R(p)$ around $p = p^*$. First, we notice that

$$p' - p^* = R(p) - R(p^*) \; . \tag{7.10}$$

The Taylor expansion of $R(p)$ for a p close to p^* is:

$$R(p) = R(p^*) + R'(p^*)(p - p^*) + o(p - p^*)^2 \; . \tag{7.11}$$

If we define $\Lambda = R'(p^*)$, we can write to first order in $p - p^*$:

$$p' - p^* \simeq \Lambda(p - p^*) \; , \tag{7.12}$$

We see that the value of Λ characterizes the fixpoint. For $\Lambda > 1$ the new point p' will be further away from p^* than the initial point p. Consequently, the fixpoint is unstable. By a similar argument, we see that for $\Lambda < 1$ the fixpoint is stable. For $\Lambda = 1$ we call the fixpoint a marginal fixpoint.

Let us now assume that the fixpoint is indeed the percolation threshold. In this case, when p is close to p_c, we know that the correlation length is

$$\xi(p) = \xi_0 (p - p_c)^{-\nu} , \tag{7.13}$$

for the initial point, and

$$\xi(p') = \xi_0 (p' - p_c)^{-\nu} \tag{7.14}$$

for the renormalized point. We will now use (7.12) for $p^* = p_c$, giving

$$p' - p_c = \Lambda (p - p_c) . \tag{7.15}$$

Inserting this into (7.14) gives

$$\xi(p') = \xi_0 (p' - p_c)^{-\nu} = \xi_0 (\Lambda (p - p_c))^{-\nu} = \xi_0 \Lambda^{-\nu} (p - p_c)^{-\nu} . \tag{7.16}$$

We can rewrite this using $\xi(p)$

$$\xi(p') = \Lambda^{-\nu} \xi(p) . \tag{7.17}$$

However, we also know that

$$\xi(p') = \frac{1}{b} \xi(p) . \tag{7.18}$$

Consequently, we have found that

$$b = \Lambda^{\nu} . \tag{7.19}$$

This implies that the exponent ν is a property of the fixpoint of the mapping $R(p)$. We can find ν from

$$\nu = \frac{\ln b}{\ln \Lambda} , \tag{7.20}$$

where we remember that $\Lambda = R'(p_c)$.

7.1.3 Application of renormalization to ξ

We will now show that we can achieve all of these results just from a simple assumption on the effect of renormalization on the correlation length. Trivially, a renormalization procedure will lead to a change in correlation length. Starting at p with a correlation length $\xi(p)$, a renormalization step will produce a new occupation probability p' and a new correlation length $\xi'(p')$. The fundamental assumption in the theory for the renormalization group is that the functional form of ξ and ξ' is the same. That is, that we can write

$$\xi'(p') = \xi(p') \ , \tag{7.21}$$

where $\xi(p)$ was the functional form of the correlation length in the original system. At least we should be able to make this assumption in some small neighborhood around p_c. That is, we assume that $\xi(p) = \xi'(p)$ for $|p - p_c| \ll 1$. In this case, we can write the correlation function as a function of the deviation from p_c: $\epsilon = p - p_c$. Similarly, we define $\epsilon' = p' - p_c$. The relation between the correlation lengths can then be written as

$$\xi(\epsilon') = \frac{\xi(\epsilon)}{b} \ , \tag{7.22}$$

where $\xi(u)$ is a particular function of u. The Taylor expansion of the renormalization mapping $R(p)$ in (7.12) can also be rewritten in terms of ϵ giving

$$\epsilon' = \Lambda\epsilon \ . \tag{7.23}$$

We can therefore rewrite (7.22) as

$$\xi(\epsilon') = \xi(\Lambda\epsilon) = \frac{\xi(\epsilon)}{b} \ , \tag{7.24}$$

or, equivalently

$$\xi(\epsilon) = b\xi(\Lambda\epsilon) \ . \tag{7.25}$$

This implies that $\xi(\epsilon)$ is a homogeneous function. Let us see how this function responds to iterations. We notice that after an iteration, the new value of ϵ is $\Lambda\epsilon$, and we can write

$$\xi(\Lambda\epsilon) = b\xi(\Lambda\Lambda\epsilon) = b\xi(\Lambda^2\epsilon) \ . \tag{7.26}$$

We can insert this value into (7.25) to get

$$\xi(\epsilon) = b\xi(\Lambda\epsilon) = b^2\xi(\Lambda^2\epsilon) \ . \tag{7.27}$$

We can continue this process up to any power n, giving

$$\xi(\epsilon) = b^n \xi(\Lambda^n \epsilon) \ , \tag{7.28}$$

for any $n \geq 1$, where we have implicitly assumed that $b > 1$.

Let us now prove that (7.28) implies that $\xi(\epsilon)$ is to leading order a power-law, and let us also find the exponent. We choose a value of n to that

$$\Lambda^n \epsilon = c \ , \tag{7.29}$$

which implies that

$$n = \frac{\ln c/\epsilon}{\ln \Lambda} \ . \tag{7.30}$$

We can always ensure that this produces a value $n > 1$ by selecting c sufficiently small. If we insert this value of n into (7.28) we get

$$\xi(\epsilon) = b^{(\frac{\ln c/\epsilon}{\ln \Lambda})} \xi(c) = e^{\ln b (\frac{\ln c/\epsilon}{\ln \Lambda}} \xi(c) \tag{7.31}$$

$$= (\frac{c}{\epsilon})^{\frac{\ln b}{\ln \Lambda}} \xi(c) \propto \epsilon^{-\nu} \ , \tag{7.32}$$

where ν is given as

$$\nu = \frac{\ln b}{\ln \Lambda} \ . \tag{7.33}$$

We have now proved that the solution to the equation $\xi(p') = \xi(p)/b$ is a power-law function $\xi \propto |p - p_c|^{-\nu}$ with the exponent ν given by (7.33).

This argument shows that the most important assumption of the renormalization theory, is that the functional form $\xi(p)$ does not change by the renormalization procedure. It is important to realize that this is an assumption, and we will then have to check whether this produces reasonable results.

7.2 Examples

In the following we provide several examples of the application of the renormalization theory. Our renormalization procedure can be summarized in the following points.

- Coarse-grain the system into cells of size b^d.
- Find a rule to determine the new occupation probability, p', from the old occupation probability, p: $p' = R(p)$.

- Determine the non-trivial fixpoints, p^*, of the renormalization mapping: $p^* = R(p^*)$, and use these points as approximations for p_c: $p_c = p^*$.
- Determine the rescaling factor Λ from the renormalization relation at the fixpoint: $\Lambda = R'(p^*)$.
- Find ν from the relation $\nu = \ln b / \ln \Lambda$.

It is important to realize that the renormalization mapping $R(p)$ is not unique. However, in order to obtain useful results we should ensure that the mapping preserves connectivity on average.

7.2.1 Example: One-dimensional percolation

Let us first address the one-dimensional percolation problem using the renormalization procedure. We have illustrated the one-dimensional percolation problem in Fig. 7.5. We generate the renormalization mapping by ensuring that it conserves connectivity. The probability for two sites to be connected over a distance b is p^b when the occupation probability for a single site is p. A renormalization mapping that conserves connectivity is therefore:

$$p' = \Pi(p, b) = p^b \ . \tag{7.34}$$

The fixpoints for this mapping are

$$p^* = (p^*)^b \ , \tag{7.35}$$

with only two possible solutions, $p^* = 0$, and $p^* = 1$. An example of a renormalization iteration is shown in Fig. 7.6. The curve illustrates that $p^* = 0$ is the only attractive or stable fixpoint, and that $p^* = 1$ is an unstable fixpoint.

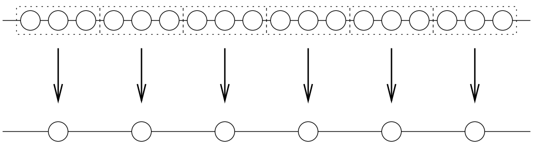

Fig. 7.5 Illustration of a renormalization rule for a one-dimensional site percolation system with $b = 3$.

We can also apply the theory directly to find the exponent ν. The renormalization relation is $p' = R(p) = p^b$. We can therefore find Λ from:

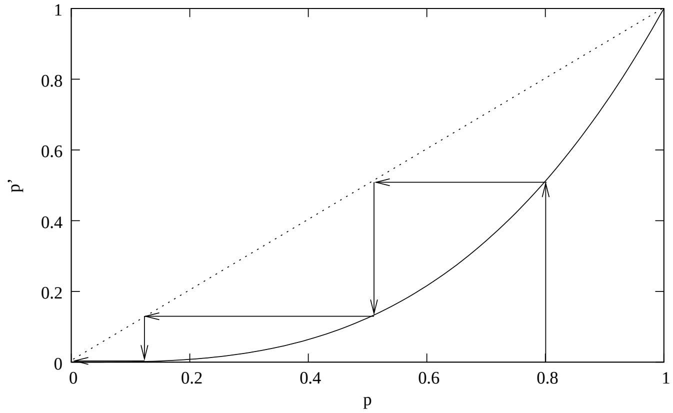

Fig. 7.6 Illustration of a renormalization rule for a one-dimensional site percolation system with $b = 3$.

$$\Lambda = \left. \frac{\partial R}{\partial p} \right|_{p^*} = b(p^*)^{b-1} = b \; , \tag{7.36}$$

where we are now studying the unstable fixpoint $p^* = 1$. We can therefore determine ν from (7.20):

$$\nu = \frac{\ln b}{\ln \Lambda} = 1 \; . \tag{7.37}$$

We notice that b was eliminated in this procedure, which is essential since we do not want the exponent to depend on details such as the size of renormalization cell. The result for the scaling of the correlation length is therefore

$$\xi \propto \frac{1}{1-p} \; , \tag{7.38}$$

when $1 - p \ll 1$.

7.2.2 Example: Renormalization on 2d site lattice

Let us now use this method to address a renormalization scheme for two-dimensional site percolation. We will use a scheme with $b = 2$. The possible configurations for a 2×2 lattice are shown in Fig. 7.7.

In order to preserve connectivity, we need to ensure that configurations $c = 1$ and $c = 2$ are occupied also in the renormalized lattice. However, for configuration $c = 3$, we may choose only to consider spanning in one direction, or spanning in both directions. If we include spanning in

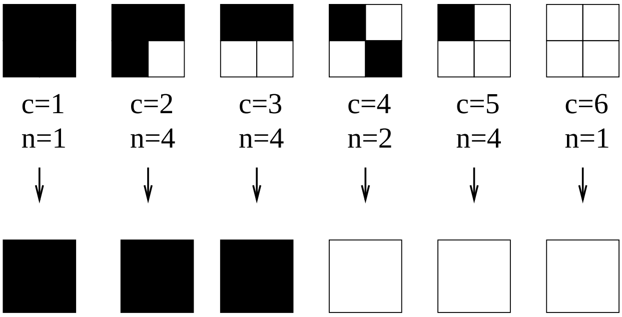

Fig. 7.7 Possible configurations for a 2×2 site percolation system. The top row indicates various clusters categorized into 6 classes c. The number of different configurations n in each class is also listed.

only one direction, there are only two of the configurations $c = 3$ that contribute the the spanning probability, and the renormalization relation becomes

$$p' = R(p) = p^4 + 4p^3(1-p) + 2p^2(1-p)^2 \; . \tag{7.39}$$

This is the probability for configurations $c = 1$, $c = 2$, or $c = 3$ to occur. The renormalization relation is illustrated in Fig. 7.8.

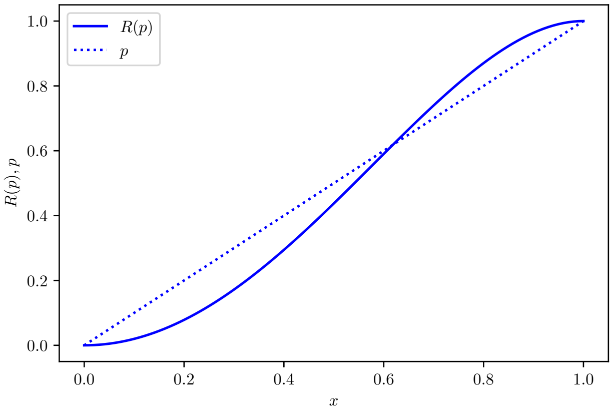

Fig. 7.8 Plot of the renormalization relation $p' = R(p) = p^4 + 4p^3(1-p) + 2p^2(1-p)^2$ for a two-dimensional site percolation problem.

We will now follow steps 3 and 4. First, in step 3, we determine the fixpoints of the renormalization relation. That is, we find the solutions to the equation

$$p^* = R(p^*) = (p^*)^4 + 4(p^*)^3(1-p^*) + 2(p^*)^2(1-p^*)^2 \; . \tag{7.40}$$

The trivial solution $p^* = 0$ is not of interest. Therefore we divide by p^* to produce

$$(p^*)^3 + 4(p^*)^2(1 - p^*) + 2(p^*)(1 - p^*)^2 = 1 \; . \tag{7.41}$$

The other trivial fixpoint is $p^* = 1$. We divide the equation by $1 - p^*$ to get

$$(p^*)^2 + p^* - 1 = 0 \; . \tag{7.42}$$

The solutions to this second order equation are

$$p^* = -\frac{1 \pm \sqrt{1+4}}{2} = \frac{\sqrt{5} \pm 1}{2} \simeq 0.62 \; . \tag{7.43}$$

We have therefore found an estimate of p_c by setting $p_c = p^*$. This does not produce the correct value for p_c in a two-dimensional site percolation system, but the result is still reasonably correct. We can similarly find the exponent ν by calculating $R'(p^*)$.

7.2.3 Example: Renormalization on 2d triangular lattice

We will now the same method to address percolation on site percolation on a triangular lattice. A triangular lattice is a lattice where each point has six neighbors. In solid state physics, the lattice is known as the hexagonal lattice because of its hexagonal rotation symmetry. Site percolation on the triangular lattice is particularly well suited for renormalization treatment, because a coarse grained version of the lattice is also a triangular lattice, as illustrated in Fig. 7.9, with a lattice spacing $b = \sqrt{3}$ times the original lattice size.

We will use the majority rule for the renormalization mapping. That is, we will map a set of three sites onto an occupied site if a majority of the sites are occupied, meaning that two or more sites are occupied. Otherwise, the renormalized site is empty. This mapping is illustrated in Fig. 7.9. This mapping does, as the reader may easily assure himself, on the average conserve connectivity. The renormalization mapping is

$$p' = R(p) = p^3 + 3p^2(1 - p) = 3p^2 - 2p^3 \; . \tag{7.44}$$

The fixpoints of this mapping are the solutions of the equation

$$p^* = 3(p^*)^2 - 2(p^*)^3 \; . \tag{7.45}$$

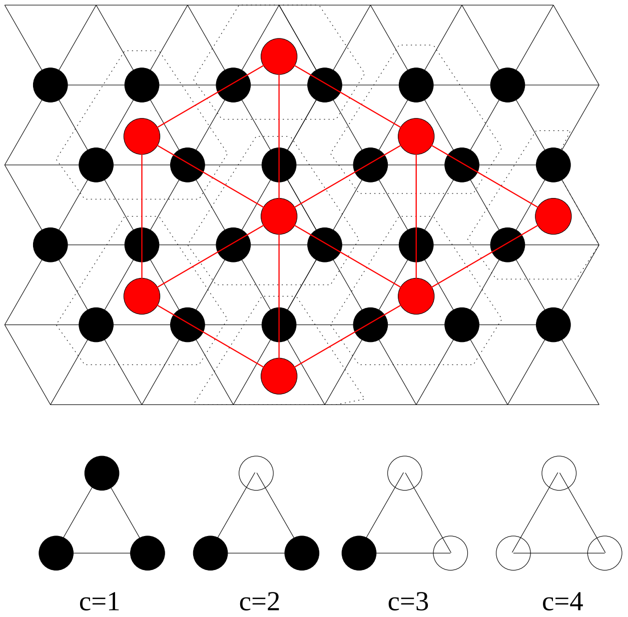

Fig. 7.9 Illustration of a renormalization scheme for site percolation on a triangular lattice. The rescaling factor is $b = \sqrt{3}$, and we use the majority rule for the mapping, that is, configurations $c = 1$ and $c = 2$ are occupied, and configurations $c = 3$ and $c = 4$ are mapped onto empty sites.

We observe that the trivial fixpoints $p^{ast} = 0$, and $p^* = 1$ indeed satisfy (7.45). The non-trivial fixpoint is $p^* = 1/2$. We are pleased to observe that this is actually the exact solution for p_c for site percolation on the triangular lattice.

We can use this relation to determine the scaling exponent ν. First, we calculate Λ:

$$\Lambda = R'(p^*) = 6p(1-p)|_{p=\frac{1}{2}} = \frac{3}{2} \, . \tag{7.46}$$

As a result we find the exponent ν from

$$\frac{1}{\nu} = \frac{\ln \Lambda}{\ln b} = \frac{\ln 3/2}{\ln \sqrt{3}} \simeq 1.355 \, , \tag{7.47}$$

which is very close to the exact result that $\nu = 4/3$ for two-dimensional percolation.

7.2.4 Example: Renormalization on 2d bond lattice

As our last example of renormalization in two-dimensional percolation problems, we will study the bond percolation problem on a square lattice. The renormalization procedure is shown in Fig. 7.10. In the renormalization procedure, we replace 8 bonds by 2 new bonds. We consider connectivity only in the horizontal direction, and may therefore simplify the lattice, by only considering the mapping of the H-cell, a mapping of five bonds onto one bond in the horizontal direction. The various configurations are shown in the figure. In table 7.1 we have shown the number of such configurations, and the probabilities for each configuration, which is needed in order to calculate the renormalization connection probability p'.

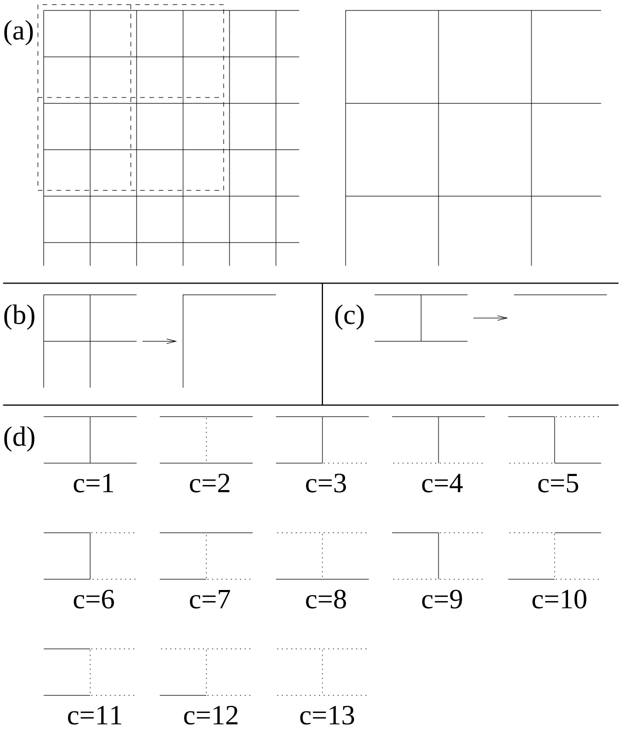

Fig. 7.10 (a) Illustration of a renormalization scheme for bond percolation on a square lattice in two dimensions. The rescaling factor is $b = 2$. (b) In general, the renormalization involves a mapping from 8 to two bonds. However, we will consider percolation only in the horizontal direction. This simplifies the mapping, to the figure shown in (c). For this mapping, the configurations are shown an enumerated in (d).

The resulting renormalization equation is given as

c		$P(c)$	$n(c)$	$\Pi\|c$
1	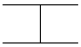	$p^5(1-p)^0$	1	1
2	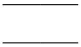	$p^4(1-p)^1$	1	1
3	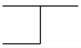	$p^4(1-p)^1$	4	1
4	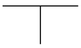	$p^3(1-p)^2$	2	1
5	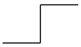	$p^3(1-p)^2$	2	1
6	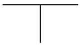	$p^3(1-p)^2$	2	0
7	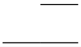	$p^3(1-p)^2$	4	1
8	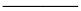	$p^2(1-p)^3$	2	1
9	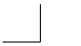	$p^2(1-p)^3$	4	0
10	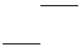	$p^2(1-p)^3$	2	0
11		$p^2(1-p)^3$	2	0
12		$p^1(1-p)^4$	5	0
13		$p^0(1-p)^5$	1	0

Table 7.1 A list of the possible configuration for renormalization of a bond lattice. The probability for percolation given that the configuration is c is denoted $\Pi|c$. The spanning probability for the whole cell is then $\Pi(p) = p' = \sum_c n(c)P(c)\Pi|c$.

$$p' = R(p) = \Pi = \sum_{c=1}^{13} n(c)P(c)\Pi|c \; , \tag{7.48}$$

where we have used c to denote the various configurations, $P(c)$ is the probability for one instance of configuration c, $n(c)$ is the number of different configurations due to symmetry consideration, and $\Pi|c$ is the spanning probability for configuration c given that the configuration is c. The resulting relation is

$$\begin{aligned} p' &= R(p) && (7.49)\\ &= p^5 + p^4(1-p) + 4p^4(1-p) + 2p^3(1-p)^2 && (7.50)\\ &\quad +2p^3(1-p)^2 + 4p^3(1-p)^2 + 2p^2(1-p)^3 && (7.51)\\ &= 2p^5 - 5p^4 + 2p^3 + 2p^2 \; . && (7.52) \end{aligned}$$

The fixpoints for this mapping are $p^* = 0$, $p^* = 1$, and $p^* = 1/2$. The fixpoints $p^* = 1/2$ provides the exact solution for the percolation threshold on the bond lattice in two dimensions. We find Λ by derivation

$$\Lambda = R'(p^*) = \frac{13}{8} \; . \tag{7.53}$$

The corresponding estimate for the exponent ν is

$$\nu = \frac{\ln b}{\ln \Lambda} \simeq 1.428 \; , \tag{7.54}$$

which should be compared with the exact result of $\nu = 4/3$ for two-dimensional percolation.

7.3 (Advanced) Universality

Even though we can choose renormalization rules that preserves connectivity statistically, the rule will not preserve connectivity exactly. The renormalization procedure is not exact. This can be illustrated by site renormalization of site percolation in two dimensions are shown in Fig. 7.11. We may speculate that various errors of this form, some of them adding together non-connected bonds, and other removing connections, would cancel out on average. However, this is not the case. For the majority rule for two-dimensional site percolation, the connectivity is not preserved, even on the average. The result is that we end up with an error in our estimate of both p_c and ν.

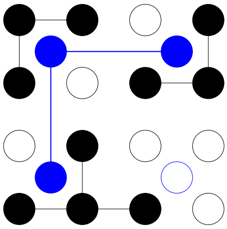

Fig. 7.11 Illustration of renormalization of connectivity for site percolation in two dimensions. The blue sites show the renormalized sites, and the lines shows which clusters are connected. In this case, we see that the renormalized lattice is spanning, even though there are no spanning clusters in the original lattice.

How can we improve this situation? We need to introduce additional bonds between the sites during the renormalization procedure to preserve connectivity, even if the original problem was a pure site problem. This will produce a mixed site-bond percolation problem. The probability q to connect two nearest-neighbors in the original site lattice must be found by counting all possible combinations of spanning between nearest neighbor sites in the original lattice. We may also have to introduce next-nearest neighbor bonds and so on.

Let us describe the renormalized problem by the two renormalized probabilities p' for sites, and x' for bonds. The renormalization procedure will be described by a set of two renormalization relations:

$$p' = R_1(p, x) \tag{7.55}$$

$$x' = R_2(p, x) \tag{7.56}$$

Now, the flow in the renormalization procedure will not simply be along the p axis, but will occur in the two-dimensional p, x-space, as illustrated in Fig. 7.12. We will no longer have a single critical points, p_c, but a set of points (p_c, x_c) corresponding to a curve in p, x-space, as shown in the figure. We also notice that when $x = 1$ we have a pure site percolation problem – all bonds will be present and connectivity depends on the presence of sites alone - and similarly for $p = 1$ we have a pure bond percolation problem.

There are still two trivial fixpoints, for $(p, x) = 0$, and for $(p, x) = (1, 1)$, and we expect these points to be attractors. We will therefore need a line that separates the two trivial fixpoints. If we start on this line, we will remain on this line. We will therefore expect there to be a fixpoint on this line, the non-trivial fixpoints (p^*, x^*). We remark that the fixpoint no longer corresponds to the critical threshold - there will be a whole family of critical values corresponding to the curved, black line in Fig. 7.12.

We can find the non-trivial fixpoint from the equations

$$p^* = R_1(p^*, x^*) \tag{7.57}$$

$$x^* = R_2(p^*, x^*) \tag{7.58}$$

Let us linearize the system near the fixpoint. We will do a Taylor expansion for the two functions $R_1(p, x)$, and $R_2(p, x)$, around the point (p^*, x^*):

$$p' - p^* = \Lambda_{11}(p - p^*) + \Lambda_{12}(x - x^*) \tag{7.59}$$

$$x' - x^* = \Lambda_{21}(p - p^*) + \Lambda_{22}(x - x^*) \tag{7.60}$$

where we have defined

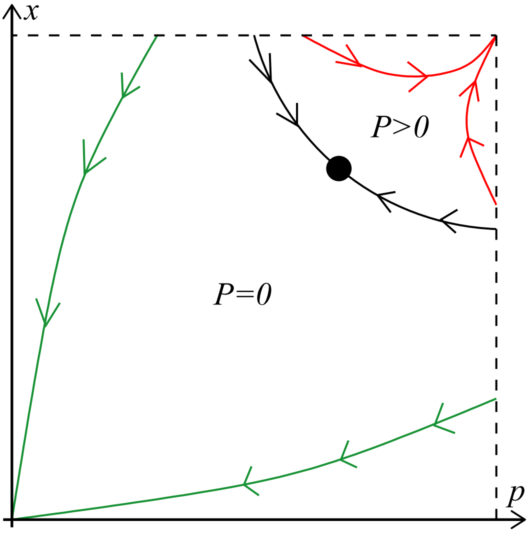

Fig. 7.12 Illustration of the flow due to renormalization in a combined site-bond percolation system. The black line shows the critical line, on which the correlation length is infinite, $\xi = \infty$. Below the critical line, renormalization will lead to the trivial fixpoint at $p, x = 0$ as illustrated by the green lines. Above the line, renormalization will lead to the fixpoint at $p, x = (1, 1)$.

$$\Lambda_{11} = \left.\frac{\partial R_1}{\partial p}\right|_{(p^*,x^*)} \quad \Lambda_{12} = \left.\frac{\partial R_1}{\partial x}\right|_{(p^*,x^*)} \tag{7.61}$$

$$\Lambda_{21} = \left.\frac{\partial R_2}{\partial p}\right|_{(p^*,x^*)} \quad \Lambda_{22} = \left.\frac{\partial R_2}{\partial x}\right|_{(p^*,x^*)} \tag{7.62}$$

We can therefore rewrite the recursion relation in matrix form, as

$$\begin{bmatrix} p' - p^* \\ x' - x^* \end{bmatrix} = \begin{bmatrix} \Lambda_{11} & \Lambda_{12} \\ \Lambda_{21} & \Lambda_{22} \end{bmatrix} \begin{bmatrix} p - p^* \\ x - x^* \end{bmatrix} . \tag{7.63}$$

We want to find the behavior after many iterations. This can be done by finding the eigenvector and the eigenvalues of the matrix. That is, we find the vectors $\mathbf{x}_i = (p_i, x_i)$ such that

$$\Lambda \mathbf{x}_i = \lambda_i \mathbf{x}_i . \tag{7.64}$$

We know that we can find two such vectors, and that the vectors are linearly independent, so that any vector $\mathbf{x}$ can be written as a linear combination of the two eigenvectors:

$$\begin{bmatrix} p - p^* \\ x - x^* \end{bmatrix} = \mathbf{x} = a_1 \mathbf{x}_1 + a_2 \mathbf{x}_2 \; . \tag{7.65}$$

Applying the renormalization mapping will therefore produce

$$\Lambda \mathbf{x} = \lambda_1 a_1 \mathbf{x}_1 + \lambda_2 a_2 \mathbf{x}_2 \; , \tag{7.66}$$

and after N iterations we get

$$\Lambda^N \mathbf{x} = \lambda_1^N a_1 \mathbf{x}_1 + \lambda_2^N a_2 \mathbf{x}_2 \; . \tag{7.67}$$

We see that if both $\lambda_1 < 1$ and $\lambda_2 < 1$, then any deviation from the fixpoint will approach zero after many iterations, because the values $\lambda_1^N \rightarrow 0$, and $\lambda_2^N \rightarrow 0$. We call eigenvalues in the range $0 < \lambda < 1$ irrelevant, and the fixpoint is stable. Eigenvalues with $\lambda > 1$ are termed relevant, because the fixpoint will move away along the direction specified be the corresponding eigenvector. Eigenvalues $\lambda = 1$ are termed marginal — there is no movement along this direction.

Let us look at the case when $\lambda_1 > 1 > \lambda_2$, which corresponds to what we will call a simple critical point. (For a simple critical point, there is only one relevant eigenvalue, and all other eigenvalues are irrelevant.) This corresponds to a stable behavior in the direction $\mathbf{x}_2$, and an unstable behavior in the $\mathbf{x}_1$ direction. That is, the behavior is like a saddle point, as illustrated in Fig. 7.13. This is consistent with the picture of a critical line. The flow along the line corresponds to the stable direction, and the flow normal to the line corresponds to the unstable direction, which is the natural generalization of the behavior we found in one dimension. Therefore any point which is originally close to the line, will first flow towards the fixpoint (p^*, x^*), before it flows out in the direction of the the relevant eigenvector.

Let us now study the behavior close to the critical line in detail for a system with $\lambda_1 > 1 > \lambda_2$. We notice that the correlation length ξ is infinite along the whole critical line, because it does not change by iterations along the critical line. That is, we have just a single fixpoint, but infinitely many critical points corresponding to a critical line. Let us start at a point $(p_0, 1)$ close to the critical line, and perform renormalization in order to find the functional shape of ξ and the exponent ν. After k iterations, the point has moved close to the fixpoint, just before it is expelled out from the fixpoint. We can therefore write

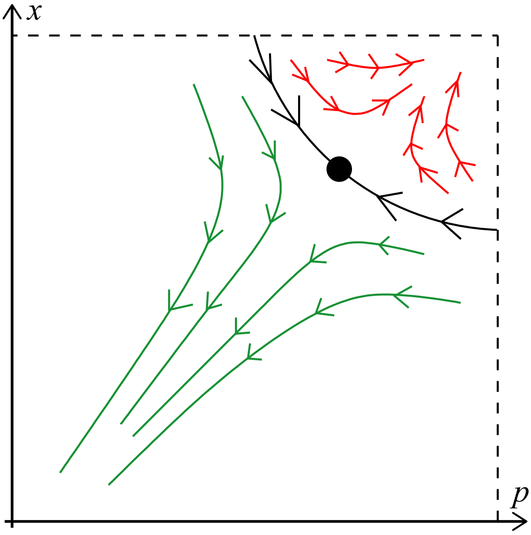

Fig. 7.13 Illustration of the flow around the unstable saddle point corresponding to the fixpoint p^*. The black line shows the critical line, on which the correlation length is infinite, $\xi = \infty$. Below the critical line, renormalization will lead to the trivial fixpoint at $p, x = 0$ as illustrated by the green lines. Above the line, renormalization will lead to the fixpoint at $p, x = (1, 1)$.

$$\begin{bmatrix} p^{(k)} - p^* \\ x^{(k)} - x^* \end{bmatrix} = a_1 \mathbf{x}_1 + a_2 \mathbf{x}_2 \ . \tag{7.68}$$

Since the iteration point is close to the fixpoint, we will assume that we can use the linear expansion around the fixpoint to address the behavior of the system. After a further l iterations we assume that we are still in the linear range, and the renormalized position in phase-space is

$$\begin{bmatrix} p^{(k+l)} - p^* \\ x^{(k+l)} - x^* \end{bmatrix} = \lambda_1^l a_1 \mathbf{x}_1 + \lambda_2^l a_2 \mathbf{x}_2 \ . \tag{7.69}$$

We stop the renormalization procedure at $l = l^*$ when $a_1^(l) \simeq 0.1$ (or some other small value that we can choose). That is

$$\lambda_1^{l^*} a_1 \simeq 0.1 \ . \tag{7.70}$$

The correlation length for this number of iterations is

$$\xi^{(k+l^*)} = \frac{\xi(p_0, 1)}{b^{(k+l^*)}} \ . \tag{7.71}$$

We have therefore found an expression for the correlation length in the point $(p_0, 1)$

$$\xi(p_0, 1) = \xi(a_1 = 0.1) b^{(k+l^*)} , \tag{7.72}$$

where the value $\xi(a_1 = 0.1)$ is a constant due to the way we have chosen l^*. The value for l^* is

$$l^* = \frac{\ln(\frac{0.1}{a_1})}{\ln \lambda_1} . \tag{7.73}$$

We have therefore found that the correlation length in the original point $(p_0, 1)$ is

$$\xi(p_0, 1) = b^k b^{\frac{\ln(0.1/a_1)}{\ln \lambda_1}} = b^k (\frac{0.1}{a_1})^{\frac{\ln b}{\ln \lambda_1}} . \tag{7.74}$$

We can express this further as:

$$\xi(p_0, 1) \propto (\frac{1}{a_1})^{\frac{\ln b}{\ln \lambda_1}} = (\frac{1}{a_1})^{\nu} = a_1^{-\nu} . \tag{7.75}$$

Now, what is a_1? This is the value of a_1 at the original point, $(p_0, 1)$, which we can relate the the critical threshold p_c for pure site percolation:

$$a_1 = a_1(p_0, 1) = a_1(p_c + (p_0 - p_c)) \tag{7.76}$$

$$\simeq a_1(p_c) + a_1'(p_c)(p_0 - p_c) \tag{7.77}$$

$$= A(p_0 - p_c) \tag{7.78}$$

where we have done a Taylor expansion around p_c. We have used that $a_1(p_c, 1) = 1$, since this is a point on the critical line, and $A = a_1'(p_c)$. If we put this relation back into (7.74), we get

$$\xi(p_0, 1) \propto a_1^{-\nu} \propto (p - p_c)^{-\nu} . \tag{7.79}$$

We have therefore shown by renormalization arguments, that ξ has a power-law behavior with exponent ν. However, we can make a similar argument starting at a point $(1, q_0)$ close the the critical point q_c. That is, we could start from a pure bond percolation problem, and we would end up with a similar relation for the correlation length

$$\xi \propto |q_0 - q_c|^{-\nu} , \tag{7.80}$$

where the exponent ν depends on λ_1.

We have therefore shown that the exponent ν is the same in these two cases. This is an example of universality. Both pure site and pure bond percolation leads to a power-law behavior for the correlation length ξ

with the same power-law exponent ν. We can also use similar arguments to argue that the critical exponent ν is the same below and above the percolation threshold.

7.4 (Advanced) Fragmentation

We will use the concepts and tools we have developed so far to address several problems of interest. First, let us address fragmentation: a large body that is successively broken into smaller part due to fracturing. There can be many processes that may induce and direct the fracturing of the grain. For example. the fracturing may depend on an external load placed on the grain, on a rapid change in temperature in the grain, on a high-amplitude sound wave propagating through the grain, or by stress-corrosion or chemical decomposition processes. Typical examples of fragment patterns are shown in Fig. 7.14.

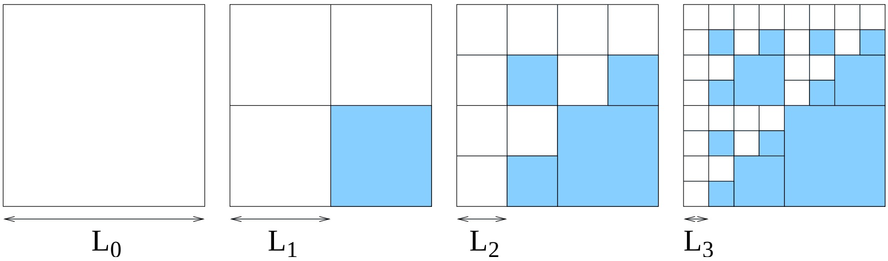

Fig. 7.14 Illustration of a deterministic fragmentation model. The shaded areas indicate the regions that will not fragment any further. That is, this drawing illustrates the case of $f = 3/4$.

Why did I choose D to denote this exponent? Let us look at the scaling properties of the structure generated by these iterations. Let us first assume that we describe the system purely geometrically, and that we are interested in the geometry of the regions that have fragmented. We will therefore assume that areas that are no longer fracturing are removed, and we are studying the mass that is left by this process. Let us start at a length-scale ℓ_n, where the mass of our system is m_n, and let us find what the mass will be when the length is doubled. For $f = 3/4$ we can then generate the new cluster by placing three of the original clusters into three of the four placed in the two-by-two square as illustrated in Fig. 7.15. The rescaling of mass and length is therefore: $\ell_{n+1} = 2\ell_n$, and

$m_{n+1} = 3m_n$. Similarly, for arbitrary f, the relations are $\ell_{n+1} = 2\ell_n$, and $m_{n+1} = 4fm_n$. As we found in section 5.5, this is consistent with a power-law scaling between the mass and length of the set

$$m(L) = m_0(\frac{L}{L_0})^D , \tag{7.81}$$

where $D = \ln 3/\ln 2$ is the fractal dimension of the structure. The value for the case of general f is similarly $D = \ln(4f)/\ln 2$.

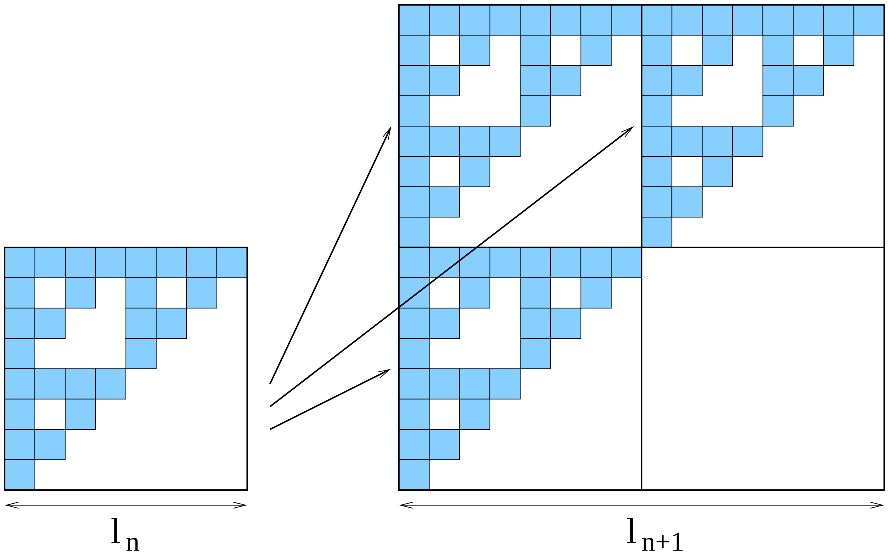

Fig. 7.15 Illustration of construction by length and mass rescaling. Three instances of the fully developed structure with mass m_n and length ℓ_n is used to generate the same structure at a length ℓ_{n+1} and with mass $m_{n+1} = 3m_n$. The mass corresponds to the mass of the regions that are not left unfragmented.

Remember that we now calculated the mass dimension of the part of the system that is present, that is the part of the system that is still fragmenting into smaller pieces. The mass dimension of the part of the system that is no longer fragmenting should be $D' = d$, which is the fractal dimension of the "dust" left by the fragmentation processes.

The methodology that we have introduced to describe fragmentation here, is consistent with the argument of Steacy and Sammis [38] for the grains size distribution in fault gouges. They argue that during the fragmentation process, two grains of the same size cannot be nearest neighbors without fragmenting. There may be various physics arguments for this assumption, but we will not discuss them in detail here. If this argument is applied in a simple cubic three-dimensional lattice, the remaining fragments will look like Fig. 7.16. However, we realize that this is identical to the fragmentation model introduced here, because features such as the size distribution (and the mass dimension of the unfractured grains), does not depend on where the remaining grains are placed in space, only in the relative density of unfractured grains in each generation. The model of Sammis *et al.* therefore corresponds to the fragmentation model with $f = 6/8$, and with spatial dimensionality $d = 3$. We have therefore found the prediction $D = \ln 6 / \ln 2 \simeq 2.58$ for the grain size distribution in fault gouges.

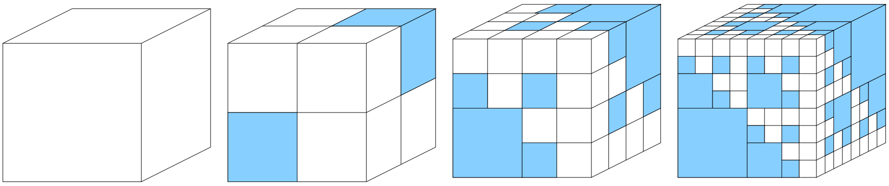

Fig. 7.16 Illustration of the fragmentation model. In each iteration, each cubical grain is divided into 8 identical smaller cubes. The fundamental rule for the model is that if there are two neighboring grains of the same size, one of them will fracture. In the figure we have shaded the regions that are not fragmented in this process for the first few steps of the iterations.

It is important to realize that the argument of Sammis *et al.* depends on the dimensionality of the system, and on the lattice used. For example, in two dimensions the argument leads to a fractal dimension $D = 1$ for a square system (corresponding to a line), whereas a triangular lattice produces a dimension between 1 and 2. We leave it as an exercise for the reader to find the dimension in this case.

7.5 Exercises

Exercise 7.1: Renormalization of nnn-model

a) Develop a renormalization scheme for a two-dimensional site percolation system with next-nearest neighbor connectivity. That is, list the 16 possible configurations, and determine what configuration they map onto in the renormalized lattice.

b) Find the renormalized occupation probability $p' = R(p)$.

c) Plot $R(p)$ and $f(p) = p$.

d) Find the fixpoints p^* so that $R(p^*) = p^*$.

e) Find the rescaling factor $\Lambda = R'(p^*)$.

f) Determine the exponent $\nu = \ln \Lambda / \ln b$.

g) How can we improve the estimates of p_c and ν?

Exercise 7.2: Renormalization of three-dimensional site percolation model

a) Find all 2^8 possible configurations for the $2 \times 2 \times 2$ renormalization cell for three-dimensional site percolation.

b) Determine a renormalization scheme - what configurations map onto an occupied site?

c) Find the renormalized occupation probability $p' = R(p)$.

d) Plot $R(p)$ and $f(p) = p$.

e) Find the fixpoints p^* so that $R(p^*) = p^*$.

f) Find the rescaling factor $\Lambda = R'(p^*)$.

g) Determine the exponent $\nu = \ln \Lambda / \ln b$.

Exercise 7.3: Renormalization of three-dimensional bond percolation model

In this exercise we will develop an H-cell renormalization scheme for bond percolation in three dimensions. The three-dimensional H-cell is illustrated in fig. 7.17.

a) Find all 2^12 possible configurations for this H-cell.

b) Determine a renormalization scheme - what configurations map onto an occupied site?

c) Find the renormalized occupation probability $p' = R(p)$.

d) Plot $R(p)$ and $f(p) = p$.

e) Find the fixpoints p^* so that $R(p^*) = p^*$.

f) Find the rescaling factor $\Lambda = R'(p^*)$.

g) Determine the exponent $\nu = \ln \Lambda / \ln b$.

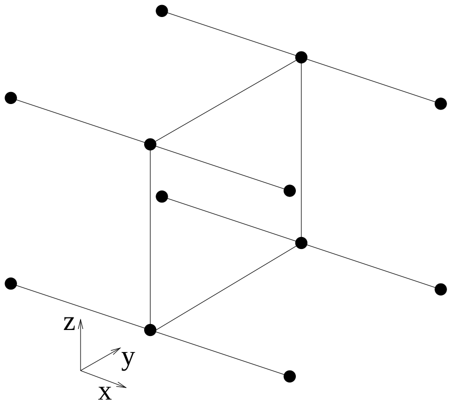

Fig. 7.17 Illustrations of the 3d H-cell.

Exercise 7.4: Numerical study of renormalization

Use the following program to study the renormalization of a given sample of a percolation system.

```
# Coarsening procedure
from pylab import *
from scipy.ndimage import measurements

def coarse(z,f):
#function zz = coarse(z,f)
# The original array is z
# The transfer function is f given as a vector with 16 possible places
# f applied to a two-by-two matrix should return
# the renormalized values
#
# The various values of f correspond to the following
# configurations of the two-by-two region that is renormalized,
# where I have used X to mark a present site, and 0 to mark an
# empty sites
#
#  0  00     4  00     8  00    12  00
#     00        X0        0X        XX
#
#  1  X0     5  X0     9  X0    13  X0
#     00        X0        0X        XX
#
#  2  0X     6  0X    10  0X    14  0X
#     00        X0        0X        XX
#
#  3  XX     7  XX    11  XX    15  XX
#     00        X0        0X        XX
#
    nx = shape(z)[0]
    ny = shape(z)[1]
    if (nx%2==1): # Must be even number
        raise ValueError(’nx must be even’)
    if (ny%2==1): # Must be even number
        raise ValueError(’ny must be even’)
    nx2 = int(nx/2)
    ny2 = int(ny/2)
    zz = zeros((nx2,ny2),float) # Generate return matrix
    x = zeros((2,2),float)
    for iy in range(0,ny,2):
        for ix in range(0,nx,2):
            x = z[ix,iy]*1 + z[ix,iy+1]*2 + \
            z[ix+1,iy]*4 + z[ix+1,iy+1]*8
            xx = f[int(x)]
            zz[int((ix+1)/2),int((iy+1)/2)] = xx
    return zz

# Example of use of the coarsening procedure
z = (rand(8,8)<0.58)*1.0
# Set up array for transformation f
f = [0,0,0,1,0,0,0,1,0,0,0,1,1,1,1,1]
lz,nz = measurements.label(z)
zz = coarse(z,f)
lzz,nzz = measurements.label(zz)
zzz = coarse(zz,f)
lzzz,nzzz = measurements.label(zzz)
zzzz = coarse(zzz,f)
lzzzz,nzzzz = measurements.label(zzzz)

# Plot the results
subplot(2,2,1)
imshow(lz)
axis(’equal’)
subplot(2,2,2)
imshow(lzz)
axis(’equal’)
subplot(2,2,3)
imshow(lzzz)
axis(’equal’)
subplot(2,2,4)
imshow(lzzzz)
axis(’equal’)
```

Perform successive iterations for $p = 0.3$, $p = 0.4$, $p = 0.5$, $p = p_c$, $p = 0.65$, $p = 0.70$, and $p = 0.75$, in order to understand the instability of the fixpoint at $p = p_c$.

Subset geometry 8

So far, we have studied the geometry of the percolation system. Now, we will gradually address the physics of processes that occur in a percolation system. We have addressed one physics-like property of the system, the *density* of the spanning cluster, and we found that we could build a theory for the density P as a function of the porosity (occupation probability) p of the system. In order to address other physical properties, we need to have a clear description of the geometry of the percolation system close to the percolation threshold. In this chapter, we will develop a simplified geometric description that will be useful, indeed essential, when we discuss physical process in disordered media. We will introduce various subsets of the spanning cluster — sets that play roles in specific physical processes. We will start by introducing *singly connected bonds*, *the backbone* and *dangling ends* and provide a simplified image of the spanning cluster in terms of the *blob* model for the percolation system [9, 2, 16, 34].

8.0.1 Singly connected bonds

We will start with an example of a subset of the spanning cluster, the set of *singly connected sites* (or bonds). This will demonstrate what we mean by a subset and how the subset is connected to a physical problem.

Singly connected site

A singly connected site is a site with the property that if it is removed, the spanning cluster will no longer be spanning.

We can relate this to a physical property: If we study fluid flow in the spanning cluster, all the fluid has to go through the singly connected sites. These sites are also often referred to as red sites, because if we were studying a set of random resistors, the highest current would have to go through the singly connected bonds, and they would therefore heat up and become “red”. Several examples of subsets of the spanning cluster, including the singly connected bonds, are shown in Fig. 8.1.

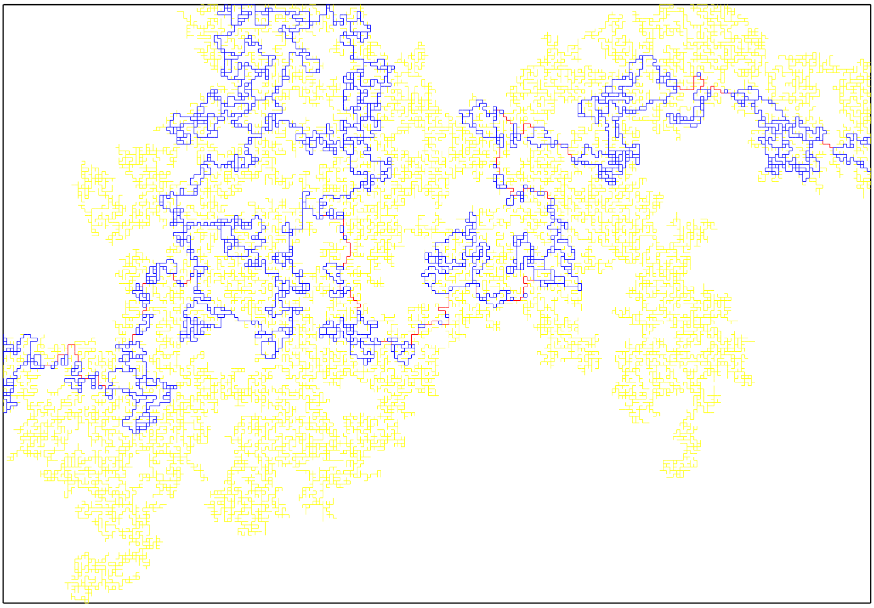

Fig. 8.1 Illustration of the spanning cluster, the singly connected bonds (red), the backbone (blue), and the dangling ends (yellow) for a 256 × 256 bond percolation system at $p = p_c$. (Figure from Martin Søreng).

Scaling hypothesis. We have learned that the spanning cluster may be described by the mass scaling relation $M \propto L^D$, where D is termed the fractal dimension of the spanning cluster. Here, we will make a daring hypothesis, which we will also substantiate: We propose that subsets of the spanning cluster obey similar scaling relations.

For example, we propose that the mass of the singly connected sites (M_{SC}) to have the scaling form

$$M_{SC} \propto L^{D_{SC}} \ , \tag{8.1}$$

where we call the dimension D_{SC} the fractal dimension of the singly connected sites.

Scaling argument. Because the set of singly connected sites is a subset of the spanning cluster, we know that $M_{SC} \leq M$. It therefore follows that

$$D_{SC} \leq D \ . \tag{8.2}$$

Generalization to other subsets. Based on this simple example, we will generalize the approach to other subsets of the spanning cluster. However, first we will introduce a new concept, a self-avoiding path on the spanning cluster.

8.1 Self-avoiding paths on the cluster

The study of percolation is the study of connectivity, and many of the physical properties that we are interested in depends on various forms of the connecting paths between the two opposite edges of the spanning cluster. We can address the structure of connected paths between the edges by studying self-avoiding paths (SAPs). A Self-Avoiding Path (SAP) is a set of connected sites that correspond to the sites on the path of a walk on the spanning cluster that does not intersect itself going from one side to the opposite side.

8.1.1 Minimal path

The shortest path between the two edges is called the shortest SAP between the two edges. (Notice, that there may be more than one path the satisfy this criterion. We chose one of these paths randomly). We call this the *minimal path* with a length L_{min}. The length here refers to the number of sites in the path, that is, we can also call this the mass of the path, $M_{\text{min}} = L_{\text{min}}$. We will use the mass instead of the length in the following to describe the paths.

Scaling hypothesis for the minimal path. We assume that mass of the minimal path also scales with the system size according to the scaling form:

$$M_{\min} \propto L^{D_{\min}} \ . \tag{8.3}$$

Where we have introduced the scaling exponent of the minimal path to be $D_{\min}$.

8.1.2 Maximum and average path

Similarly, we call the longest SAP between the two edges the *longest path* with a mass $M_{\max}$. Again, we assume that the mass has a scaling form, $M_{\max} \propto L^{D_{\max}}$. We notice that $M_{min} \leq M_{max}$. Consequently, a similar relation holds for the exponents $D_{\min} \leq D_{\max}$.

We also introduce the term the *average path*, meaning the average mass (length) of all possible SAPs going between opposite sides of the system, $\langle M_{SAP} \rangle \propto L^{D_{SAW}}$. The dimension D_{SAW} will lie between the dimensions of the minimal and the maximal path.

8.1.3 Backbone

Intersection of all self-avoiding paths. The notion of SAPs can also be used to address the physical properties of the cluster, such as we saw for the singly connected bonds. The set of singly connected bonds is the intersections between all SAPs connecting the two sides. That is, the singly connected bonds is the set of points that any path must go through in order to connect the two sides. From this definition, we notice that the dimension $D_{SC} < D_{\min}$, and as we will see further on, $D_{SC} = 1/\nu$ which is smaller than 1 for two-dimensional systems.

Union of all self-avoiding paths. Another useful set is the union of all SAPs that connect the two edges of the cluster. This set is called the backbone with dimension D_B.

Backbone

The *backbone* is the union of all self-avoiding paths on the spanning cluster that connect two opposite edges.

This set has a simple physical interpretation for a random porous material, since it corresponds to the sites that are accessible to fluid flow if a pressure is applied accross the material. The remaining sites are called *dangling ends*. The backbone are all the sites that have at least two different paths leading into them, one path from each side of the cluster. The remaining sites only have one (self-avoiding) path leading into them, and we call this set of sites the dangling ends. The spanning cluster consists of the backbone plus the dangling bonds, as illustrated in Fig. 8.2. The dangling ends are therefore pieces of the cluster that can be cut away by the removal of a single bond.

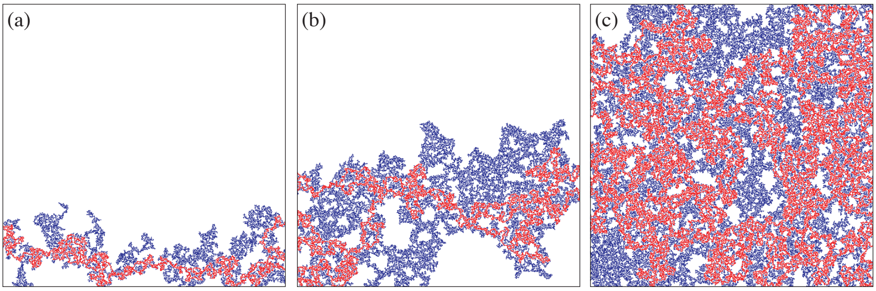

Fig. 8.2 Illustration of the spanning cluster consisting of the backbone (red) and the dangling ends (blue) for a 512×512 site percolation system for (a) $p = 0.58$, (b) $p = 0.59$, and (c) $p = 0.61$.

We have arrived at the following hierarchy of exponents describing various subsets of paths through the cluster:

$$D_{SC} \leq D_{\min} \leq D_{SAW} \leq D_{\max} \leq D_B \leq D \leq d \, , \tag{8.4}$$

8.1.4 Scaling of the dangling ends

Generally, we will find that the dimension of the backbone, D_B, is smaller than the dimension of the spanning cluster. For example, in two dimensions, we find that $D_B \simeq 1.6$, whereas $D \simeq 1.89$. This has implications for the relative size of the backbone and the dangling ends.

The spanning cluster consists of the backbone and the dangling ends. Therefore, the mass of the spanning cluster, M, must equal the sum of the masses of the backbone and the dangling ends $M = M_B + M_{DE}$. Since we know that $M \propto L^D$ and $M_B \propto L^{D_B}$, we find that

$$M_{DE} = M - M_B = M_0 L^D - M_{0,B} L^{D_B} \, . \tag{8.5}$$

To see what happens when $L \to \infty$, we divide by M:

$$\frac{M_{DE}}{M} = 1 - \frac{M_{0,B} L^{D_B}}{M_0 L^D} = 1 - cL^{D_B - D} \ , \tag{8.6}$$

Since $D_B \leq D$, we see that this fraction goes to a constant (one) as L approaches infinity. Consequently, we have found that $M_{DE} \propto M \propto L^D$. This also implies that as the system size goes to infinity most of the mass is in the dangling ends and that the backbone occupies a smaller and smaller portion of the total mass of the system.

8.1.5 Argument for the scaling of subsets

We can provide a better argument for why the various subsets should scale with the system size L to various exponents. We notice that the following relation between the masses must be true:

$$L^1 \leq M_{\min} \leq M_{SAW} \leq M_{\max} \leq M_{BB} \leq M \leq L^d \ , \tag{8.7}$$

where the first inequality $L^1 \leq M_{\min}$ follows because even the minimum path must be at least of length L to go from one side to the opposite side.

Now, if this is to be true for all values of L, it can be argued that because all the masses are between two scaling relations, L^1 and L^d, also the scaling of the intermediate masses, M_x, must be power-laws with some power-law exponents, $M_x \propto L^{D_x}$, with the hierarchy of exponents given in (8.4).

8.1.6 Blob model for the spanning cluster

Let us now try to formulate our geometric description of the spanning cluster into a *model* of the spanning cluster [36]. We have found that the spanning cluster can be subdivided first into two parts: the backbone and the dangling ends. The backbone may again be divided into two parts: a set of blobs where the are several parallel paths and a set of sites, the singly connected sites, that connect the blobs to each other and the blobs to the dangling ends. Thus, we have ended up with a model with three components:

- the dangling ends,

- a set of blobs where there are several parallel paths
- the singly connected points, connecting the blobs to each other and the blobs to the dangling ends.

Each of the blobs and the dangling ends will again have a similar substructure of dangling ends, blobs with parallel paths, and singly connected bonds as illustrated in Fig. 8.3. This cartoon image of the clusters will prove itself to provide useful intuition on the geometrical structure of percolation clusters when we address the physics of disordered systems in the next chapters.

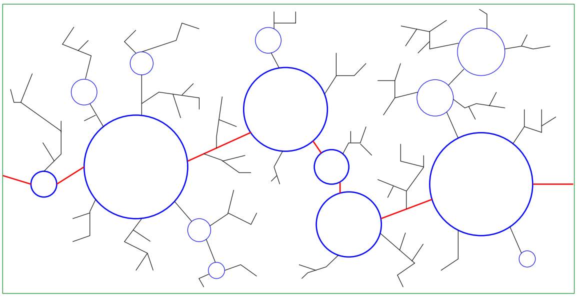

Fig. 8.3 Illustration of the hierarchical blob-model for the percolation cluster showing the backbone (bold), singly connected bonds (red) and blobs (blue).

8.1.7 Mass-scaling exponents for subsets of the spanning clusters

The exponents can be calculated either by numerical simulations, where the masses of the various subsets are measured as a function of system size at $p = p_c$, or by the renormalization group method. Numerical results based on computer simulations are listed in the following table.

d	D_{SC}	$D_{\min}$	$D_{\max}$	D_B	D	D_{DE}
2	3/4	1.1	1.5	1.6	1.89	

8.2 Renormalization calculation

We will now use the renormalization group approach to address the scaling exponent for various subsets of the spanning cluster at $p = p_c$. For this, we will here use the renormalization procedure for bond percolation on a square lattice in two dimensions following Hong and Stanley [17], where we have found that the renormalization procedure produces the exact result for the percolation threshold, $p_c = p^* = 1/2$. This is a fixpoint of the mapping.

Our strategy will be to assume that all the bonds have a mass $M = 1$ in the original lattice, and then find the mass M' in the renormalized lattice, when the length has been rescaled by b. For a property that displays a self-similar scaling, we will expect that

$$M' \propto b^{D_x} M \ , \tag{8.8}$$

where D_x denotes the exponent for the particular subset we are looking at. We can use this to determine the fractal exponent D_x from

$$D_x = \frac{\ln M'/M}{\ln b} \ . \tag{8.9}$$

We will do this be calculating the average value of the mass of the H-cell, by taking the mass of the subset we are interested in for each configuration, $M_x(c)$, and multiplying it by the probability of that configuration, summing over all configurations:

$$\langle M \rangle = \sum_c M_x(c) P(c) \ . \tag{8.10}$$

We have now calculated the average mass in the original 2 by 2 lattice, and this should correspond to the average renormalized mass, $\langle M' \rangle = p' M'$, which is the mass of the renormalized bond, M' multiplied with the probability for that bond to be present p'. That is, we will find M' from:

$$p' M' = \sum_c M(c) P(c) \ , \tag{8.11}$$

We will study our system at the nontrivial fixpoint $p = p^* = 1/2 = p_c$. The spanning configurations c for bond renormalization in two dimensions, are shown together with their probabilities and the masses of various subsets in following table:

c		$P(c)$	M_{SC}	L_{min}	L_{AVG}	L_{max}	M_{BB}	M
1	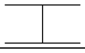	$p^5(1-p)^0$	0	2	2.5	3	5	5
2	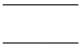	$p^4(1-p)^1$	0	2	2	2	4	4
3	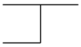	$4p^4(1-p)^1$	1	2	2.5	3	4	4
4	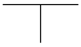	$2p^3(1-p)^2$	2	2	2	2	2	3
5	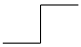	$2p^3(1-p)^2$	3	3	3	3	3	3
6	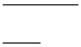	$4p^3(1-p)^2$	2	2	2	2	2	3
7	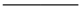	$2p^2(1-p)^3$	2	2	2	2	2	2
$\langle M_x \rangle$			$26/2^5$	$34/2^5$	$36.5/2^5$	$39/2^5$	$47/2^5$	$53/2^5$
D_x			$\frac{\ln \frac{13}{8}}{\ln 2}$	$\frac{\ln \frac{17}{8}}{\ln 2}$	$\frac{\ln \frac{36.5}{16}}{\ln 2}$	$\frac{\ln \frac{39}{16}}{\ln 2}$	$\frac{\ln \frac{47}{16}}{\ln 2}$	$\frac{\ln \frac{53}{16}}{\ln 2}$
D_x			0.7004	1.0875	1.1898	1.2854	1.5546	1.7279
$D_{x,n}$			3/4	1.13		1.4	1.6	91/48

Table 8.1 Numerical exponents for the exponent describing various subsets of the spanning cluster defined using the set of Self-Avoiding Walks going from one side to the opposite side of the cluster. The last line shows the exponents found from numerical simulations in a two-dimensional system.

This use of the renormalization group method to estimate the exponents demonstrates the power of the renormalization arguments. Similar arguments will be used to address other properties of the percolation system.

8.3 (Advanced) Singly connected bonds and ν

Let us also use this technique to develop an interpretation of the exponent ν and how it is related to the singly connected sites (See Coniglio [8] for a detailed argument). Because the exponent ν can be found from the renormalization equation at the fixpoint, which corresponds to the percolation threshold, it is reasonable to assume that the exponent ν can be derived from some property of the fractal structure at $p = p_c$.

Let us address bond percolation in two dimensions, described by the occupation probability p for bonds, and let us introduce an additional variable $1 - \pi$: the probability to remove an occupied bond from the system. We will consider the percolation problem to be described by these two values. When we are at $p = p_c$, we would expect that for any $1 - \pi > 0$, the spanning cluster will break into a set of unconnected clusters. The only fixpoint value when $p = p_c$ is therefore for $1 - \pi = 0$, that is, $\pi = 1$.

Can we derive a recursion relation for $1 - \pi$? For our renormalized cell of size b, the probability to break connectivity between the end nodes should be $1 - \pi'$. This corresponds to the probability that the renormalized bond is broken, because after renormalization there is only one bond in the box of size b. We write the recursion relation as a Taylor expansion around the fix-point $1 - \pi = 0$, or $\pi = 1$:

$$1 - \pi' = A(1 - \pi) + \mathcal{O}((1 - \pi)^2) \ , \tag{8.12}$$

where A is given as

$$A = \left. \frac{\partial \pi'}{\partial \pi} \right|_{\pi = 1} \ . \tag{8.13}$$

We realize that the new p in the system after the introduction of π is given by $p = \pi p_c$, when the ordinary percolation system is at p_c. Similarly, the renormalized occupation probability is $p' = \pi' p_c$, and we have therefore found that

$$A = \left. \frac{\partial \pi'}{\partial \pi} \right|_{\pi = 1} = \left. \frac{\partial p'}{\partial p} \right|_{p = p_c} = b^{1/\nu} \ . \tag{8.14}$$

8.4 Deterministic fractal models

We have found that we can calculate the behavior of infinite-dimensional and one-dimensional systems exactly. However, for finite dimensions such as for $d = 2$ or $d = 3$ we must rely on numerical simulations and renormalization group arguments to determine the exponents and the behavior of the system. However, in order to learn about physical properties in systems with scaling behavior, we may be able to construct simpler models that contain many of the important features of the percolation cluster. For example, we may be able to introduce deterministic, iterative fractal structures that reproduce many of the important properties of the percolation cluster at $p = p_c$, but that is deterministic and not a random system. The idea is that we can use this system to study other properties of the physics on fractal structures.

An example of an iterative fractal structure that has many of the important features of the percolation clusters at $p = p_c$ is the Mandelbrot-Given curve. The curve is generated by the iterative procedure described in Fig. 8.4. Through each generation, the length is rescaled by a factor

$b = 3$, and the mass is rescaled by a factor 8. That is, for generation l, the mass is $m(l) = 8^l$, and the linear size of the cluster is $L(l) = 3^l$. If we assume a scaling on the form $m = L^D$, we find that

$$D = \frac{\ln 8}{\ln 3} \simeq 1.89 \ . \tag{8.15}$$

This is surprisingly similar to the fractal dimension of the percolation cluster. We can also look at other dimensions, such as for the singly connected bonds, the minimum path, the maximum path and the backbone.

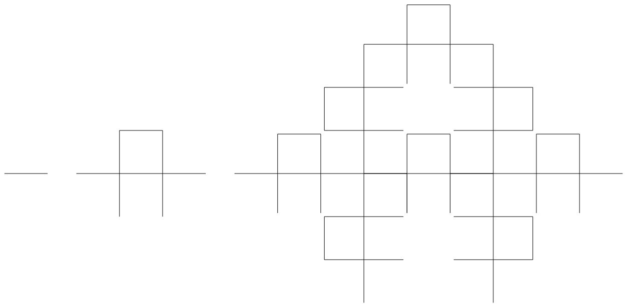

Fig. 8.4 Illustration of first three generations of the Mandelbrot-Given curve. The length is rescaled by a factor $b = 3$ for each iteration, and the mass of the whole structure is increased by a factor of 8. The fractal dimension is therefore $D = \ln 8/\ln 3 \simeq 1.89$.

Let us first address the singly connected bonds. In the zero'th generation, the system is simply a single bond, and the length of the singly connected bonds, L_{SC} is 1. In the first generation, there are two bonds that are singly connecting, and in the second generation there are four bonds that are singly connecting. The general relation is that

$$L_{SC} = 2^l \ , \tag{8.16}$$

where l is the generation of the structure. The dimension, D_{SC}, of the singly connected bonds is therefore $D_{SC} = \ln 2/\ln 3 \simeq 0.63$, which should be compared with the exact value $D_{SC} = 3/4$ for two-dimensional percolation.

The minimum path will for all generations be the path going straight through the structure, and the length of the minimal path will therefore be equal to the length of the structure. The scaling dimension D_{min} is therefore $D_{min} = 1$.

The maximum path increases by a factor 5 for each iteration. The dimension of the maximum path is therefore $D_{max} = \ln 5/\ln 3 \simeq 1.465$.

We can similarly find that the mass of the backbone increases by a factor 6 for each iteration, and the dimension of the backbone is therefore $D_B = \ln 6/\ln 3 \simeq 1.631$.

The Mandelbrot-Given curve can be optimized by selecting the lengths L_i illustrated in Fig. 8.5 in the way that provides the best estimate for the exponents of interest.

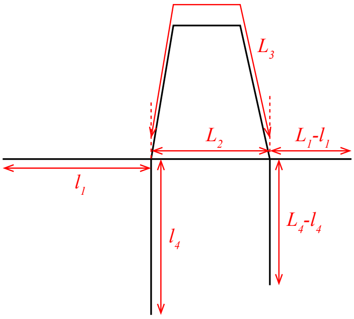

Fig. 8.5 The Mandelbrot-Given construction can be optimized by choosing particular values for the lengths l_1, L_2, L_3, l_4, and L_4. Here, L_3 gives the length around the whole curved path. The choice of l_1 and l_4 does not affect the scaling properties we have been addressing, and are therefore not relevant parameters. The ordinary Mandelbrot-given curve corresponds to $b = 3$, $L_1 = 2$, $L_2 = 1$, $L_3 = 3$, $L_4 = 2$, $l_1 = 1$, and $l_4 = 1$.

This deterministic iterative fractal can be used to perform quick calculations of various properties on a fractal system, and may also serve as a useful hierarchical lattice on which to perform simulations when we are studying processes occurring on a fractal structure.

8.5 Lacunarity

The fractal dimension describes the scaling properties of structures such as the percolation cluster at $p = p_c$. However, structures that have the same fractal dimension, may have a very different appearance. As an example, let us study several variations of the Sierpinski gasket introduced in section 5.5. As illustrated in Fig. 8.6, we can construct several rules for the iterative generation of the fractal that all result in the same fractal dimension, but have different visual appearance. The fractal dimension $D = \ln 3/\ln 2$ for both of the examples in Fig. 8.6, but by increasing the number of triangles that are used in each generation, the structures become more homogeneous. How can we quantify this difference?

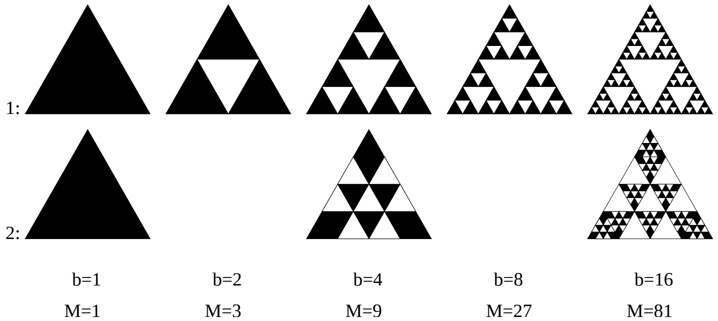

Fig. 8.6 Two versions of the Siepinski gasket. In version 1, the next generation is made from 3 of the structures from the last generation, and the spatial rescaling is by a factor $b = 3$. In version 2, the next generation is made from 9 of the structures from the last generation, and the spatial rescaling is by a factor $b = 6$. The resulting fractal dimension is $D_2 = \ln 9/\ln 4 = \ln 3^2/\ln 2^2 = \ln 3/\ln 2 = D_1$. The two structures therefore have the same fractal dimension. However, version 1 have large fluctuations that version 2.

In order to quantify this difference, Mandelbrot invented the concept of lacunarity . We measure lacunarity from the distribution of mass-sizes. We can characterize and measure the fractal dimension of a fractal structure using box-counting, as explained in section 5.5. The structure, such as the percolation cluster, is divided into boxes of size ℓ. In each box, i, there will be a mass $m_i(\ell)$. The fractal dimension was found by calculating the average mass per box of size ℓ:

$$\langle m_i(\ell) \rangle_i = A\ell^D \ . \tag{8.17}$$

However, there will be a full distribution of masses $m(\ell)$ in the boxes, characterized by a distribution $P(m, \ell)$, which gives the probability for mass m in a box of size ℓ. We can characterize this distribution by its moments:

$$\langle m^k(\ell) \rangle = A_k \ell^{kD} \ , \tag{8.18}$$

where this particular scaling form implies that the structure is unifractal: the scaling exponents for all the moments are linearly related.

For a unifractal structure, we expect the distribution of masses to have the scaling form

$$P(m, \ell) = \ell^x f(\frac{m}{\ell^D}) \ , \tag{8.19}$$

where the scaling exponent x is yet undetermined. In this case, the moments can be found by integration over the probability density

$$\begin{aligned}\langle m^k \rangle &= \int P(m,\ell) m^k dm && (8.20)\\ &= \int m^k \ell^x f(\frac{m}{\ell^D}) dm && (8.21)\\ &= \ell^{(kD+x+D} \int (\frac{m}{\ell^D})^k f(\frac{m}{\ell^D}) d(\frac{m}{\ell^D}) && (8.22)\\ &= \ell^{D(k+1)+x} \int x^k f(x) dx && (8.23)\end{aligned}$$

We can determine the unknown scaling exponent x from the scaling of the zero'th moment, that is, from the normalization of the probability density: $\langle m^0 \rangle = 1$ implies that $D(0+1)+x=0$, and therefore, that $x=-D$. The scaling ansatz for the distribution of masses is therefore

$$P(m,\ell) = \ell^{-D} f(\frac{m}{\ell^D}) \; . \tag{8.24}$$

And we found that the moments can be written as

$$\langle m^k \rangle = \ell^{D(k+1)-D} \int x^k f(x) dx = A_k \ell^{kD} \; , \tag{8.25}$$

as we assumed above.

We therefore see that the distribution of masses is characterized by the distribution $P(m,\ell)$, which in turn is described by the fractal dimension, D, and the scaling function $f(u)$, which gives the shape of the distribution.

The distribution of masses can be broad, which would correspond to "large holes", or narrow, which would correspond to a more uniform distribution of mass. The width of the distribution can be characterized by the mean-square deviation of the mass from the average mass:

$$\varDelta = \frac{\langle m^2 \rangle - \langle m \rangle^2}{\langle m \rangle^2} = \frac{A_2 - A_1^2}{A_1^2} \; . \tag{8.26}$$

This number describes another part of the mass distribution relation than the scaling relation, and can be used to characterize fractal set. For the percolation problem, this number is assumed to be universal, independent of lattice type, but dependent on the dimensionality.

8.6 Exercises

Exercise 8.1: Singly connected bonds

Use the example programs from the text to find the singly connected bonds.

a) Run the programs to visualize the singly connected bonds. Can you understand how this algorithms finds the singly connected bonds? Why are some of the bonds of a different color?

b) Find the mass, M_{SC}, of the singly connected bonds as a function of system size L for $p = p_c$ and use this to estimate the exponent D_{SC}: $M_{SC} \propto L^{D_{SC}}$.

c) Can you find the behavior of $P_{SC} = M_{SC}/L^d$ as a function of $p - p_c$?

Exercise 8.2: Left/right-turning walker

We have provided a subroutine and an example program that implements the left/right-turning walker algorithm. The algorithm works on a given clusters. From one end of the cluster, two walkers are started. The walkers can only walk according to the connectivity rules on the lattice. That is, for a nearest-neighbor lattice, they can only walk to their nearest neighbors. The left-turning walker always tries to turn left from its previous direction. If this site is empty, it tries the next-best site, which is to continue straight ahead. If that is empty, it tries to move right, and if that is empty, it moves back along the direction it came. The right-turning walker follows a similar rule, but prefers to turn right in each step. The first walker to reach the other end of the cluster stops, and the other walker stops when it reaches this site.

The path of the two walkers is illustrated in the figure below. The sites that are visited by both walkers consitute the singly connected bonds. The union of the two walks consitutes what is called the external perimeter (Hull) of the cluster.

a) Use the following programs to generate and illustrate of the singly connected bonds for a 100 × 100 system. Check that the illustrated bonds correspond to the singly connected bonds.

```
from pylab import *
from scipy.ndimage import measurements
import numba
```

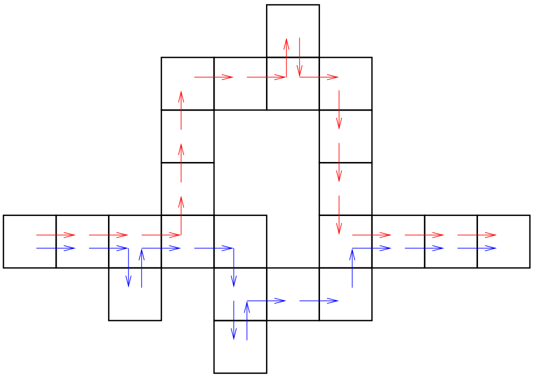

Fig. 8.7 Illustrations of the left-right turning walker.

```
@numba.njit(cache=True)
def walk(z):
    # Left turning walker
    # Returns left: nr of times walker passes a site
    # First, ensure that array only has one contact point at
    #   left and right : topmost points chosen
    nx = z.shape[0]
    ny = z.shape[1]
    i = where(z[0,:] > 0)
    ix0 = 0 # starting row for walker is always 0
    iy0 = i[0][0] # starting column (first element where
    #               there is a matching column which is zero)
    print("Starting walk in x=" + str(ix0) + " y=" + str(iy0))
    # First do left-turning walker
    directions = zeros((4,2), int)
    directions [0,0] = -1 # west
    directions [0,1] = 0
    directions [1,0] = 0 # south
    directions [1,1] = -1
    directions [2,0] = 1 # east
    directions [2,1] = 0
    directions [3,0] = 0 # north
    directions [3,1] = 1
    nwalk = 1
    ix = ix0
    iy = iy0
    direction = 0 # 0 = west, 1 = south, 2 = east, 3 = north
    left = zeros((nx,ny),int)
    right = zeros((nx,ny),int)
    while (nwalk >0):
        left[ix,iy] = left[ix,iy] + 1
        # Turn left until you find an occupied site
        nfound = 0
        while (nfound==0):
            direction = direction - 1
            if (direction < 0):
                direction = direction + 4
            # Check this direction
            iix = ix + directions[direction,0]
            iiy = iy + directions[direction,1]
            if (iix >= nx):
                nwalk = 0 # Walker escaped
                nfound = 1
                iix = nx
                ix1 = ix
                iy1 = iy
            # Is there a site here?
            elif(iix >= 0):
                if(iiy >= 0):
                    if (iiy < ny):
                        if (z[iix,iiy]>0): # site present, move here
                            ix = iix
                            iy = iiy
                            nfound = 1
                            direction = direction + 2
                            if (direction > 3):
                                direction = direction - 4
    #left
    nwalk = 1
    ix = ix0
    iy = iy0
    direction = 1 # 1=left, 2 = down, 3 = right, 4 = up
    while(nwalk >0):
        right[ix,iy] = right[ix,iy] + 1
        # ix,iy
        # Turn right until you find an occupied site
        nfound = 0
        while (nfound==0):
            direction = direction + 1
            if (direction > 3):
                direction = direction - 4
            # Check this directionection
            iix = ix + directions[direction,0]
            iiy = iy + directions[direction,1]
            if (iix >= nx):
                if (iy >= iy1):
                    nwalk = 0 # Walker escaped
                    nfound = 1
                    iix = nx
            # Is there a site here?
            elif(iix >= 0):
                if(iiy >= 0):
                    if (iiy < ny):
                        if (iix < nx):
                            if (z[iix,iiy]>0): # site present, move here
                                ix = iix
                                iy = iiy
                                nfound = 1
                                direction = direction - 2
                                if (direction <0):
                                    direction = direction + 4
    return left, right
```

```
from pylab import *
from scipy.ndimage import measurements
# Generate spanning cluster (l-r spanning)
lx = 100
ly = 100
p = 0.6
ncount = 0
perc = []
while (len(perc)==0):
    ncount = ncount + 1
    if (ncount >1000):
        print("Couldn’t make percolation cluster...")
        break
    z=rand(lx,ly)<p
    lw,num = measurements.label(z)
    perc_x = intersect1d(lw[0,:],lw[-1,:]) # Testing using intersect
    perc = perc_x[where(perc_x > 0)]
    print("ncount = ",ncount)
if len(perc) > 0:
    zz = (lw == perc[0])
    # zz now contains the spanning cluster
    figure() # Display spanning cluster
    imshow(zz, interpolation=’nearest’, origin=’upper’)
    l,r = walk(zz)
    figure()
    imshow(l, interpolation=’nearest’, origin=’upper’)
    figure()
    imshow(r, interpolation=’nearest’, origin=’upper’)
    zzz = l*r # Find points where both l and r are non-zero
    figure()
    imshow(zzz, interpolation=’nearest’, origin=’upper’)
    colorbar()
    zadd = zz + zzz
    figure()
    imshow(zadd, interpolation=’nearest’, origin=’upper’)
    colorbar()
```

b) Measure the dimension D_{SC}.

c) Modify the programs to find the external perimeter (Hull) of a spanning cluster in a 100×100 system.

d) Measure the dimension D_P of the perimeter.

e) (Advanced) Develop a theory for the behavior of $P_H(p, L)$, the probability for a site to belong to the Hull as a function of p and L for $p > p_c$.

f) (Advanced) Measure the behavior of $P_H(p, L)$ as a function of p for $L = 512 \times 512$.

9 Introduction to disorder

We have now developed the tools to address the statistical properties of the geometry of a disordered system such as a model porous medium: the percolation system. In this part, we will apply this knowledge to address physical properties of disordered systems and to study physical processes in disordered materials.

We have learned that the geometry of a disordered system displays fractal scaling close to the percolation threshold. Material properties such as the density of singly connected sites, or the backbone of the percolation cluster, display self-similar scaling. The backbone is the part of the spanning cluster that participates in fluid flow. The mass, M_B, of the backbone scales with the system size, L, according to the scaling relation $M_B = L^{D_B}$, where D_B is smaller than the Euclidean dimension. The density of the backbone therefore decreases with system size. This implies that material properties which we ordinarily would treat as material constants, depend on the size of the sample. In this part we will develop an understanding of the origin of this behavior, and show how we can use the tools from percolation theory to address the behavior in such systems.

The behavior of a disordered system can in principle always be addressed by direct numerical simulation. For example, for incompressible, single-phase fluid flow through a porous material, the effective permeability of a sample can be found to very good accuracy from a detailed numerical model of fluid flow through the system. However, it is not practical to model fluid flow down to the smallest scaling in practical problems such as in oil migration. We would therefore need to extrapolate from the small scale to the large scaling. This process, often referred to as up-scaling, requires that we know the scaling properties of our system. We will address up-scaling in detail in this chapter.

We may argue that the point close to the percolation threshold is anomalous and that any realistic system, such as a geological system, would typically be far away from the percolation threshold. In this case, the system will only display an anomalous, size-dependent behavior up to the correlation length, and over larger lengths the behavior will be that of a homogeneous material. We should, however, be aware that many physical properties are described by broad distributions of material properties, and this will lead to a behavior similar to the behavior close to the percolation threshold, as we will discuss in detail in this part. In addition, several physical processes ensure that the system is driven into or is exactly at the percolation threshold. One such example is the invasion-percolation process, which gives a reasonable description of oil-water emplacement processes such as secondary oil migration. For such systems, the behavior is best described by the scaling theory we have developed.

In this part, we will first provide an introduction to the scaling of material properties such as conductivity and elasticity. Then we will demonstrate how processes occurring in systems with frozen disorder, such as a porous material, often lead to the formation of fractal structures.

Flow in disordered media 10

We will start our studies of physics in disordered media by addressing flow, either in the form of incompressible fluid flow in a random, porous system or in the form of electric current in a random, porous materials. We will first introduce the basic properties of flow of current or fluids, and then address flow in a percolating system close to p_c. We will study the behavior numerically, develop a scaling theory, and find properties using the renormalization group approach. Our initial studies will be on the binary porous medium of the percolation system. However, we can also extend our results to more general random media, and we demonstrate how this can be done towards the end of the chapter.

10.0.1 Electrical conductivity and resistor networks

Traditionally, the conductive properties of a disordered material have been addressed by studying the behavior of random networks of resistors called *random resistor networks* [24, 23, 1]. In this case, a voltage V is applied across the disordered material, such as a bond-percolation network, and the total current, I, through the sample is measured, giving the conductance G of the sample as the constant of proportionality $I = GV$. (We recall that the current I is the amount of charge flowing through a given cross-sectional area per unit time).

We remember from electromagnetism that we discern between *conductance* and *conductivity*:

- conductance, G, is a property of a specific sample — a given medium — with specific dimensions
- conductivity, g, is a material property

For an L^d sample in a d-dimensional system, the conductance of a homogeneous material with conductivity σ is

$$G = L^{d-1} g/L = L^{d-2} g \; . \tag{10.1}$$

It is common in electromagnetism to use σ for conductivity. Here, we will instead use g to avoid confusion with the exponent σ we introduced previously for the behavior of s_ξ. The conductance is inversely proportional to the length of the sample in the direction of flow, and proportional to the cross-sectional $d-1$-dimensional area. We can understand this by considering that there are L^{d-1} parallel parts that contribute to the flow. Parallel-parts add to the conductance. In addition, each part has a length L, and we recall from electromagnetism that conductance decreases with length.

10.0.2 Flow conductivity of a porous system

We can also use fluid flow in porous medium as our basic physical system. If done in the limit of slow, incompressible fluid flow these two systems are practically identical. For fluid flow in a porous medium of length L and cross-sectional area A, the system is described by Darcy's law which provide a relation between the amount of fluid volume flowing through a given cross-sectional area, A, per unit time, Φ, and the pressure drop Δp across the sample:

$$\Phi = \frac{kA}{\eta}\frac{\Delta p}{L} \; , \tag{10.2}$$

where k is the called permeability of the material and is a property of the material geometry, and η is the viscosity of the fluid. Again, we would like a description so that k is material property, and all the information about the geometry of the material goes into the flow conductance of the sample through the length L and the cross-sectional area A. Generalized to a d-dimensional system, the relation is

$$\Phi = \frac{kL^{d-1}}{\eta L}\Delta p = L^{d-2}\frac{k}{\eta}\Delta p \; . \tag{10.3}$$

From this, we see that the electric conductivity problem in this limit is the same as the Darcy-flow permeability problem. We will therefore not discern between the two problems in the following. We will simply call them flow problems and describe them using the current, I, the conductivity, g, the conductance G, and the potential V. We will study these problems on a L^d percolation lattice, using the theoretical, conceptual and computational tools we have developed so far.

10.1 Conductance of a percolation lattice

Let us first address the conductance of a L^d sample of a percolation system. The system may be either a site or a bond percolation system, but many of the concepts we introduce are simpler to explain if we just consider a bond percolation system.

We will start with a simplified system: The system will be a network of bonds that are present with probability p. We assume that all bonds have the same conductance, which we can set to 1 without loss of generality. The bonds are removed with probability $1 - p$, and we model this by setting the conductance of a removed bond to be zero.

10.1.1 Finding the conductance of the system

The conductance of the L^d sample is found by solving the flow problem illustrated in fig. 10.1. A potential difference V is applied across the whole sample, and we find (measure) the resulting current I. We find the conductance from Ohm's law (or similarly from Darcy's law for fluid flow):

$$I = GV \quad \Rightarrow \quad G = \frac{I}{V} \, . \tag{10.4}$$

In general, the conductance G will be a function of p and L: $G = G(p, L)$.

Local potentials and currents. Let us look at the network in more detail. Fig. 10.1b illustrates a small part of the whole system. The two adjacent sites i and j are connected with a bond of conductance $G_{i,j}$. If the bond is present (with probability p in the percolation system), the conductance is $G_{i,j}$ is 1, otherwise it is zero.

The current from site i to site j is related to the difference in potential between the two sites:

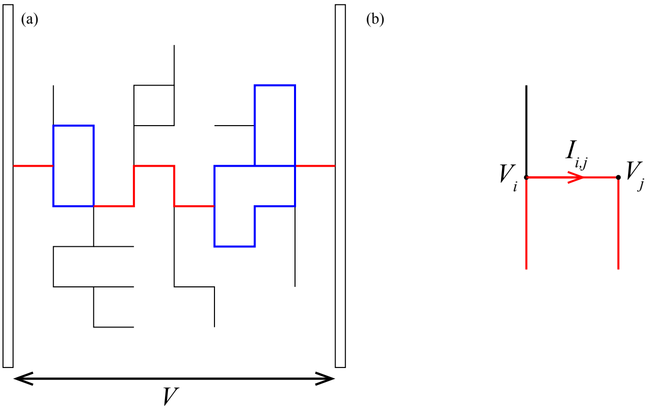

Fig. 10.1 (a) Illustration of flow through a bond percolation system. The bonds shown in red are the singly connected bonds: all the flux has to go through these bonds. The bonds shown in blue are the rest of the backbone: The flow only takes place on the singly connected bonds and the backbone, the remaining bonds are the dangling ends, which do not participate in fluid flow. (b) Illustration of the potentials V_i and V_j in two adjacent sites and the current $I_{i,j}$ from site i into site j.

$$I_{i,j} = G_{i,j}\left(V_i - V_j\right) \ , \tag{10.5}$$

where we notice that the current is positive if the potential is higher in site i than in site j.

Conservation of current. In addition, the continuity condition provides a conservation equation for the currents: Charges (or fluid mass for Darcy flow) cannot change, and therefore the net current into any point inside the lattice must be zero. This corresponds to the condition that the sum of the current from site i into all its neighboring sites k must be zero:

$$\sum_k I_{i,k} = 0 \tag{10.6}$$

In electromagnetism this is called Kirchhoff's rule for currents. We can rewrite this in terms of the local potentials V_i instead by inserting (10.5) in (10.6):

$$\sum_k G_{i,k}\left(V_i - V_k\right) = 0 \ . \tag{10.7}$$

This provides us with a set of equations for all the potentials V_i, which we must solve to find the potentials and hence the currents between all the sites in a percolation system.

Finding currents and potentials. We can use this to find all the potentials for a percolation system. Let us adress a two-dimensional system of size $L \times L$. The potential in a position (x, y) on the lattice is $V(x, y)$, where x and y are integers, $x = 0, 1, 2, \ldots, L-1$ and $y = 0, 1, 2, \ldots, L-1$. We denote $G_{i,j}$ as $G(x_i, y_i; x_j, y_j)$. We can then rewrite (10.7) as

$$G(x, y; x+1, y)\,(V(x, y) - V(x+1, y)) + \tag{10.8}$$
$$G(x, y; x-1, y)\,(V(x, y) - V(x-1, y)) + \tag{10.9}$$
$$G(x, y; x, y+1)\,(V(x, y) - V(x, y+1)) + \tag{10.10}$$
$$G(x, y; x, y-1)\,(V(x, y) - V(x, y-1)) = 0 \tag{10.11}$$

In order to solve this two-dimensional problem, it is usual to rewrite it as a one-dimensional system of equations with a single index. The index $i = x + yL$ uniquely describes a point so that $V(x, y) = V_i$. We see that $(x, y) = i$, $(x+1, y) = i+1$, $(x-1, y) = i-1$, $(x, y+1) = i+L$, and $(x, y-1) = i-L$. We can rewrite (10.11) using this indexing system:

$$G_{i,i+1}\,(V_i - V_{i+1}) + G_{i,i-1}\,(V_i - V_{i-1}) + \tag{10.12}$$
$$G_{i,i+L}\,(V_i - V_{i+L}) + G_{i,i-L}\,(V_i - V_{i+L}) = 0 \tag{10.13}$$

This is effectively a set of L^d equations for V_i. In addition we have the boundary conditions that $V(0, j) = V$ and $V(L-1, j) = 0$ for $j = 0, 1, \ldots, L-1$. This defines the system as a tri-diagonal set of linear equations that can be solved easily numerically.

10.1.2 Computational methods

We have now reformulated the conductivity problem on a percolation lattice to a computational problem that we can solve. We do this by generating random lattices of size $L \times L$, solve to find the potential $V(x, y)$, and then study the effective conductivity, $G = I/V$ of the system by summing up all the currents exiting the system (or entering — these should be the same).

We can do this by generating a bond-lattice, where the values $G_{i,j}$ are either 0 or 1. However, so far all our visualization methods have been constructed for site lattices. We will therefore study a site lattice, but instead generate $G_{i,j}$ between two sites based on whether the sites are present. We set $G_{i,j}$ for two nearest-neighbors to be present (1) if *both* sites i and j are present (1). Otherwise we set $G_{i,j}$ to zero, that is, if at least one of the sites is empty we set $G_{i,j}$ to be zero. We assume all the sites on the left and right outsides to be present. This is where current flows in and where the potentials are set. In addition, we assume all the sites on the top and bottom outsides to be empty. It is therefore now flow in from the top or bottom. We therefore only study percolation from the left to the right.

We have written subroutines to help you with these studies. The function `sitetobond` transforms your percolation matrix `z` to a bond matrix. The function `FIND_CON` solves the system of equations to find the potentials, V_i, and the function `coltomat` transforms the resulting array of potentials back into a matrix form, $V(x, y)$. The following programs are used to calculate the potentials and currents and visualize the results. The resulting plots are shown in Fig. 10.2.

```
from pylab import *
from scipy.sparse import spdiags, dia_matrix, coo_matrix
from scipy.sparse.linalg import spsolve
from scipy.ndimage import measurements

# Written by Marin Soreng 2004
# Calculates the effective flow conductance Ceff of the
# lattice A as well as the potential V in every site .
def FIND_COND (A , X , Y ):
    V_in = 1.
    V_out = 0.
    # Calls MK_EQSYSTEM .
    B,C = MK_EQSYSTEM (A , X , Y )
    # Kirchhoff ' s equations solve for V
    V = spsolve(B, C)
    # The pressure at the external sites is added
    # ( Boundary conditions )
    V = concatenate((V_in * ones (X), V,  V_out * ones (X)))
    # Calculate Ceff
    # second-last X elements of V multiplied with second-last elem. of A
    # these are the second last column of the system
    # gives the conductivity of the system per row?
    Ceff = dot((V[-1-2*X:-1-X] - V_out).T, A[-1-2*X:-1-X, 1]) \
      / ( V_in - V_out )
    return V , Ceff

# Sets up Kirchoff ' s equations for the 2 D lattice A .
# A has X * Y rows and 2 columns . The rows indicate the site ,
# the first column the bond perpendicular to the flow direction
# and the second column the bond parallel to the flow direction .
#
# The return values are [B , C ] where B * x = C . This is solved
# for the site pressure by x = B \ C .

def MK_EQSYSTEM (A , X , Y ):
    # Total no of internal lattice sites
    sites = X *( Y - 2)
    # Allocate space for the nonzero upper diagonals
    main_diag = zeros(sites)
    upper_diag1 = zeros(sites - 1)
    upper_diag2 = zeros(sites - X)
    # Calculates the nonzero upper diagonals
    main_diag = A[X:X*(Y-1), 0] + A[X:X*(Y-1), 1] + \
      A[0:X*(Y-2), 1] + A[X-1:X*(Y-1)-1, 0]
    upper_diag1 = A [X:X*(Y-1)-1, 0]
    upper_diag2 = A [X:X*(Y-2), 1]
    main_diag[where(main_diag == 0)] = 1
    # Constructing B which is symmetric , lower = upper diagonals .
    B = dia_matrix ((sites , sites)) # B *u = t
    B = - spdiags ( upper_diag1 , -1 , sites , sites )
    B = B + - spdiags ( upper_diag2 ,-X , sites , sites )
    B = B + B.T + spdiags ( main_diag , 0 , sites , sites )
    # Constructing C
    C = zeros(sites)
    #    C = dia_matrix ( (sites , 1) )
    C[0:X] = A[0:X, 1]
    C[-1-X+1:-1] = 0*A [-1 -2*X + 1:-1-X, 1]
    return B , C

def sitetobond ( z ):
    # Function to convert the site network z(L,L) into a (L*L,2) bond
    # network
    # g [i,0] gives bond perpendicular to direction of flow
    # g [i,1] gives bond parallel to direction of flow
    # z [ nx , ny ] -> g [ nx * ny , 2]
    nx = size (z ,1 - 1)
    ny = size (z ,2 - 1)
    N = nx * ny
    gg_r = zeros ((nx , ny)) # First , find these
    gg_d = zeros ((nx , ny )) # First , find these
    gg_r [:, 0:ny - 1] = z [:, 0:ny - 1] * z [:, 1:ny]
    gg_r [: , ny  - 1] = z [: , ny  - 1]
    gg_d [0:nx - 1, :] = z [0:nx - 1, :] * z [1:nx, :]
    gg_d [nx - 1, :] = 0
    # Then , concatenate gg onto g
    g = zeros ((nx *ny ,2))
    g [:, 0] = gg_d.reshape(-1,order='F').T
    g [:, 1] = gg_r.reshape(-1,order='F').T
    return g

def coltomat (z, x, y):
    # Convert z(x*y) into a matrix of z(x,y)
    # Transform this onto a nx x ny lattice
    g = zeros ((x , y))
    for iy in range(1,y):
        i = (iy - 1) * x + 1
        ii = i + x - 1
        g[: , iy - 1] = z[ i - 1 : ii]
    return g
```

```
# Generate spanning cluster (l - r spanning )
lx = 400
```

```
ly = 400
p = 0.5927
ncount = 0
perc = []

while (len(perc)==0):
    ncount = ncount + 1
    if (ncount >100):
        break
    z=rand(lx,ly)<p
    lw,num = measurements.label(z)
    perc_x = intersect1d(lw[0,:],lw[-1,:])
    perc = perc_x[where(perc_x > 0)]
    print("Percolation attempt", ncount)
zz = asarray((lw == perc[0]))
# zz now contains the spanning cluster
zzz = zz.T # Transpose
g = sitetobond ( zzz ) # Generate bond lattice
V, c_eff = FIND_COND (g, lx, ly) # Find conductivity
x = coltomat ( V , lx , ly ) # Transform to nx x ny lattice
V = x * zzz
g1 = g[:,0]
g2 = g[: ,1]
z1 = coltomat( g1 , lx , ly )
z2 = coltomat( g2 , lx , ly )

# Plot results
figure(figsize=(16,16))
ax = subplot(221)
imshow(zzz, interpolation='nearest')
title("Spanning cluster")
subplot(222, sharex=ax, sharey=ax)
imshow(V, interpolation='nearest')
title("Potential")

# Calculate current from top to down from the potential
f2 = zeros ( (lx , ly ))
for iy in range(ly -1):
    f2[: , iy ] = ( V [: , iy ] - V [: , iy +1]) * z2 [: , iy ]
# Calculate current from left to right from the potential
f1 = zeros ( (lx , ly ))
for ix in range(lx-1):
    f1[ ix ,:] = ( V [ ix ,:] - V [ ix +1 ,:]) * z1 [ ix ,:]
# Find the sum of (absolute) currents in and out of each site
fn = zeros (( lx , ly ))
fn = fn + abs ( f1 )
fn = fn + abs ( f2 )
# Add for each column (except leftmost) the up-down current, but offset
fn [: ,1: ly ] = fn [: ,1: ly ] + abs ( f2 [: ,0: ly -1])
# For the left-most one, add the inverse potential
#   multiplied with the spanning cluster bool information
fn [: ,0] = fn [: ,0] + abs (( V [: ,0] - 1.0)*( zzz [: ,0]))
# For each row (except topmost) add the left-right current, but offset
fn [1: lx ,:] = fn [1: lx ,:] + abs ( f1 [0: lx -1 ,:])
```

```
# Plot results
subplot(223, sharex=ax, sharey=ax)
imshow(fn, interpolation=’nearest’)
title (" Current ")
# Singly connected
zsc = fn > (fn.max() - 1e-6)
# Backbone
zbb = fn>1e-6
# Combine visualizations
ztt = ( zzz*1.0 + zsc*2.0 + zbb*3.0 )
zbb = zbb / zbb.max()
subplot(224, sharex=ax, sharey=ax)
imshow(ztt, interpolation=’nearest’)
title (" SC, BB and DE ")
```

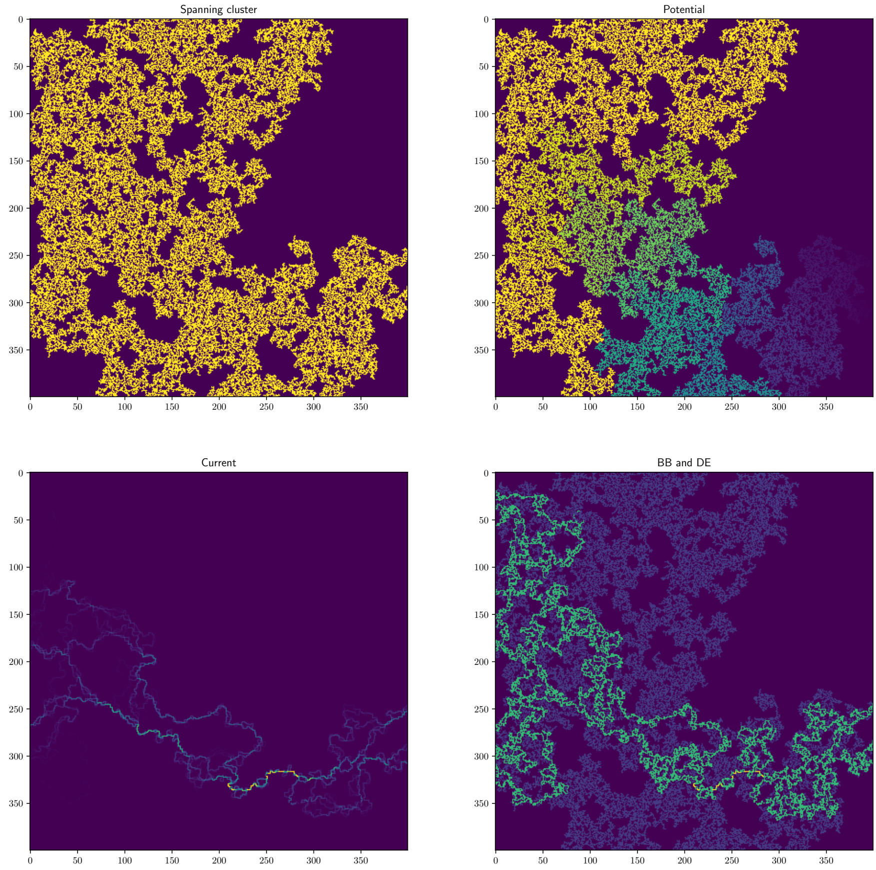

Fig. 10.2 Plots of the spanning cluster, the potential, $V(x, y)$, the absolute value of the current flowing into each site, and the singly connected bonds, the backbone and the dangling ends.

10.1.3 Measuring the conductance

Using this program we can measure the conductance of the system and how it varies with both p and L. First, we perform simulations for M samples and calculate the conductance from $G(p, L) = I(p, L)/V$, where V is given, and we calculate I. Here, I is the sum of all the currents escaping (or entering) the system. We have set all the potentials on the left side to $V = 1$, that is, $V_{iL} = 1$ for $i = 0, 1, \ldots, L - 1$. For these sites, $G_i, i + 1$ is always 1. The current I is therefore:

$$I = \sum_{i=0}^{L-1} I_{iL,iL+1} = G_{iL,iL+1} \left(V_{iL} - V_{iL+1}\right) = V_{iL} - V_{iL+1} \; . \tag{10.14}$$

We use the following program to find the conductance, $G(p, L)$, for an $L \times L$ system for $L = 400$, as well as the density of the spanning cluster $P(p, L)$. The resulting behavior for $L = 400$ and $M = 600$ is shown in Fig. 10.3. We observe two things from this plot: First we see that the behavior of $G(p, L)$ and $P(p, L)$ is qualitatively different around $p = p_c$: $P(p, L)$ increases very rapidly as $(p - p_c)^\beta$ where β is less than 1. However, it appears that $G(p, L)$ increases more slowly. Indeed, from the plot it looks as if $G(p, L)$ increases as $(p - p_c)^x$ with an exponent x that is larger than 1. How can this be? Why does the density of the spanning cluster increase very rapidly, but the conductance increases much slower? This may be surprising, but we will develop an explanation for this below.

```
from pylab import *
from scipy.ndimage import measurements
Lvals = [400]
pVals = logspace(log10(0.58), log10(0.85), 20)
C = zeros((len(pVals),len(Lvals)),float)
P = zeros((len(pVals),len(Lvals)),float)
nSamples = 600
G = zeros(len(Lvals))
for iL in range(len(Lvals)):
    L = Lvals[iL]
    lx = L
    ly = L
    for pIndex in range(len(pVals)):
        p = pVals[pIndex]
        ncount = 0
        for j in range(nSamples):
            ncount = 0
            perc = []
            while (len(perc)==0):
                ncount = ncount + 1
                if (ncount > 1000):
```

```
          print("Couldn't make percolation cluster...")
          break
        z=rand(lx,ly)<p
        lw,num = measurements.label(z)
        perc_x = intersect1d(lw[0,:],lw[-1,:])
        perc = perc_x[where(perc_x > 0)]
      if len(perc) > 0: # Found spanning cluster
        area = measurements.sum(z, lw, perc[0])
        P[pIndex,iL] = P[pIndex,iL] + area # Find P(p,L)
        zz = asarray((lw == perc[0])) # zz=spanning cluster
        zzz = zz.T
        g = sitetobond (zzz) # Generate bond lattice
        Pvec, c_eff = FIND_COND(g, lx, ly) # Find conducance
        C[pIndex,iL] = C[pIndex,iL] + c_eff
    C[pIndex,iL] = C[pIndex,iL]/nSamples
    P[pIndex,iL] = P[pIndex,iL]/(nSamples*L*L)
plot(pVals,C[:,-1],'-ob',label='$C$')
plot(pVals,P[:,-1],'-or',label='$P$')
legend()
xlabel(r"$p$")
ylabel(r"$C,P$")
```

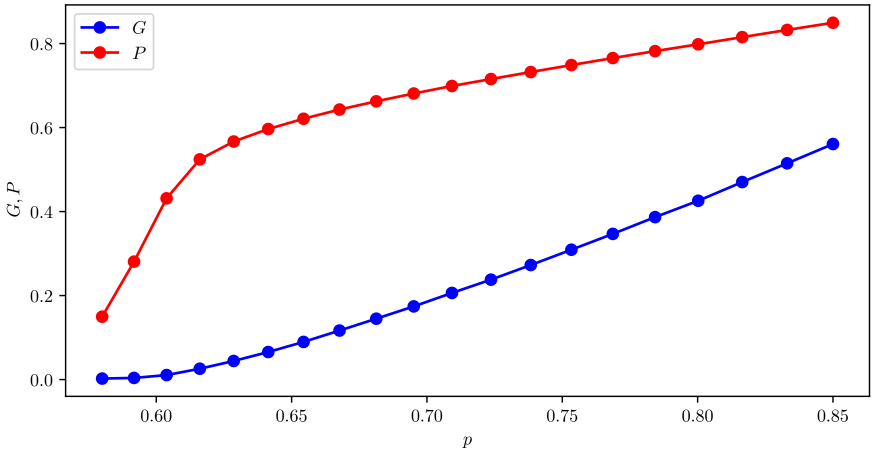

Fig. 10.3 Plots of the conductance $G(p, L)$ and the density of the spanning cluster $P(p, L)$ for $L = 400$.

10.1.4 Conductance and the density of the spanning cluster

For an infinite system, that is when $L \to \infty$, we cannot define a conductance G. Instead, we must describe the system by its conductivity $g = L^{d-2}G$ (see (10.1)). The two-dimensional system is a special case where the conductance and the conductivity are identical. However, in general, we need to use this transformation to relate G and g.

For an infinite system, we know that for $p < p_c$ there will be no spanning cluster. The effective conductivity is therefore zero. When p is close to 1, the density of the spanning cluster will be proportional to p, and we also expect the conductance to be proportional to p in this range. This may lead us to assume that the density of the spanning cluster and the conductance of the sample is proportional also when p is close to p_c. However, our direct measurements above (originally done by Last and Thouless [24]) show that P and G are not proportional when p approaches p_c.

We have the tools to understand this behavior. The spanning cluster consists of the backbone and dangling ends. However, it is only the backbone that contributes to conductance of the sample. We could remove all the dangling ends, and still get the same behavior the the conductance. This suggests, that it is the scaling behavior of the backbone that is important. However, we have found that the mass-scaling exponent of the backbone, D_B, is smaller than D, the mass scaling exponent for the spanning cluster. This indicates that most of the mass of the spanning cluster is found in the dangling ends. This is the reason for the difference between the behavior of $P(p)$, and $G(p)$ for p close to p_c. In the following we will develop a detailed scaling argument for the behavior of the conductance G and the conductivity g of the percolation system.

10.2 Scaling arguments for conductance and conductivity

We will now use the same scaling techniques we introduced to find the behavior of $P(p, L)$ to develop a theory for the conductance $G(p, L)$. First, we realize that we instead of p may describe the conductance as a function of ξ and L: $G(p, L) = G(\xi, L)$. Second, we realize that we want to describe the system in the range where $p > p_c$. We will address two limits of the behavior: When $L \gg \xi$ and then at p_c, that is, when $\xi \gg L$.

10.2.1 Scaling argument for $p > p_c$ and $L \gg \xi$

When $L \gg \xi$, we know that over length scales larger than ξ, the system is effectively homogeneous. We can see this by subdividing the system into cells of size ξ, giving us a total of $(L/\xi)^d$ such cells.

For a homogeneous system of ℓ^d boxes of size ℓ, we know that the conductance G of the whole system is $G = \ell^{d-2} G_\ell$, where G_ℓ is the conductance of a single box. We apply the same principle to this system: The conductance $G(\xi, L)$ is given as

$$G(\xi, L) = (\frac{L}{\xi})^{d-2} G(\xi, \xi) \; , \tag{10.15}$$

where we have written $G(\xi, \xi)$ for the conductivity within the box — the conductance of a system where the correlation length is ξ and $L = \xi$.

From (10.1), the conductivity $g(\xi, L)$ is given as

$$g(\xi, L) = L^{-(d-2)} G(\xi, L) = \frac{G(\xi, \xi)}{\xi^{d-2}} \; . \tag{10.16}$$

What is $G(\xi, \xi)$? A system with correlation length equal to the system size is indistinguishable from a system at $p = p_c$. The conductance $G(\xi, \xi)$ is therefore the conductance of the spanning cluster at $p = p_c$ in a system of size $L = \xi$. Let us therefore find the conductance of a finite system — a system of size L — at the percolation threshold.

10.2.2 Conductance of the spanning cluster

This leads us to address the conductance, $G(\infty, L)$, of the spanning cluster at $p = p_c$. We know that the spanning cluster consists of the backbone and the dangling ends, and that only the backbone will contribute to the conductivity. The backbone can be described by the blob model (see section 8.1 for a discussion of the blob model): The backbone consists of blobs of bonds in parallel, and links of singly connected bonds between them.

We will start from a scaling hypothesis — a scaling ansatz for the conductance — derive the consequences of this assumption, and then finally test these consequences to see if the data is consistent with our assumption. This will then validate, or at least not invalidate to be more precise, the hypothesis. Our scaling hypothesis will be that the conductance of a system of size L at p_c can be described by the scaling exponent $\tilde{\zeta}_R$:

$$G(\infty, L) \propto L^{-\tilde{\zeta}_R} \; . \tag{10.17}$$

Finding bounds for the scaling behavior. In many cases, we cannot find the scaling exponents directly, but we may be able to find bounds for the scaling exponents. We will pursue this approach here. We will see if we can find bounds for the scaling of $G(\infty, L)$, and thereby determine bounds for the exponent $\tilde{\zeta}_R$?

Lower bound for the scaling exponent. First, we know that the spanning cluster consists of blobs in series with the singly connected bonds. This implies that the resistivity $R = 1/G$ of the spanning cluster is given as the resistivity of the singly connected bonds R_{SC} plus the resistivity of the blobs, R_{blob} since resistivities are added for a series of resistances:

$$1/G = R = R_{SC} + R_{blob} \; . \tag{10.18}$$

This implies that $R > R_{SC}$. The resistance of the singly connected bonds can easily be found, since the definition of singly connected bonds is that they are connected in series, one after another. We know the effective resistance of a series of resistors from basic electromagnetism: The resistance of a series of resistors is the sum of the resistances. The resistance of the singly connected bonds is therefore the resistance of a single bond multiplied with the number of singly connected bonds, M_{SC}. We have therefore found that

$$M_{SC} < R \; . \tag{10.19}$$

Because $M_{SC} \propto L^{D_{SC}}$, and we have assumed that $R \propto L^{\tilde{\zeta}_R}$, we find that

$$D_{SC} \leq \tilde{\zeta}_R \; . \tag{10.20}$$

We have found a lower bound for the exponent!

Upper bound for the scaling exponent. We can find an upper bound by examining the minimal path. The resistance of the spanning cluster will be smaller than or equal to the resistance of the minimal path, since the spanning cluster will have some regions, the blobs, where there are bonds in parallel. Adding parallel bonds will always lower the resistance. Hence, the resistance is smaller than or equal to the resistance of the minimal path. Since the minimal path is a series of resistances in series, the total resistance of the minimal path is the mass of the minimal path multiplied by the resistance of a single bond. Consequently, the resistance of the spanning cluster is smaller than the mass of the minimal path, $M_{\min}$, which we know scales with system size, $M_{\min} \propto L^{D_{\min}}$. We have therefore found an upper bound for the exponent

$$L^{\tilde{\zeta}_R} \propto R \leq L_{min} \propto L^{D_{min}} \ , \tag{10.21}$$

and therefore

$$\tilde{\zeta}_R \leq D_{min} \ . \tag{10.22}$$

Upper and lower bound demonstrate the scaling relation. We have therefore demonstrated (or proved) the scaling relation

$$D_{SC} \leq \tilde{\zeta}_R \leq D_{min} \ . \tag{10.23}$$

Because this scaling relation shows that the scaling of R is bounded by two power-laws in L, we have also proved that the resistance R is a power-law, and that the exponents are within the given bounds. We notice that when dimensionality of the system is high, the probability of loops will be low, and blobs will be unlikely. In this case

$$D_{SC} = \tilde{\zeta}_R = D_{min} = D_{max} \ . \tag{10.24}$$

10.2.3 Conductivity for $p > p_c$

By scaling arguments, we have established that the conductance $G(\infty, L)$ of the spanning cluster in a system of size L is described by the exponent $\tilde{\zeta}_R$:

$$G(\infty, L) \propto L^{-\tilde{\zeta}_R} \text{ when } L \leq \xi \ . \tag{10.25}$$

We use this to find an expression for $G(\xi, \xi)$, which is the conductance of the spanning cluster at $p = p_c$ in a system of size $L = \xi$. Therefore

$$G(\xi, \xi) \propto \xi^{-\tilde{\zeta}_R} \ . \tag{10.26}$$

We insert this in (10.16) in order to establish the behavior of the conductivity, g, for $p > p_c$, finding that

$$g = \frac{G(\xi, \xi)}{\xi^{d-2}} \propto \xi^{-(d-2+\tilde{\zeta}_R)} \tag{10.27}$$

$$\propto (p - p_c)^{\nu(d-2+\tilde{\zeta}_R)} \propto (p - p_c)^{\mu} \tag{10.28}$$

We have introduced the exponent μ:

$$\mu = \nu(d - 2 + \tilde{\zeta}_R) \ . \tag{10.29}$$

We notice that for two-dimensional percolation, any value of $\tilde{\zeta}_R$ larger than $1/\nu$ will lead to a value for $\mu > 1$, which was what was observed in Fig. 10.3. The exponent μ is therefore larger than 1, which is significantly different from the exponent β, which is less than 1, that describes the mass of the spanning cluster.

Can the results be generalized? We have therefore explained the difference between how $P(p, L)$ and $G(p, L)$ (or $g(p, L)$) scales with $(p - p_c)$ close to p_c. This is a useful insight and a useful result the provide important information about how we expect a random porous material to behave just as flow is starting to occur through it. Notice that when we study percolation systems here, we have generally assumed that the porosity is uncorrelated. For real systems, the porosity may have correlations due to the physical processes that have generated the porosity or the underlying materials. However, when we know how to describe uncorrelated systems like the percolation system, we may be able to use similar theoretical, scaling and computational approaches to study the behavior of real systems.

10.3 Renormalization calculation

Another theoretical approach to address and understand the behavior of the system is through the renormalization group calculation. Here, we will use the renormalization group approach for a square bond lattice in order to estimate the exponent $\tilde{\zeta}_R$.

In order to apply the renormalization group approach, we calculate the average resistance $\langle R' \rangle$ of a 2×2 cell. We use the H-cell approach and only look at percolation in the horizontal direction. The various configurations c and their degeneracy $g(c)$ is illustrated in table 10.1. (The degeneracy is the number of configurations of the same type). We assume that the resistance of a single bond is R. The renormalized resistance R' is then given as $p'R' = \langle R' \rangle$. Using the scaling relation for the resistance, $R \propto L^{\tilde{\zeta}_R}$, we can determine the exponent from

$$\tilde{\zeta}_R = \frac{\ln \frac{\langle R' \rangle}{p'}}{\ln b} \ . \tag{10.30}$$

The renormalization scheme and the values used are shown in the table 10.1. The resulting value for the renormalized resistance is

$$
\begin{aligned}
R' &= \frac{1}{p'}\sum_c g(c)P(c)R(c) && (10.31)\\
&= \frac{1}{p'}\left(\frac{1}{2}\right)^5\left(1+4\cdot\frac{5}{3}+1+2\cdot 2+2\cdot 3+4\cdot 2+2\cdot 2\right) && (10.32)\\
&\simeq 1.917\;. && (10.33)
\end{aligned}
$$

Consequently, the exponent $\tilde{\zeta}_R$ is given by

$$\tilde{\zeta}_R \simeq \frac{\ln 1.917}{\ln 2} \simeq 0.939\;. \tag{10.34}$$

This value is consistent with the scaling bounds set by the scaling relation in (10.24).

c		$P(c)$	$g(c)$	R_c
1	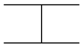	$p^5(1-p)^0$	1	1
2	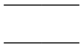	$p^4(1-p)^1$	1	1
3	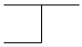	$p^4(1-p)^1$	4	5/3
4	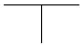	$p^3(1-p)^2$	2	2
5	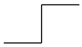	$p^3(1-p)^2$	2	3
6	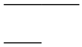	$p^3(1-p)^2$	4	2
7	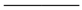	$p^2(1-p)^3$	2	2

Table 10.1 Renormalization scheme for the scaling of the resistance R in a random resistor network. The value $R(c)$ gives the resistance of configuration c, and $g(c)$ is the degeneracy, that is, the number of such configurations.

10.4 Finite size scaling

General scaling of the conductivity. In general, the conductance and the conductivity is related by:

$$G(p,L) = L^{d-2}g(p,L) \tag{10.35}$$

We found that the scaling of the conductivity is:

$$g \propto (p-p_c)^{\mu} \propto \xi^{-\mu/\nu} \,, \tag{10.36}$$

with the exponent μ given as $\mu = \nu\left(d-2+\tilde{\zeta}_R\right)$.

Finite size scaling ansatz for the conductivity. How can we use this scaling behavior as a basis for a finite-size scaling ansatz? We apply the usual approach, where we assume that we can extend the behavior of the infinite system to the finite size system by the introduction of a finite size scaling function $f(L/\xi)$:

$$g(\xi, L) = \xi^{-\mu/\nu} f(\frac{L}{\xi}) \,. \tag{10.37}$$

10.4.1 (Advanced) Developing the scaling form from renormalization

This scaling relation can be developed systematically using the renormalization group approach. Through each renormalization iteration, the conductivity g is mapped onto itself as all length are rescaled by a factor b, by multiplying the whole expression by b to some exponent x, yet to be determined:

$$g(\xi, L) = b^{x} g(\frac{\xi}{b}, \frac{L}{b}) \,. \tag{10.38}$$

The result after l iterations is

$$g(\xi, L) = (b^{l})^{x} g(\frac{\xi}{b^{l}}, \frac{L}{b^{l}}) \,. \tag{10.39}$$

For the case $L < \xi$ we choose to continue iterations until $b^{l} = L$, which gives

$$g(\xi, L) = L^{x} g(1, \frac{\xi}{L}) \,. \tag{10.40}$$

Similarly, when $L > \xi$, we continue iterations until $b^{l} = \xi$, which gives

$$g(\xi, L) = \xi^{x} g(\frac{L}{\xi}, 1) \,. \tag{10.41}$$

Now, we have already established the scaling behavior when $L > \xi$, where we found that $g \propto \xi^{-\mu/\nu}$. We recognize that the exponent $x = -\mu/\nu$, and that the function $g(x, y)$ is a constant both when $x = 1$, and $y \gg 1$, and when $y = 1$, and $x \gg 1$. We have therefore found the limiting scaling behavior:

$$g(\xi, L) = \begin{cases} \xi^{-\mu/\nu} & L \gg \xi \\ L^{-\mu/\nu} & L \ll \xi \end{cases} . \qquad (10.42)$$

10.4.2 The finite-size scaling ansatz

The result for $L \ll \xi$ we can also find by a direct scaling argument. When $L \ll \xi$, the system behaves as if it is at $p = p_c$. In this case we have that $G \propto L^{-\tilde{\zeta}_R}$. We insert this into the expression for g and find $g = GL^{-(d-2)}$, which gives

$$g = GL^{-(d-2)} \propto L^{-\zeta_R} L^{-(d-2)} \propto L^{-(d-2+\tilde{\zeta}_R)} \propto L^{-\mu/\nu} . \qquad (10.43)$$

This means that we have two possible finite-size scaling assumptions. Either

$$g(\xi, L) = \xi^{-\mu/\nu} f\left(\frac{L}{\xi}\right) , \qquad (10.44)$$

where the scaling function $f(u)$ has the form

$$f(u) = \begin{cases} \text{const.} & u \gg 1, \; L \to \infty \\ u^{-\mu/\nu} & u \ll 1, \; \xi \to \infty \end{cases} \qquad (10.45)$$

or

$$g(\xi, L) = L^{-\mu/\nu} \tilde{f}\left(\frac{L}{\xi}\right) , \qquad (10.46)$$

where we leave it to the reader to develop the form of the scaling function $\tilde{f}(u)$.

10.4.3 Finite-size scaling observations

How does the scaling ansatz correspond to the observations? We can use the program we have developed to measure the conductivity as a function of both p and system size L. The following program has been modified for this type of measurement:

```
from pylab import *
from scipy.ndimage import measurements
from matplotlib.colors import ListedColormap
Lvals = [25,50,100,200,400]
pVals = logspace(log10(0.58), log10(0.85), 20)
```

```
C = zeros((len(pVals),len(Lvals)),float)
P = zeros((len(pVals),len(Lvals)),float)
nSamples = 600
mu = zeros(len(Lvals))
for iL in range(len(Lvals)):
    L = Lvals[iL]
    for pIndex in range(len(pVals)):
        p = pVals[pIndex]
        ncount = 0
        for j in range(nSamples):
            ncount = 0
            perc = []
            while (len(perc)==0):
                ncount = ncount + 1
                if (ncount > 1000):
                    print("Couldn’t make percolation cluster...")
                    break
                z=rand(L,L)<p
                lw,num = measurements.label(z)
                perc_x = intersect1d(lw[0,:],lw[-1,:])
                perc = perc_x[where(perc_x > 0)]
            if len(perc) > 0:
                zz = asarray((lw == perc[0]))
                # zz now contains the spanning cluster
                zzz = zz.T
                #    # Generate bond lattice from this
                g = sitetobond ( zzz )
                #    # Generate conductivity matrix
                Pvec, c_eff = FIND_COND(g, lx, ly)
                C[pIndex,iL] = C[pIndex,iL] + c_eff
        C[pIndex,iL] = C[pIndex,iL]/nSamples
for iL in range(len(Lvals)):
    L = Lvals[iL]
    plot(pVals,C[:,iL],label="L="+str(L))
xlabel(r"$p$")
ylabel(r"$C$")
legend()
```

The results for $L = 25, 50, 100, 200, 400$ are shown in Fig. 10.4. Here, we plot both the raw data, $g(p, L)$, and the behavior of $g(p_c, L)$ as a function of L on a $\log-$log-scale, showing that $g(p_c, L)$ indeed scales as a power-law with L.

Scaling data collapse. We can also test the scaling ansatz by plotting a finite-size scaling data collapse. We expect that the conductivity will behave as

$$g(p, L) = L^{-\mu/\nu} \tilde{f}\left(L/\xi\right) \ , \tag{10.47}$$

which we can rewrite by introducing $\xi = \xi_0 (p - pc)^{-\nu}$ to get:

$$g(p, L) = L^{-\mu/\nu} \tilde{f}\left(\left(L^{1/\nu} (p - p_c) \right)^{\nu} \right) \ . \tag{10.48}$$

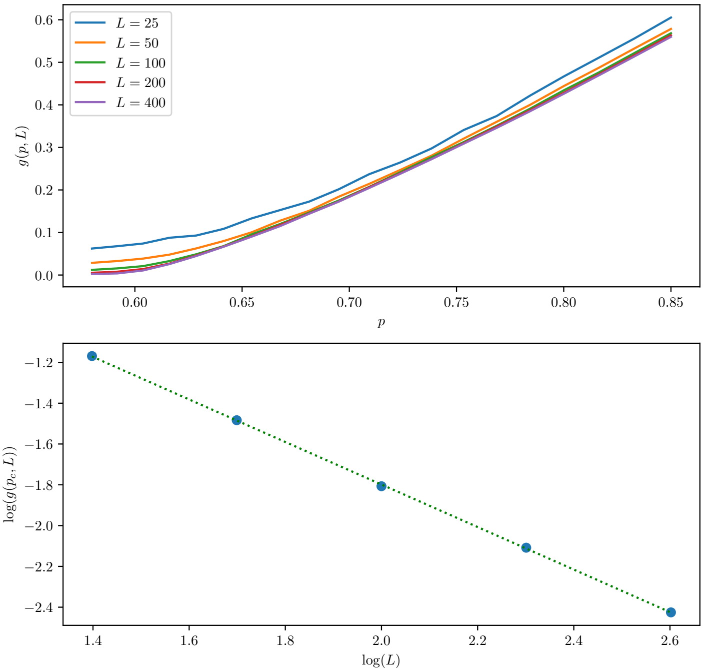

Fig. 10.4 (a) Illustration of the conductivity $g(p, L)$ as a function of p for $L = 25, 50, 100, 200, 400$. (b) We see that at p_c the conductivity $g(p_c, L)$ is scaling according to $g \propto L^{-\mu/\nu}$.

We test this by plotting $L^{\mu/\nu} g(p, L)$ as a function of $L^{1/\nu}(p - p_c)$. This is shown in Fig. 10.5.

Estimating the exponent μ from the data. We can also use the results from the simulations to measure μ directly by plotting $g(p, L)$ as a function of $(p - p_c)$ and fitting a linear function on a log-log plot. We do this for increasing values of L in Fig. 10.6. (Notice that the curves for small values of L clearly are not linear, and we should, ideally, have fitted the linear curve to only the part of the curve that is approximately linear. We will not address methods to do this here, but you should develop such methods in your own research.)

Implications of the scaling ansatz. Our conclusion is that the conductivity is a function of p, but also of system size, which implies that the conductivity of a disordered system close to p_c is not a simple material property as we are used to — we need to address the scaling behavior of the system in detail in order to understand the behavior of the conductivity and the conductance of the system.

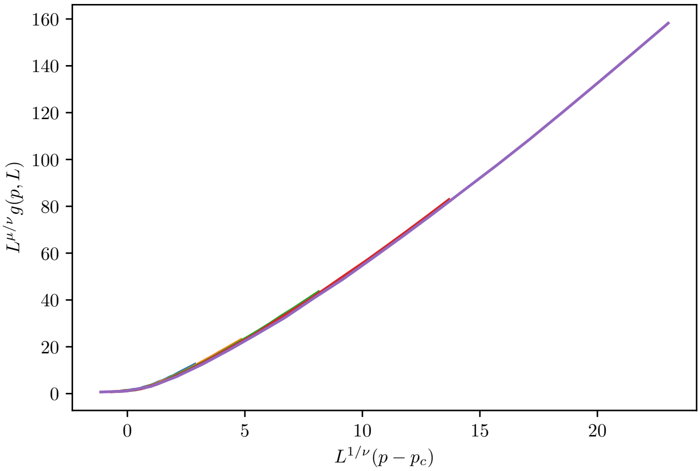

Fig. 10.5 Finite-size data scaling collapse for $g(p, L)$ showing the validity of the scaling ansatz.

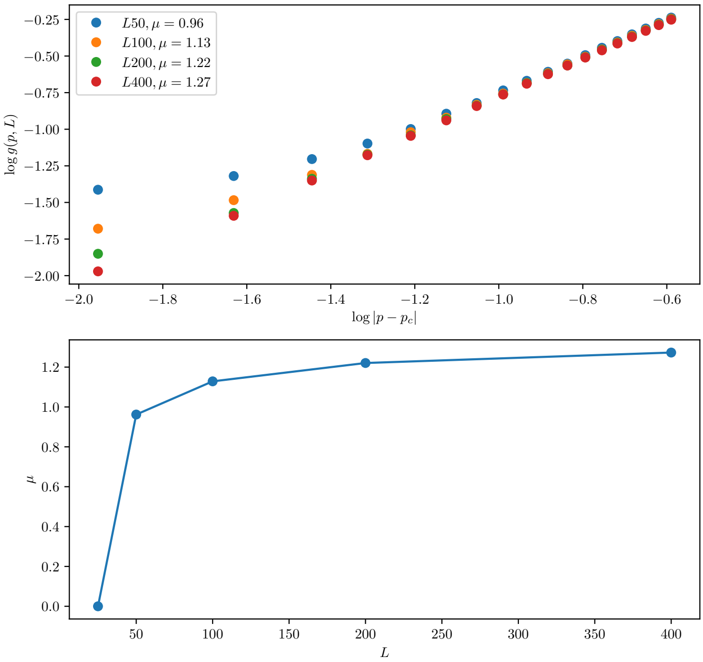

Fig. 10.6 (a) Plot of $g(p, L)$ for increasing values of L. (b) Plot of the exponent μ calculated by a linear fit for increasing system sizes L.

10.5 (Advanced) Internal flux distribution

When we solve the flow problem, for electricity or fluids, on the percolation cluster, we find a set of currents $I_b = I_{i,j}$ for each bond $b = (i, j)$ on the backbone. For all other bonds, the flux will be identically zero. How can we describe the distribution of fluxes on the backbone?

For electrical flow, the conservation of energy is formulated in the expression:

$$RI^2 = \sum_b r_b I_b^2 \ , \tag{10.49}$$

where R is the total resistance of the system, I is the total current, r_b is the resistivity of bond b and I_b is the current in bond b. We can therefore rewrite the total resistance R as

$$R = \sum_b r_b (\frac{I_b}{I})^2 = \sum_b r_b i_b^2 \ , \tag{10.50}$$

where we have introduced the fractional current $i_b = I_b/I$. We have written the total resistance as a sum of the square of the fractional currents in each of the bonds.

The fractional current i_b is assigned to each bond of the backbone. We can describe the fractional currents by the probability distribution for various values of i_b. We can count the number of bonds $n(i)$ having the fractional current i. The total number of bonds is the mass of the backbone:

$$\sum_b 1 = M_B \propto L^{D_B} \ . \tag{10.51}$$

The distribution of fractional currents is therefore given by $P(i) = n(i)/M_B$.

We characterize the distribution $P(i)$ through the moments of the distribution:

$$\langle i^{2q} \rangle = \frac{1}{M_B} \sum_b i_b^{2q} = \frac{1}{M_B} \int i^{2q} n(i) di \ . \tag{10.52}$$

However, there is no general way to simplify this relation, since we do not know whether the function $n(i)$ has a simple scaling form.

However, we can address specific moments of the distribution. We know that the mass of the backbone has a fractal scaling with exponent D_B. This corresponds to the zero'th moment of the distribution. We expect (or hypothesize) that at $p = p_c$, the other moments has a scaling form:

$$\sum_b i_b^{2q} \propto L^{y(q)} \ . \tag{10.53}$$

What can we say about the scaling exponents $y(q)$ for moment q?

Scaling exponent for $q = 0$. For $q = 0$, the sum is

$$\sum_b (i_b^2)^0 \propto L^{y(0)} \propto L^{D_B} \ , \tag{10.54}$$

that is, $y(0) = D_B$.

Scaling exponent for $q \to \infty$. What happens in the limit of $q \to \infty$? In this case, the only terms that will be important in the sum are the terms where $i_b = 1$, because all other terms will be zero. The bonds with $i_b = 1$ are the singly connected bonds: all the current passes through these bonds. Therefore, we have

$$\sum_b (i_b^2)^\infty \propto L^{y(\infty)} \propto M_{SC} \propto L^{D_{SC}} \ , \tag{10.55}$$

and we find that $y(\infty) = D_{SC}$.

Scaling exponent for $q = 1$. When $q = 1$, we find from (10.50) that the sum is given as the total resistance of the cluster

$$\sum_b (i_b^2)^1 = R \propto L^{\tilde{\zeta}_R} \ , \tag{10.56}$$

which implies that $y(1) = \tilde{\zeta}_R$.

The shape of $y(q)$. We can in general argue that because each term in the sum $\sum_b (i_b)^{2q}$ is monotonically decreasing in q, the sum is also monotonically decreasing. We can therefore illustrate the curve $y(q)$ in Fig. 10.7.

Fluctuations in real resistors. In real resistor-networks, the case is even more complex, because the resistivity is due to impurities, and the impurities diffuse. Therefore, the fluctuations in the resistivity will also have a time-dependent part. This is the origin of thermal noise in the circuit. If we keep the total current I constant, fluctuations in the resistivity will lead to fluctuations in the voltage.

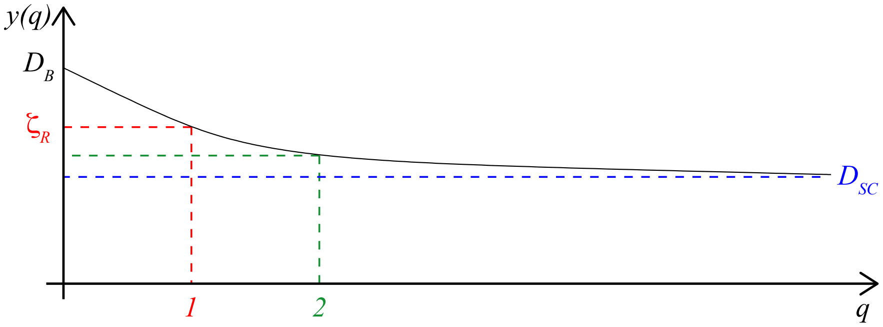

Fig. 10.7 Illustration of the exponents $y(q)$ characterizing the scaling of the moments of the distribution of fractional currents, as a function q, the order of the moment.

10.5.1 Scaling of current fluctuations

What can we learn about the second moment, $q = 2$? We know that the total resistance, R, is

$$R = \sum_b r_b i_b^2 \; . \tag{10.57}$$

So far, we have only addressed the case when $r_b = 1$ for all the bonds on the backbone. However, in reality there will be some variations in the local resistances, so that we can write

$$r_b = 1 + \delta r_b \; , \tag{10.58}$$

where $\langle \delta r_b \rangle = 0$.

10.5.2 Potential fluctuations

Let us estimate the fluctuations in the potential (voltage):

$$\delta V = V - \langle V \rangle = \sum_b \delta r_b (i_b)^2 \; . \tag{10.59}$$

However, the fractional currents i_b are now also different, since $i_b = I_b/I$ depends on the overall current I. Therefore we introduce

$$R_0 = \sum_b (i_b^{(0)})^2 \; , \tag{10.60}$$

where

$$i_b = i_b^{(0)} + \delta i_b \; . \tag{10.61}$$

There is a general theorem giving that

$$\sum_b 1 \cdot \delta(i_b^2) \simeq 0 \,, \tag{10.62}$$

to leading order. We can therefore conclude that

$$\delta V = V - \langle V \rangle = \sum_b \delta r_b i_b^2 + \sum_b 1 \cdot (\delta i_b^2) \simeq 0 \,. \tag{10.63}$$

However, what about the fluctuations in the deviations?

$$\langle (\delta V)^2 \rangle = \langle \sum_{b,b'} \langle \delta r_b \delta r_{b'} \rangle i_b^2 i_{b'}^2 \langle = \sum_{b,b'} \langle \delta r_b \delta r_{b'} \rangle i_b^2 (i_b')^2 \,. \tag{10.64}$$

If we assume that the fluctuations are independent:

$$\langle \delta r_b \delta r_{b'} \rangle = \delta_{bb'} \mathit{\Delta} \,, \tag{10.65}$$

where we have introduced

$$\mathit{\Delta} = \langle \delta r_b^2 \rangle \,. \tag{10.66}$$

We therefore find that

$$\langle \delta V^2 \rangle = \mathit{\Delta} \sum_b (i_b)^4 \propto \mathit{\Delta} L^{y(2)} \,. \tag{10.67}$$

Consequently, we find that the noise is related to the second moment. We know that the exponent $y(2)$ is bounded: $D_{SC} \geq y(2) \geq \tilde{\zeta}_R$, which places the value for $y(2) \simeq 0.9$ for a two-dimensional system.

10.6 (Advanced) Multi-fractals

The distribution of fractional currents in the random resistor network is an example of a *multi-fractal distribution*. The higher moments of this distribution have the non-trivial scaling relation

$$M_q \propto L^{y(q)} \,, \tag{10.68}$$

Unifractal distributions. Previously, we have studied *unifractal distributions*, such as the distribution of percolation cluster sizes when p is close to p_c. We found that the moments of the distribution of clusters sizes could be written as:

$$M_q \langle s^{q-1} \rangle \propto |p - p_c|^{-\gamma q(\beta+1)} \; , \tag{10.69}$$

This is an example of a unifractual distribution. All the moments are described by a single exponent and have a simple scaling form:

$$M_q \propto |p - p_c|^{xq} \; , \tag{10.70}$$

where the exponent $x = -\gamma(\beta + 1)$. The whole distrubtion is only described by this single exponent, and this is why we use the word unifractal to describe the distribution.

Multi-fractal distributions. We have now studied on example of a multifractal: the distribution of fractional currents in the random resistor network. In this case, we found that the moments of the distribution was described by

$$M_q = \langle i^{2q} \rangle = \frac{\sum_b i_b^{2q}}{M_B} \propto L^{y(q)-D_B} \; . \tag{10.71}$$

This is different from the unifractal case, where the exponent $y(q)$ is linear in q: $y(q) = Dq$. For the multifractal there is a whole spectrum of different exponents — each moment is described by a different exponent and there is no simple relation that relates the exponents. In practice, multifractals are typically encountered when measures, such as the fractional current through a bond, is imposed on a fractal structure.

Moments pick out various aspects of the distribution. What does the moments of order q measure in the system? Let us assume that the distribution $n(i)$ of fractional current in the system has the functional form illustrated in Fig. 10.8(a). In Fig. 10.8(b) we illustrate the function $n(i)i^{2q}$. The maximum of this function is found at i_q (that is, i_q gives the maximum of the function $n(i)i^{2q}$). We will assume that the distribution is sharp, so that we can calculate the moment by only using the values in a small neighborhood of i_q. The q-th moment is therefore approximately

$$M_q = \int n(i) i^{2q} di \simeq n(i_q) i_q^{2q} \; . \tag{10.72}$$

This approximation becomes better as $q \to \infty$ since the distribution $n(i)i^{2q}$ is then approaching a delta function around i_q.

This implies that the various moments will pick out various values of i. That is, the moment q will address the structure of sites that have currents that are close to i_q, since it is the currents close to i_q that contribute to the moment. Looking at the different moments of the distribution therefore corresponds to looking at different substructures of

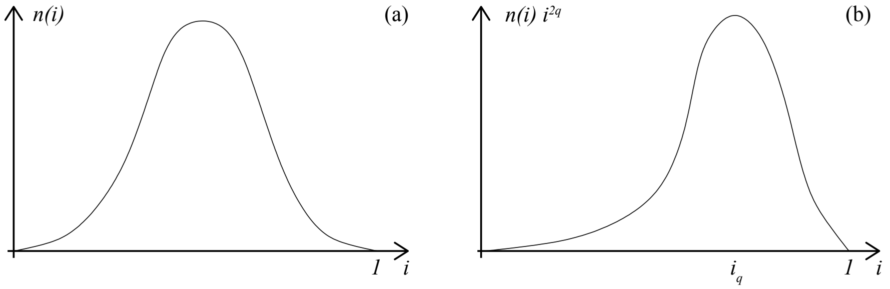

Fig. 10.8 Illustration of the distribution $n(i)$ of fractional currents i in a random resistor network. Part (a) shows the direct distribution, and part (b) shows $n(i)i^{2q}$. The distribution has a maximum at i_q.

the cluster. For example, we saw that the zeroth moment of the current distribution picks out the singly connected bonds and the infinite moment picks out the backbone.

System-size dependence. Let us now address the system-size L-dependence of $n(i)$ and i_q^{2q}. Let us assume that i_q^2 and $n(i_q)$ is scaling with system size according to

$$i_q^2 \propto L^{-\alpha(q)} , \tag{10.73}$$

and

$$n(i_q) \propto L^{f(\alpha(q))} . \tag{10.74}$$

And we will assume that the q-th moment depends on the distribution at i_q:

$$m_q \simeq n(i_q) i_q^{2q} \propto L^{f(\alpha(q)) - q\alpha(q)} \propto L^{y(q) - D_B} . \tag{10.75}$$

The value i_q is found from the maximum of $n(i)i^{2q}$. The condition for this maximum is

$$\frac{\partial}{\partial i} \left[n(i) i^{2q} \right]_{i_q} = 0 , \tag{10.76}$$

or

$$\frac{\partial}{\partial i} \left[\ln n(i) + 2q \ln i \right]_{i_q} = 0 , \tag{10.77}$$

which gives

$$\left. \frac{\left(\frac{\partial \ln n(i)}{\partial i} \right)}{\ln i} \right|_{i_q} = -2q . \tag{10.78}$$

Now we can substitute the L-dependent expressions for $n(i_q)$ and i_q^2, getting

$$\ln n(i_q) = f \ln L , \tag{10.79}$$

and

$$\ln i_q^2 = -\alpha \ln L \ , \tag{10.80}$$

and therefore we find that

$$\frac{\partial f}{\partial \alpha} = q \ . \tag{10.81}$$

We therefore have two equations relating $y(q)$ to $f(\alpha)$ and $\alpha(q)$:

$$f(\alpha(q)) = [y(q) - D_B] + q\alpha(q) \tag{10.82}$$

$$\frac{\partial f}{\partial \alpha} = q \tag{10.83}$$

We can also find the reverse equations, using a Legendre transformation:

$$\frac{\partial}{\partial q}(f(\alpha(q)) = \frac{\partial f}{\partial \alpha}\frac{\partial \alpha}{\partial q} \tag{10.84}$$

$$= \frac{\partial y}{\partial q} + \alpha(q) + q\frac{\partial \alpha}{\partial q} \tag{10.85}$$

$$\frac{\partial y}{\partial q} = -\alpha \tag{10.86}$$

Interpretation. What is the interpretation of $f(\alpha)$? Because $n(i_q)L^{D_B}$ is the total number of bonds with current i_q, we can interpret $f(\alpha(q)) + D_B$ as the fractal dimension of the set of bonds with a current i_q.

Numerically, we estimate $f(\alpha)$ by selecting i_q, and then measure the fractal dimension of the subset with $i = i_q$, and plot the relation between i_q and the fractal dimension using as $f(\alpha)$.

Notice that it is generally assumed that $f(\alpha)$ (and $y(q)$) are universal values that do not depend on the details of the lattice, but do depend on the dimensionality of the systems.

10.7 Real conductivity

So far we have addressed conductivity of a percolation cluster. That is a system where the local conductances (or permeabilities) are either zero or a given constant conductance. That is, we have studied a system with local conductances $G_{i,j}$ so that

$$G_b = G_{i,j} = \begin{cases} 1 \, p \\ 0 \, 1-p \end{cases} \ . \tag{10.87}$$

Binary mixture of conductors. However, in practice, we want to address systems with some distribution of conductances, such as a binary mixture of good and bad conductors, with conductances:

$$G_b = G_{i,j} = \begin{cases} G_2 \, p \\ G_1 \; 1-p \end{cases} . \tag{10.88}$$

Superconductor networks. However, in order to address this problem, let us first look at the conjugate problem to the random resistor network, the random superconductor network. We will assume that the conductances are

$$G_b = G_{i,j} = \begin{cases} \infty \; p \\ 1 \quad 1-p \end{cases} . \tag{10.89}$$

In this case, we expect the conductance to diverge when p approaches p_c from below, and that the conductance is infinite when $p > p_c$. It can be shown that the behavior for the random superconductor network is similar to that of the random resistor network, but that the exponent describing the divergence of the conductance (and consequently conductivity) when p approaches p_c is s:

$$G \propto (p_c - p)^{-s} , \tag{10.90}$$

Combining the two approaches. How can we address both these problems? For any system with a finite smallest conductance, $G_<$, we can always use the smaller conductance as the unit for conductance, and write the functional form for the conductance of the whole system as

$$G(G_1, G_2, p) = (\frac{G(\frac{G_1}{G_1}, \frac{G_2}{G_1}, p)}{G_1}) = G(\frac{G_2}{G_1}, p) , \tag{10.91}$$

Scaling ansatz for binary mixture of conductances. We will make a scaling ansatz for the general behavior of G:

$$G = G_2 (p - p_c)^{\mu} f_{\pm}(\frac{(\frac{G_1}{G_2})}{(p-p_c)^y}) , \tag{10.92}$$

where the exponent y is yet to be determined.

The random resistor network we studied above corresponds to $G_1 \to 0$, and $G_2 = c$. In this case, we retrieve the scaling behavior for p close to p_c, by assuming that $f_+(0)$ is a constant.

For the random superconductor network, the conductances are $G_2 \to \infty$, and $G_1 = \text{const.}$. We will therefore need to construct $f_-(u)$ in such a way that the infinite conductance is canceled from the prefactor. That is, we need $f_-(u) \propto u$. We insert this into (10.92), getting

$$G \propto G_2 (p - p_c)^{\mu} \frac{\frac{G_1}{G_2}}{(p - p_c)^y} \propto G_1 |p - p_c|^{\mu + y} \ . \tag{10.93}$$

Because we know that the scaling exponent should be $\mu + y = -s$ in this limit, we have determined y: $y = -\mu - s$, where μ and s are determined from the random resistor and random superconductor networks respectively.

Finite G_2 and G_1. When $p \to p_c$ the conductance G should approach a constant number when both G_2 and G_1 are finite. However, $p \to p_c$ corresponds to the argument $x \to +\infty$ in the function $f_{\pm}(x)$. However, the only way to ensure that the total conductance is finite, is to require that the two dependencies on $(p - p_c)$ cancel exactly. We achieve this by selecting

$$f_{\pm}(x) \propto x^{\mu/(\mu+s)} \ . \tag{10.94}$$

We can insert this relation into (10.92), getting

$$G = G_2 |p - p_c|^{\mu} \left(\frac{\frac{G_1}{G_2}}{|p - p_c|^{\mu+s}} \right)^{\mu/(\mu+s)} \ , \tag{10.95}$$

which results in

$$G = G_2 (\frac{G_1}{G_2})^{\frac{\mu}{\mu+s}} \ . \tag{10.96}$$

This expression can again be simplified to

$$G(p = p_c) = G_2^{\frac{s}{\mu+s}} G_1^{\frac{\mu}{\mu+s}} \ , \tag{10.97}$$

Numerical values in two dimensions. In two dimensions, $\mu = s \simeq 1.3$, and the relation becomes:

$$G \propto (G_1 G_2)^{\frac{1}{2}} \ , \tag{10.98}$$

10.8 Exercises

Exercise 10.1: Density of the backbone

The backbone of a spanning cluster is the union of all self-avoiding walks from one side of the cluster to the opposite. The backbone corresponds to the sites the contribute to the flow conductivity of the spanning cluster. The remaining sites are the dangling ends.

We call the mass of the backbone M_B, and the density of the backbone $P_B = M_B/L^d$, where L is the system size, and d the dimensionality of the percolation system. Here, we will study two-dimensional site percolation.

a) Argue that the functional form of $P_B(p)$ when $p \to p_c^+$ is

$$P_B(p) = P_0(p - p_c)^x \; , \tag{10.99}$$

and find an expression for the exponent x. You can assume that the fractal dimension of the backbone, D_B, is known.

b) Assume that the functional form of $P_B(p)$ when $p \to p_c^+$ and $\xi \ll L$ is

$$P_B(p) = P_0(p - p_c)^x \; , \tag{10.100}$$

Determine the exponent x by numerical experiment. If needed, you may use that $\nu = 4/3$.

Exercise 10.2: Flow on fractals

Use the example programs from the text to study fluid flow in a percolation system.

a) Run the example programs provided in the text to visualize the currents on the spanning cluster.

b) Modify the program to find the backbone and the dangling ends of the spanning cluster.

c) Use the program to find the singly connected bonds in the spanning cluster.

Exercise 10.3: Conductivity

a) Find the conductivity as a function of $p - p_c$. Determine the exponent $\tilde{\zeta}_R$ by direct measurement.

b) Find the conductivity at $p = p_c$ as a function of system size L.

Exercise 10.4: Current distribution

Use the example programs from the text to find the currents I_b in each bonds b on a spanning cluster at $p = p_c$, $p = 0.585$, and $p = 0.60$.

a) Find the total current I going through the system.
In the following we will study the normalized currents, $i_b = I_b/I$.

b) Find the distribution $P(i)$ of the normalized currents.

c) Measure moments of the distribution.

Exercise 10.5: Bivariate porous media

Rewrite the programs in the text to study a bivariate distribution of conductances. That is, for each site, the conductance is 1 with probability p and $g_0 < 1$ with probability $1 - p$.

a) Visualize the distribution of currents for $g_0 = 0.1$.

b) Find the conductivity $g(p)$ for $\sigma_0 = 0.1$, 0.01, and 0.001.

c) Plot $\sigma(p_c)$ as a function of σ_0.

d) (Advanced) Can you find a way to rescale the conductivities to produce a data-collapse?

11 Elastic properties of disordered media

There are various physical properties that we may be interested in for a disordered material. In the previous chapter, we studied flow problems in disordered materials using the percolation system as a model disordered material. In this chapter we will address mechanical properties of the disordered material, such as the coefficients of elasticity [11, 4, 20, 28, 41].

We will address the behavior of the disordered material in the limit of fractal scaling. In this limit we expect material properties such as Young's modulus to display a non-trivial dependence on system size. That is, we will expect material properties such as Young's modulus to have an explicit system size dependence. We will use the terminology and techniques already developed to study percolation to address the mechanical behavior of disordered systems.

11.1 Rigidity percolation

What are the elastic properties of a percolation system? First, we need to decide on how to convert a percolation system onto an elastic system. We will start by modeling an elastic material as a bond lattice, where each bond represents a local elastic element. The element will in general have resistance to stretching and bending. Systems with only stretching stiffness are termed central force lattices. Here, we will address systems with both stretching and bending stiffness.

Models for stretching and bending stiffness. We can formulate the effect of bending and stretching through the elastic energy of the system. The energy will have terms that depend on the elongation of bonds — these will be the terms that are related to stretching resistance. In addition, there will be terms related to the bending of bonds. Here we will introduce the bending terms through the angles between bonds. For any two bonds connected to the same site, there will be an energy associated with changes in the angle of the bond. This can be expressed as

$$U = \sum_{ij} \frac{1}{2} k_{ij} (\mathbf{u}_i - \mathbf{u}_j)^2 + \sum_{ijk} \frac{1}{2} \kappa_{ijk} \phi_{ijk}^2 \ , \tag{11.1}$$

where U is the total energy, the sums are over all particle pairs ij or all particle triplets ijk. The force constant is $k_{ij} = k$ for bonds in contact and zero otherwise, and $\kappa_{ijk} = \kappa$ for triplets with a common vertice, and zero otherwise. The vector $\mathbf{u}_i$ gives the displacement of node i from its equilibrium position. The various quantities are illustrated in Fig. 11.1

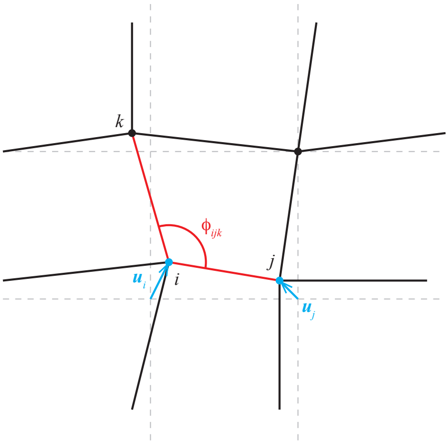

Fig. 11.1 Illustration of the initial bond lattice (dashed, gray), and the deformed bond lattice. Three nodes i, j, k are illustrated. The angle ϕ_{ijk} is shown. The displacements $\mathbf{u}_i$ and $\mathbf{u}_j$ are shown respectively with cyan vectors.

Elastic modulus. Let us address the effective elastic behavior of the percolation system. We would like to describe the material using a material property such as Young's modulus, E, or the shear modulus, G. Let us consider a three-dimensional sample with cross-sectional area $A = L^2$ and length L. Young's modulus, E, relates the tensile stress, σ_{zz}, applied normal to the surface with area A to the elongation ΔL in the

z-direction.

$$\sigma_{zz} = \frac{F_z}{A} = E\frac{\Delta L_z}{L} \ , \tag{11.2}$$

We can therefore write the relation between the force F_z and the elongation ΔL_z as

$$F_z = \frac{EA}{L}\Delta L = \frac{EL^2}{L}\Delta L = L^{d-2}E\Delta L \ . \tag{11.3}$$

We recognize this as a result similar to the relation between the conductance and the conductivity of the sample, and we will call $K = L^{d-2}E$ the compliance of the system. We recognize this as being similar to the spring constant of a spring.

Elastic properties when $p < p_c$. What happens to the compliance of the system as a function of p? When $p < p_c$ there are no connecting paths from one side to another, and the compliance will therefore be zero. It requires zero force F_z to generate an elongation ΔL_z in the system. Notice that we are only interested in the infinitesimal effect of deformation. If we compress the sample, we will of course eventually generate a contacting path, but we are only interested in the initial response of the system.

Elastic properties when $p > p_c$. When $p \geq p_c$ there will be at least one path connecting the two edges. For a system with a bending stiffness, there will be a load-bearing path through the system, and the deformation ΔL_z of the system requires a finite force, F_z. The compliance K will therefore be larger than zero. We have therefore established that for a system with bending stiffness, the percolation threshold for rigidity coincides with the percolation threshold for connectivity. However, for a central force lattice, we know that the spanning cluster at p_c will contain may singly connected bonds. These bonds will be free to rotate, and as a result a central force network will have a rigidity percolation threshold which is higher than the connectivity threshold. Indeed, rigidity percolation for central force lattices will have very high percolation thresholds in three dimensions and higher. Here, we will only focus on lattices with bond bending terms.

Behavior of E close to p_c. Based on our experience with percolation systems, we may hypothesize that Young's modulus will follow a power-law in $(p - p_c)$ when p approaches p_c:

$$E \propto \begin{cases} 0 & p < p_c \\ (p-p_c)^{\tau} & p > p_c \end{cases} \ . \tag{11.4}$$

where τ is an exponent describing the elastic system. We will now use our knowledge of the percolation systems to show that this behavior is indeed expected, and to determine the value of the exponent τ.

11.1.1 Developing a theory for $E(p, L)$

Let us address the Young's modulus $E(p, L)$ of a percolation system with occupation probability p and a system size L. We could also write E as a function of the correlation length $\xi = \xi(p)$, so that $E = E(\xi, L)$. Young's modulus is in general related to the compliance through $E(\xi, L) = K(\xi, L)L^{d-2}$. We can therefore address the compliance of the system and then calculate Young's modulus.

Dividing the system into boxes of size ξ. We will follow an approach similar to what we used to derive the behavior of $P(p, L)$. First, we address the case when the correlation length $\xi \ll L$. In this case, we can subdivide the L^d system into boxes of linear size ξ as illustrated in Fig. 11.2. There will be $(L/\xi)^d$ such boxes. On this scale the system is homogeneous. Each box will have a compliance $K(\xi, \xi)$, and the total compliance will be $K(\xi, L)$.

Compliance of the combined system. We know that the total compliance of n elements in series is $1/n$ times the compliance of a single element. You can easily convince yourself of this addition rule for spring constants, by addressing two springs in series. Similarly, we know that adding n elements in parallel will make the total system n times stiffer, that is, the compliance will be n times the compliance of an individual element. The total compliance $K(\xi, L)$ of this system of $(L/\xi)^d$ boxes is therefore:

$$K(\xi, L) = K(\xi, \xi)(\frac{L}{\xi})^{d-2} . \tag{11.5}$$

Young's modulus can then be found as

$$E(\xi, L) = L^{-(d-2)}K(\xi, L) = \frac{K(\xi, \xi)}{\xi^{d-2}} . \tag{11.6}$$

In order to progress further we need to find the compliance $K(\xi, \xi)$. However, we recognize that this is the compliance of the percolation system at $p = p_c$ when the system size L is the correlation length L. We are therefore left with the problem of finding the compliance of the spanning cluster at $p = p_c$ as a function of system size L.

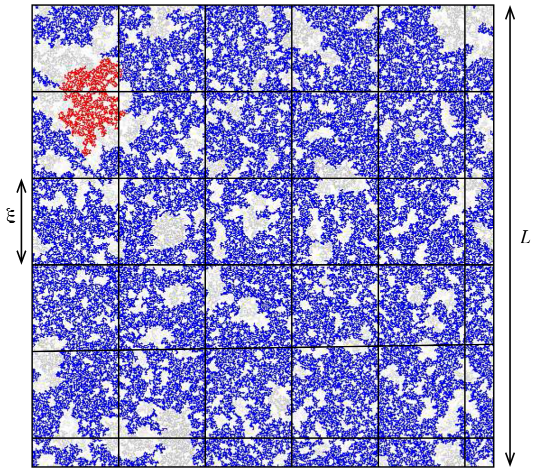

Fig. 11.2 Illustration of subdivision of a system with $p = 0.60$ into regions with a size corresponding to the correlation length, ξ. The behavior inside each box is as for a system at $p = p_c$, whereas the behavior of the overall system is that of a homogeneous system of boxes of linear size ξ.

11.1.2 Compliance of the spanning cluster at $p = p_c$

Again, we expect from our experience from the behavior of scaling structures that the compliance will scale with the system size with a fractal dimension $\tilde{\zeta}_K$:

$$K \propto L^{\tilde{\zeta}_K} \ . \tag{11.7}$$

We will follow our standard approach: we assume a scaling behavior, establish a set of bounds for K, which will also serve as a proof of the scaling behavior of K, and then use this result to develop a general theory for $K(p, L)$.

Energy, force and elongation of the system. We will use arguments based on the total energy of the system. The total energy of a system subjected to a force $F = F_z$ resulting in an elongation ΔL is:

$$U = \frac{1}{2} K (\Delta L)^2 \ , \tag{11.8}$$

where the elongation ΔL is related to the force F through, $\Delta L = F/K$. Consequently,

$$U = \frac{1}{2} K (\frac{F}{K})^2 = \frac{1}{2} \frac{F^2}{K} \ . \tag{11.9}$$

We can therefore relate the elastic energy of a system subjected to the force F directly to the compliance of that system.

Upper bound for the compliance. Our arguments will be based on the geometrical picture we have of the spanning cluster when $p = p_c$. The cluster consists of singly connected bonds, blobs, and dangling ends. The dangling ends do not influence the elastic behavior, and can be ignored in our discussion. It is only that backbone that contribute to the elastic properties of the spanning cluster. We can find an upper bound for the compliance by considering the singly connected bonds. The system consists of the blob and the singly connected bonds in series. The compliance must include the effect of all the singly connected bonds in series. However, adding the blobs in series as well will only contribute to lowering the compliance. We will therefore get an upper bound on the compliance, by assuming all the blobs to be infinitely stiff, and therefore only include the effects of the singly connected bonds.

Let us therefore study the elastic energy in the singly connected bonds when the cluster is subjected to a force F. The energy, U, can be decomposed in a stretching part, U_s, and a bending part, U_b: $U = U_s + U_b$.

For a singly connected bond from site i to site j, the change in length, $\delta\ell_{ij}$, due to the applied force F is $\delta\ell_{ij} = F/k$, where k is the force constant for a single bond. The energy due to stretching, U_s, is therefore

$$U_s = \sum_{ij} \frac{1}{2} k \delta\ell_{ij}^2 = \sum_{ij} \frac{1}{2} k (\frac{F}{k})^2 = \frac{1}{2} \frac{M_{SC}}{k} F^2 \ , \tag{11.10}$$

where M_{SC} is the mass of the singly connected bonds.

We can find a similar expression for the bending terms. For a bond between sites i and j, the change in angular orientation, $\delta\phi_{ij}$ is due to the torque $T = r_i F$, where r_i is the distance to bond i in the direction normal to the direction of the applied force F: $\delta\phi_{ij} = T/\kappa$. The contribution from bending to the elastic energy is therefore

$$U_b = \sum_{ij} \frac{1}{2} \kappa (\delta\phi_{ij})^2 = \frac{1}{2} \sum_{ij} \kappa (\frac{r_i F}{\kappa})^2 = \frac{1}{2\kappa} M_{SC} R_{SC}^2 F^2 \ , \tag{11.11}$$

where

$$R_{SC}^2 = \frac{1}{M_{SC}} \sum_{ij} r_i^2 \ , \tag{11.12}$$

where the sum is taken over all the singly connected bonds.

The elastic energy of the singly connected bonds is therefore:

$$U_{SC} = (\frac{1}{2k} + \frac{R_{SC}^2}{2\kappa}) M_{SC} F^2 \ , \tag{11.13}$$

and the compliance of the singly connected bonds is

$$K_{SC} = \frac{F^2}{2U} = \frac{1}{(1/k + R_{SC}^2/\kappa)M_{SC}} \; . \tag{11.14}$$

which is an upper bound for the compliance K of the system.

Lower bound for the compliance. We can make a similar argument for a lower bound for the compliance K of the system. The minimal path on the spanning cluster provides the minimal compliance. The addition of any bonds in parallel will only make the system stiffer, and therefore increase the compliance. We can determine the compliance of the minimal path by calculating the elastic energy of the minimal path. We can make an identical argument as we did above, but we need to replace M_{SC} with the mass, M_{min}, of the minimal path, and the radius of gyration R_{SC}^2 with the radius of gyration of the bonds on the minimal path R_{min}^2.

Kantor [20] has provided numerical evidence that both R_{min}^2 and R_{SC}^2 is proportional to ξ^2. When we are studying the spanning cluster at $p = p_c$ this corresponds to R_{min} and R_{SC} being proportional to L. This shows that the dominating term for the energy is the bending and not the stretching energy when p is approaching p_c.

Bounded expression for the compliance K. We have therefore determined the scaling relation

$$K_{min} \leq K \leq K_{SC} \; , \tag{11.15}$$

where we have found that when $L \gg 1$, $K_{min} \propto L^{-(D_{min}+2)}$ and $K_{SC} \propto L^{-(D_{SC}+2)}$. That is:

$$L^{-(D_{min}+2)} \leq K(L) \leq L^{-(D_{SC}+2)} \; . \tag{11.16}$$

Because $K(L)$ is bounded by two power-law in L (for all values of L), we have also demonstrated that $K(L)$ also is a power-law in L with an exponent $\tilde{\zeta}_K$ satisfying the relation

$$-(D_{min} + 2) \leq \tilde{\zeta}_K \leq -(D_{SC} + 2) \; . \tag{11.17}$$

11.1.3 Finding Young's modulus $E(p, L)$

This scaling relation gives us $K(p_c, L)$. We use this expression to find $K(\xi, \xi)$, the compliance of a system of size ξ from (11.6):

$$E(\xi, L) = \frac{K(\xi,\xi)}{\xi^{d-2}} \propto \frac{\xi^{\tilde{\zeta}_K}}{\xi^{d-2}} \propto \xi^{\tilde{\zeta}_K-(d-2)} \; . \tag{11.18}$$

We have therefore found a relation for the scaling exponent τ:

$$E(p, L) = \xi^{-(d-2-\tilde{\zeta}_K)} \propto (p-p_c)^{(d-2-\tilde{\zeta}_K)\nu} \propto (p-p_c)^{\tau} \; . \tag{11.19}$$

The exponent τ is therefore in the range:

$$(d-2+D_{SC}+2)\nu \le \tau \le (d-2+D_{min}+2)\nu \; , \tag{11.20}$$

Bounds on the exponent τ. The resulting bounds on the scaling exponents are:

$$(D_{SC}+2)\,\nu \le \tau \le (D_{min}+2)\,\nu \; , \tag{11.21}$$

For two-dimensional percolation the exponents are approximately

$$3.41 \le \tau \le 3.77 \; , \tag{11.22}$$

Similarity between the flow and the elastic problems. We see that the bounds are similar to the bounds we found for the exponent $\tilde{\zeta}_R$. This similarity lead Sahimi [29] and Roux [27] to conjecture that the elastic coefficients E and G, and the conductivity σ is related through

$$\frac{E}{\sigma} \propto \xi^{-2} \; . \tag{11.23}$$

and therefore that

$$\tau = \mu + 2\nu = (d + \tilde{\zeta}_R)\nu \; . \tag{11.24}$$

which is well supported by numerical studies.

In the limit of high dimensions, $d \ge 6$, the relation $\tau = \mu + 2\nu = 4$ becomes exact. However, we can use as a rule of thumb that the exponent $\tau \simeq 4$ in all dimensions $d \ge 2$.

Diffusion in disordered media 12

In this chapter we will study diffusional transport in disordered media. We can model diffusional transport either by solving the diffusion equation or by studying the time developments of random walks — both approaches produce the same results. We will use the statistical approach and study how random walkers spread with time in free space as well as on percolation clusters. We will introduce a scaling theory for the behavior of this process in both space and time — extending our previous scaling approaches and proving us with new tools and insights. We will do this in several steps, starting with a brief introduction to random walks and diffusion in uniform media, then introduce a computational model for random walks on the percolation cluster, and finally apply our full set of tools to develop scaling theories for the observed behavior [15, 13, 26].

12.1 Diffusion and random walks in homogeneous media

A typical example of a random walk is the random motion of a small dust particle due to random collisions with air molecules, a process called Browian motion. Random walks are general processes that we often use as physicial, theoretical or conceptual models.

A two-dimensional random walk. If a random walker starts at $\mathbf{r} = 0$, its position $\mathbf{r}_n$ after n steps can be written as

$$\mathbf{r}_n = \mathbf{r}_0 + \sum_{i=1}^{n} \mathbf{u}_i \ , \tag{12.1}$$

where $\mathbf{u}_i$ is step i. We will usually assume that the steps $\mathbf{u}_i$ are independent and isotropically distributed.

Generating a random walk. We can generate an example of random walk by selecting $\mathbf{u}_i = (x_i, y_i)$, where x_i and y_i are selected from e.g. a uniform random distribution from -1 to 1. The following program calculates and visualizes the resulting path starting from the origin, and the resulting path is shown in Fig. 12.1.

```
from pylab import *
n=1000
u = 2*random(size=(n,2))-1
r = cumsum(u,axis=0)
plot(r[:,0],r[:,1])
```

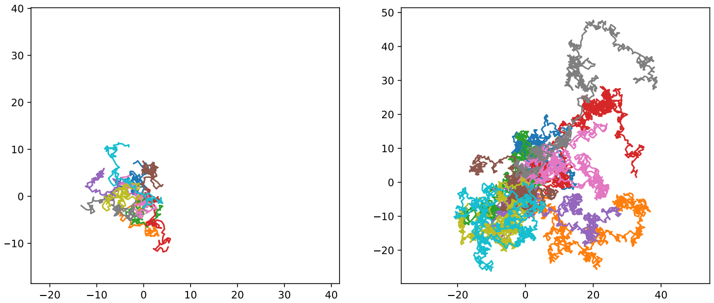

Fig. 12.1 Plots of 10 random walks of size $n = 100$ (left) and $n = 1000$ (right).

We notice that the random walker spreads out gradually, leaving behind a trace with a complex geometry. Let us now see if we can develop a theory for growth of random walker and for their geometry.

12.1.1 Theory for the time development of a random walk

We can develop a theory for the position $\mathbf{r}_n$ as a function of the number of steps n. For simplicity, we start the walker at the origin, so that $\mathbf{r}_0 = 0$. First, we see find the average position after n steps:

$$\langle \mathbf{r}_n \rangle = \langle \sum_{i=1}^{n} \mathbf{u}_n \rangle = \sum_{i=1}^{n} \langle \mathbf{u}_i \rangle = 0 \ , \tag{12.2}$$

where we have used that since $\mathbf{u}_i$ are isotropic, $\langle \mathbf{u}_i \rangle = 0$. This is not surprising, the random walker has the same probability to walk in all directions and therefore does not get anywhere on average.

However, from Fig. 12.1 we see that the extent of the path increases with the number of steps n. We can characterize this using similar measures to what we used to describe the geometry of the percolation clusters, by measuring r_n^2 instead. We find the average value of r_n^2 using the same approach:

$$\begin{aligned}
\langle r_n^2 \rangle &= \langle \left(\sum_i \mathbf{u}_i \right) \cdot \left(\sum_j \mathbf{u}_j \right) \rangle && (12.3) \\
&= \langle \sum_i \sum_j \mathbf{u}_i \cdot \mathbf{u}_j \rangle && (12.4) \\
&= \langle \sum_{i=j} \mathbf{u}_i \cdot \mathbf{u}_j \rangle + \langle \sum_{i \neq j} \mathbf{u}_i \cdot \mathbf{u}_i \rangle && (12.5) \\
&= \sum_i \langle \mathbf{u}_i \cdot \mathbf{u}_i \rangle + \sum_{i \neq j} \underbrace{\langle \mathbf{u}_i \cdot \mathbf{u}_i \rangle}_{=0} && (12.6) \\
&= n\delta^2 \, , && (12.7)
\end{aligned}$$

where $\langle \mathbf{u}_i \cdot \mathbf{u}_i \rangle = \delta^2$ is a property of the distribution of $\mathbf{u}_i$ corresponding to the variance of the distribution. And where we have used that because $\mathbf{u}_i$ and $\mathbf{u}_j$ are independent, the average of their product is equal to the product of their averages:

$$\langle \mathbf{u}_i \cdot \mathbf{u}_j \rangle = \langle \mathbf{u}_i \rangle \cdot \langle \mathbf{u}_j \rangle = 0 \cdot 0 = 0 \, . \qquad (12.8)$$

Consequently, we have shown that $r_n^2 = n\delta^2$. This is a *very general result.* We have found that the size of the diffusion path increases slowly with the number of steps: $r_n = \delta n^{1/2}$. This result is valid in any dimension as long as the two basic assumptions are satisfied: The individual steps are independent and each individual step has an isotropic distribution so that the average displacement from a single step is zero.

The dimension of the random walk. Here we have demonstrated that the size of the random walk, measured as r^2, is proportional to the number of elements in the random walk. This is similar to the way we measured the size of a cluster using the radius of gyration of the cluster. Indeed, it can be shown that these two definitions give the same relation $r_n^2 = b^2 n$, where b is a constant of unit length that describes the distribution of a single step. We realize that n is the number of elements in the random walk, corresponding to s, the number of sites in a cluster. We have therefore found that $r_n = bn^{1/2}$, or similarly, that $n = (r_n/b)^2 \propto r^{D_w}$. This implies that the dimension, D_w, of the random walk always is $D_w = 2$ — independent of the embedding dimension d. This means that for $d = 1$ the random walk will overfill space. Indeed, we expect it to step on top of itself repeatedly. For $d = 2$ the random walk will just fill space since $D_w = d$, whereas for $d = 3$ and higher dimensions the random walk will fill a diminishing portion of space. (Just like the spanning cluster had a smaller scaling exponent than the spatial dimension, and hence the density of the spanning cluster decreased for larger systems).

12.1.2 Continuum description of a random walker

We can also describe the motion of the random walker through the probability density $P(\mathbf{r}, t)$, where $P(\mathbf{r}, t)d\mathbf{r}dt$ is the probability for the random walker to be in the volume $\mathbf{r}d\mathbf{r}$ in the time period t to $t + dt$.

For a random walker on a grid, the probability to be at a grid position i is given as $P_i(t)$. The probability for the walker to be at a position i at the time $t = t + \delta t$ is then

$$P_i(t + \delta t) = P_i(t) + \sum_j [\sigma_{j,i} P_j(t) - \sigma_{i,j} P_i(t)]\delta t \ , \tag{12.9}$$

where the sum is over all neighbors j of the site i. The term $\sigma_{i,j}$ is the transition probability. The first term in the sum represents the probability that the walker during the time period δt walks into site i from site j, and the second term represents the probability that the walker during the time period δt walks from site i to one of the neighboring sites j.

When $\delta t \to 0$ this equation approaches a differential equation

$$\frac{\partial P_i}{\partial t} = \sum_j [\sigma_{j,i} P_j(t) - \sigma_{i,j} P_i(t)] \ . \tag{12.10}$$

If we assume that the transition probability is equal for all the neighbors, so that $\sigma_{i,j} = 1/Z$, where Z is the number of neighbors, the differential equation simplifies to

$$\frac{\partial P}{\partial t} = D \nabla^2 P \ , \tag{12.11}$$

which we recognize as the diffusion equation, where the diffision constant D is related to the transition probabilities $\sigma_{i,j}$ and Z.

The general solution to this equation is

$$P(\mathbf{r},t) = \frac{1}{(2\pi Dt)^{d/2}} e^{-r^2/2Dt} = \frac{1}{(2\pi)^{d/2}|\mathbf{R}|^2} e^{-\frac{1}{2}(\frac{r}{|\mathbf{R}|})^2} , \tag{12.12}$$

where we have introduced $|\mathbf{R}| = \sqrt{Dt}$.

It can be shown that the moments of this distribution are

$$\langle r^k \rangle = A_k R(t)^k \propto t^{k/2} , \tag{12.13}$$

and specifically, that

$$\langle r^2 \rangle = \int P(\mathbf{r},t) r^2 d\mathbf{r} = R^2(t) = Dt . \tag{12.14}$$

We are now ready to address the behavior of random walkers on percolation clusters.

12.2 Random walks on clusters

We now have the basic tools to understand diffusion in homogeneous media: by studying the position $\mathbf{r}(t)$ of a random walker as a function of the number of steps n or the time $t = n\delta t$, where δt is the time for a single step.

How can we use this method to study diffusion on a percolation cluster? We want to address how a particle diffuses on the cluster. That is, we want to study how a random walker moves on the occupied sites in the percolation system. We will assume that the walker only can move onto connected neighbor sites in each step.

There are many different ways we can construct such measurements, and as always, we need to be very precise when we define both the experiment and our set of measures. Our plan is to drop a random walker onto a random site in the percolation system and measure the position $\mathbf{r}(t)$ of the walker as a function of time.

12.2.1 Developing a program to study random walks on clusters

In order to *study* the behavior we need to develop a program to generate a random walk on top of a percolation lattice, generate many such paths and collect, analyze and visualize the resulting behavior.

The rules for such a walker would be that we select a position at random and then parachute the walker into this position. We start with a percolation system given by the $L \times L$ matrix `cluster`, where `cluster` is `True` in the points where the sites are present. The initial positions, `ix`, `iy`, in the x- and y-direction for the walker are therefore random numbers between 0 and $L - 1$ respectively:

```
ix = randint(L)
iy = randint(L)
```

where `L` is the system size. If this site is empty, the walk stops immediately and its length is zero:

```
if not cluster[ix,iy]:
   return
```

Storing the trajectory of the walker. We store the trace of the walker in two arrays (we need both to handle periodic boundary conditions later): `walker_map` which consists of the positions `ix,iy` of the walker for each step, and `displacement`, which consists of the positions relative to the initial position of the walker.

Random selection of next step. How do we select where the walker can move? The walker is restricted to move to nearest neighbor sites that are present. There are several approaches:

- We may select a direction at random and try to move in this direction. If the walker cannot move in this direction it stays put for this step, and then tries again in the next step. In this case, the walker may have many steps without any motion.
- We may find all the directions the walker can possibly move in, and then select one of these directions at random. In this case the walker will move onto a new site in each step.

Both these methods effectively produce the same behavior. We will select the second method. We therefore need to create a list of the possible directions to move in. In order to make this list, we have a list called `directions` of possible movement directions:

```
    directions = np.zeros((2, 4), dtype=np.int64)
    # X-dir: east and west, Y-dir: north and south.
    directions[0, 0] = 1
    directions[1, 0] = 0
    directions[0, 1] = -1
    directions[1, 1] = 0
    directions[0, 2] = 0
    directions[1, 2] = 1
    directions[0, 3] = 0
    directions[1, 3] = -1
```

For each step, we need to collect all the possible steps into a list called `neighbor_arr`. This is done by the following loop:

```
    neighbor = 0
        for idir in range(directions.shape[1]):
            dr = directions[:,idir]
            iix = ix + dr[0]
            iiy = iy + dr[1]
            if 0 <= iix < L and 0 <= iiy < L and cluster[iix, iiy]:
                neighbor_arr[neighbor] = idir
                neighbor += 1
```

If this list is empty, that is, if `neighbor` is zero, there are *no possible places to move*. This means that the walker has landed on a cluster of size $s = 1$. In this case, we stop and return with $n = 1$.

Finally, we select one of the `neighbor` directions at random, move the walker into this site, update `walker_map` and `displacement` and repeat the process.

```
        # Select random direction from 0 to neighbor-1
        randdir = randint(neighbor)
        dir = neighbor_arr[randdir]
        ix += directions[0, dir]
        iy += directions[1, dir]
        step += 1
        walker_map[0, step] = ix
        walker_map[1, step] = iy
        displacement[:,step]=displacement[:,step-1]+directions[:,dir]
```

Here, `step` corresponds to n, the current step number.

Preparing the function. We put this into a function and use the `numba` library to speed up simulation times.

```
import numba
import numpy as np

@numba.njit(cache=True)
def percwalk(cluster, max_steps):
    """Function performing a random walk on the spanning cluster.
    Parameters
    ----------
    cluster : np.ndarray
        Boolean array with 1's signifying a site in the spanning cluster.
    max_steps : int
        Maximum number of walker steps to perform.
    Returns
    -------
    walker_map : np.ndarray
        A coordinate map of the walk performed, x in [0] and y in [1]
    displacement : np.ndarray
        A coordinate map of relative positions, x in [0] and y in [1]
    num_steps : int
        Number of steps performed.
    """
    walker_map = np.zeros((2, max_steps))
    displacement = np.zeros_like(walker_map)
    directions = np.zeros((2, 4), dtype=np.int64)
    neighbor_arr = np.zeros(4, dtype=np.int64)
    # X-dir: east and west, Y-dir: north and south.
    directions[0, 0] = 1
    directions[1, 0] = 0
    directions[0, 1] = -1
    directions[1, 1] = 0
    directions[0, 2] = 0
    directions[1, 2] = 1
    directions[0, 3] = 0
    directions[1, 3] = -1
    # Initial random position
    Lx, Ly = cluster.shape
    ix = np.random.randint(Lx)
    iy = np.random.randint(Ly)
    walker_map[0, 0] = ix
    walker_map[1, 0] = iy
    step = 0
    if not cluster[ix, iy]: # Landed outside the cluster
        return walker_map, displacement, step
    while step < max_steps-1:
        # Make list of possible moves
        neighbor = 0
        for idir in range(directions.shape[1]):
            dr = directions[:,idir]
            iix = ix + dr[0]
            iiy = iy + dr[1]
            if 0 <= iix < Lx and 0 <= iiy < Ly and cluster[iix, iiy]:
                neighbor_arr[neighbor] = idir
                neighbor += 1
        if neighbor == 0: # No way out, return
            return walker_map, displacement, step
        # Select random direction from 0 to neighbor-1
        randdir = randint(neighbor)
        dir = neighbor_arr[randdir]
        ix += directions[0, dir]
        iy += directions[1, dir]
        step += 1
        walker_map[0, step] = ix
        walker_map[1, step] = iy
        displacement[:,step]=displacement[:,step-1]+directions[:,dir]
    return walker_map, displacement, step
```

Testing the function. Let us test the newly generated function on a few simplified cases. First, we try it on a system with $p = 1$, that is, on a homogeneous system.

```
from pylab import *
L = 50
p = 1
z=rand(L,L)<p
imshow(z,origin="lower")
walker_map, displacement, steps = percwalk(z,200)
# walker_map is oriented as row-column (ix, iy)
plot(walker_map[1,:steps],walker_map[0,:steps])
```

Walks from 10 such simulations are shown in Fig. 12.2. This looks reasonable and nice, but we do notice that quite a few of these walks reach the boundaries of the system. We may wonder how this finite system size affects the behavior and statistics of the system.

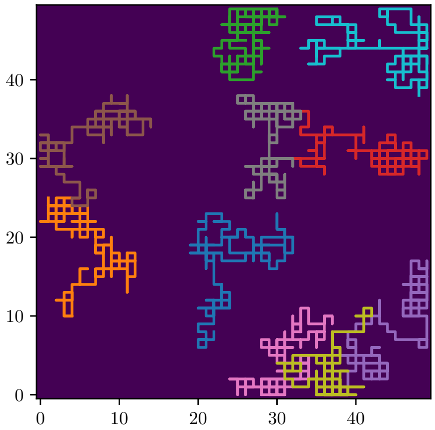

Fig. 12.2 Trajectories of 10 random walks for a (homogeneous) system with $L = 50$ and $p = 1$.

Measuring $r^2(t)$ for a random walker. The function `percwalk` returns the displacements, $\mathbf{r}_n$, for the walking starting from $\mathbf{r}_0 = 0$. We find r_n^2 and visualize the result for a single walk:

```
from pylab import *
L = 50
p = 1
z=rand(L,L)<p
walker_map, displacement, steps = percwalk(z,200)
r2 = sum(displacement**2,axis=0)
```

```
t = arange(len(r2))
plot(t,r2)
```

The resulting plot is shown in Fig. 12.3. We do not really learn much from this plot — we need to collect more statistics. We need to generate many different walks and then average over all the walks to find a statistically better measure for $r^2(t)$.

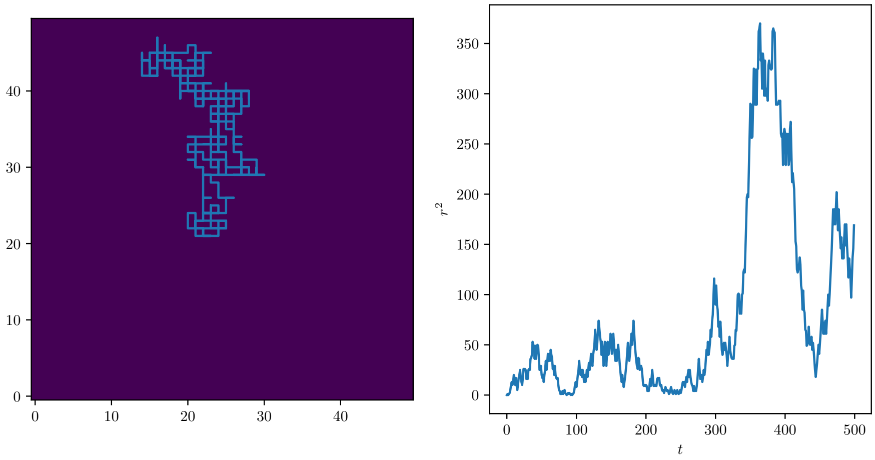

Fig. 12.3 (a) Trajectory of a random walk for a (homogeneous) system with $L = 50$ and $p = 1$. (b) Plot of the corresponding $r^2(t)$.

Collecting statistics for $r^2(t)$. We therefore write a small function to generate a given number of clusters with the given p. For each such cluster we will generate a given number of walks. Notice, that we must also specify the maximum number of steps that we model for each walk. The following function implements these features:

```
@numba.njit(cache=True)
def find_displacements(p,L,num_systems,num_walkers,max_steps):
    displacements = zeros(max_steps)
    for system in range(num_systems):
        z = rand(L,L)<p
        for j in range(num_walkers):
            num_steps = 0
            while num_steps <= 1:
                walker_map,displacement,num_steps = percwalk(z,max_steps)
        displacements += sum(displacement**2, axis=0)
    displacements = displacements/(num_walkers*num_systems)
    return displacements
```

Notice a few details: If the number of steps is 1 or smaller it means that the walker landed either on an empty size ($n = 0$) or on a single site ($n = 1$). We do not want to include these in our statistics since they provide little information about the behavior of the random walker. We use this program to collect statistics from $M = 500$ random walks of length $n = 10000$ steps on a $L = 100$ system:

```
p = 1
L = 100
max_steps = 10000
num_walkers = 500
num_systems = 100
displacements = find_displacements(p,L,num_systems,num_walkers,max_steps)
dr1 = displacements[1:]
t = arange(len(dr))
loglog(t,dr)
```

The resulting plot in Fig. 12.4(a) shows that the system indeed behaves as we expect — for small values of t. However, as t increases, we see that the effect of the finite system size L starts to affect the results. This is because the random walker is limited by the wall and eventually we will be limited the $L \times L$ system. This problem will also arise when we study the percolation system. How can we reduce this problem?

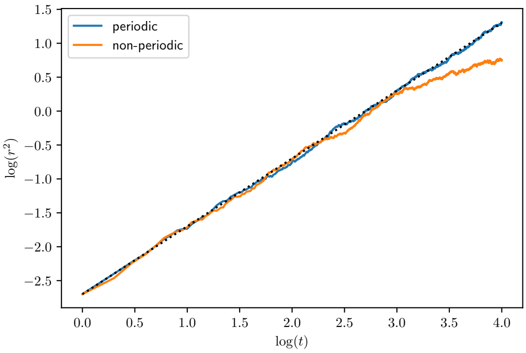

Fig. 12.4 Plot of $r^2(t)$ for a $L = 100$ system with non-periodic and periodic boundary conditions.

Introducing periodic boundary condition. One way of reducing this problem is by introducing *periodic boundary conditions*. The idea is that is the random walker steps outside the lattice on the left side, it appears on the right-hand side instead. That is, if `ix` becomes -1, it is instead set to $L - 1$. We implement this in the `percwalk` function in the following.

The resulting plot of $r^2(t)$ in Fig. 12.4 shows that this solves the problem with the boundaries. This aspect will be even more important when we study percolation systems in non-uniform media.

```python
# With periodic boundary conditions - essential for good statistics
import numba
import numpy as np

@numba.njit(cache=True)
def percwalk(cluster, max_steps):
    """Function performing a random walk on the spanning cluster.
    Parameters
    ----------
    cluster : np.ndarray
        Boolean array with 1's signifying a site in the spanning cluster.
    max_steps : int
        Maximum number of walker steps to perform.
    Returns
    -------
    walker_map : np.ndarray
        A coordinate map of the walk performed, x in [0] and y in [1]
    displacement : np.ndarray
        A coordinate map of relative positions, x in [0] and y in [1]
    num_steps : int
        Number of steps performed.
    """
    walker_map = np.zeros((2, max_steps))
    displacement = np.zeros_like(walker_map)
    directions = np.zeros((2, 4), dtype=np.int64)
    neighbor_arr = np.zeros(4, dtype=np.int64)
    # X-dir: east and west, Y-dir: north and south.
    directions[0, 0] = 1
    directions[1, 0] = 0
    directions[0, 1] = -1
    directions[1, 1] = 0
    directions[0, 2] = 0
    directions[1, 2] = 1
    directions[0, 3] = 0
    directions[1, 3] = -1
    # Initial random position
    Lx, Ly = cluster.shape
    ix = np.random.randint(Lx)
    iy = np.random.randint(Ly)
    walker_map[0, 0] = ix
    walker_map[1, 0] = iy
    step = 0
    # Check if we landed outside the spanning cluster
    if not cluster[ix, iy]:
        # Return the map with starting position and number of steps
        return walker_map, displacement, step
    while step < max_steps-1:
        # Make list of possible moves
        neighbor = 0
        for idir in range(directions.shape[1]):
            dr = directions[:,idir]
            iix = ix + dr[0]
            iiy = iy + dr[1]
            # Periodic BC
            if iix>=Lx:
                iix = iix-Lx
            if iix<0:
                iix = iix+Lx
            if iiy>=Ly:
                iiy = iiy-Ly
            if iiy<0:
                iiy = iiy+Ly
            if cluster[iix, iiy]:
                neighbor_arr[neighbor] = idir
                neighbor += 1
        if neighbor == 0: # No way out, return
            return walker_map, displacement, step
        # Select random direction from 0 to neighbor-1
        randdir = np.random.randint(neighbor)
        dir = neighbor_arr[randdir]
        ix += directions[0, dir]
        iy += directions[1, dir]
        step += 1
        walker_map[0, step] = ix
        walker_map[1, step] = iy
        displacement[:,step]=displacement[:,step-1]+directions[:,dir]
    return walker_map, displacement, step
```

12.2.2 Diffusion on a finite cluster for $p < p_c$

We now have all the tools to stary studying the behavior of a random walker on top of a percolation system. We select $p = p_c$ and drop the random walker on a random position on the lattice. The resulting set of walks from such a simulation can be seen in Fig. 12.5.

```
from pylab import *
L = 100
p = 0.5927
z=rand(L,L)<p
imshow(z,origin="lower")
for i in range(30):
    walker_map, displacement, steps = percwalk(z,10000)
    plot(walker_map[1,:steps],walker_map[0,:steps],’o’,markersize=4)
```

Understanding behavior for $p > p_c$. We then simulate a larger set of walks for $p = 0.45, 0.50, 0.55, p_c$. The resulting plots of $r^2(t)$ are shown in Fig. 12.6. We see that when $p < p_c$, $r^2(t) \propto t^x$ for some time, but then

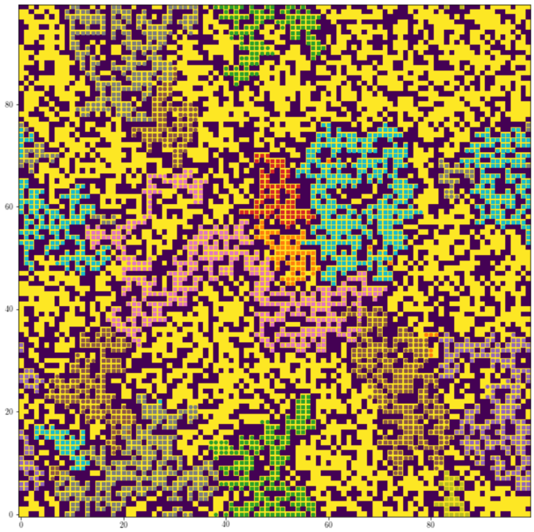

Fig. 12.5 Plot of 30 walks in a $L = 100$ system at $p = p_c$.

aften some time, $r^2(t)$ crosses over to a constant instead. How can we understand this behavior?

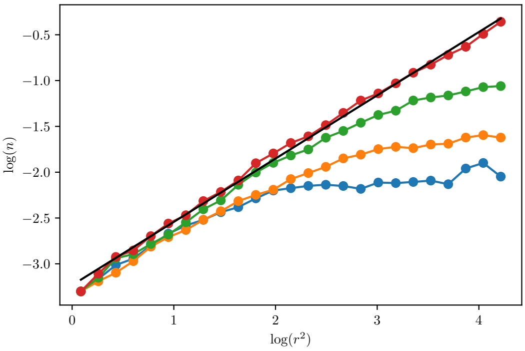

Fig. 12.6 Plots of $r^2(t; p, L)$ for $p = 0.45, 0.50, 0.55, p_c$

Long-term behavior when $p < p_c$. For a single walker that lands on a cluster of size s, we expect that the walker will be limited to walk on this cluster and therefore cannot reach positions that are much further away than R_s. Thus, after a long time, we expect $r^2(t) \propto R_s^2$. If we repeat this experiment many times, each time dropping the walker onto a random occupied point in the system, we need to take the average over all clusters of size s and over all starting positions, to find the average of $r^2(t)$ for all these different walks. If we drop the walker at a random position, the probability for that walker to land on a cluster of size s is $sn(s,p)$, and the contribution from this cluster to $r^2(t)$ after a long time is R_s^2. Therefore, the average $\langle r^2(t)\rangle$ for the walker is:

$$\left[\langle r^2\rangle\right] \propto \left[R_s^2\right] = \sum_s R_s^2 sn(s,p) \ . \tag{12.15}$$

We approximate this sum by an integral and replace $n(s,p)$ by the scaling ansatz $n(s,p) = s^{-\tau}F(s/s_\xi)$, getting

$$\left[R_s^2\right] = \int_1^\infty R_s^2 s s^{-\tau} F(s/s_\xi) ds \ . \tag{12.16}$$

We realize that the function $F(s/s_\xi)$ falls to zero very rapidly when $s > s_\xi$ and it is effectively constant below that, we therefore replace the integral with an integral up to s_ξ:

$$\left[R_s^2\right] = \int_1^{s_\xi} R_s^2 s s^{-\tau} ds \ . \tag{12.17}$$

We now insert that $R_s^2 \propto s^{2/D}$ and perform the integral, getting:

$$\left[R_s^2\right] \propto s_\xi^{2/D+2-\tau} \propto s_\xi^{2/D} s_\xi^{2-\tau} \ . \tag{12.18}$$

where we recognize the first factor as $\xi^2 \propto (p-p_c)^{-2\nu}$ and the second factor from (4.34) as $(p-p_c)^\beta$ so that

$$\left[R_s^2\right] \propto (p-p_c)^{\beta-2\nu} \ . \tag{12.19}$$

We notice that in this case the average is of R_s^2 over $sn(s,p)$, but when we calculated the correlation length in (5.21) the average was of R_s^2 over $s^2n(s,p)$, and this is the reason for the appearance of the exponent $\beta-2\nu$ and not simply -2ν as we got for the correlation length.

Short term behavior. There is a transition in $r^2(t)$ to $\left[R^2\right]$ after some crossover time t_0. For times shorter than t_0 we see from Fig. 12.6 that the behavior appears to be that $r^2(t) \propto t^{2k}$ for some exponent $2k$. We notice that as p approaches p_c, the crossover time t_0 increases. All the curves for various p-values appear to have similar, or possibly the same behavior for $t < t_0$.

In Fig. 12.6 we notice that the exponent $2k$ is not 1, as we found for the homogeneous case. It is clearly lower than 1. If we measure it, we find that $2k \simeq 0.66$ and $k \simeq 0.33$. We call this behavior *anomalous diffusion* because the mean squared distance $r^2(t)$ does not grow linearly with time, but with an exponent different than 1. What can we say about the crossover time t_0? We will return to this after examining the case when $p > p_c$.

12.2.3 Diffusion at $p = p_c$

From Fig. 12.6 we also see that for $p = p_c$ the random walk follows $r^2(t) \propto t^{2k}$. This behavior is as expected. For times shorter than t_0, the walker behaves as if it is on p_c, whereas after a long time, $t > t_0$, we start noticing that the walker is restricted when it diffuses on the finite clusters. Another way to think of this is that the crossover time t_0 increases as $p \to p_c$, and diverges at $p = p_c$. The exponent k is a universal exponent for diffusion on percolation systems. It does not depend on the lattice structure or the rules for connectivity, but it does depend on the embedding dimension d.

12.2.4 Diffusion for $p > p_c$

We can use the same computational approach to study the behavior of the random walker when $p > p_c$. The resulting plots for $p = 0.8, 0.75, 0.70, 0.65$ and p_c are shown in Fig. 12.7. The plots show that when $p > p_c$, for short times the $r^2(t)$ curve follows the behavior for $p = p_c$ with $r^2(t) \propto t^{2k}$. But for a crossover time t_0, the behavior changes and crosses over to a behavior where $r^2(t) \propto t^1$, that is, it crosses over to the behavior of a homogeneous system. How can we understand this?

Developing a model for $p > p_c$. We know that when $p = 1$, the system is homogeneous, and $\langle r^2 \rangle = D(1)t$. We will therefore write the general relation for $p > p_c$:

$$\langle r^2 \rangle = D(p)t \ , r \gg \xi \ . \tag{12.20}$$

What behavior do we expect from $D(p)$? We expect $D(p)$ to increase in a way similar to the density of the backbone or the conductivity g. In fact, the Einstein relation for diffusion relates the diffusion constant to the conductance through:

$$D(p) \propto g(p) \propto (p - p_c)^{\mu} \ . \tag{12.21}$$

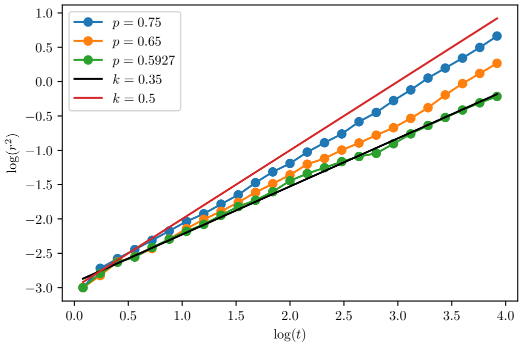

Fig. 12.7 Plots of $r^2(t; p, L)$ for $p = 0.8, 0.75, 0.70, 0.65, p_c$

We therefore expect that when $p > p_c$, and the time is larger than a crossover time $t_0(p)$, that the behavior is scaling with exponent μ, identical to that of conductivity. And for a time shorter than the crossover time, the behavior is identical to the behavior at $p = p_c$. We can understand this in the same way as above: When $t < t_c$ the walker does still not experience that the characteristic clusters are limited by a finite characteristic length ξ.

12.2.5 Scaling theory

Let us develop a scaling theory for the behavior of $\langle r^2 \rangle$. We will assume that when the time is smaller than a cross-over time, the behavior is according to a power-law with exponent $2k$, and that when the time is larger than the cross-over time, the behavior is either that of diffusion with diffusion constant $D(p)$ for $p > p_c$, or it reaches a constant plateau for the case when $p < p_c$.

Let us introduce a scaling ansatz with these properties:

$$\langle r^2 \rangle = t^{2k} f[(p - p_c)t^x] \ . \tag{12.22}$$

We could also have started from any of the end-points, such as from the assumption that

$$\langle r^2 \rangle = (p_c - p)^{\beta - 2\nu} G_1(\frac{t}{t_0}) \ , \tag{12.23}$$

or

$$\langle r^2 \rangle = (p - p_c)^{\mu} G_2(\frac{t}{t_0}) \ . \tag{12.24}$$

We have two unknown exponents k and x that must be determined from independent knowledge. We will assume that the function $f(u)$ has the behavior

$$f(u) = \begin{cases} \text{const.} & |u| \ll 1 \\ u^{\mu} & u \gg 1 \\ (-u)^{\beta - 2\nu} & u \ll -1 \end{cases} \quad (12.25)$$

Let us now address the various limits in order to determine the scaling exponents k and x in terms of known exponents.

Scaling behavior in the limit $p > p_c$. First, we know that when $p > p_c$, that is when $u \gg 1$, we have that

$$\langle r^2 \rangle \propto (p - p_c)^{\mu} t \ , \quad (12.26)$$

which should correspond to the functional form from the ansatz:

$$(p - p_c)^{\mu} t \propto t^{2k} f((p - p_c)t^x) \propto t^{2k} [(p - p_c)t^x]^{\mu} \ . \quad (12.27)$$

This results in the exponent relation

$$2k = 1 - \mu x \ , \quad (12.28)$$

or

$$k = \frac{1 - \mu x}{2} \ . \quad (12.29)$$

Scaling behavior in the limit $p < p_c$. Similarly, we know that the behavior in the limit of $u \ll -1$ should be proportional to $(p_c - p)^{\beta - 2\nu}$. Consequently, the scaling ansatz gives

$$(p_c - p)^{\beta - 2\nu} \propto t^{2k} f((p - p_c)t^x) \propto t^{2k} [(p_c - p)t^x]^{\beta - 2\nu} \ , \quad (12.30)$$

which results in the exponent relation:

$$2k + x(\beta - 2\nu) = 0 \ . \quad (12.31)$$

Solving to find the exponents. We solve the two equations for x and k, finding

$$k = \frac{1}{2}[1 - \frac{\mu}{2\nu + \mu - \beta}] \ , \quad (12.32)$$

and

$$x = \frac{1}{2\nu + \mu - \beta} \ . \quad (12.33)$$

Our argument therefore shows that the scaling ansatz is indeed consistent with the limiting behaviors we have already determined, and it allows us to make a prediction for k and x.

Testing the scaling ansatz. We can test the scaling function by a direct plot of the simulated result. The scaling relation states that $r^2(t) = t^{2k} f[(p-p_c)t^x]$, which means that $r^2(t)t^{-2k} = f[(p-p_c)t^x]$. If we therefore plot $r^2(t)t^{-2k}$ on one axis and $(p-p_c)t^x$ on the other axis, all the data for the various values of p should fall onto a common curve corresponding to the function $f(u)$. This is illustrated in Fig. 12.8, which shows that the scaling ansatz is in good correspondence with the data. Indeed, the plot also shows that the assumptions about the shape of the scaling function $f(u)$ are correct.

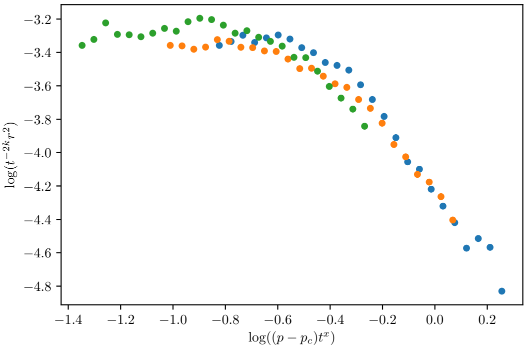

Fig. 12.8 Plots of $r^2(t;p,L)$ for $p = 0.45, 0.50, 0.55$ rescaled according to the scaling theory.

Interpreting the dimension of the walk at $p = p_c$. When $p = p_c$, we find that

$$\langle r^2 \rangle \propto t^{2k} = t^{\frac{2\nu-\beta}{2\nu+\mu-\beta}} , \tag{12.34}$$

We can write this relation in the same way as we wrote the behavior of an ordinary random walk,

$$t \propto r^{d_w} , \tag{12.35}$$

where d_w is the dimension of the random walk. We have therefore found that

$$d_w = \frac{1}{k} = 2 + \frac{\mu}{\nu - \frac{\beta}{2}} , \tag{12.36}$$

which is a number larger than 2. This means that for a given time, the walk remains more compact, which is consistent with our intuition.

Defining the cross-over time. We have introduced a cross-over time, t_0, which is defined so that

$$(p - p_c)t_0^x \simeq 1 \ , \tag{12.37}$$

which gives

$$t_0 \propto |p - p_c|^{-1/x} \propto |p - p_c|^{-(2\nu+\mu-\beta)} \ . \tag{12.38}$$

Interpreting the crossover time. How can we interpret this relation? We could decompose the relation to be:

$$t_0 \propto \frac{|p - p_c|^{\beta-2\nu}}{|p - p_c|^{\mu}} \ , \tag{12.39}$$

where we know that the average radius of gyration for clusters are

$$[R_s^2] \propto |p - p_c|^{\beta-2\nu} \ , \tag{12.40}$$

This gives us an interpretation of the cross-over time for diffusion:

$$t_0(p) \propto \frac{[R_s^2]}{D} \ , \tag{12.41}$$

where D is the diffusion constant. Why is this time not proportional to ξ^2/D, the time it takes to diffuse a distance proportional to the correlation length? The difference comes from the particular way we devised the experiment: the walker was dropped onto a randomly selected occupied site.

Interpreting the behavior for $p > p_c$. Let us now address what happens when $p > p_c$. In this case, the contributions to the variance of the position has two main terms: one term from the spanning cluster and one term from the finite clusters.

$$[\langle r^2 \rangle] = Dt = \frac{P}{p} D't + R_s^2 \ , \tag{12.42}$$

where the first term, $P/pD't$ is the contribution from the random walker on the infinite cluster. This term consists of the diffusion constant D' for a walker on the spanning cluster, and the prefactor P/p which comes from the probability for the walker to land on the spanning cluster: For a random walker placed randomly on an occupied site in the system, the probability for the walker to land on the spanning cluster is P/p, and the probability to land on any of the finite clusters is $1 - P/p$. The second term is due to the finite cluster. This term reaches a constant value for large times t. The only time dependence is therefore in the first term, and we can write:

$$Dt = \frac{P}{p} D' t \; , \tag{12.43}$$

for long times, t. That is:

$$D' = \frac{Dp}{P} \propto (p - p_c)^{\mu - \beta} \propto \xi^{-\frac{\mu - \beta}{\nu}} \propto \xi^{-\theta} \; . \tag{12.44}$$

where we have introduce the exponent

$$\theta = \frac{\mu - \beta}{\nu} \; . \tag{12.45}$$

Interpreting the crossover time for $p > p_c$. We have therefore found an interpretation of the cross-over time t_0, and, in particular for the appearance of the β in the exponent. We see that the cross-over time is

$$t_0 \propto \frac{|p - p_c|^{\beta - 2\nu}}{|p - p_c|^{\mu}} \propto \frac{\xi^2}{D'} \; . \tag{12.46}$$

The interpretation of t_0 is therefore that t_0 is the time the walker needs to travel a distance ξ when it is diffusing with diffusion constant D' on the spanning cluster.

12.2.6 Diffusion on the spanning cluster

How does the random walker behave on the spanning cluster? We have found that for $p > p_c$ and for $t > t_0$ the mean square displacement increases according to

$$\langle r^2 \rangle = D' t \propto (p - p_c)^{\mu - \beta} t \; , \tag{12.47}$$

For $t < t_0$, we expect the behavior to be

$$\langle r^2 \rangle \propto t^{2k'} \; , \tag{12.48}$$

as illustrated in Fig. 12.6.

Interpretation of t_0 for walks on the spanning cluster. We expect the relations to be valid up to the point (t_0, ξ^2), where both descriptions should provide the same result. Therefore we expect

$$\xi \propto t_0^{2k'} \propto D' t_0 \; , \tag{12.49}$$

and therefore that

$$t_0 \propto \frac{\xi^2}{D'} \propto \frac{(p-p_c)^{-2\nu}}{(p-p_c)^{\mu-\beta}} \propto (p-p_c)^{-(2\nu+\mu-\beta)} \ . \tag{12.50}$$

Consequently, the value of t_0 is the same for diffusion on the spanning cluster only as for the diffusion on any cluster including the spanning clsuter. In general, we can interpret t_0 as the time it takes for the walker to diffuse to the end of the cluster when $p < p_c$, and the time it takes to diffuse to a distance ξ on the spanning cluster when $p > p_c$.

Interpretation of k for walks on the spanning cluster. Let us check the other exponent, k'. We find that

$$\xi^2 \propto (p-p_c)^{-2(2\nu+\mu-\beta)k'} \ , \tag{12.51}$$

and therefore that

$$k' = \frac{\nu}{2\nu+\mu-\beta} \ , \tag{12.52}$$

which is not the same as we found in (12.32) for all clusters. We find that k' is slightly larger than k.

Interpretation of k' and k. What is the interpretation of k'? If we consider random walks on the spanning cluster only, the behavior at $p = p_c$ is described by

$$\langle r^2 \rangle \propto t^{2k'} \ , \tag{12.53}$$

this gives

$$r^{1/k'} \propto t \propto r^{d_w} \ , \tag{12.54}$$

where d_w can be interpreted as the dimension of the random walk. For the case of random walkers on the spanning cluster at $p = p_c$ we have therefore found that4

$$d_w = 2 + \frac{\mu-\beta}{\nu} \ . \tag{12.55}$$

The fractal dimension is larger than 2. This corresponds to the walker getting stuck on the percolation cluster, and the structure of the walk is therefore more dense or compact.

12.2.7 (Advanced) The diffusion constant D

We can use the theory we have developed so far to address the behavior of the diffusion constant with time. Fick's law can generally be formulated as

$$\langle r^2 \rangle = \mathcal{D} t \; , \tag{12.56}$$

or, equivalently, we can find the diffusion constant for Fick's law from:

$$\mathcal{D} = \frac{\partial}{\partial t} \langle r^2 \rangle \; . \tag{12.57}$$

Now, we have established that for diffusion on the spanning cluster for $p = p_c$, the diffusion is anomalous. That is, the relation between the square distance and time is not linear, but a more complicated power-law relationship

$$\langle r^2 \rangle \propto t^{2k'} \; . \tag{12.58}$$

As a result, we find that the diffusion constant $\mathcal{D}'$ for diffusion on the spanning cluster defined through Fick's law is

$$\mathcal{D}' \propto \frac{\partial}{\partial t} t^{2k'} \propto t^{2k'-1} \; . \tag{12.59}$$

We can therefore interpret the process as a diffusion process where $\mathcal{D}$ decays with time.

In the anomalous regime, we find that

$$r \propto t^{k'} \; , \tag{12.60}$$

and therefore that

$$r^{1/k'} \propto t \; . \tag{12.61}$$

We can therefore also write the diffusion constant $\mathcal{D}'$ as

$$\mathcal{D}' \propto t^{2k'-1} \propto r^{2-1/k'} \propto r^{-\theta} \; . \tag{12.62}$$

We could therefore also say that the diffusion constant is decreasing with distance. The reverse is also generally true: Whenever $\mathcal{D}$ depends on the distance, we will end up with anomalous diffusion.

We can also relate these results back to the diffusion equation. The diffusion equation for the random walk was:

$$\frac{\partial P}{\partial t} = \mathcal{D}' \nabla^2 P = \nabla \mathcal{D}' \nabla P \; , \tag{12.63}$$

where the last term is the correct term if the diffusion constant depends on the spatial coordinate.

We can rewrite the dimension, d_w, of the walk to make the relation between the random walker and the dimensionality of the space on which it is moving more obvious:

$$d_w = 2 - d + \frac{\mu}{\nu} + d - \frac{\beta}{\nu} \ , \tag{12.64}$$

where we recognize the first term as

$$\tilde{\zeta}_R = 2 - d + \frac{\mu}{\nu} \ , \tag{12.65}$$

and the second term as the fractal dimension, D, of the spanning cluster:

$$D = d - \frac{\beta}{\nu} \ . \tag{12.66}$$

We have therefore established the relation

$$d_w = \tilde{\zeta}_R + D \ . \tag{12.67}$$

This relation is actually generalizable, so that for a random walker restricted to only walk on the backbone, the dimension of the walker is

$$d_{w,B} = \tilde{\zeta}_R + D_B \ . \tag{12.68}$$

12.3 Exercises

Exercise 12.1: Random walks on the spanning cluster

In this exercise we will use and modify the program `percwalk` from the text to study random walks in percolation systems, and on the spanning cluster in particular. We want to find the dimension d_w of a two-dimensional random walk on the spanning cluster.

a) Find the distance $\langle r^2 \rangle$ as a function of the number of steps N for random walks on the spanning cluster for $p = p_c$.

b) Find the dimension, d_w of the walk, from the relation $\langle r^2 \rangle \propto N^{2/d_w}$.

c) Find the distribution $P(r, N)$ for the position r as a function of the number of steps N for a random walker on the percolation cluster.

d) (Advanced) Can you produce a data-collapse for the distribution $P(r, N)$.

e) (Advanced) Can you determine the functional form of the distributoin $P(r, N)$. Is it a Gaussian?

Exercise 12.2: Random walks on percolation clusters

In this exercise we will use and modify the program `percwalk` to study random walks on the spanning cluster of a percolation system.

a) Find the distance $\langle r^2 \rangle$ as a function of the number of steps N for random walks on the spanning cluster for $p < p_c$ and for $p > p_c$.

b) Plot $\log\langle R^2 \rangle$ as a function of N for various values of p.

c) Can you find the behavior of the correlation length ξ from this plot?

d) Discuss the behavior of the characteristic cross-over time t_0 based on the plot.

Exercise 12.3: Self-avoiding walks on fractals

(Advanced) In this exercise we will use the program `percwalk` to study a self-avoiding random walker on the spanning cluster. In this exercise you will need to collect extensive statistics to be able to determine the scaling behavior.

a) Find the distance $\langle R^2 \rangle$ as a function of the number of steps N for random walks on the spanning cluster for $p = p_c$.

b) Find the dimension, d_w of the walk, from the relation $\langle R^2 \rangle \propto N^{2/d_w}$.

13 Dynamic processes in disordered media

So far, we have studied the behavior and properties of systems with *disorder*, such as the model porous material we call the percolation system. That is, we have studied properties that depend on the existing disorder of the material. In this chapter, we will start to address dynamical processes that generate percolation-like disordered structures, but where the structures evolve, develop, and change in time.

The first dynamic problem we will address is the formation diffusion fronts, and we will demonstrate that the front of a system of diffusing particles can be described as a percolation system.

The second dynamic problem we will address is the slow displacement of one fluid by another in a porous medium. We will in particular demonstrate that the invasion percolation process generates a fractal structure similar to the percolation cluster by itself - it is a process that drives itself to a critical state, similar to the recently introduced notion of Self-Organized Criticality [3]. We will then address how we can study similar processes in the gravity field, and, in particular, the influence of stabilizing and destabilizing mechanisms. Invasion percolation in a destabilizing gravity field provides a good model to describe and understand the process of primary migration.

13.1 Diffusion fronts

The first dynamical problem we will address is the structure of a diffusion front [31]. Let us address a diffusion process on a square lattice. One example of such a process is the two-dimensional diffusion of particles from a source at $x = 0$ into the $x > 0$ plane, when particles are not allowed to overlap. The system of diffusing particles is illustrated in Fig. 13.1.

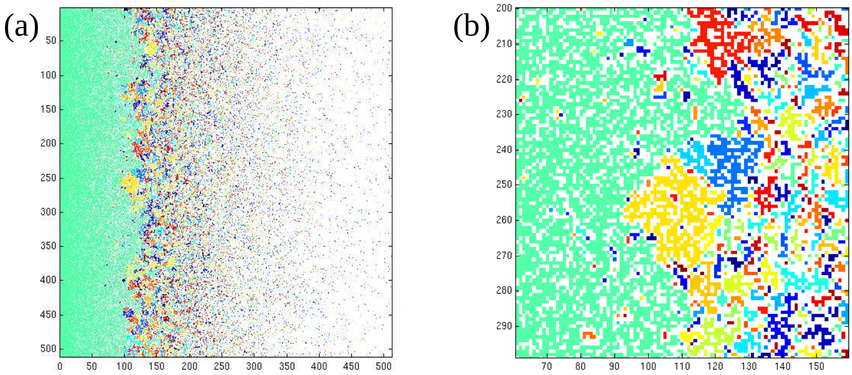

Fig. 13.1 Illustration of the diffusion front. Particles are diffusing from a source at the left side. We address the front separating the particles connected to the source from the particles not connected to the source. The average distance is given by x_c shown in the figure. The width of the front, ξ, is also illustrated in the figure. The different clusters are colored to distinguish them from each other. The close-up in figure (b) illustrates the finer details of the diffusion fronts, and the local cluster geometries.

Exact solution for concentration. For this problem we know the exact solution for the concentration, $c(x,t)$, or particles, corresponding to the occupation probability $P(x,t)$. The solution to the diffusion equation with a constant concentration, or $P(x = 0, t) = 1$, is the error function given as the integral over a Gaussian function:

$$P(x,t) = 1 - erf(\frac{x}{\sqrt{Dt}}) \ , \tag{13.1}$$

where the error function is defined as the integral:

$$erf(u) = \frac{2}{\sqrt{2\pi}} \int_0^u e^{\frac{-v^2}{2}} dv \ . \tag{13.2}$$

This solution produces the expected deviation $\langle x^2 \rangle = Dt$, where D is the diffusion constant for the particles. There is no y (or z) dependence for the solution.

Structure of clusters connected to diffusion front. We will address the structure of connected clusters of diffusing particles. Two particles are connected if they are neighbors so that they inhibit each others diffusion in a particular direction. If we fix t, we notice that the system will be compact close to $x = 0$, and that there only will be a few thinly spread particles when $x \gg \sqrt{Dt}$. In this system, the occupation probability varies with both time t and spatial position x. However, we expect the system of diffusing particles to be connected to the source out to a distance x_c corresponding to the point where the occupation probability is equal to the percolation threshold p_c for the lattice type studied. That is:

$$P(x_c, t) = p_c \ , \tag{13.3}$$

defines the center of the diffusion front: the front separating the particles that are connected to the source from the particles that are not connected to the source. We notice that $x_c(t) = \sqrt{Dt}$.

Width of the diffusion front. idxwidth of diffusion front]

What is the width of the diffusion front? For a given time t, the occupation probability decreases with $\delta x = x - x_c$. Similarly, the correlation length will therefore also depend on the distance δx to the average position of the front. We expect that a cluster may be connected to the front if it is within a distance ξ of x_c. Particles that are further away than the local correlation length, ξ, will not be connected over such distances, and will therefore not be connected. Particles that are closer to x_c than ξ will typically by connected through some connecting path. We will therefore introduce ξ as the width of the front, corresponding to the distance at which the local correlation length, due to the occupation probability $P(x, t)$, is equal to the distance from x_c. The local correlation length $\xi(x)$ is given as

$$\xi(x) = \xi_0 |P(x, t) - p_c|^{-\nu} \ , \tag{13.4}$$

The distance w at which $\xi(x_c + w) = w$ gives the width of the front. We can write this self-consistency equation for w as

$$w = \xi_0 |P(x + w, t) - p_c|^{-\nu} \ . \tag{13.5}$$

Let us introduce a Taylor expansion of $P(x)$ around $x = x_c$:

$$P(x, t) \simeq P(x_c, t) + \left.\frac{dP}{dx}\right|_{x_c} (x - x_c) \ , \tag{13.6}$$

where we recognize that $x_c \propto \sqrt{Dt}$ gives

$$\left.\frac{dP}{dx}\right|_{x_c} \propto \frac{1}{\sqrt{Dt}} \propto \frac{1}{x_c} \ . \tag{13.7}$$

We insert this into the self-consistency equation (13.5) getting

$$w = \xi_0 |w \left.\frac{dP}{dx}\right|_{x_c} |^{-\nu} \propto (w/x_c)^{-\nu} \ , \tag{13.8}$$

which gives

$$w \propto x_c^{\nu/(1+\nu)} \ . \tag{13.9}$$

The width of the front therefore scales with the average position of the front, and the scaling exponent is related to the scaling exponent of the correlation length for the percolation problem.

Time development. What happens in this system with time? Since x_c is increasing with time, we see that the relative width decreases:

$$\frac{w}{x_c} \propto \frac{x_c^{\nu/(1+\nu)}}{x_c} \propto x_c^{-\frac{1}{1+\nu}} \ . \tag{13.10}$$

This effect will also become apparent under renormalization. Applying a renormalization scheme with length b, will result in a change in the front width by a factor $b^{\nu/(1+\nu)}$, but along the y-direction the rescaling will simply be by a factor b. Successive applications will therefore make the front narrower and narrower. This difference in scaling along the x and the y axis is referred to as self-affine scaling, in contrast to the self-similar scaling where the rescaling is the same in all directions.

13.2 Invasion percolation

We will now study the slow injection of a non-wetting fluid into a porous medium saturated with a wetting fluid. In the limit of infinitely slow injection, this process is termed *invasion percolation* for reasons that will soon become obvious [39, 12].

Physical system — fluid saturated porous medium. When a non-wetting fluid is injected slowly into a saturated porous medium, the pressure in the non-wetting fluid must exceed the capillary pressure in a pore-throat for the fluid to propagate from one pore to the next, as illustrated in Fig. 13.2. The pressure difference, δP needed corresponds to the capillary pressure P_c, given as

$$P_c = \frac{\Gamma}{\epsilon} \; , \tag{13.11}$$

where Γ is the interfacial surface tension, and ϵ is the characteristic size of the pore-throats in the porous medium. However, there will be some disorder present in the porous medium corresponding to local variation in the characteristic pore sizes ϵ. This will lead to a distribution of capillary pressures threshold P_c needed to invade a particular pore. We will assume that the medium can be described as a set of pores connected with pore throats with a uniform distribution of capillary pressure thresholds, and we will assume that the capillary pressure thresholds are not correlated but statistically independent. We can therefore rescale the pressure scale, by subtracting the minimum pressure threshold and dividing by the range of pressure thresholds, and describe the system as a matrix of critical pressures P_i required to invade a particular site.

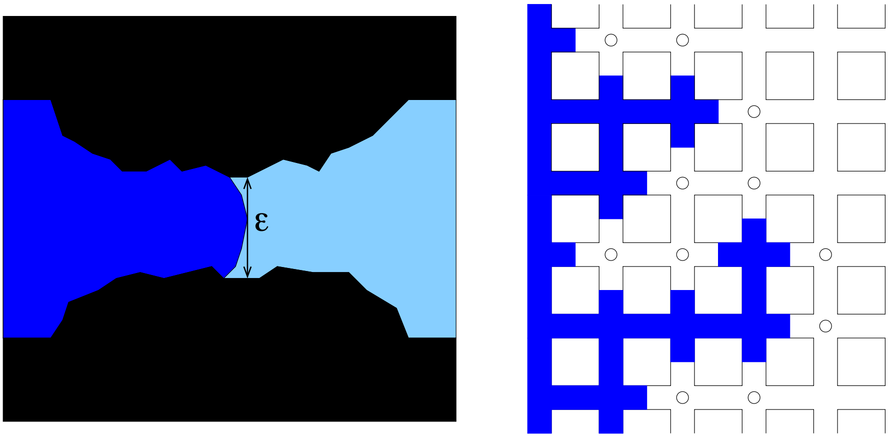

Fig. 13.2 Illustration of the invasion percolation process in which a non-wetting fluid is slowly displacing a wetting fluid. The left figure shows the interface in a pore throat: the pressure in the invading fluid must exceed the pressure in the displaced fluid by an amount corresponding to the capillary pressure $P_c = \Gamma/\epsilon$, where Γ is the interfacial surface tension, and ϵ is a characteristic length for the pore throat. The right figure illustrates the invasion front after injection has started. The fluid may invade any of the sites along the front indicated by small circles. The site with the smallest capillary pressure threshold will be invaded first, changing the front and exposing new boundary sites.

Modeling the fluid displacement process. The fluid displacement process can then be modeled by assuming that all the sites on the left side of the matrix are in contact with the invading fluid. The pressure in the invading fluid is increased slowly, until the fluid invades the connected site with the lowest pressure threshold. This generates a new set of invaded sites in contact with the inlet, and a new set of neighboring sites. The invasion process continues until the invading fluid reaches the opposite side. Further injection will then not produce any further fluid displacement, the fluid will flow through the system through the open path generated.

Computational implementation. How can we transfer this model description to a computational model? We introduce a lattice of pores to represent the pore throat sizes. For each lattice site, there is a critical pore size into that pore, with a critical pressure, p_i, needed to push the fluid into this pore. We map the pressure onto a scale from 0.0 to 1.0, where 1.0 represents the pressure needed to invade all pores in the lattice.

We then start to gradually increase the pressure in the fluid and allow the fluid to invade from the left side of the lattice. Let us say we have increased the pressure to the value p ($0 \leq p \leq 1$). This would mean that all sites that have $p_i \leq p$ *and* that are connected to the left side would be invaded.

This corresponds to a percolation problem. If we make a percolation system with occupation probability p, then the fluid will have invaded all the clusters that are connected to the left side. Thus, we have mapped the invasion percolation problem onto a percolation problem. Let us implement this approach.

First, we generate a random lattice of critical pressures and an array of pressures p that we will loop through:

```
from pylab import *
from scipy.ndimage import measurements
L = 400
z = rand(L,L) # Random distribution of thresholds
p = arange(0.0,0.7,0.01)
```

We step gradually through this set of p-values, finding the clusters of connected sites that have p-values smaller than `p[npstep]`

```
for nstep in range(len(p)-1):
    zz = z<p[nstep]
    lw,num = measurements.label(zz)
```

Then, we find the labels of all the clusters on the left side of the lattice. All the clusters with these labels are connected to the left side and are part of the invasion percolation cluster called `cluster`. We do this in two steps. First, we find a list of unique labels that are on the left side. Then we find all the clusters with labels that are in this list using the `numpy`-function `isin`:

```
    leftside = lw[:,0]
    leftnonzero = leftside[where(leftside>0)]
    uniqueleftside = unique(leftnonzero)
    cluster = isin(lw,uniqueleftside)
```

Then we make a matrix that stores at what time t (pressure value $p(t)$) a particular site was invaded. This is done by simply adding a 1 for all set sites at t to a matrix `pcluster`. The first clusters invaded will then have the highest value in the `pcluster` matrix. We use the `pcluster` matrix to visualize the dynamics.

```
    pcluster = pcluster + 1.0*cluster
```

Finally, we check if the fluid has reached the right-hand side by comparing the labels on the left-hand side with those on the right-hand side. If any labels are the same, there is a cluster connecting the two sides (a spanning cluster), and the fluid invasion process stops:

```
    # Check if it has reached the right hand side
    span = intersect1d(lw[:,1],lw[:,-1])
    if (len(span[where(span > 0)])>0):
        break
```

The whole program for the simulation, including initialization of `pcluster` is then:

```
# Example program for studying invasion percolation problems
# NOTE: This is not an optimal but an educational algorithm
from pylab import *
from scipy.ndimage import measurements
L = 400
p = arange(0.0,0.7,0.01)
z = rand(L,L) # Random distribution of thresholds
pcluster = zeros((L,L),float)
for nstep in range(len(p)-1):
    zz = z<p[nstep]
    lw,num = measurements.label(zz)
    leftside = lw[:,0]
    leftnonzero = leftside[where(leftside>0)]
    uniqueleftside = unique(leftnonzero)
    cluster = isin(lw,uniqueleftside)
    pcluster = pcluster + 1.0*cluster
    # Check if it has reached the right hand side
    span = intersect1d(lw[:,1],lw[:,-1])
    if (len(span[where(span > 0)])>0): break
```

```
imshow(log(pcluster),origin="lower")
```

Results for fluid displacement process. The resulting pattern of injected nodes is illustrated in Fig. 13.3, where the colors indicate the pressure at which the injection took place. It can be seen from the figure that the injection occurs in bursts. When a site is injected, many new connected neighbors are available as possible sites to invade. As the pressure approaches the pressure needed to percolate to the other side, these newly appearing sites of the front will typically also be invaded, and invasion will occur in gradually larger regions. These bursts have been characterized by Furuberg *et al.* [12], and it can be argued that the distribution of burst sizes as well as the time between bursts are power-law distributed.

Mapping invasion percolation onto percolation. Based on this algorithmic model for the fluid displacement process, it is also easy to connect the invasion percolation problem with ordinary percolation. For an injection pressure of p, all sites with critical pressure below or equal to p are in principle available for the injection process. However, it is only the clusters of such sites connected to the left side that will actually be invaded, since the invasion process requires a connected path from the inlet to the site for a site to be filled. We will therefore expect that the width of the invasion percolation front corresponds to the correlation length $\xi = \xi_0 (p_c - p)^{-\nu}$ as p approaches the percolation threshold p_c, because this is the length at which clusters are connected. That is, cluster that are a distance ξ from the left side will typically be connected to the left side, and therefore connected, whereas clusters that are further away than ξ will typically not be connected and therefore not invaded. This shows that the critical pressure will correspond to p_c. This also shows that when the fluid reaches the opposite side, the system is exactly at p_c, and we expect the invasion percolation cluster to have the same scaling properties as the spanning cluster at $p = p_c$. There will be small differences, because the invasion percolation cluster also contains smaller clusters connected to the left side, but we do not expect these to change the scaling behavior of the cluster. That is, we expect the fractal dimension of the invasion percolation cluster to be D. This implies that the density of the displaced fluid decreases with system size.

Invasion percolation with and without trapping. The process outlined above does, however, not contain all the essential physics of the fluid displacement process. For displacement of an incompressible fluid, a

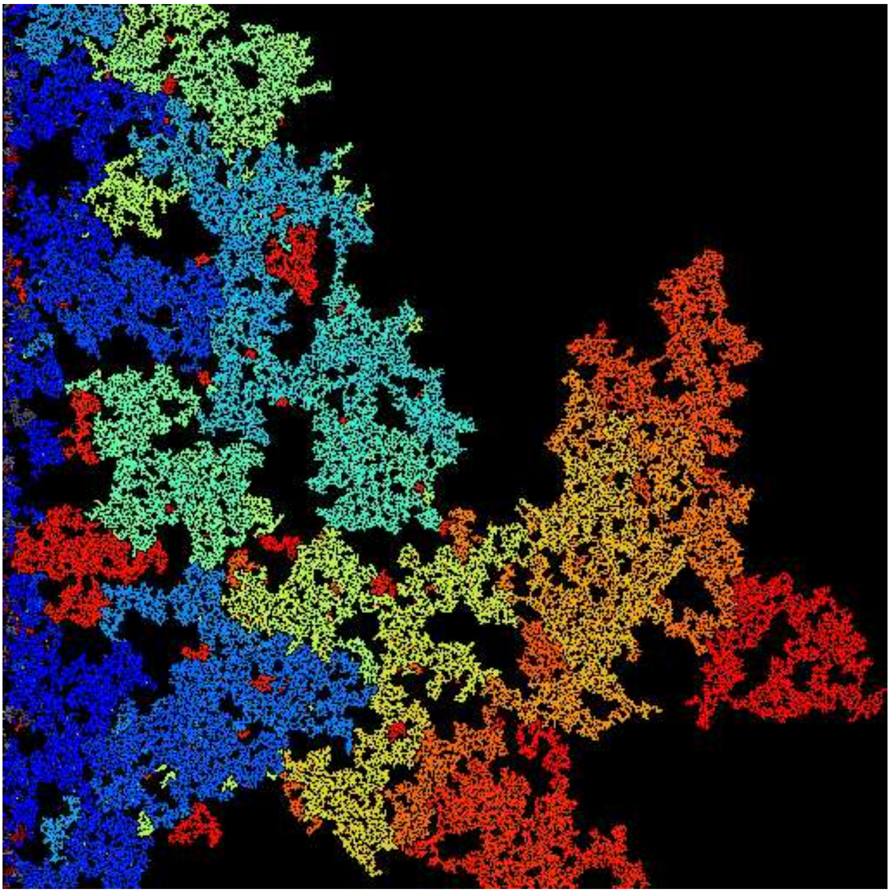

Fig. 13.3 Illustration of the invasion percolation cluster. The color-scale indicates normalized pressure at which the site was invaded.

region that is fully bounded by the invading fluid cannot be invaded, since the displaced fluid does not have any place to go. Instead, we should study the process called invasion percolation with trapping. It has been found that when trapping is included, the fractal dimension of the invasion percolation cluster is slightly smaller [10]. In two dimensions, the dimension is $D \simeq 1.82$.

This difference between the process with and without trapping disappears for three-dimensional geometries because trapping become unlikely in dimensions higher than 2. Indeed, direct numerical modeling shows that the fractal dimension for both the ordinary percolation system and invasion percolation is $D \simeq 2.5$ for invasion percolation with and without trapping.

13.2.1 Gravity stabilization

The invasion percolation cluster displays self-similar scaling similar to that of ordinary percolation. This implies that the position $h(x, p)$ of the fluid front as a function of the non-dimensional applied pressure p is given as the correlation length - since this is how far clusters connected to the left side typically are connected. That is, when p approaches p_c, the average position of the front is $\bar{h}(x, p) = \xi(p) = \xi_0(p_c - p)^{-\nu}$. The width, $w(p)$ of the front is also given as the correlation length:

$$w(p) = \xi_0(p_c - p)^{-\nu} , \tag{13.12}$$

as p approaches p_c both the front position and the front width diverges, that is, both the front position $\bar{h}$ and the width, w, are proportional to the system size L:

$$\bar{h} \propto w \propto L , \tag{13.13}$$

However, when the system size increases, we would expect other stabilizing effects to become important. For a very small, but finite fluid injection velocity, the viscous pressure drop will eventually become important and comparable to the capillary pressure. Also, any deviation from a completely flat system or for a system with a slight different in densities, the effect of the hydrostatic pressure term will also eventually become important. We will now demonstrate how we may address the effect of such a stabilizing (or destabilizing) effect [5, 25].

Invasion percolation in a gravity field. Let us assume that the invasion percolation occurs in the gravity field. This implies that the pressure needed to invade a pore depends both on the capillary pressure, and on a hydrostatic term. The pressure P_i^c needed to invade site i at vertical position x_i in the gravity field is:

$$P_i^c = \frac{\Gamma}{\epsilon} + \Delta\rho g x_i , \tag{13.14}$$

We can again normalize the pressures, resulting in

$$p_i^C = p_i^0 + \frac{\Delta\rho g}{\Gamma\epsilon^2} x_i' , \tag{13.15}$$

where the coordinates are measured in units of the pore size, ϵ, which is the unit of length in our system. The last term is called the Bond number:

$$Bo = \frac{\Delta\rho g}{\Gamma\epsilon^2} , \tag{13.16}$$

Here, we will include the effect of the bond number in a single number g, so that the critical pressure at site i is:

$$p_i^c = p_i^0 + g x_i' \ , \tag{13.17}$$

where p_i^0 is a random number between 0 and 1.

Computational implementation. We implement this by changing the values of the pressure threshold p_i in the computational code:

```
g = 0.001
grad = g*meshgrid(range(L),range(L))[0]
z = z + grad
```

The whole program then becomes

```
# Now we add the effect on gravity - modifying the values of z
from pylab import *
from scipy.ndimage import measurements
L = 400
p = arange(0.0,0.7,0.01)
z = rand(L,L) # Random distribution of thresholds
g = 0.001
grad = g*meshgrid(range(L),range(L))[0]
z = z + grad
pcluster = zeros((L,L),float)
for nstep in range(len(p)-1):
    zz = z<p[nstep]
    lw,num = measurements.label(zz)
    leftside = lw[:,0]
    leftnonzero = leftside[where(leftside>0)]
    uniqueleftside = unique(leftnonzero)
    cluster = isin(lw,uniqueleftside)
    pcluster = pcluster + 1.0*cluster
    # Check if it has reached the right hand side
    span = intersect1d(lw[:,1],lw[:,-1]) # Testing using intersect
    if (len(span[where(span > 0)])>0):
        break
imshow(log(pcluster),origin="lower")
```

Visualization of results. The resulting invasion percolation front for various numbers of g is illustrated in Fig. 13.4. How can we understand the gradual flattening of the front as g increases from g?

Front width analysis. This problem is similar to the diffusion front problem. For an applied pressure p the front will typically be connected up to an average distance x_c given as

$$p = p^0 + x_c g \ . \tag{13.18}$$

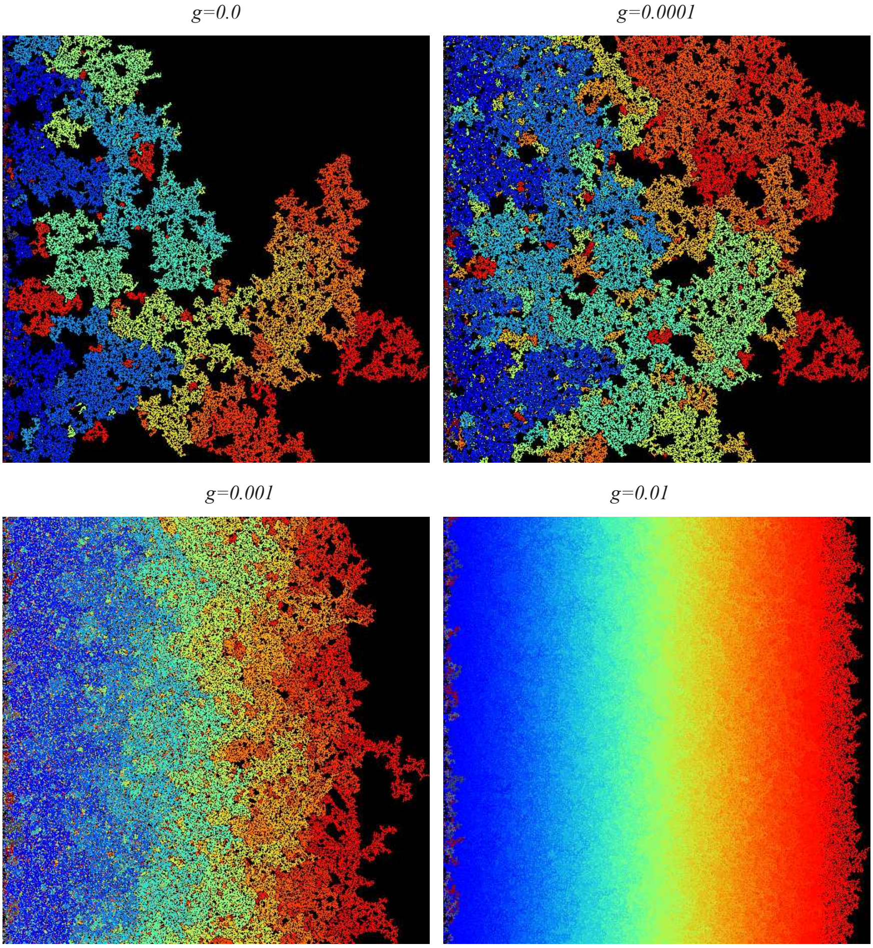

Fig. 13.4 Illustration of the gravity stabilized invasion percolation cluster for $g = 0$, $g = 10^{-4}$, $g = 10^{-3}$, and $g = 10^{-2}$. The color-scale indicates normalized pressure at which the site was invaded.

The front will also extend beyond the average front position. The occupation probability at a distance a from the front is $p' = p_c - ag$, since fewer sites will be set beyond the front due to the stabilizing term g. A site at a distance a is connected to the front if this distance a is shorter to or equal to the correlation length for the occupation probability p' at this distance. The maximum distance a for which a site is connected to the front therefore occurs when

$$a = \xi(p') = \xi_0(p_c - p')^{-\nu} . \tag{13.19}$$

This gives

$$a = \xi(p') = \xi_0(p_c - p')^{-\nu} = \xi_0(p_c - (p_c - ag))^{-\nu} = \xi_0(ag)^{-\nu}a \; . \quad (13.20)$$

This gives

$$a \propto g^{-\nu/(1+\nu)} \; , \quad (13.21)$$

as the front width. We leave it as an exercise to show find the form of the position $h(p, g)$, and the width, $w(p, g)$, as a function of p and g. We observe that the width has a reasonable dependence on g. When g approaches 0, the width diverges. This is exactly what we expect since the limit $g = 0$ corresponds to the limit of ordinary invasion percolation.

This discussion demonstrates a general principle that we can use to study several stabilizing effects, such as the effect of viscosity or other material or process parameters that affect the pressure needed to advance the front. The introduction of a finite width or characteristic length ξ that can systematically be varied in order to address the behavior of the system when the characteristic length diverges is also a powerful method of both experimental and theoretical use.

13.2.2 Gravity destabilization

The gravity destabilized invasion percolation process corresponds to the case when a less dense fluid is injected at the bottom of a denser fluid. This is similar to the process known as secondary migration, where the produced oil is migrating up through the sediments filled with denser water. Examples of the destabilizing front is shown in Fig. 13.5.

We can make a similar argument for the case when $g < 0$, but in this case the front is destabilized, and the correlation length $\xi \propto (-g)^{-\nu/(1+\nu)}$ corresponds to the width of the finger extending front the front. The extending finger can be modeled as a sequence of blobs of size ξ extending from the flat surface. This implies that the region responsible for the transport of oil in secondary migration is essentially one-dimensional structures: lines with a finite width w. The amount of hydrocarbons left in the sediments during this process is therefore negligible. However, there will be other effects, such as the finite viscosity and the rate of production compared to the rate of flow, which will induce more than one finger. However, the full process has only to a small degree been addressed. Gravity destabilized invasion percolation is used as a modeling tool in studies of petroleum plays and commercial software packages are available for such simulation.

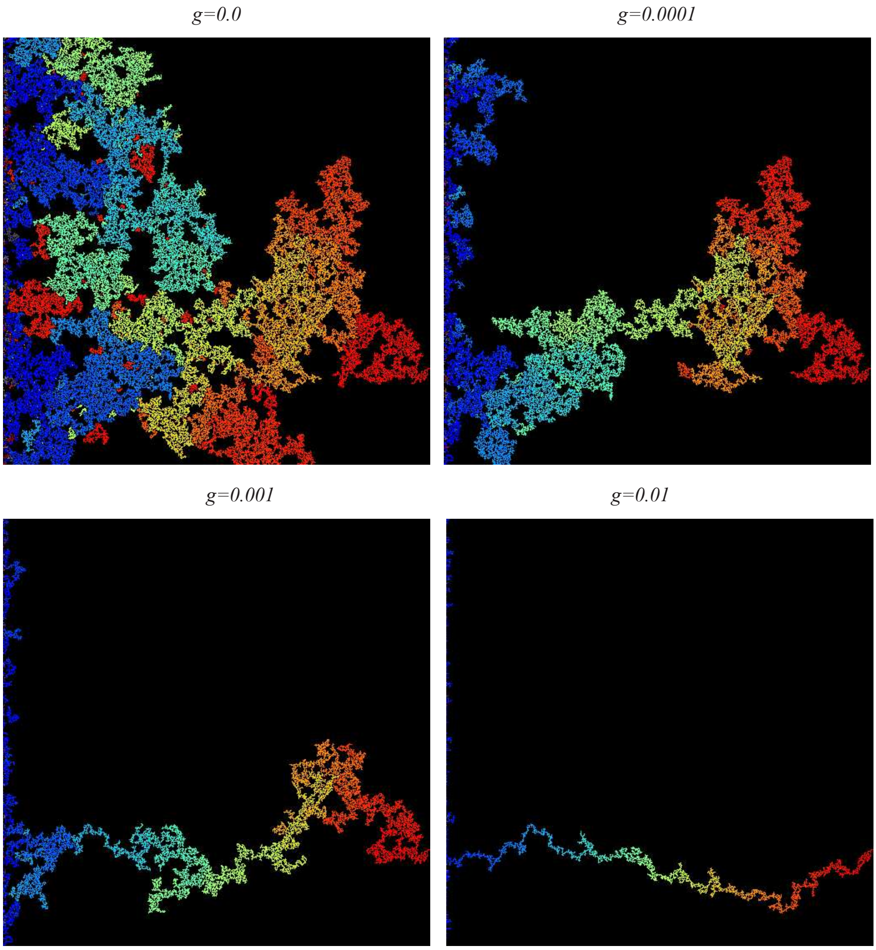

Fig. 13.5 Illustration of the gravity de-stabilized invasion percolation cluster for $g = 0$, $g = -10^{-4}$, $g = -10^{-3}$, and $g = -10^{-2}$. The color-scale indicates normalized pressure at which the site was invaded.

References

[1] Joan Adler, Yigal Meir, Amnon Aharony, A. B. Harris, and Lior Klein. Low-concentration series in general dimension. *Journal of Statistical Physics*, 58(3):511–538, 1990.

[2] A. Aharony, Y. Gefen, and A. Kapitulnik. Scaling at the percolation threshold above six dimensions. *Journal of Physics A: Mathematical and General*, 17(4):L197–L202, 1984.

[3] Per Bak. *How Nature Works: the Science of Self-Organized Criticality.* Copernicus, 1996.

[4] David J. Bergman and Yacov Kantor. Critical Properties of an Elastic Fractal. *Physical Review Letters*, 53(6):511–514, 1984.

[5] A. Birovljev, L. Furuberg, J. Feder, T. Jssang, K. J. Mly, and A. Aharony. Gravity invasion percolation in two dimensions: Experiment and simulation. *Physical Review Letters*, 67(5):584–587, 1991.

[6] John L. Cardy. Introduction to Theory of Finite-Size Scaling. In *Current Physics–Sources and Comments*, volume 2 of *Finite-Size Scaling*, pages 1–7. Elsevier, 1988.

[7] Kim Christensen and Nicholas R. Moloney. *Complexity and Criticality.* Imperial College Press, 2005.

[8] A. Coniglio and R. Figari. Droplet structure in Ising and Potts models. *Journal of Numerical Mathematics*, 16(14):L535–L540, 1983.

[9] P. G. de Gennes. La percolation: Un concept unificateur. *La Recherche*, 7:919, 1976.

[10] M. M. Dias and D. Wilkinson. Percolation with trapping. *Journal of Physics A: Mathematical and General*, 19(15):3131–3146, 1986.

[11] Shechao Feng and Pabitra N. Sen. Percolation on Elastic Networks: New Exponent and Threshold. *Physical Review Letters*, 52(3):216–219, 1984.

[12] Liv Furuberg, Jens Feder, Amnon Aharony, and Torstein Jøssang. Dynamics of Invasion Percolation. *Physical Review Letters*, 61(18):2117–2120, 1988.

[13] Yuval Gefen, Amnon Aharony, and Shlomo Alexander. Anomalous Diffusion on Percolating Clusters. *Physical Review Letters*, 50(1):77–80, 1983.

[14] Geoffrey R. Grimmett. *Percolation*. Grundlehren der mathematischen Wissenschaften. Springer, Berlin Heidelberg, 2 edition, 1999.

[15] Shlomo Havlin and Daniel Ben-Avraham. Diffusion in disordered media. *Advances in Physics*, 36(6):695–798, 1987.

[16] H. J. Herrmann and H. E. Stanley. The fractal dimension of the minimum path in two- and three-dimensional percolation. *Journal of Physics A: Mathematical and General*, 21(17):L829–L833, 1988.

[17] D. C. Hong and H. E. Stanley. Cumulant renormalisation group and its application to the incipient infinite cluster in percolation. *Journal of Numerical Mathematics*, 16(14):L525–L529, 1983.

[18] Allen Hunt, Robert Ewing, and Behzad Ghanbarian. *Percolation Theory for Flow in Porous Media*. Lecture Notes in Physics. Springer, 3 edition, 2014.

[19] Leo P. Kadanoff. Scaling laws for ising models near ${T}_{c}$. *Physics Physique Fizika*, 2(6):263–272, 1966.

[20] Yacov Kantor and Itzhak Webman. Elastic Properties of Random Percolating Systems. *Physical Review Letters*, 52(21):1891–1894, 1984.

[21] Harry Kesten. *Percolation Theory for Mathematicians*. Progress in Probability. Birkhäuser Basel, 1982.

[22] Peter R. King and Mohsen Masihi. *Percolation Theory in Reservoir Engineering*. WORLD SCIENTIFIC (EUROPE), 2018.

[23] Scott Kirkpatrick. Percolation and Conduction. *Reviews of Modern Physics*, 45(4):574–588, 1973.

[24] B. J. Last and D. J. Thouless. Percolation Theory and Electrical Conductivity. *Physical Review Letters*, 27(25):1719–1721, 1971.

[25] Paul Meakin, Aleksandar Birovljev, Vidar Frette, Jens Feder, and Torstein Jøssang. Gradient stabilized and destabilized invasion percolation. *Physica A: Statistical Mechanics and its Applications*, 191(1):227–239, 1992.

[26] Yigal Meir, Raphael Blumenfeld, Amnon Aharony, and A. Brooks

Harris. Series analysis of randomly diluted nonlinear resistor networks. *Physical Review B*, 34(5):3424–3428, 1986.

[27] S. Roux. Relation between elastic and scalar transport exponent in percolation. *Journal of Numerical Mathematics*, 19(6):L351–L356, 1986.

[28] M. Sahimi. Relation between the critical exponent of elastic percolation networks and the conductivity and geometrical exponents. *Journal of Physics C: Solid State Physics*, 19(4):L79–L83, 1986.

[29] Muhammad Sahimi and Joe D. Goddard. Elastic percolation models for cohesive mechanical failure in heterogeneous systems. *Physical Review B: Condensed Matter and Materials Physics*, 33(11):7848–7851, 1986.

[30] M. Sahini and M. Sahimi. *Applications Of Percolation Theory*. Wiley Press, 2003.

[31] B. Sapoval, M. Rosso, and J. F. Gouyet. The fractal nature of a diffusion front and the relation to percolation. *Journal de Physique Lettres*, 46(4):149–156, 1985.

[32] Waclaw Sierpinski. Sur une courbe dont tout point est un point de ramification. *Comp. Rend. Acad. Sci. Paris*, 160:302–305, 1915.

[33] Sorin Solomon, Gerard Weisbuch, Lucilla de Arcangelis, Naeem Jan, and Dietrich Stauffer. Social percolation models. *Physica A: Statistical Mechanics and its Applications*, 277(1):239–247, 2000.

[34] H. E. Stanley. Cluster shapes at the percolation threshold: and effective cluster dimensionality and its connection with critical-point exponents. *Journal of Physics A: Mathematical and General*, 10(11):L211–L220, 1977.

[35] H. E. Stanley. *Introduction to Phase Transitions and Critical Phenomena*. Oxford University Press USA, New York, reprint edition edition, 1987.

[36] H. E. Stanley and A. Coniglio. Fractal structure of the incipient infinite cluster in percolation. In G. Deutsher, R. Zallen, and J. Adler, editors, *Percolation Structures and Processes*. Adam Hilger, Bristol, 1983.

[37] Dietrich Stauffer and Ammon Aharony. *Introduction To Percolation Theory: Second Edition*. Wiley Press, 1992.

[38] Sandra J. Steacy and Charles G. Sammis. An automaton for fractal patterns of fragmentation. *Nature*, 353(6341):250–252, 1991.

[39] D. Wilkinson and J. F. Willemsen. Invasion percolation: a new form of percolation theory. *Journal of Numerical Mathematics*, 16(14):3365–3376, 1983.

[40] Kenneth G. Wilson. Renormalization Group and Critical Phenomena. I. Renormalization Group and the Kadanoff Scaling Picture. *Physical Review B: Condensed Matter and Materials Physics*, 4(9):3174–3183, 1971.

[41] J. G. Zabolitzky, D. J. Bergman, and D. Stauffer. Precision calculation of elasticity for percolation. *Journal of Statistical Physics*, 44(1):211–223, 1986.

Index